

Regulation of endocytosis and secretion by Rab GTPase activating proteins

Dissertation

zur Erlangung des Doktorgrades der Naturwissenschaften

(Dr. rer. nat.)

der Fakultät für Biologie

der Ludwigs-Maximilians-Universität München

vorgelegt von

Alexander Haas

München 2008

1. Gutachter: PD Dr. Angelika Böttger

2. Gutachter: Prof. Dr. Michael Schleicher

Tag der mündlichen Prüfung: 17.06.2008

Ehrenwörtliche Versicherung und Erklärung über frühere Promotionsversuche

Hiermit versichere ich, Alexander Haas, ehrenwörtlich, dass die vorgelegte Dissertation von mir selbständig und ohne unerlaubte Hilfe angefertigt ist. Des Weiteren erkläre ich, dass die vorgelegte Dissertation weder ganz noch in wesentlichen Teilen einer anderen Prüfungskommission vorgelegt wurde. Ich habe mich anderweitig keiner Doktorprüfung unterzogen.

München, 13. Februar 2008

Alexander Haas

“All there is to thinking (...) is seeing something noticeable which makes you see something you weren’t noticing which makes you see something that isn’t even visible.”

Norman Maclean

Zusammenfassung

Vesikulärer Transport ist ein hochgradig regulierter Prozess. Eine Schlüsselfunktion übernehmen hierbei Proteine der Rab Familie, die mit 60 Mitgliedern die größte Gruppe innerhalb der Ras Superfamilie kleiner monomerer GTPasen darstellt. Rabs rekrutieren als Effektoren bezeichnete Proteine zur Membran von Organellen, deren Identität sie hierdurch definieren. Rabs können sowohl in einer aktiven, GTP gebundenen, als auch in einer inaktiven Gestalt, gebunden an GDP, auftreten. Eine Schlüsselfunktion in ihrer Regulation kommt RabGAPs zu, die katalytisch die Hydrolyse gebundenen GTPs beschleunigen.

Durch Datenbankanalyse wurden im humanen Genom 40 dieser GAPs, die durch eine TBC Domäne charakterisiert sind, identifiziert. Um spezifische Rab-RabGAP Paare erkennen zu können, wurde ein neuartiges Hefe-Hybrid Verfahren entwickelt. Mittels dieses Verfahrens wurde ein RabGAP-5 benanntes GAP identifiziert, das spezifisch die GTP Hydrolyse durch Rab5 stimulierte. Die Expression von RabGAP-5 führte zur Inaktivierung von Rab5 und dem Verlust des Rab5 Effektors EEA1 von Endosomen. RabGAP-5 war des Weiteren in der Lage, die von Rab5 abhängige Aufnahme von EGF und Transferrin zu blockieren. Die Depletion von RabGAP-5 führte durch die erhöhte Menge von GTP gebundenem Rab5 zu vergrößerten Endosomen und blockierte den Transport von EGF.

Um im Weiteren an der Regulation der Sekretion beteiligte Rabs und ihre GAPs zu identifizieren, wurde eine neue Methode etabliert, die es, basierend auf der Inaktivierung von endogenen Rabs durch Expression ihrer GAPs, ermöglicht, beide Partner zugleich zu erkennen.

Mittels dieses Verfahrens wurde der Einfluss von RabGAPs auf den Golgi Apparat, das ERGIC und die Sekretion untersucht. Dies führte zur Identifikation von TBC1D20 als alleinigem gemeinsamem Regulator dieser Prozesse und Organellen, einem hochgradig konservierten Protein. Dieses Protein stimulierte die GTP Hydrolyse sowohl durch Rab1 als auch durch Rab2, und reguliert *in vivo* in erster Linie Rab1. Als einziges RabGAP besitzt TBC1D20 eine Transmembran-Domäne, durch die es im ER verankert wird. Hier interagiert TBC1D20 mit RTN-1, welches seine Aktivität moduliert.

Diese Ergebnisse zeigen eine bisher unbekannt Funktion von Rab1 bei der Regulation von Prozessen auf der Ebene des ER auf. Des Weiteren wird das klassische Bild von RabGAPs als Regulatoren der Lebensspanne aktiver, GTP gebundener Rab GTPasen, durch diese Ergebnisse erweitert.

Abstract

Vesicle traffic in eukaryotic cells is a tightly organized process involving a multitude of regulatory proteins. Key regulators of this traffic are small GTPases called Rabs. With about 60 members in the human genome, they constitute the largest subgroup in the superfamily of Ras like monomeric GTPases. They recruit effector proteins to specific membranes and thus define the identity of organelles. Rabs switch between an active, GTP bound state and an inactive GDP bound state. Key regulators of this conversion are RabGAPs, which accelerate the hydrolysis of bound GTP. All RabGAPs are characterized by the presence of a TBC domain.

In the human genome 40 RabGAPs were identified, most of which had not been studied so far. To assign them to their specific Rab proteins, a novel reverse yeast two-hybrid screening method was developed. This identified a GAP for Rab5 termed RabGAP-5. RabGAP-5 stimulated the GTPase activity of Rab5. Its expression inactivated Rab5 and redistributed the Rab5 effector EEA1 from early endosomes to the cytoplasm. RabGAP-5 also blocked the Rab5 dependent uptake of EGF and transferrin from the plasma membrane. When RabGAP-5 was depleted, the size of endosomes was increased, indicating elevated Rab5-GTP levels. Endocytosed EGF was unable to exit the endosome, indicating that trafficking through endosomes was also blocked.

To identify GAPs and Rabs implicated in the regulation of early secretory events simultaneously, a second novel screening method was established. It involved the analysis of phenotypes caused by the inactivation of endogenous target Rabs via the overexpression of RabGAPs.

Changes in Golgi morphology, ERGIC organisation and the proceeding of secretion were only observed with one candidate RabGAP, the highly conserved protein TBC1D20. TBC1D20 showed activity towards Rab1 and Rab2 *in vitro*, and acted primarily on Rab1 *in vivo*. In contrast to all other RabGAPs it has a transmembrane domain, which localises it to the ER. TBC1D20 interacts with RTN-1 on ER membranes. This interaction modulates the activity of TBC1D20.

These data indicate a novel function for Rab1 in regulating ER exit, and thus extend the classical view of RabGAPs as regulators of active Rab lifetime.

Zusammenfassung	I
Abstract	II
1 Introduction	6
1.1 Intracellular membrane trafficking	6
1.1.1 Organelles and vesicle trafficking	6
1.1.2 Trafficking pathways	6
1.1.3 Vesicle trafficking has defined stages	8
1.2 Small GTPases and membrane traffic	10
1.2.1 The G domain	10
1.2.2 GTPases function as molecular switches	11
1.2.3 GTPases in vesicle trafficking	12
1.2.4 Rab GTPases	12
1.2.5 Rabs define membrane compartments	14
1.2.6 Rabs modulate multiple steps in vesicular trafficking	15
1.2.7 The classic Rab Cycle	16
1.3 RabGAPs regulate GTP hydrolysis by Rabs	18
1.3.1 The TBC domain	18
1.3.2 The GTP hydrolysis reaction	19
1.3.3 Open questions about Rab and their GAPs	21
2 Regulation of endocytosis by RabGAP-5	22
2.1 Aim of this Work	22
2.2 Results	22
2.2.1 Bioinformatic identification and characterisation of human RabGAPs	22
2.2.2 Cloning of human RabGAPs	24
2.2.3 Yeast two-hybrid screening to identify RabGAPs regulating endocytosis	24
2.2.4 RabGAP-5 specifically activates GTP hydrolysis by Rab5	27
2.2.5 RN-tre is a specific Rab43 GAP	28
2.2.6 RabGAP-5 redistributes Rab5 effectors <i>in vivo</i>	30
2.2.7 RabGAP-5 causes redistribution of Rab5	32
2.2.8 RN-tre does not function as a GAP for Rab5 <i>in vivo</i>	34
2.2.9 Expression of RabGAP-5 blocks the endocytosis of EGF	35
2.2.10 RabGAP-5 blocks transferrin receptor trafficking	37
2.2.11 RabGAP-5 is an essential regulator of Rab5	39
2.2.12 Elevated levels of Rab5 cause a phenotype resembling RabGAP-5 depletion	42
2.2.13 Depletion of RabGAP-5 blocks trafficking through early endosomes	42
2.3 Summary	45
3 Regulation of secretion by TBC1D20	46
3.1 Aim of this Work	46
3.2 Results	46
3.2.1 Rab inactivation screening	46
3.2.2 A Rab inactivation screen for Golgi fragmentation	47
3.2.3 A Rab inactivation screen for changes in ERGIC morphology	50
3.2.4 A Rab inactivation screen for a block of VSV-G trafficking	53
3.2.5 TBC1D20 is a highly conserved TBC domain protein	55
3.2.6 Over-expression of TBC1D20 causes a unique “loss of Golgi” phenotype	57
3.2.7 TBC1D20 blocks exit of VSV-G from the ER	62
3.2.8 TBC1D20 expression causes scattering of COPII	65
3.2.9 TBC1D20 expression does not interfere with COPII dynamics	67
3.2.10 The cargo receptor p24 reveals a sorting defect caused by TBC1D20	68
3.2.11 TBC1D20 is a GAP for Rab1 and Rab2 <i>in vitro</i>	71
3.2.12 Dominant negative Rab1 ^{N121I} mimics the TBC1D20 phenotype	72
3.2.13 Depletion of Rab1 causes Golgi fragmentation	75

3.2.14	Depletion of Rab1 but not Rab2 blocks VSV-G transport	77
3.2.15	Dominant negative Rab1 ^{N121I} blocks VSV-G transport	79
3.2.16	TBC1D20 depletion causes increased p115 clustering	81
3.2.17	The depletion of TBC1D20 does not block VSV-G trafficking	84
3.2.18	TBC1D20 is a RabGAP localising to the ER	86
3.2.19	TBC1D20 localises to the ER via a C-terminal TMD	87
3.2.20	The TMD of TBC1D20 is required for its ER localisation	89
3.2.21	TBC1D20 interacts with Reticulon 1 variant 2	91
3.2.22	RTN-1 modulates the activity of TBC1D20 <i>in vivo</i>	94
3.3	Summary	98
4	Discussion	99
4.1	RabGAPs are a highly diverse protein family	99
4.2	Novel methods to study the interactions of Rabs and their GAPs	99
4.2.1	A novel yeast two-hybrid system to identify Rab-GAP pairs	99
4.2.2	Rab inactivation screening as a novel method to analyse trafficking	101
4.3	RabGAP-5 is a specific Rab5 GAP	103
4.3.1	RabGAP-5 links signalling to membrane traffic	104
4.3.2	RabGAP-5 and Merlin	106
4.4	RN-tre is a GAP for Rab43	107
4.5	TBC1D20 regulates secretion by inactivating Rab1	108
4.5.1	The Rab1 GAP TBC1D20 regulates Golgi morphology and ER exit	108
4.5.2	RTN-1 is an ER associated TBC1D20 interactor that modulates its activity	110
4.5.3	Rab1 is the conserved key regulator of the early secretory pathway	112
4.5.4	TBC1D20 and the Rab cascade	113
4.5.5	Rab1 and Golgi biogenesis	114
4.6	An additional model of GAP mediated Rab regulation	115
4.7	The specificity of Rab-GAP interactions	118
5	Material and Methods	120
5.1	Materials	120
5.1.1	Reagents	120
5.1.2	Equipment	120
5.1.3	Solutions	121
5.1.4	PCR primer	122
5.1.5	siRNA oligonucleotides	124
5.1.6	Antibodies	126
5.1.6.1	Primary antibodies	126
5.1.6.2	Secondary antibodies	127
5.2	Bacterial methods	127
5.2.1	Growth and maintenance of <i>E. coli</i>	127
5.2.2	Bacterial strains	127
5.2.3	Preparation and transformation of chemically competent bacteria	128
5.2.4	Preparation and transformation of electrocompetent bacteria	129
5.2.5	Plasmid DNA preparation from bacteria	129
5.2.6	Purification of 6xHis-tagged proteins from bacteria	130
5.3	DNA methods	131
5.3.1	"Shortway" cloning strategy	131
5.3.2	Compatible vectors	131
5.3.3	Restriction digests and agarose gel electrophoresis of DNA	132
5.3.4	Cloning digested DNA fragments	132
5.3.5	cDNA synthesis	132
5.3.6	PCR and cloning of PCR products	133
5.3.7	Site-directed mutagenesis	134

5.3.8	DNA sequencing	134
5.4	Protein methods	135
5.4.1	SDS-PAGE and Coomassie staining	135
5.4.2	Western blotting	136
5.4.3	Determination of protein concentration	136
5.4.4	Protein precipitation with TCA	136
5.4.5	Antibody generation and purification	137
5.5	Yeast methods	138
5.5.1	Strains, media and growth	138
5.5.2	Yeast transformation (frozen cell method)	138
5.5.3	Plasmid DNA minipreps from yeast cells	139
5.5.4	Yeast two-hybrid screening	139
5.6	Mammalian cell culture	140
5.6.1	Cell culture	140
5.6.2	Transient transfection of mammalian cells	140
5.6.3	RNA interference	140
5.7	Mammalian cell methods	141
5.7.1	Immunofluorescence	141
5.7.2	Cell extracts	142
5.7.3	Immunoprecipitation	142
5.7.4	Cell fractionation	143
5.7.5	Carbonate extraction	143
5.7.6	Proteinase K digestion	144
5.8	Cellular and biochemical assays	144
5.8.1	EGF uptake assay	144
5.8.2	VSV-G transport assay	145
5.8.3	GTP-hydrolysis assay	145
Abbreviations		147
References		149
Publications		161
Presentations		162
Acknowledgements		163
Curriculum Vitae		164

1 Introduction

1.1 Intracellular membrane trafficking

1.1.1 Organelles and vesicle trafficking

Eukaryotic cells are compartmentalised into membrane bound organelles that establish and maintain functionally discrete environments. Organelles therefore differ in their protein and lipid composition as well as in their luminal content.

To equip the organelles with their unique protein and lipid composition as well as to exchange material between them, membrane trafficking is required. Membrane traffic describes a series of steps by which proteins and lipids are exchanged between compartments in the form of small membrane bound carriers termed vesicles. This exchange is a highly organised and tightly regulated process generating and maintaining the different properties of each organelle.

To organise the various steps along the route of a vesicle from one to the other compartment, many regulatory and accessory proteins are required at each step. Even though the understanding of these proteins and the processes needed for proper vesicle mediated transport has made great progress in recent years (Jahn and Scheller, 2006; van Vliet et al., 2003), many questions still remain to be answered.

1.1.2 Trafficking pathways

Membrane trafficking can be divided into two general pathways (Figure 1-1). Material taken up from the plasma membrane and transported towards the inside of the cell follows the endocytic pathway. Proteins and lipids produced by the cell that traffic to destinations within the cell or become secreted, follow the secretory pathway.

Proteins trafficking through the secretory pathway are synthesised at the endoplasmatic reticulum (ER) by ER attached ribosomes. They leave the ER at ER exit sites (ERES) in vesicles coated with the Coat Protein Complex II (COPII) (Tang et al., 2005). These vesicles fuse with each other and form the ER-Golgi intermediate compartment (ERGIC) (Appenzeller-Herzog and Hauri, 2006). The next stage is the Golgi apparatus where cargo is modified and sorted. ER resident proteins recycle back to the ER in COPI vesicles. The Golgi is divided in functionally discrete sub-compartments termed *cis*-, *medial*- and *trans*-Golgi. The final compartment of the Golgi is called the trans-Golgi network (TGN) (Griffiths and Simons, 1986). Here cargo is sorted into clathrin-coated vesicles

(McNiven and Thompson, 2006), which traffic to the plasma membrane (PM) or other sub-cellular compartments (Gu et al., 2001). The TGN also receives vesicles from organelles of the endocytic pathway (Bonifacino and Rojas, 2006), and thus functions as an integrator of both the secretory and the endocytic pathway.

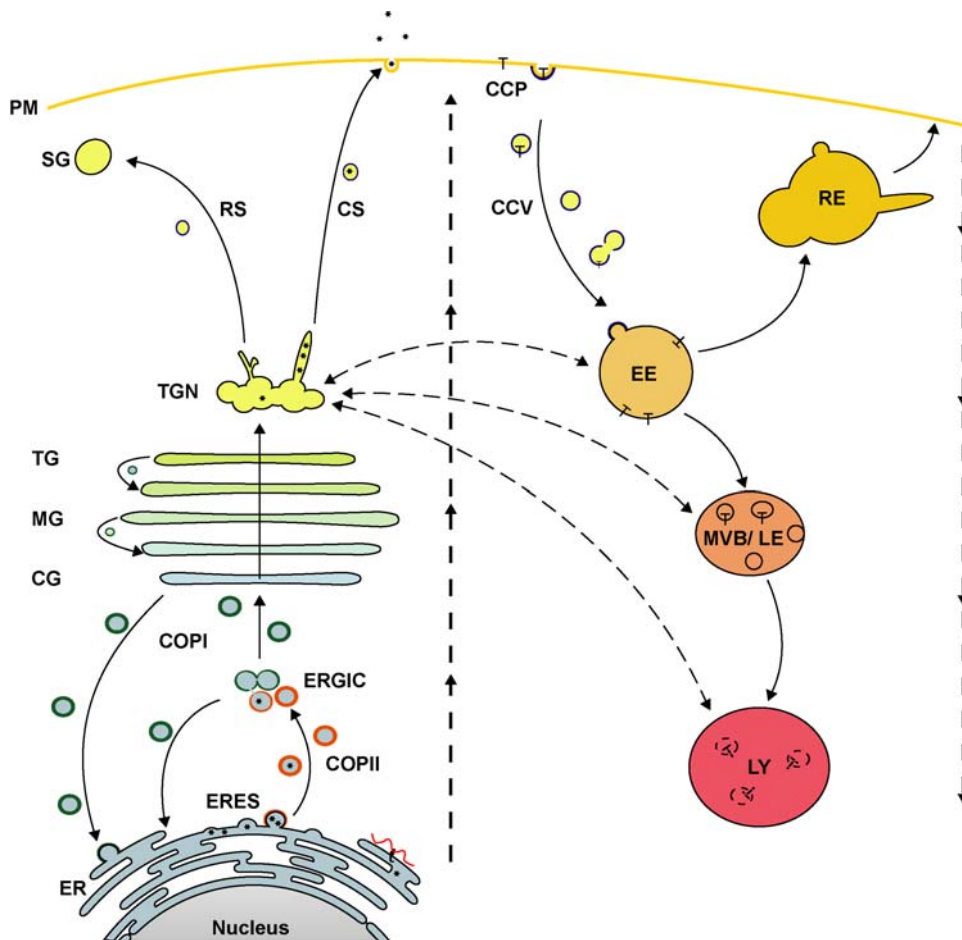


Figure 1-1 Mammalian membrane compartments and trafficking pathways. Left hand side: The secretory pathway is initiated at the endoplasmic reticulum (ER). Cargo proteins (*) are produced by ER associated ribosomes. Cargo leaves the ER in COPII (orange coat) vesicles at ER exit sites (ERES). Cargo traffics via the ER-Golgi intermediate compartment (ERGIC) to the *cis*- *medial*- and *trans*-Golgi (CG, MG, TG). ER resident proteins are recycled in COPI (green coat) vesicles. The final stage of the Golgi is the *trans*-Golgi network (TGN) that functions as an integrator of secretory and endocytic traffic. Cargo can undergo regulated secretion (RS) and traffic to the plasma membrane (PM) via secretory granules (SG) or directly traffic to the PM via the constitutive secretory pathway (CS). **Right hand side:** The endocytic pathway is initiated at the PM. Activated receptors (T) are endocytosed via clathrin-coated (blue coat) pits (CCP) and clathrin-coated vesicles (CCV) to early endosomes (EE). Cargo can be recycled via recycling endosomes (RE). Cargo destined for degradation traffics via late endosomes or multi vesiculated bodies (LE/MVB) to lysosomes (LY). Drawing is not to scale.

Multiple parallel endocytic pathways are initiated at the PM (Mayor and Pagano, 2007). In clathrin dependent endocytosis, activated receptors accumulate in clathrin-coated pits (CCP), which are pinched off and form clathrin-coated vesicles (CCV) (McNiven and

Thompson, 2006). These vesicles fuse with early endosomes (EEs). Cargo designated to be recycled traffics through the recycling endosome (RE) back to the PM (Maxfield and McGraw, 2004). Cargo designated for degradation remains in the EE, which matures into the late endosome (LE) or multivesicular body (MVB). Internal vesicles are generated at the MVB that remove the active receptors from the cytoplasm and stop signalling events (Katzmann et al., 2002). MVBs finally fuse with lysosomes (LY) and degrade their content (Futter et al., 1996).

1.1.3 Vesicle trafficking has defined stages

Vesicle trafficking is initiated from a donor compartment at specific vesicle formation sites that are enriched in cargo (Figure 1-2A). Cytosolic coat components are recruited to these sites and promote vesicle formation. Coats are supra-molecular assemblies of proteins that cover vesicles. Three main coat complexes can be distinguished in mammalian cells: the clathrin coats, associated with trafficking between the PM, the TGN and endosomal compartments; the COPI coat which functions in intra-Golgi and Golgi to ER traffic; and the COPII coat that is involved in anterograde trafficking from the ER to the Golgi.

As coats or coat associated proteins recognize sorting signals, their association leads to further concentration of cargo at the vesicle formation site. The addition of further coat components leads to the polymerisation of the coat into a regulatory lattice. This polymerisation deforms flat membrane patches into buds (Figure 1-2B) and ultimately vesicles (Bonifacino and Lippincott-Schwartz, 2003). The neck still connecting the budding vesicle to the donor membrane (Figure 1-2C) is then severed either directly by the action of the coat (Matsuoka et al., 1998) or by accessory proteins like dynamin (McNiven and Thompson, 2006). After abscission from the donor membrane, the newly formed vesicles un-coat (Figure 1-2D). The coat is lost from vesicles either by the direct activity of the coat (Bi et al., 2002) or accessory proteins triggering uncoating (Lafer, 2002). The coat proteins then recycle to the vesicle formation site and participate in the formation of further vesicles.

Motor proteins are recruited to the vesicle and mediate its transport along cytoskeletal structures such as actin fibres or microtubules (Figure 1-2E). This ensures long-distance movement, and may not be essential for short distance traffic.

Long distance docking and target recognition of the vesicle (Figure 1-2F) requires cytosolic proteins called tethers (Sztul and Lupashin, 2006). Tethers are proteins or protein complexes that usually form elongated rod like structures and bind to proteins on both the

vesicle and the target. The proximity generated by tethers is thought to enhance the efficiency of vesicle transport and facilitate the subsequent fusion (Pfeffer, 1999).

The docking (Figure 1-2G) of vesicles to their acceptor membranes requires specific soluble NSF attachment protein receptors (SNAREs) (Jahn and Scheller, 2006). Specific SNAREs are found on both the vesicle and the donor membrane. All these SNAREs have a SNARE motif. Four SNARE motifs associate into a complex of four intertwined parallel α -helices, in with each helix is provided by a different SNARE motif. This complex of extraordinary stability is called a SNAREpin (Weber et al., 1998). The SNAREpin assembly is thought to exert mechanical force on membranes, and thus causes fusion (Figure 1-2H). The fusion leads to the release of the cargo into the lumen of the acceptor compartment. The SNAREpin is then unwound by the combined action of the NEM-sensitive factor (NSF) (Block et al., 1988) and the soluble NSF attachment protein (SNAP) (Clary et al., 1990). The SNAREs and cargo receptor molecules are then recycled (Figure 1-2I) in vesicles to the donor membrane.

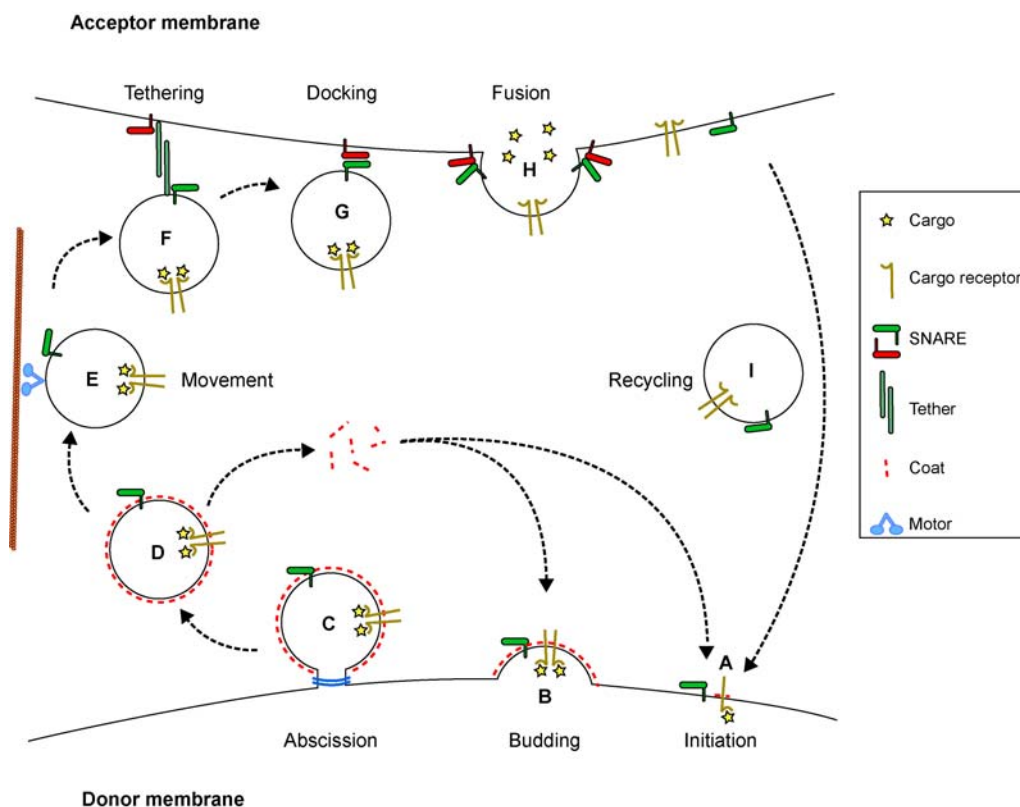


Figure 1-2 Overview of vesicle transport. (A) Initiation of coat assembly at the donor membrane. (B) Budding and (C) abscission of the newly formed vesicle. (D) Uncoating of the vesicle and recycling of coat proteins. (E) Movement of the vesicle along cytoskeletal structures. (F) Tethering of the vesicle to the target membrane. (G) Docking and *trans*-SNARE complex formation. (H) SNAREpin formation driven membrane fusion and cargo release. (I) SNAREs and cargo receptors recycle to the donor compartment. Drawing is not to scale.

1.2 Small GTPases and membrane traffic

1.2.1 The G domain

Small monomeric GTPases belong to the so-called Ras superfamily. The family members, usually about 25 kDa in size, make one of the largest protein families in the human genome. Sequence analysis has revealed about 200 members (Wennerberg et al., 2005). This superfamily is divided into the five major groups Ras, Rho, Ran, Arf and Rab.

The members of this family are characterised by a G domain that binds to guanine nucleotides. This domain is built by six β -strands surrounded by five α -helices (Figure 1-3), a typical conformation for nucleotide-binding domains. The nucleotide-interacting portion of the G domain, the G box, consists of five sequence elements, G1 to G5 (Bourne et al., 1991). Nucleotide binding is mediated by interactions of both the nucleotide base with an N/TKxD motif in G4 and the β - and γ -phosphates with the G1 phosphate-binding loop (P-loop), a GxxxxGKS/T motif. The G domain also coordinates a magnesium ion that is required for binding nucleotides. The DxxGQ motif in G3 is involved in GTP hydrolysis. Specificity for guanine nucleotides is due to an aspartate that forms hydrogen bonds with the guanine ring and hinders binding of adenine by the GTPase (Vetter and Wittinghofer, 2001).

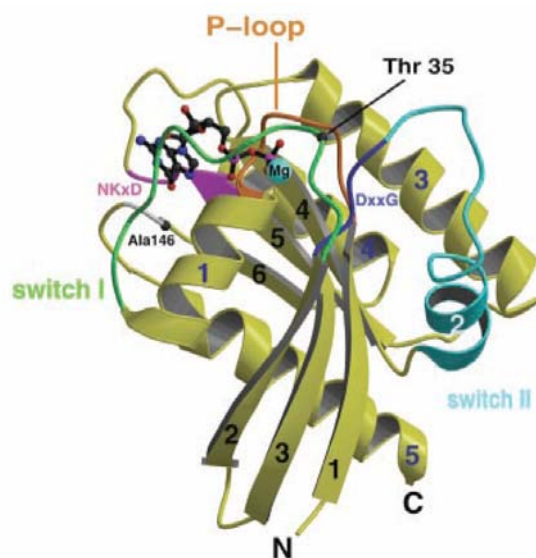


Figure 1-3 The G-domain. Protein in ribbon representation bound to GTP in ball and stick representation. The switch-I region is in green, the switch-II in lavender. Magnesium is represented as a blue sphere. Adapted from Vetter, 2001.

1.2.2 GTPases function as molecular switches

A conserved characteristic of these GTPases is their ability to form stable complexes with both GTP and GDP. Two regions of the G-domain called switch-I and switch-II (Figure 1-3) undergo conformational changes dependent on the state of the bound nucleotide. The ability of small GTPases to exist in two conformations makes them molecular switches (Figure 1-4). In the active, GTP-bound form, two hydrogen bonds from the γ -phosphate are formed to invariant threonine and glycine residues in switch-I and switch-II. These hydrogen bonds are lost when hydrolysis from GTP to GDP occurs and the switch regions relax into the inactive GDP bound conformation. The conformational change therefore works like a loaded spring (Vetter and Wittinghofer, 2001).

To activate the GTPases, GTP is exchanged to GDP by guanine nucleotide exchange factors (GEFs). Even though different domains catalyse nucleotide exchange, they use similar mechanisms. GEFs open the nucleotide-binding cleft by destabilising it. This destabilisation reduces the nucleotide affinity and leads to dissociation of GDP (Vetter and Wittinghofer, 2001). There is no preference which nucleotide will be inserted by the GEF reaction. As the cellular GTP concentration is higher than the concentration of GDP and the interaction of the active GTPases with downstream interacting proteins sequesters them, the equilibrium is shifted into the GDP-to-GTP direction (Cherfils and Chardin, 1999).

GTPase activating proteins (GAPs) stimulate the weak basal GTP hydrolysis activity of the GTPases and thus inactivate them. The mechanism of GAP accelerated GTP hydrolysis will be discussed in more detail later.

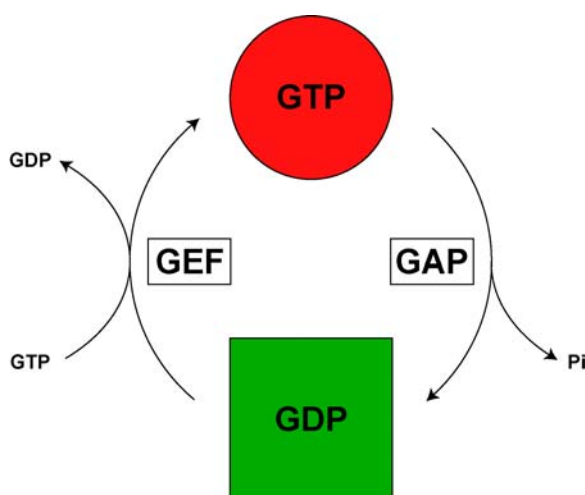


Figure 1-4 The GTPase cycle. GTPases cycle between an active conformation bound to GTP (red) and a inactive conformation bound to GDP (green). Hydrolysis of GTP to GDP is stimulated by GAPs. The exchange of GDP to GTP is catalysed by GEFs.

The downstream interacting proteins of small GTPases, so-called effectors have much higher affinity to the GTPases in their active GTP bound conformation (Vetter and Wittinghofer, 2001). They bind to surfaces of the GTPases including the switch regions. The switch regions also contribute to the specificity of this interaction (Pereira-Leal and Seabra, 2000). When the switch regions change their conformation upon hydrolysis from GTP to GDP, the interaction of the effector with the GTPase is lost.

1.2.3 GTPases in vesicle trafficking

Most tethers and coat subunits are recruited to membranes by the action of small GTPases (Munro, 2002). COPII requires Sar1 to associate with membranes and initiate the coat formation. Sar1 also functions as the timer for coat release, as a subunit of the coat also functions as a GAP for Sar1 (Bi et al., 2002). COPI on the other hands requires the small GTPase ARF (Serafini et al., 1991) that is closely related to Sar1. One group of Golgi associated tethers and structural elements termed Golgins (Short et al., 2005) have a so-called GRIP domain (Munro and Nichols, 1999) that specifically binds to small GTPases of the Arl family (Panic et al., 2003). The related GRAB domain present in another group of golgins binds Arf1 (Gillingham et al., 2004). The exocyst, a huge multi subunit complex involved in exocytosis (Short and Barr, 2002), requires Rho and CDC42 for its proper spatial regulation (Guo et al., 2001; Zhang et al., 2001).

1.2.4 Rab GTPases

Many proteins or protein complexes involved in membrane trafficking require a member of the Rab family of small GTPases to be recruited to specific membranes. Rab GTPases were first identified as **Ras-like from brain**, (Gallwitz et al., 1983) and soon after shown to be involved in trafficking (Salminen and Novick, 1987).

While coat proteins and SNARE machineries have only diversified modestly in the course of eukaryotic evolution, the Rab GTPase family expanded substantially during the specialization of the endomembrane system (Gurkan et al., 2007). With more than 60 members (Wennerberg et al., 2005) in the human genome, the Rab family is the largest group of the Ras superfamily. *S.cerevisiae* has only eleven Rabs (Lazar et al., 1997) called Ypts (yeast protein transport). However, alignments of Rab and Ypt proteins show a high degree of conservation, and human and yeast Rab proteins can be grouped according to their segregation pattern in a phylogenetic tree (Figure 1-5). These groups that reflect similarity of sequence also represent shared ancestry (Pereira-Leal and Seabra, 2001).

Most Rabs that co-segregate in the phylogenetic tree share similar sub-cellular localisation and function. Ypt51/52/53 regulates endocytic events in yeast (Lazar et al., 1997). It falls into one group with the mammalian Rabs Rab5a,b,c, Rab22a and Rab31 (Figure 1-5). These Rabs regulate endocytosis in mammalian cells (Zerial and McBride, 2001). Other Rabs of this group like Rab17, which are less closely related to Ypt51/52/53, are also involved in regulation of endosome associated trafficking (Zacchi et al., 1998). This suggests that specialised Rabs for different sorting events arose early in evolution. The increase in number of regulatory proteins reflects the increased complexity of higher eukaryotic cells. On the other hand, yeast Ypt1 is in a group with only two almost identical isoforms, Rab1a and Rab1b. This suggests that ER to Golgi trafficking, which is regulated by these Rabs was not subject to diversification throughout evolution.

Some groups in this phylogenetic tree, like the Rab3/Rab27 group that is involved in regulated secretion (Zerial and McBride, 2001) do not have a yeast member. This suggests that these Rabs regulate trafficking events that are specific for higher eukaryotic cells.

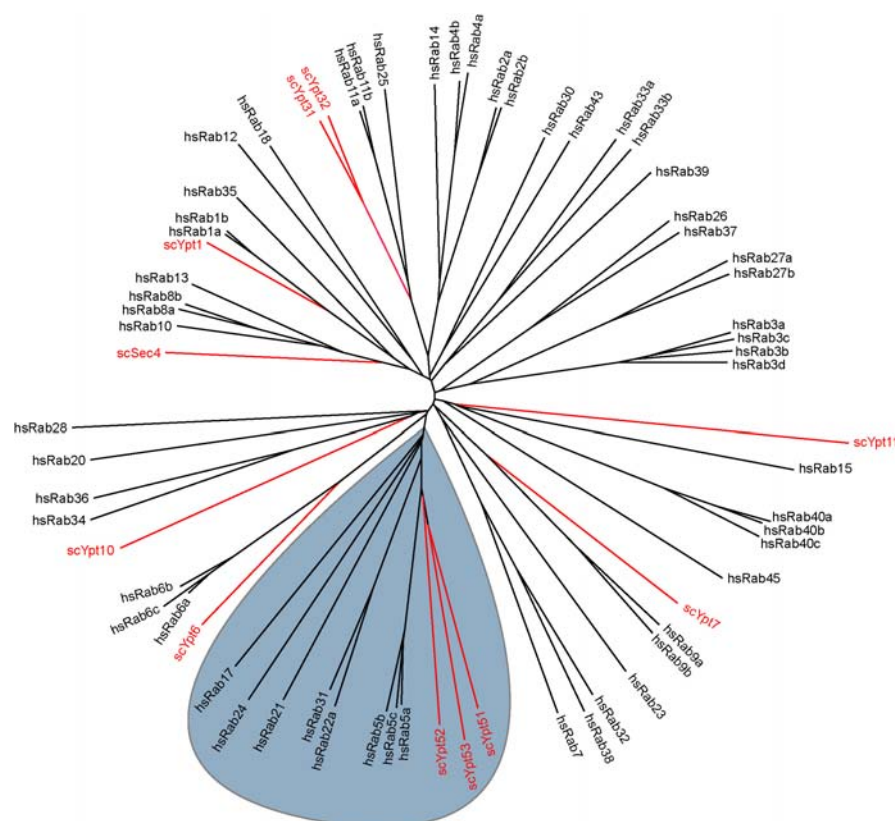


Figure 1-5 A phylogenetic tree of human and *S.cerevisiae* Rabs. *S.cerevisiae* Ypt proteins are depicted in red for easier discrimination. A blue background highlights one group of Rabs regulating endocytosis that are related to Ypt51/52/53. Length of lines represents similarity of amino acid sequence.

Many Rabs have isoforms with almost identical sequences. The differences between these isoforms are so far poorly studied. Most probably they regulate the same process redundantly or are tissue or developmental stage specific in their expression. Without isoforms, approximately 40 independent Rab proteins with a distinct function are found in the human genome.

1.2.5 Rabs define membrane compartments

Rabs localise to specific sub-cellular compartments (Figure 1-6) (Zerial and McBride, 2001). Every membrane compartment and trafficking step necessary to make a functioning cell is identified by a specific set of Rabs.

Rabs tightly associate to membranes with two highly hydrophobic geranyl-geranyl moieties that are covalently linked to cysteine residues at their very C-terminus. Active Rabs recruit effectors to specific membranes (Grosshans et al., 2006). Rab effectors can be integral and peripheral membrane proteins as well as cytosolic proteins and complexes. Rabs usually have multiple effectors but most effectors are specific for one Rab. Rabs provide identity to the membrane they are localising to by specifically concentrating these effector molecules (Pfeffer, 2001). This mechanism is not limited to entire organelles, as Rabs also define sub-domains (Pfeffer, 2003). Recycling endosomes for example are characterised by both Rab4 and Rab11 (Figure 1-6).

Rabs define membrane compartments in combination with their effectors. Rab9 for example generates a functional sub-domain on late endosomes (Pfeffer, 2001). Rab9 is involved in the transport of MPRs from late endosomes to the TGN. The tail interacting protein of 47 kDa (TIP47) is a Rab9 effector that binds to MPRs. TIP47 preferentially binds to MPRs in the presence of Rab9. Its interaction with Rab9 enhances the affinity of TIP47 for MPRs (Carroll et al., 2001). Active Rab9 therefore generates membrane domain enriched in MPRs and TIP47 designated to traffic to the TGN.

Rabs can act in combination with specific lipids, mostly phosphoinositides. Phosphoinositides are generated by phosphorylation of PtdIns on specific inositol ring positions by PtdIns-kinases (Behnia and Munro, 2005). The Rab5 effector EEA1 for example requires both PtdIns(3)P and Rab5 to be recruited to early endosomes (Simonsen et al., 1998).

Hypervariable sequences at the C-terminus of Rabs were previously thought to confer the membrane specificity (Chavrier et al., 1991). More recent findings challenge this view and show that a cooperative mode of Rabs and their effectors (Aivazian et al., 2006)

ensures proper membrane localisation. This suggests a model in which effectors need Rabs as much as Rabs need their effectors for specific localization.

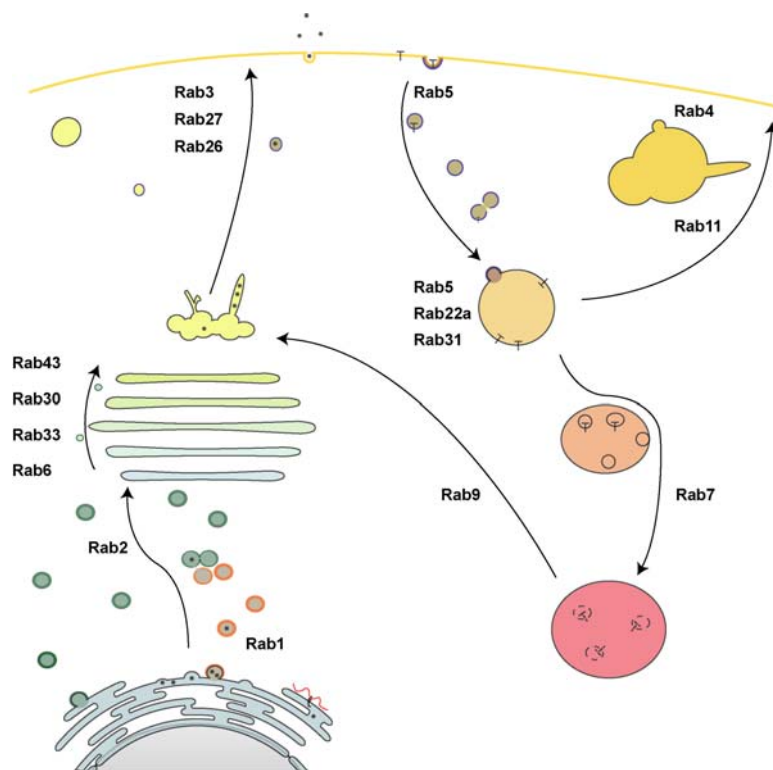


Figure 1-6 Rab proteins provide membrane identity. A selection of human Rab proteins linked to processes and organelles they regulate is depicted. The figure layout is based on Figure 1-1. Drawings are not to scale.

1.2.6 Rabs modulate multiple steps in vesicular trafficking

Rabs are involved in the regulation of multiple steps of vesicle trafficking. Their effectors exert various functions at these steps. In general, five distinct levels of trafficking have been shown to require Rabs (Segev, 2001).

First, Rabs are involved at the step of vesicles formation and cargo or SNARE recruitment. The Rab1 effector p115 programs budding COPII vesicles by the incorporation of SNAREs necessary for their subsequent docking and fusion (Allan et al., 2000). Rab5 as another example is required for sequestration of activated receptors into CCPs prior to CCVs abscission (McLauchlan et al., 1998).

Second, a role for Rabs in vesicle motility is suggested by several findings (Hammer and Wu, 2002). Rab6 interacts with the dynein/ dynactin complex and thus links vesicles to microtubules (Short et al., 2002). Melanosome localised Rab27 binds Melanophilin, which in turns binds myosin Va. This generates a tripartite protein complex that is required for melanosome motility along the actin skeleton (Fukuda et al., 2002).

Third, Rabs are proposed to be involved in active membrane remodelling processes. Rab5 and its effector EEA1 are proposed to interact with PI(3)-kinase, which generates PtdIns(3)P (Christoforidis et al., 1999b; Simonsen et al., 1998). The Rab5 effector Rabenosyn-5 binds to the Rab5 GEF Rabex-5 and is recruited by PtdIns(3)P as well (Nielsen et al., 2000). Thus a positive feedback loop is formed that generates more active Rab5 and a local increase of PtdIns(3)P.

Fourth, Rabs are involved in long range docking of vesicles to their target by tethering. The tether p115 is recruited onto ER derived vesicles by Rab1 and interacts with the Golgi associated proteins GM130 and Giantin (Short et al., 2005). Furthermore, p115 is necessary for clustering of COPII vesicles to form the ERGIC (Alvarez et al., 1999). The Rab5 effector EEA1 is involved in homotypic early endosome docking and fusion (Christoforidis et al., 1999a; Mills et al., 1998; Simonsen et al., 1998). It is also required for the heterotypic fusion of early endosomes with CCVs (Rubino et al., 2000).

Fifth, evidence is pointing to a role for Rabs in the event of membrane fusion by regulating the SNAREpin formation. Rabs themselves appear not to be directly involved in the regulation of SNARE function. However, in numerous cases, for example in the case of Rab1 (Allan et al., 2000) or Rab5 (McBride et al., 1999; Simonsen et al., 1999), their effectors interact with and modulate the activity of SNAREs.

1.2.7 The classic Rab Cycle

The regulation of Rabs is a process that involves multiple accessory and regulatory proteins. It is called the Rab cycle (Goody et al., 2005; Seabra and Wasmeier, 2004).

Due to their highly hydrophobic geranyl-geranyl moieties, Rabs need a special chaperone called GDP dissociation inhibitor (GDI) (Sasaki et al., 1990) to be extracted from membranes and shuttle through the cytoplasm (Figure 1-7). GDI only associates with Rabs that are both prenylated and bound to GDP (Rak et al., 2003). This ensures that only inactive Rabs are extracted from membranes. GDI binds to the Rab and also provides a binding platform and a cavity to shield both prenyl groups from the cytoplasm (Pylypenko et al., 2006).

To release Rabs from GDI and insert them into membranes additional factors called GDI displacement factors (GDF) are required (Figure 1-7) (Wu et al., 2007). Only few of these are characterised so far, called either Ypt interacting proteins (YIP) (Sivars et al., 2003) or prenylated Rab acceptors (PRA) (Hutt et al., 2000). These transmembrane proteins probably form a pore that facilitates the insertion of Rabs into the membrane. The kinetics of

the insertion and extraction of prenylated Rabs from membranes by GDI are thermodynamically similar (Pylypenko et al., 2006). To prevent recurrent membrane extraction the Rab must therefore become bound to GTP (Soldati et al., 1994).

This exchange of GDP to GTP is mediated by GEFs (Figure 1-7). The substrate specificity of GEFs is crucial for the fidelity of membrane association of Rabs. GEFs are so far only poorly characterised. In contrast to other regulatory proteins GEFs do not share a common domain. Proteins with a VPS9 domain mediate nucleotide exchange in Rab5 related Rabs (Delprato et al., 2004). Sec2, which is the GEF for Sec4, catalyses the exchange reaction with a coiled coil (Dong et al., 2007). The transport protein particle complex I (TRAPPI) (Sacher et al., 1998) consists of multiple sub-units and has GEF activity towards YPT1. The addition of three further subunits changes both its localization and properties; the complex is then called TRAPPII and shows GEF activity towards YPT31 (Jones et al., 2000; Wang et al., 2000).

The affinity of the Rab for its effector molecules rises by several orders of magnitude when it is in to the active conformation bound to GTP. The active Rab therefore recruits specific effector molecules to the membrane (Figure 1-7), which fulfil their downstream functions at the membrane specified by the Rab. The Rab-effector complex is dynamically regulated. When a vesicle fuses with its target membrane, the Rab has to be inactivated. As active Rabs define the identity of a membrane, this termination of their active state is mandatory to maintain the identity of the acceptor membrane after fusion with vesicles of different identity.

To inactivate Rabs GAPs are needed (Figure 1-7). When the Rab is inactivated by the GAP, its affinity for its effectors is strongly reduced. The effectors relocate to the cytoplasm and recycle to the pool of GTP bound Rab. The inactive Rab is then extracted from the membrane by GDI. GDI shuttles the prenylated Rab through the cytoplasm and the Rab is reinserted in the donor membrane (Figure 1-7).

1.3 RabGAPs regulate GTP hydrolysis by Rabs

GAPs are key regulators of this classic Rab cycle. They regulate the lifetime of GTP bound Rab, and therefore regulate and maintain the identity of membranes conferred by Rabs. RabGAPs were first identified in *S. cerevisiae* (Strom et al., 1993), a decade after the first discovery of Rab GTPases (Gallwitz et al., 1983). A biochemical activity, which accelerated the GTP hydrolysis by Ypt6, was found in extracts generated by multi-copy plasmid based overexpression. Analysis of the plasmid revealed a gene named GAP for Ypt6 (GYP6) that encodes a 458 aa protein. After the identification of further Ypt GAPs (Albert and Gallwitz, 1999; Vollmer and Gallwitz, 1995; Vollmer et al., 1999) it was noted that these proteins

share a common protein domain. Due to its sequence similarity with the human oncogene *Tre2*, with *S.cerevisiae* *Bub2*, and *S.pombe* *Cdc16* (Neuwald, 1997) it was called a TBC domain. An arginine in the TBC domain is required to catalyse GTP hydrolysis similar to RasGAP (Albert et al., 1999). Human RabGAPs are TBC domain proteins as well (Cuif et al., 1999; Lanzetti et al., 2000).

Bioinformatic analysis showed that the TBC domain is comprised of six sequence motifs termed A to F (Neuwald, 1997). Three of these motifs contain invariant so-called signature sequences: RxxxW in motif A; IxxDxxR in motif B; and YxQ in motif C. The sequence motifs A to F are part of the catalytically active region of the Ypt GAPs (Albert et al., 1999). The arginine required for hydrolysis is found in the signature sequence in motif B. The overall structure of the TBC domain is fully α -helical, and adopts the shape of the letter “V” (Rak et al., 2000). Invariant hydrophobic amino acids, which are contributed by multiple α -helices, form the core of the structure. The sequence motifs B and C are located in a rectangular groove inside the V. Co-crystallisation of yeast Gyp1 with human Rab33b showed that the Rab is bound in this rectangular groove (Pan et al., 2006).

The TBC domain makes contact with the Rab via multiple α -helices. They mainly interact with both switch regions and the P-loop. This explains the nucleotide specificity and the substrate selectivity of RabGAPs. Mutations of residues contributing to this interaction decrease GAP activity. The specific recognition and interaction with target Rabs is therefore mandatory for specific acceleration of GTP hydrolysis. The interaction with the GAP is needed to position the Rab correctly relation to the GAP as the B and C motifs of the TBC domain form a loop that extends into the nucleotide-binding cleft of the Rab.

1.3.2 The GTP hydrolysis reaction

The GTP hydrolysis reaction cleaves the high-energy phosphoanhydride bond between the γ - and the β -phosphate. This leads to the conversion of GTP to GDP and inorganic phosphate (P_i) (Wittinghofer, 2006). After this reaction the two switch regions can no longer form hydrogen bonds to the γ -phosphate and thus change their conformation.

The mechanism by which TBC domain proteins accelerate the GTP hydrolysis by Rabs was believed to be similar to the mechanism described for Ras. Here an arginine finger provided in *trans* by the GAP and a conserved glutamine provided by Ras in *cis* mediate GTP hydrolysis (Wittinghofer et al., 1997). However, recent co-crystallisation of a TBC domain with a Rab showed that a variation of this mechanism is used by RabGAPs (Pan et

al., 2006). Both the arginine and the glutamine are provided by the GAP in *trans* (Figure 1-8). The conserved glutamine provided by the Rab mediates interaction with the backbone carbonyl of a tyrosine and the amino group of the glutamine provided by the TBC domain. This interaction is crucial to position the glutamine of the GAP properly.

This *trans* glutamine of the TBC domain coordinates a water molecule for a nucleophilic attack on the γ -phosphate (Feuerstein et al., 1989). It is therefore equivalent to the *cis* glutamine in other GTPases (Vetter and Wittinghofer, 2001). The nucleophilic attack leads to a shift of negative charge from the γ - to the β -phosphate (Figure 1-8). This charge distribution is closer to GDP than to GTP (Allin et al., 2001). The accumulating negative charge is compensated by the positively charged arginine provided by the GAP in *trans* (Figure 1-8). It was shown that this charge compensation by the arginine reduces the activation energy for the β - γ bond cleavage (Kotting et al., 2006). This arginine therefore helps to destabilise the bond between the γ - and the β -phosphate. It also promotes the formation of a dissociative transition state with a penta-coordinated phosphate group (Scheffzek et al., 1998). The P_i released during GTP hydrolysis can either fuse back to form GTP again or become the leaving group. Therefore the release of P_i is the rate-limiting step of the GTP hydrolysis reaction (Allin et al., 2001). Structures of Ras and its GAP show that the GAP covers the leaving group. The GAP is therefore thought to block P_i release (Scheffzek et al., 1997; Scheffzek et al., 1998). These structures suggest that the GAP acts as the rate-limiting factor in GAP activated GTP hydrolysis.

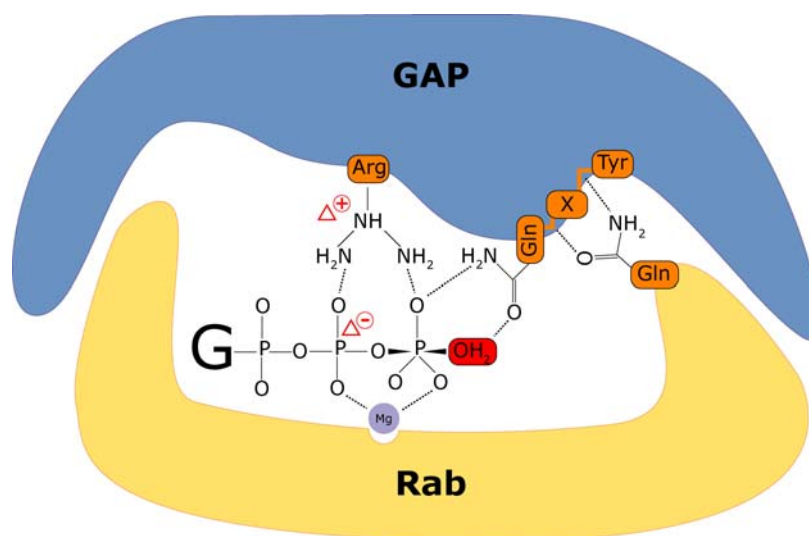


Figure 1-8 Rab-GAP mediated GTP hydrolysis. This schematic depicts the probable transition state in TBC domain activated GTP hydrolysis. The amino acids involved directly or indirectly in catalysis are shown in orange. They are labelled with the common three letter abbreviations. The lavender sphere indicates the magnesium ion required for nucleotide coordination by the Rab. The

letter “G” indicates the guanine nucleotide. Attacking water molecule in red. Solid lines indicate bonds dashed lines indicate hydrogen bonds or ionic interactions. Drawing is not to scale.

1.3.3 Open questions about Rab and their GAPs

Many of the steps and factors involved in vesicle trafficking have been analysed in great detail. Both the vesicle formation by coats (Matsuoka et al., 1998) and SNARE mediated fusion (Weber et al., 1998) have been reconstituted *in vitro*. Much less is known about the other steps in vesicle trafficking. Rab GTPases and their effectors regulate most of these steps. The sheer amount of Rabs and their effectors has made the understanding of these steps so difficult. A better understanding of their regulation will help to gain further insight into this complex network.

GAPs for Ras and Rho as prototypes for the Ras superfamily of monomeric GTPases have been studied in great detail (Bos et al., 2007). On the other hand, little is known about the GAPs of Rabs. Multiple GAPs for Rab GTPases have been identified by database research (Bernards, 2003). The attempt to match pairs of Rabs and their GAPs was only made in *S. cerevisiae*. In the human system so far only very few TBC domain proteins have been described or assigned to the Rabs they regulate.

Work on RabGAPs in yeast led to the idea that these proteins are promiscuous in recognizing their substrate (Albert and Gallwitz, 1999). This is a very puzzling idea since GAPs bind the switch regions contributing to the specificity of effector binding (Pereira-Leal and Seabra, 2000). They furthermore regulate Rabs that regulate specific events in membrane trafficking.

This work establishes the tools necessary to match pairs of human Rabs and GAPs and investigate the specificity of RabGAP substrate recognition. It also provides new insights into the trafficking processes they regulate.

2 Regulation of endocytosis by RabGAP-5

2.1 Aim of this Work

Endocytosis is a highly controlled process that involves many conserved families of proteins. One of the key players in this tightly orchestrated network of proteins is the family of Rab GTPases (Miaczynska and Zerial, 2002; Zerial and McBride, 2001). Rabs coordinate many steps of endocytic transport (Markgraf et al., 2007). One of the key Rabs regulating endocytosis and trafficking events at early endosomes is Rab5 (Zerial and McBride, 2001).

GEFs and GAPs regulate the state of activity of Rabs. To find RabGAPs involved in the regulation of endocytosis, and for Rab5 in particular, the complete GAP family first had to be identified in the human genome. In a second step a system to identify the human GAP for Rab5 had to be established. Finally, this regulation had to be verified in cells by studying endocytic trafficking.

2.2 Results

2.2.1 Bioinformatic identification and characterisation of human RabGAPs

It was known from work in yeast that RabGAPs contain a TBC domain (Albert et al., 1999; Strom et al., 1993; Vollmer et al., 1999). Human RabGAPs were known to contain TBC domains as well (Cuif et al., 1999; Lanzetti et al., 2004) but only very few members of this protein family were identified so far. The human genome was therefore searched for proteins containing a TBC domain using the online Basic Local Alignment Search Tool (BLAST) (<http://www.ncbi.nlm.nih.gov/blast/>). After eliminating splicing variants 40 proteins containing a TBC domain remained. The sequences of these proteins were aligned using the Vector NTI® software and further analysed (Figure 2-1).

Even though these proteins showed enough similarity in their TBC domains for the algorithms to identify their relatedness, the TBC domain and the signature sequence IxxDxxR (T/S) in motif B are mutable. The arginine in the signature sequence that is involved in GTP hydrolysis is highly conserved, but not invariant. In some proteins, for example in USP6, part of the human *trc* oncogene, the arginine is shifted one position towards the N-terminus. Others like the TBC1D3 group showed no arginine in the catalytic motif. Some proteins like TBC1D7 have a TBC domain that lacks the signature sequence in motif B.

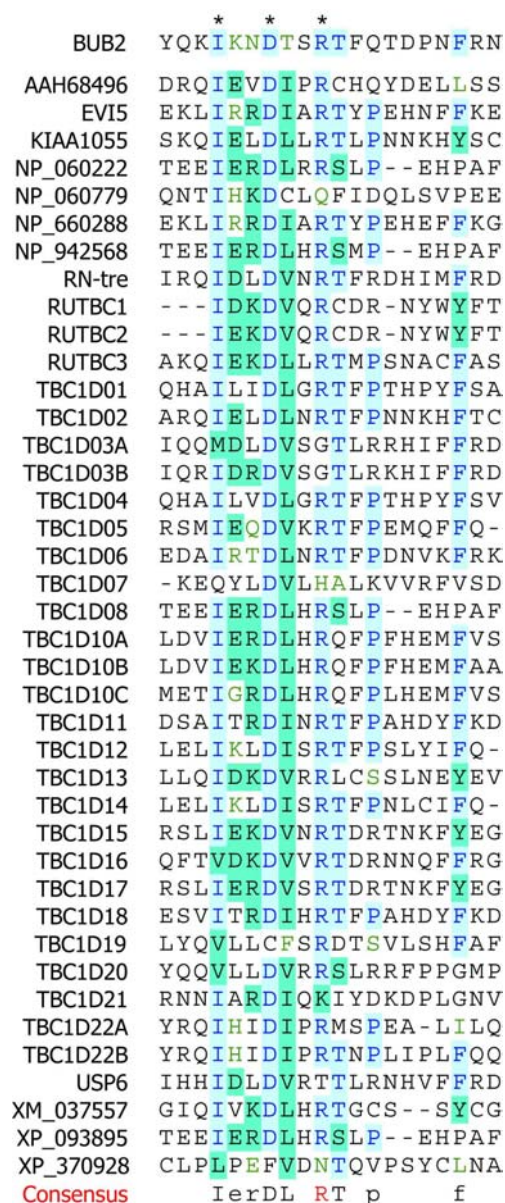


Figure 2-1 Sequence alignment of human TBC domain containing proteins. Only a part of the B motif with the signature sequence (IxxDxxR) containing the catalytic arginine is shown here. *S.Cerevisiae* BUB2 is added as a founding member of the TBC domain. In the consensus sequence the arginine involved in GTP hydrolysis is depicted in red.

Most human TBC domain proteins are multi-domain proteins. The smallest proteins of this family only contain a TBC domain and have molecular weights between 30 and 40 kDa like TBC1D20. The largest TBC domain proteins reach up to 160 kDa (e.g. USP6). The TBC domain can be situated at any position in the protein (Figure 2-2). Many different domains were found in RabGAPs, including phosphotyrosine-binding PTB domains; lipid binding PH domains; GRAM domains that are found in membrane associated phosphatases; ubiquitin ligase domains; SH3 domains involved in receptor tyrosine kinase signalling. Five examples of these diverse domain structures are shown in Figure 2-2.

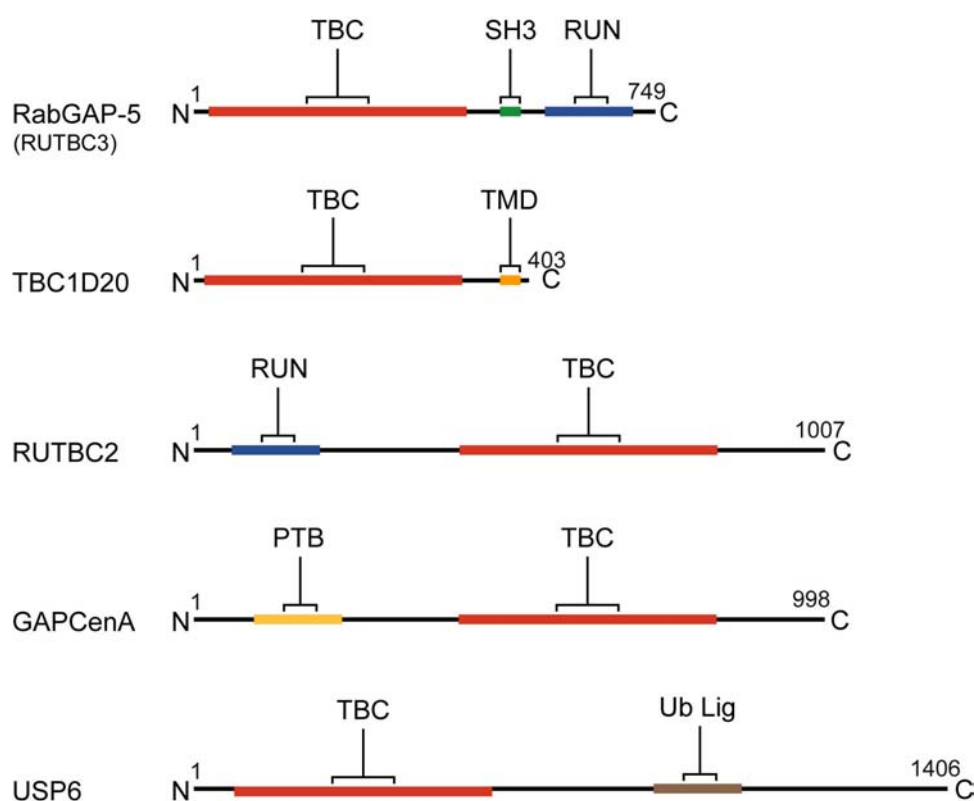


Figure 2-2 Schematic representation of the domain structure of selected TBC domain proteins. Domains are indicated by the common abbreviations. Drawings are not to scale.

2.2.2 Cloning of human RabGAPs

After their bioinformatic identification, the RabGAPs were amplified from human cDNA libraries using PCR technology. The libraries used were either commercially available libraries generated from whole Foetus, Testis, Liver or Kidney, or were generated from mRNA purified from HeLa L cells.

As a general strategy a mixture of these libraries was used as a source. PCR reactions were carried out using a nested PCR method described in (5.3.6). After excision of bands of the appropriate size from agarose gels, the DNA was integrated into a parental pCRIITOP Vector. All inserts were verified by DNA sequencing and subsequently sub-cloned into mammalian and yeast expression vectors.

2.2.3 Yeast two-hybrid screening to identify RabGAPs regulating endocytosis

To identify a GAP for Rab5 the yeast two-hybrid technique was used. In a reverse screening system all TBC-domain proteins were tested against all human Rabs. All Rabs were sub-cloned into the pGBT9 vector, which carries the GAL4 DNA binding domain. The TBC domain proteins were sub-cloned into the pACT2 vector, which contributes the GAL4 activation domain to the synthetic transcription factor. Competent yeast cells were

transfected with both plasmids and plated onto selective media to select for co-transfection. After three days 5 independent colonies were transferred to quadruple dropout medium (QDO) to select for growth on medium lacking histidine and adenine as a readout of potential interactions.

When the GAPs were tested against wild-type Rabs no specific signals were obtained. This was due to the fact that the interaction of a GAP and its target GTPase is transient (Allin et al., 2001) and is lost after GTP hydrolysis has occurred (Albert et al., 1999).

A conserved glutamine of all Rabs was therefore mutated to leucine to generate hydrolysis deficient Rabs that are restricted to their GTP bound conformation (Scheffzek et al., 1997). Each TBC domain protein was then tested against these Q-L Rabs. This approach identified several Rab- RabGAP interactions. Out of these only the RUN- and TBC-domain containing protein 3 interacted with Rab5^{Q79L}. It also interacted with Rab22a^{Q64L} and Rab31^{Q65L} (Figure 2-3A) in this assay. The phylogenetic tree of Rabs (Figure 1-5) shows that these Rabs form a subfamily. This suggests that some, but not full specificity was gained using this approach. It led to the speculation that the introduction of the hydrophobic leucine in the Rabs prevented the correct insertion of the arginine finger of the GAP into the active site. This steric hindrance probably allowed the interaction of the GAP with several closely related Rabs.

To overcome this steric hindrance, the arginine in the TBC domain was replaced by alanine. Each R-A mutant GAP was then tested against all Q-L Rabs. Again, several Rab- RabGAP pairs were identified. Out of all RabGAPs tested, only the RUN- and TBC-domain containing protein 3^{R165A} interacted with Rab5^{Q79L} (Figure 2-3B). The interaction was stronger than in the previous experiments. In this assay the RUN- and TBC-domain containing protein 3 no longer showed an interaction with Rab22a^{Q64L} and Rab31^{Q65L}. Therefore it was referred to as RabGAP-5 to conform to the naming of the Rab5 exchange factor Rabex-5 (Horiuchi et al., 1997).

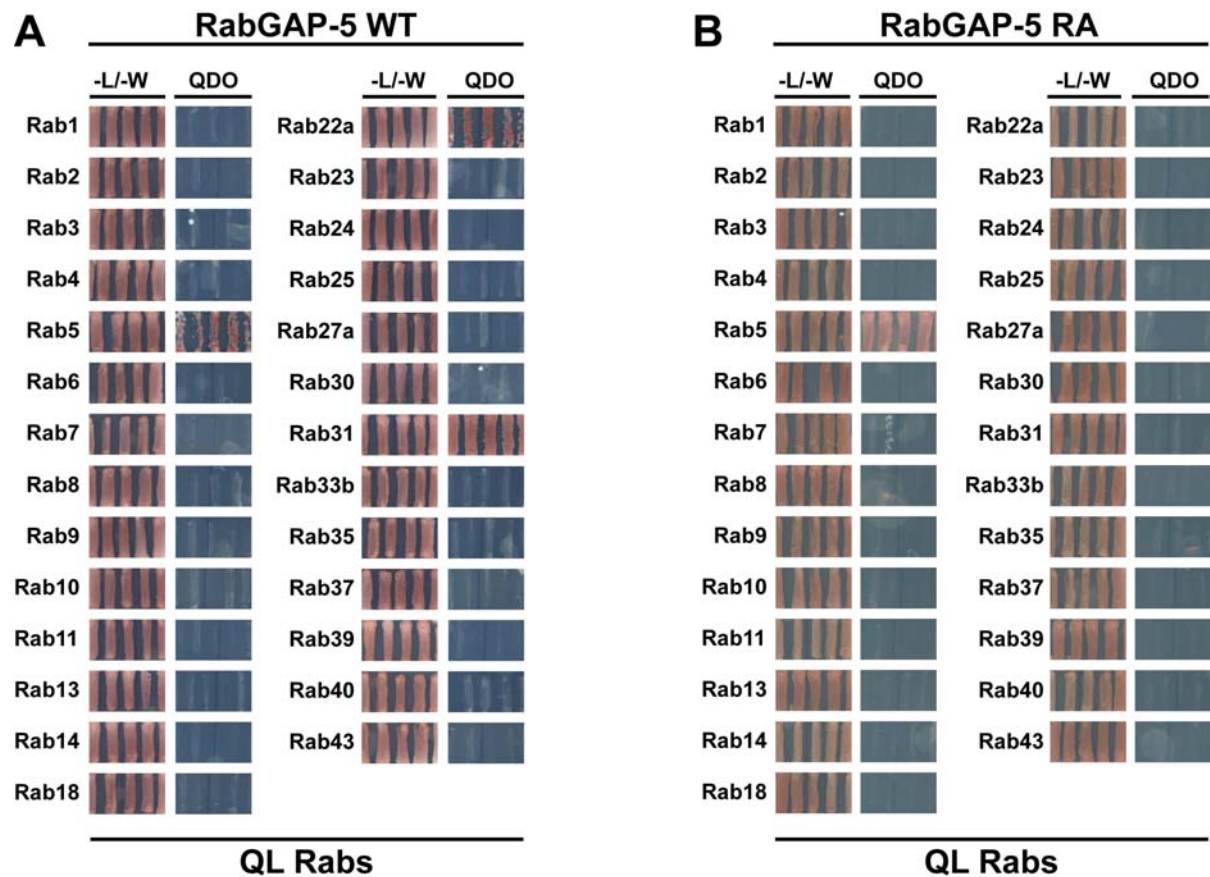


Figure 2-3 A system with two mutations is used for screening GAPs against Rabs. Five independent colonies were tested on SC-LW and QDO. Growth on QDO indicates an interaction between the two proteins. (A) Wild-type RabGAP-5 was tested against all human Rabs locked in their GTP bound state by introduction of Q-L point mutations. On selective QDO medium growth with Rab5^{Q79L}, Rab22a^{Q64L} and Rab31^{Q65L} was observed. (B) RabGAP-5^{R165A} was tested against a library of human Rabs locked in their GTP bound state. In this double mutant approach, RabGAP-5^{R165A} only interacted with Rab5^{Q79L}.

Conformation specific Rab5 mutants were then used to confirm that the interaction between RabGAP-5 and Rab5 is dependent on the nucleotide state of Rab5 (Figure 2-4).

When RabGAP-5 was tested against the Rab5 mutants the interaction was strongest with Rab5^{Q79L} and RabGAP-5^{R165A}. The interaction was weaker with Rab5^{WT} and RabGAP-5^{R165A}. When both proteins were used as wild-type, no interaction was observed. Further demonstrating specificity, RabGAP-5 did not show any interaction with GDP-locked Rab5^{S20N}.

As a control for the nucleotide state of the mutant Rabs, the Rab5 exchange factor Rabex-5 (Horiuchi et al., 1997) and the Rab5 effector EEA1 (Simonsen et al., 1998) were used. Rabex-5 exclusively interacted with GDP-locked Rab5^{S20N} whereas EEA1 only interacted with the GTP restricted Rab5^{Q79L}.

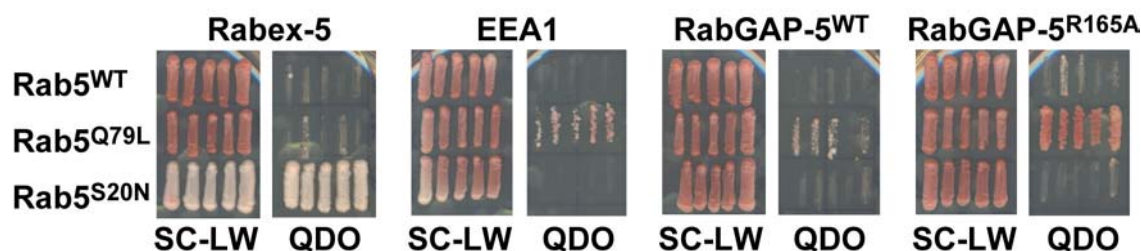


Figure 2-4 Conformation specific mutants of Rab5 identify GEFs, effector molecules and GAPs. Directed two-hybrid tests of 3 different conformations of Rab5 against Rabex-5, EEA1, wild-type RabGAP-5, and RabGAP-5^{R165A}. Five independent colonies were tested on SC-LW and QDO. Growth on QDO indicates an interaction between the two proteins.

Like most other TBC domain proteins, RabGAP-5 is a multi-domain protein (Figure 2-2). The TBC domain is localised at its N-terminus. RabGAP-5 contains an Src-homology-3 (SH3) domain C-terminal of the TBC domain. This domain recognizes proline-rich sequences (Mayer, 2001) and is mostly found in proteins involved in signal transduction. The third domain of RabGAP-5 is a RPIP8, UNC-14 and NESCA (RUN) domain (Callebaut et al., 2001) at its very C-terminus. The RUN domain is present in several proteins that are linked to GTPases of both the Rab and the Rap families. However, its molecular function is not known.

2.2.4 RabGAP-5 specifically activates GTP hydrolysis by Rab5

Next, the ability of RabGAP-5 to accelerate GTP-hydrolysis by Rab5 was tested using purified proteins. To address the question of specificity other Rabs related to Rab5 or reported to be involved in the regulation of endocytosis were tested as well. The Golgi associated Rab6 was used as a negative control.

Rab proteins were generated as 6xHis and GST-tagged recombinant proteins in *E.coli*. They were purified using the 6xHis tag on Ni-NTA columns and dialysed into TBS containing 2mM DTT. RabGAP-5 was purified from *E.coli* tagged with maltose-binding protein (MBP) on the N-terminus. The C-terminus of the protein was tagged with a 6xHis tag. Recombinant RabGAP-5 was purified using the 6xHis tag on Ni-NTA agarose to ensure purification of full-length protein only. It was dialysed into TBS containing 2mM DTT.

RabGAP-5 accelerated GTP-hydrolysis only by the three Rab5 isoforms Rab5a, 5b, and 5c (Figure 2-5A). None of the other Rabs tested showed significant increase of GTP hydrolysis upon addition of RabGAP-5 (Figure 2-5A). Also Rab22a and Rab31, which interacted with RabGAP-5 in the first yeast two-hybrid screen, were not stimulated by the addition of RabGAP-5. The N-terminal TBC-domain including aa 1-451 was purified in the

same way as the full-length protein. When tested under the same conditions, it activated GTP hydrolysis by Rab5 equivalent to the full-length protein (Figure 2-5B). This confirms the idea that the TBC domain acts as a RabGAP domain. The mutation of arginine¹⁶⁵ in the catalytic site to alanine strongly reduced the ability of RabGAP-5 to stimulate GTP-hydrolysis by Rab5 (Figure 2-5C). The constitutive active Rab5^{Q79L} mutant did not hydrolyze GTP and was not stimulated upon addition of wild-type RabGAP-5 (Figure 2-5C).

Taken together, these results indicate that RabGAP-5 is a GAP acting specifically on Rab5. They also support the data obtained by yeast two-hybrid screening using R-A mutant GAPs and Q-L Rabs.

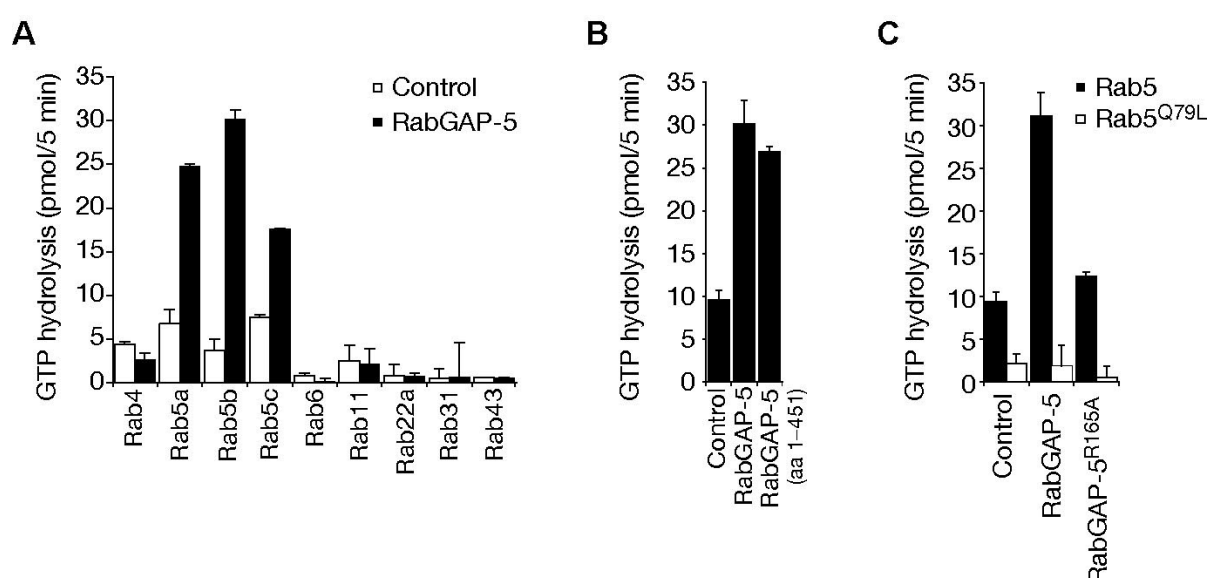


Figure 2-5 GTP- hydrolysis by Rab5 is accelerated by RabGAP-5. Gap assays were carried out using 100pmoles of the Rabs indicated. 10pmoles of RabGAP-5 indicated by filled bars or buffer as indicated by open bars were added. (A) Rabs were tested for their ability to hydrolyse GTP in the presence of buffer or RabGAP-5. (B) The TBC-domain of RabGAP-5 shows similar activity to the full-length protein. (C) RabGAP-5^{R165A} did not stimulate GTP hydrolysis by Rab5. Rab5^{Q79L} is hydrolysis deficient.

2.2.5 RN-tre is a specific Rab43 GAP

Another TBC-domain protein called RN-tre (related to the N-terminus of tre) has previously been reported to have GAP activity towards Rab5 (Lanzetti et al., 2004; Lanzetti et al., 2000). RN-tre was therefore analysed using the reverse yeast two-hybrid screening method.

When wild-type RN-tre was tested against a library of GTP-restricted Rabs no growth of yeast on selective medium was observed. When RN-Tre^{R150A} was tested against a library of GTP-locked Rabs it interacted with Rab43^{Q77L} and Rab30^{Q68L} (Figure 2-6). These two Rabs form a group in the phylogenetic tree of human Rabs (Figure 1-5). While a weak

background signal was seen with Rab4^{Q72L}, no interaction of RN-tre with Rab5^{Q79L} was observed.

Rab30 is known to associate with the Golgi apparatus (de Leeuw et al., 1998) but not with endosomal compartments. Rab43, formerly known as Rab41, was previously only described as a cDNA clone (Guo et al., 2003).

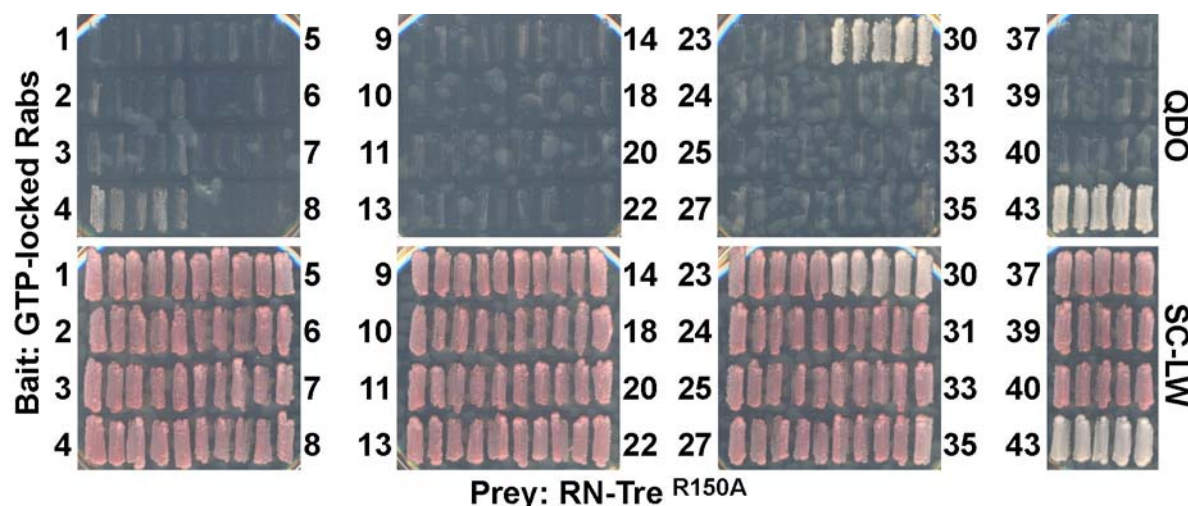


Figure 2-6 RN-tre interacts with Rab30 and Rab43. A weak background signal was observed for Rab4. Five independent colonies were tested on SC-LW and QDO. Growth on QDO indicates an interaction between the two proteins.

To further investigate the interaction of RN-tre with Rab43, recombinant RN-tre was produced as a MBP and 6xHis tagged protein as described for RabGAP-5. In an *in vitro* assay under the same conditions used for RabGAP-5, RN-Tre activated GTP-hydrolysis by Rab43 100-fold over the level observed in the absence of the GAP (Figure 2-7 A). RN-tre also weakly activated GTP-hydrolysis by Rab5, but to a much lesser extent. GTP Hydrolysis by Rab30 was stimulated by RN-tre to a minor extent. Based on the close relationship of Rab43 and Rab30 such a background activity *in vitro* is not surprising. When the catalytic arginine¹⁵⁰ of RN-tre was mutated to alanine, the activity of RN-Tre towards Rab43 was lost (Figure 2-7B). It was therefore concluded that RN-tre acts as a GAP specific for Rab43 and not for Rab5.

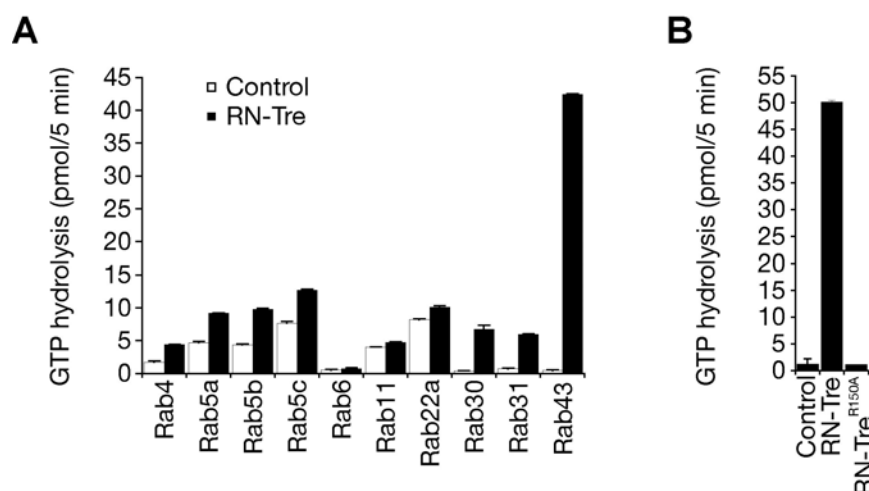


Figure 2-7 RN-tre specifically activates GTP hydrolysis by Rab43. GAP assays were carried out using 100pmoles of the Rabs indicated. 10pmoles of RN-tre indicated by filled bars or buffer as indicated by open bars were added. (A) Rabs were tested for their ability to hydrolyse GTP in the presence of buffer or RN-tre. (B) RN-tre^{R150A} was not able to stimulate hydrolysis by Rab43.

2.2.6 RabGAP-5 redistributes Rab5 effectors *in vivo*

If RabGAP-5 acts as a GAP for Rab5 *in vivo*, then overexpression of the protein should redistribute Rab5 effectors such as EEA1 (Mu et al., 1995) to the cytosol.

To localise to the early endosome, EEA1 requires both active Rab5 and PtdIns(3)P (Lawe et al., 2000; Simonsen et al., 1998). Neither factor in isolation is sufficient to localise EEA1 to early endosomes. If RabGAP-5 functions as a Rab5 specific GAP *in vivo* and inactivates Rab5, EEA1 would be lost from early endosomes.

Consistent with this prediction, the expression of full-length myc-epitope tagged RabGAP-5 in HeLa cells resulted in the loss of EEA1 from punctate endosomal structures (Figure 2-8). The same was true for expression of the N-terminal TBC domain ranging from aa 1-451 (Figure 2-8). A faint staining of EEA1 throughout the cytoplasm was observed in both cases. Expression of the C-terminal SH3 and RUN domain containing part of RabGAP-5 did not redistribute EEA1 (Figure 2-8). This indicates that EEA1 is lost from early endosomes as a result of the expression of the TBC domain of RabGAP-5. Expression of full-length inactive RabGAP-5^{R165A} did not have an effect on the distribution of EEA1 (Figure 2-8). This suggests that the redistribution of EEA1 depends on the catalytic inactivation of Rab5 by RabGAP-5. These data show that RabGAP-5 acts as a GAP for Rab5 *in vivo*.

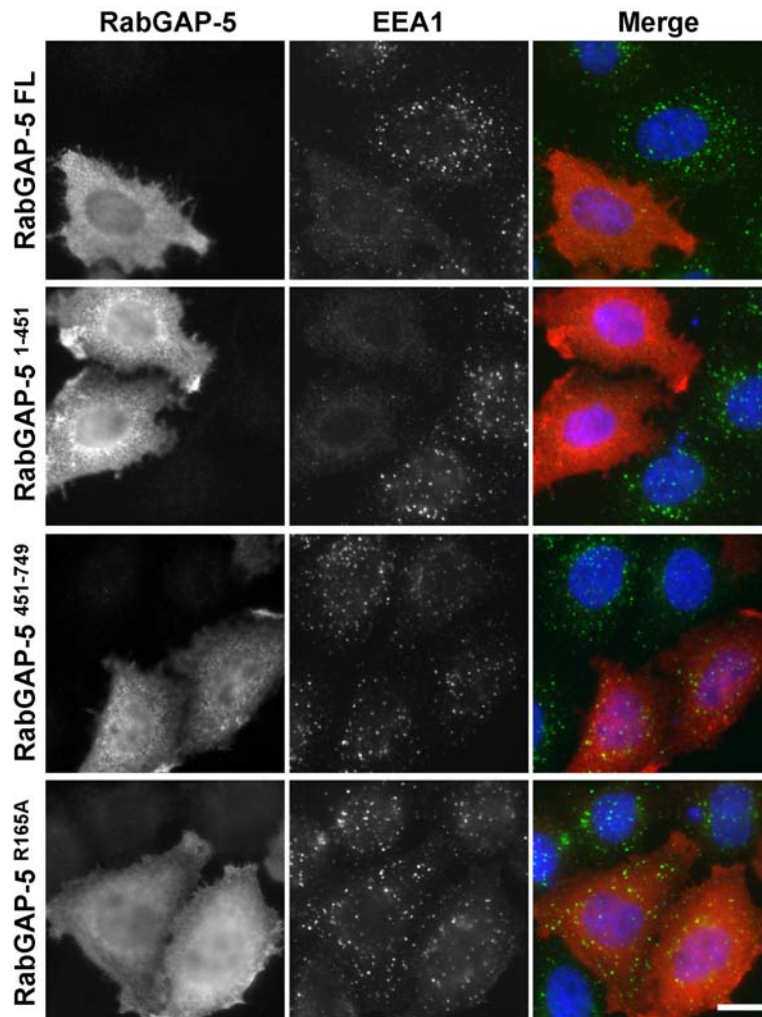


Figure 2-8 RabGAP-5 redistributes EEA1. 24 hours after transfection with myc-epitope tagged full-length wild-type RabGAP-5, truncation constructs or RabGAP-5^{R165A} HeLa cells were fixed and stained with antibodies against the Myc epitope (red) and EEA1 (green). The bar indicates 10 μ m.

If RabGAP-5 is a specific GAP for Rab5, then organelles independent of Rab5 for their formation and function will not be affected by expression of RabGAP-5.

No effect of RabGAP-5 expression was observed on lysosomes (Figure 2-9A) stained with antibodies against the lysosomal protein LAMP1 (Rohrer et al., 1996). The Golgi apparatus stained with antibodies against the *cis*-Golgi marker GM130 (Nakamura et al., 1995) was not affected by expression of RabGAP-5 as well (Figure 2-9B).

This suggests that EEA1 is lost from early endosomes due to the specific inactivation of Rab5 by RabGAP-5. Non-specific side effects of RabGAP-5 expression on vesicle trafficking in general or inactivation of other Rab GTPases appear unlikely, as Rab5 independent organelles like lysosomes and the Golgi remained unaffected.

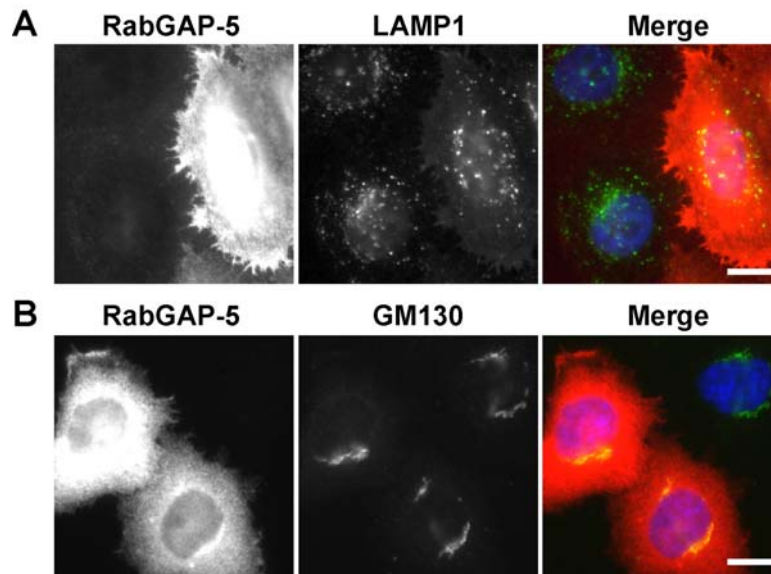


Figure 2-9 RabGAP-5 expression does not affect Rab5 independent organelles. HeLa cells were transfected with myc-epitope tagged RabGAP-5 for 24h. The cells were then fixed and stained with for the Myc epitope (red) and (A) LAMP1 (green) or (B) GM130 (green) respectively. Bars indicate 10 μ m.

2.2.7 RabGAP-5 causes redistribution of Rab5

To investigate the inactivation of Rab5 by RabGAP-5, the fate of GFP-tagged Rab5 was followed.

Wild-type Rab5 localized to early endosomes stained with EEA1 (Figure 2-10A). Expression of constitutive active Rab5^{Q79L} caused the formation of enlarged endosomes (Figure 2-10A) as previously reported (Stenmark et al., 1994). Surprisingly, the GDP restricted Rab5^{S34N} predominantly localized to the Golgi apparatus (Figure 2-10A). Co-expression of myc-epitope tagged wild-type RabGAP-5 with GFP-tagged wild-type Rab5 relocated Rab5 to the Golgi apparatus (Figure 2-10B) similar to the inactive Rab5^{S34N} mutant (Figure 2-10A). This effect was due to the inactivation of Rab5 by RabGAP-5, as catalytically inactive RabGAP-5^{R165A} did not redistribute wild-type Rab5 to the Golgi (Figure 2-10B).

These findings indicate that Rab5 is inactivated by the catalytic activity of RabGAP-5. RabGAP-5 therefore functions as a specific Rab5 GAP *in vivo*.

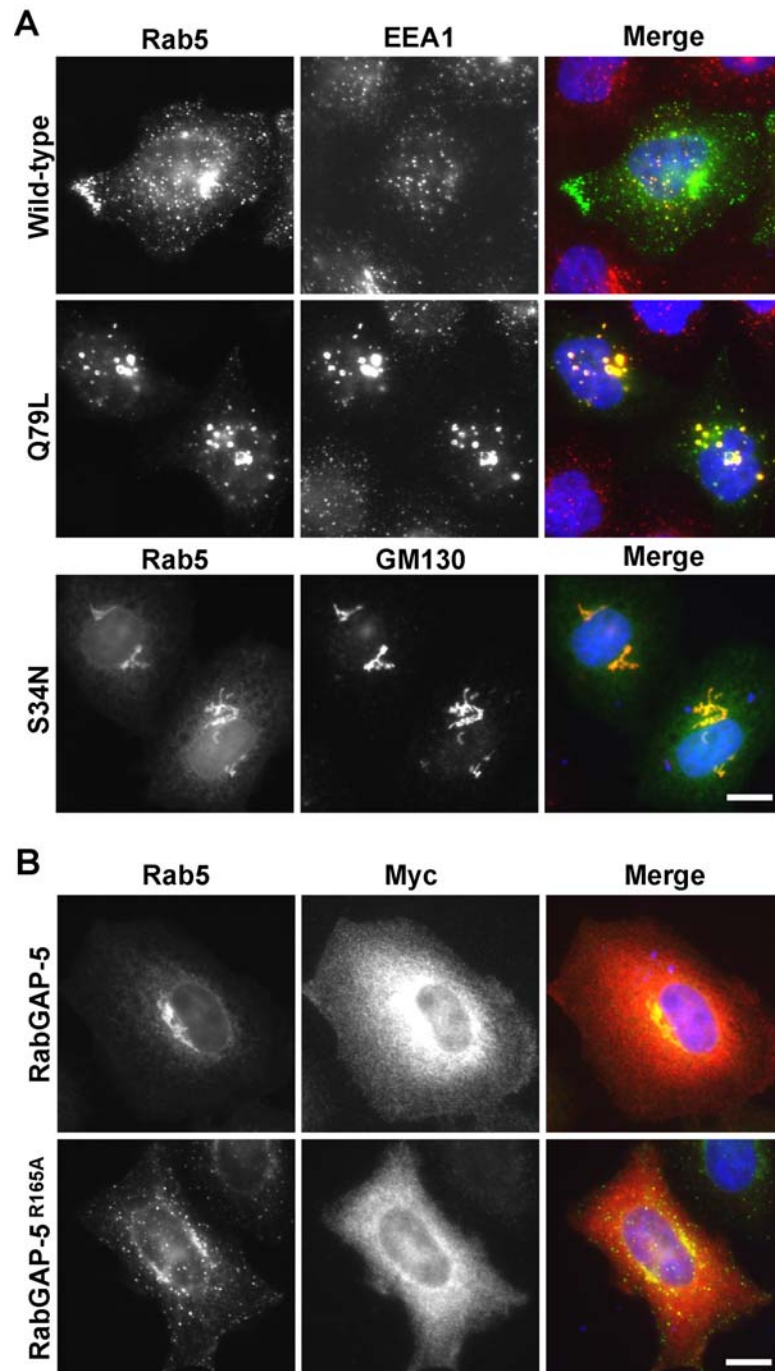


Figure 2-10 RabGAP-5 inactivates Rab5. (A) HeLa cells were transfected with GFP-tagged wild-type and mutant Rab5 for 24h. The cells were then fixed and stained for EEA1 (red) or GM130 (red) respectively. (B) HeLa cells were co-transfected with myc-epitope tagged wild-type and inactive RabGAP-5^{R165A} together with GFP-tagged wild-type Rab5 for 24h. The cells were then fixed with PFA and stained with for the myc-epitope tag (red). Bars indicate 10 μ m.

2.2.8 RN-tre does not function as a GAP for Rab5 *in vivo*

Even though RN-tre was previously reported to act as a GAP for Rab5 it predominantly acted on Rab43 *in vitro* (Figure 2-7).

To investigate the activity of RN-tre towards Rab5 *in vivo*, its influence on the distribution of EEA1 and Rab5 was analysed. In contrast to RabGAP-5, RN-Tre did not redistribute EEA1 (Figure 2-11A). The localisation of GFP-tagged wild-type Rab5 was also not affected by expression of RN-tre (Figure 2-11C). Rab43 localized to the Golgi (Figure 2-11B) and is therefore unlikely to play a direct role in the regulation of endocytosis.

These results suggest that RN-tre does not function as a specific Rab5 GAP *in vivo*. It rather appears to be involved in the regulation of Golgi associated trafficking.

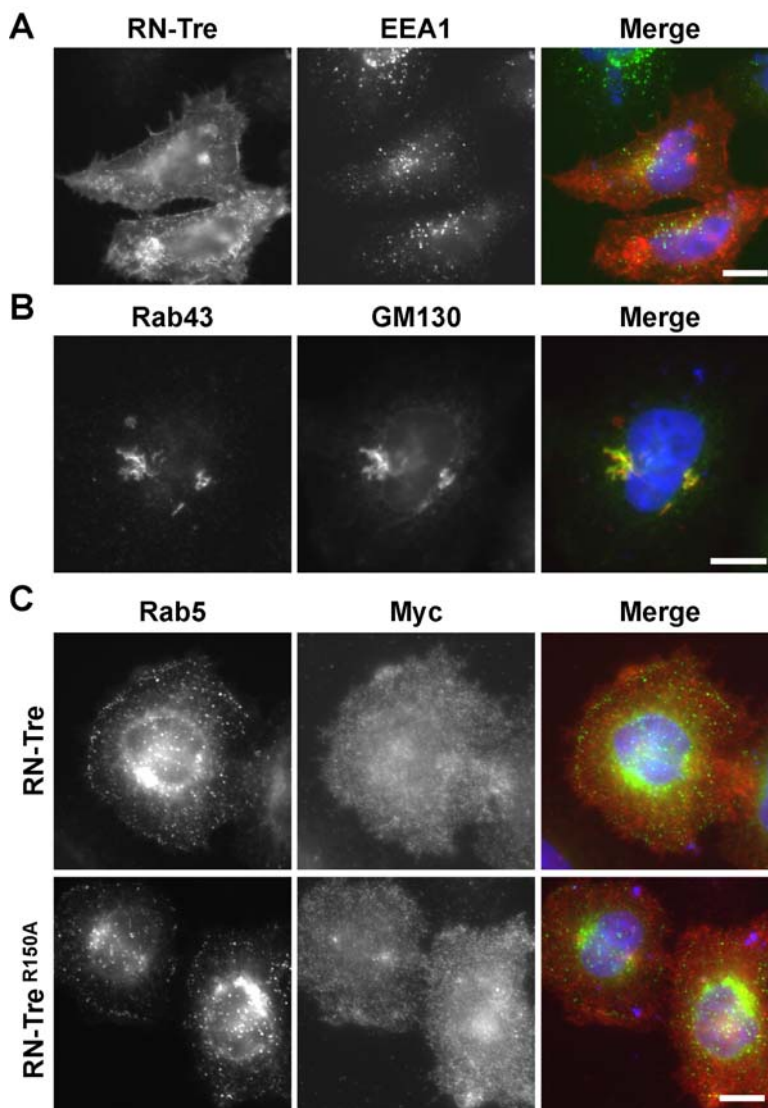


Figure 2-11 RN-tre does not function as a Rab5 GAP *in vivo*. (A) HeLa cells were transfected with myc-tagged RN-tre for 24 hours. The cells were then fixed and stained for the myc-epitope (red) and

EEA1 (green). (B) HeLa cells were transfected with GFP-tagged wild-type Rab43 for 24 hour. The cells were the fixed with PFA and stained for GM130 (red). (C) HeLa cells were co-transfected with myc-epitope tagged wild-type or inactive RN-tre^{R150A} together with GFP-tagged wild-type Rab5 24 hours. The cells were then fixed with PFA and stained for the myc-epitope (red). Bars indicate 10µm.

2.2.9 Expression of RabGAP-5 blocks the endocytosis of EGF

Rab5 and its effector EEA1 are required on early endosomes for the regulation of several trafficking events (Christoforidis et al., 1999a; Rubino et al., 2000). Therefore, it was possible that RabGAP-5 overexpression might lead to a defect in early endosomal trafficking. To test this hypothesis, the endocytosis of the EGF receptor was investigated.

After binding to its ligand the EGF receptor dimerises, auto-phosphorylates and signalling cascades are initiated (Carpenter, 2000). The EGF receptor is subsequently endocytosed into CCVs in a process that requires Rab5 (McLauchlan et al., 1998). CCVs fuse with each other and EEs in a Rab5 dependent process (Ceresa, 2006; Christoforidis et al., 1999a). Receptor signalling is propagated and amplified at EEs (Miaczynska et al., 2004). After inactivation of Rab5 and activation of Rab7 (Feng et al., 1995; Rink et al., 2005) the EGF receptor is sorted to MVBs and degraded (Stahl and Barbieri, 2002).

When RabGAP-5 expression inactivates Rab5, trafficking of the EGF receptor from the cell surface through the early endocytic compartment should be blocked. This was analysed by following the fate of fluorescently labelled EGF. HeLa L cells were transfected with either wild-type or inactive RabGAP-5^{R165A} 24 hours prior to the incubation with labelled EGF. Non-expressing neighbouring cells were used as control. The cells were incubated at 4°C in the presence of labelled EGF to allow binding to the receptor and then shifted to 37°C to initiate endocytosis of the activated receptor.

Comparable amounts of EGF were bound to the surface of both RabGAP-5 expressing and non-expressing cells (Figure 2-12A,B). After 10 minutes at 37°C EGF was found in small punctate structures, most likely clathrin coated vesicles, in non-expressing cells. In adjacent cells expressing RabGAP-5 EGF was still present at the plasma membrane (Figure 2-12A). After 30 minutes EGF was present in larger punctate structures resembling early endosomes in control cells. EGF was essentially lost from the PM of RabGAP-5 expressing cells at this time point (Figure 2-12A). This loss was probably due to competition of excess unlabelled EGF in the growth medium. In cells expressing the inactive RabGAP-5^{R165A} EGF behaved exactly as in control cells was at any time point (Figure 2-12B).

These data show that the expression of RabGAP-5 blocks the endocytosis of the EGF-receptor by the inactivation of Rab5.

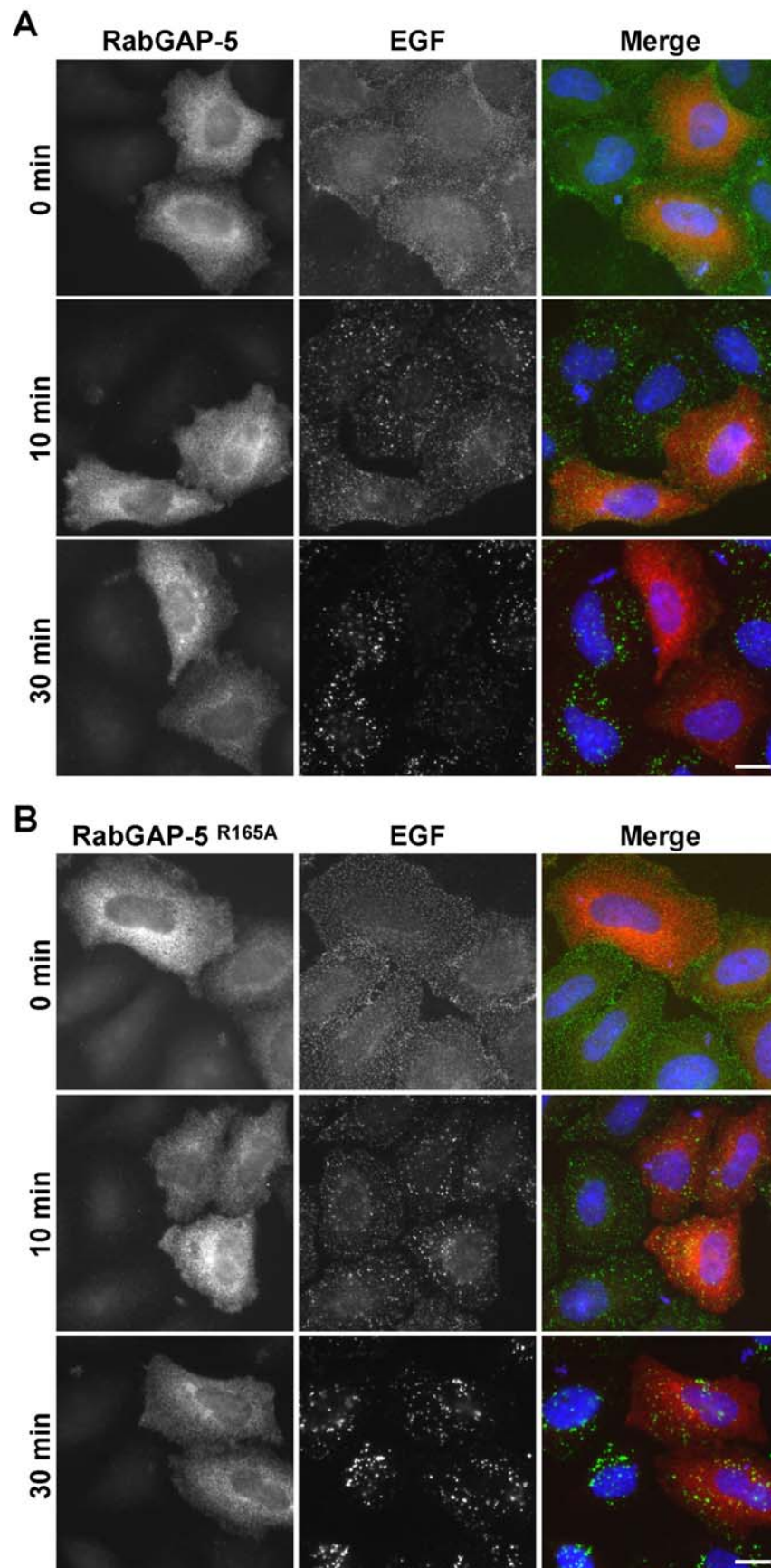


Figure 2-12 Trafficking of EGF is blocked by RabGAP-5. HeLa cells were transfected with myc-tagged (A) wild-type or (B) catalytically inactive RabGAP-5^{R165A} for 24 hours. The cells were shifted

to 4°C and incubated with fluorescent EGF (green). Endocytosis of EGF was initiated by shifting of the cells to 37°C. The cells were fixed at the time points indicated, and stained for the myc-epitope tag (red). Bars indicate 10µm.

2.2.10 RabGAP-5 blocks transferrin receptor trafficking

After studying the fate of EGF receptor, a receptor undergoing degradation after endocytosis (Carpenter, 2000), a receptor recycling to the PM was analysed.

The transferrin receptor recycles between endocytic compartments and the PM. EGF receptor and transferrin receptor are both endocytosed by the same pathway, but they are separated before EGF receptor is sorted into MVBs (Futter et al., 1996). The transferrin receptor is involved in iron homeostasis (Dautry-Varsat, 1986). Transferrin, a glycoprotein of the blood, transports iron. The iron-free form, apotransferrin, binds iron and forms ferrotransferrin. The transferrin receptor binds to ferrotransferrin and is endocytosed by a Rab5 dependent process into EEs. At the low pH of endosomes iron is released and apotransferrin is formed. Apotransferrin remains bound to the receptor. The receptor then recycles via REs in a Rab11 dependent process back to the PM (Sheff et al., 1999). At the neutral pH of the interstitial fluid apotransferrin is released from the transferrin receptor.

To examine the effect of the expression of RabGAP-5 the fate of fluorescently labelled transferrin was followed. HeLa L cells were transfected with either wild-type or mutant RabGAP-5^{R165A} 24 hours prior to the incubation with labelled transferrin. Neighbouring non-expressing cells were used as control. The cells were incubated with fluorescent transferrin at 4°C to allow binding to the receptor and subsequently shifted to 37°C to initiate receptor endocytosis.

Comparable amounts of transferrin were bound to the surface of both expressing and non-expressing cells (Figure 2-13A, B). After 5 minutes at 37°C, transferrin was internalised into small punctate structures in control cells. In adjacent RabGAP-5 expressing cells transferrin was still present as a diffuse haze characteristic of the plasma membrane (Figure 2-13A). After 7.5 minutes transferrin was mainly seen in punctate structures in control cells. After this time point the fluorescence signal faded due to the recycling process. In cells expressing RabGAP-5 transferrin was still present at the plasma membrane at this time point (Figure 2-13A). When the catalytically inactive RabGAP-5^{R165A} mutant was used, no difference in the trafficking of transferrin was observed between transfected and adjacent non-transfected control cells at any time-point (Figure 2-13B).

These data show that endocytosis of the transferrin receptor is blocked in cells over-expressing RabGAP-5 dependent on its ability to inactivate Rab5.

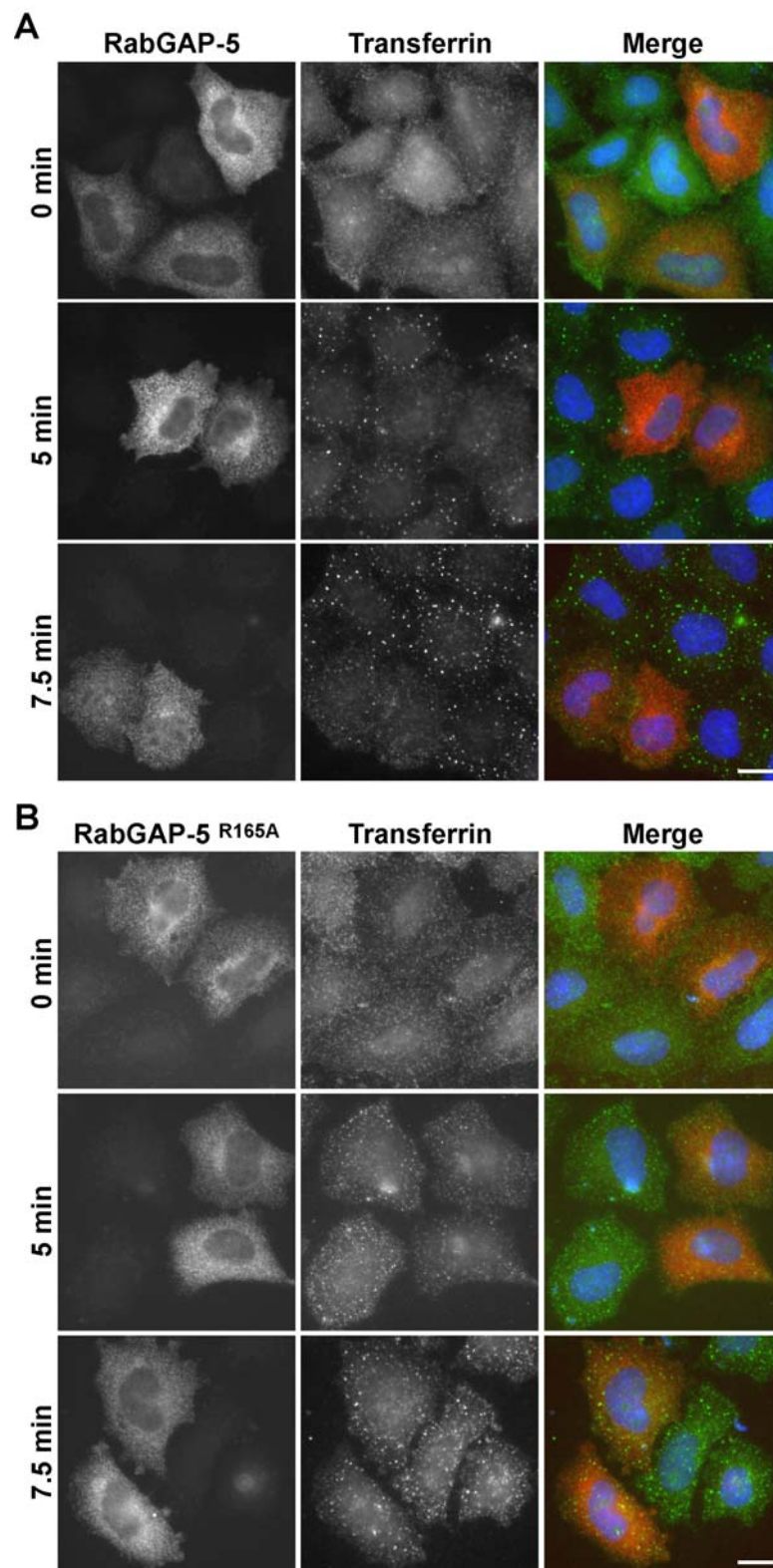


Figure 2-13 RabGAP-5 blocks endocytosis of the transferrin receptor. HeLa cells were transfected with myc-tagged (A) wild-type or (B) catalytically inactive RabGAP-5^{R165A} for 24 hours. The cells were shifted to 4°C and incubated with fluorescent transferrin (green). Endocytosis of transferrin was initiated by shifting the cells to 37°C. The Cells were fixed at the time points indicated and stained for the myc-epitope tag (red). Bars indicate 10µm.

Next, the steady state distribution of the transferrin receptor was analysed in cells over-expressing RabGAP-5. The steady state distribution of this recycling receptor depends on various trafficking routes, at least one of which is dependent on the activity of Rab5.

Various pools of the transferrin receptor can be observed in HeLa cells (Figure 2-14). One pool is on the cell surface to bind transferrin. This pool consists of recycled and newly synthesized receptors. The second pool is found in punctate structures inside the cell and corresponds to early endosomes. A third pool accumulates in the perinuclear region and corresponds to recycling endosomes. This normal distribution of the transferrin receptor was changed in cells expressing wild-type RabGAP-5 (Figure 2-14). The pool of transferrin receptor at the plasma membrane appeared unchanged, but the pools of transferrin receptor inside the cell were reduced. This effect was not observed in cells expressing RabGAP-5^{R165A} (Figure 2-14).

Taken together, these findings show that RabGAP-5 interferes with trafficking of recycling proteins such as the transferrin receptor. The steady state of recycling proteins dependent on the activity of Rab5 is altered by RabGAP-5 expression as well. Therefore these data indicate that RabGAP-5 functions as a GAP for Rab5 *in vivo*.

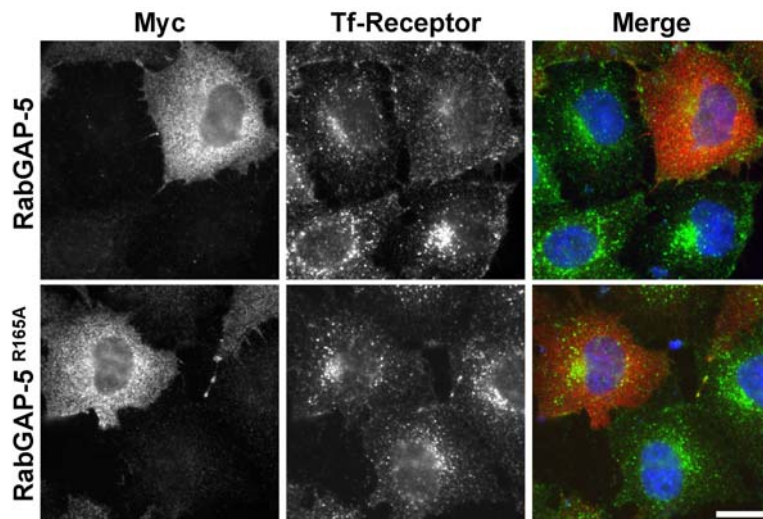


Figure 2-14 RabGAP-5 changes the steady state distribution of the transferrin receptor. HeLa cells were transfected with myc-tagged wild-type or catalytically inactive RabGAP-5^{R165A} for 24 hours. The cells were then fixed and stained with antibodies against the myc-epitope (red) and transferrin receptor (green). The bar indicates 10µm.

2.2.11 RabGAP-5 is an essential regulator of Rab5

As RabGAP-5 is a GAP for Rab5 both *in vitro* and *in vivo*, the question arose of whether or not endogenous RabGAP-5 is essential for the regulation of Rab5.

To address this question small interfering RNA (siRNA) oligonucleotides were used. Antibodies against RabGAP-5 were generated to show the depletion of the endogenous protein. The antibodies were raised in rabbits against RabGAP-5 aa 1-451 tagged with MBP. MBP specific antibodies were removed by adsorption over an Affigel-15 column with 1mg MBP coupled per ml of gel. Subsequently, RabGAP-5 antibodies were affinity purified using a RabGAP-5¹⁻⁴⁵¹ column. This purified antibody was used at 1 µg/ml for western blot and staining of cells. The antibody did not stain endogenous RabGAP-5 by immunofluorescence independent of the fixation method. However, the antibody recognized a band of the appropriate molecular weight on western blot. This binding was competed by pre-incubation of the purified antibody with recombinant RabGAP-5 (Figure 2-15). This shows that the antibody specifically binds to RabGAP-5.

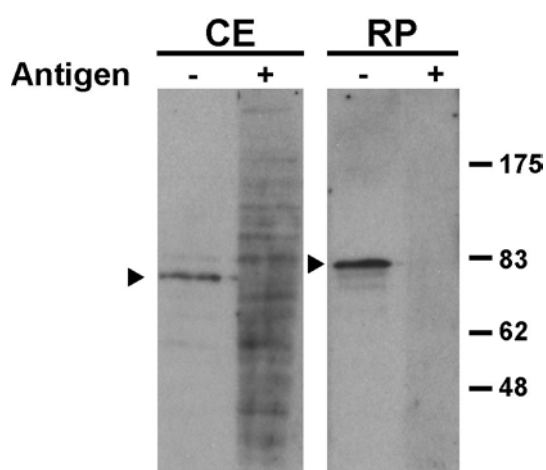


Figure 2-15 Antigen competition of the RabGAP-5 antibody. Western blot strips loaded with either 25 µg cell extracts (CE) or 1ng recombinant MBP-RabGAP-5¹⁻⁴⁵¹ (RP) were probed with the α -RabGAP-5 antibody. The Antibody was pre-incubated with 10µg/ml recombinant RabGAP-5 for 1 hour (+) or left untreated (-).

HeLa cells were treated with RabGAP-5 specific siRNA duplexes for 72 hours. Western blots of extracts generated from these cells revealed that RabGAP-5 was efficiently depleted by specific siRNA oligonucleotides (Figure 2-16A, marked by an arrowhead). The levels of α -tubulin as a loading control as well as the levels of EEA1 and LAMP1 were not affected by depletion of RabGAP-5 (Figure 2-16A).

In cells depleted of RabGAP-5 the staining of EEA1 was more intense and present on larger clustered structures than in control cells where EEA1 was found on smaller dispersed structures typical of early endosomes (Figure 2-16B). This distribution of EEA1 in RabGAP-

5 depleted cells is similar to cells expressing GTP restricted Rab5^{Q79L} (Lawe et al., 2002; Stenmark et al., 1994). The staining for the lysosomal marker LAMP1 was strongly reduced in cells depleted of RabGAP-5 (Figure 2-16C). When these cells were stained without detergent extraction of the plasma membrane, LAMP1 was found on the cell surface (Figure 2-16C). This finding argues that endosomal trafficking is defective in cells depleted of RabGAP-5, since newly synthesized LAMP1 is transported from the TGN via early endosomes to lysosomes (Cook et al., 2004; Rohrer et al., 1996).

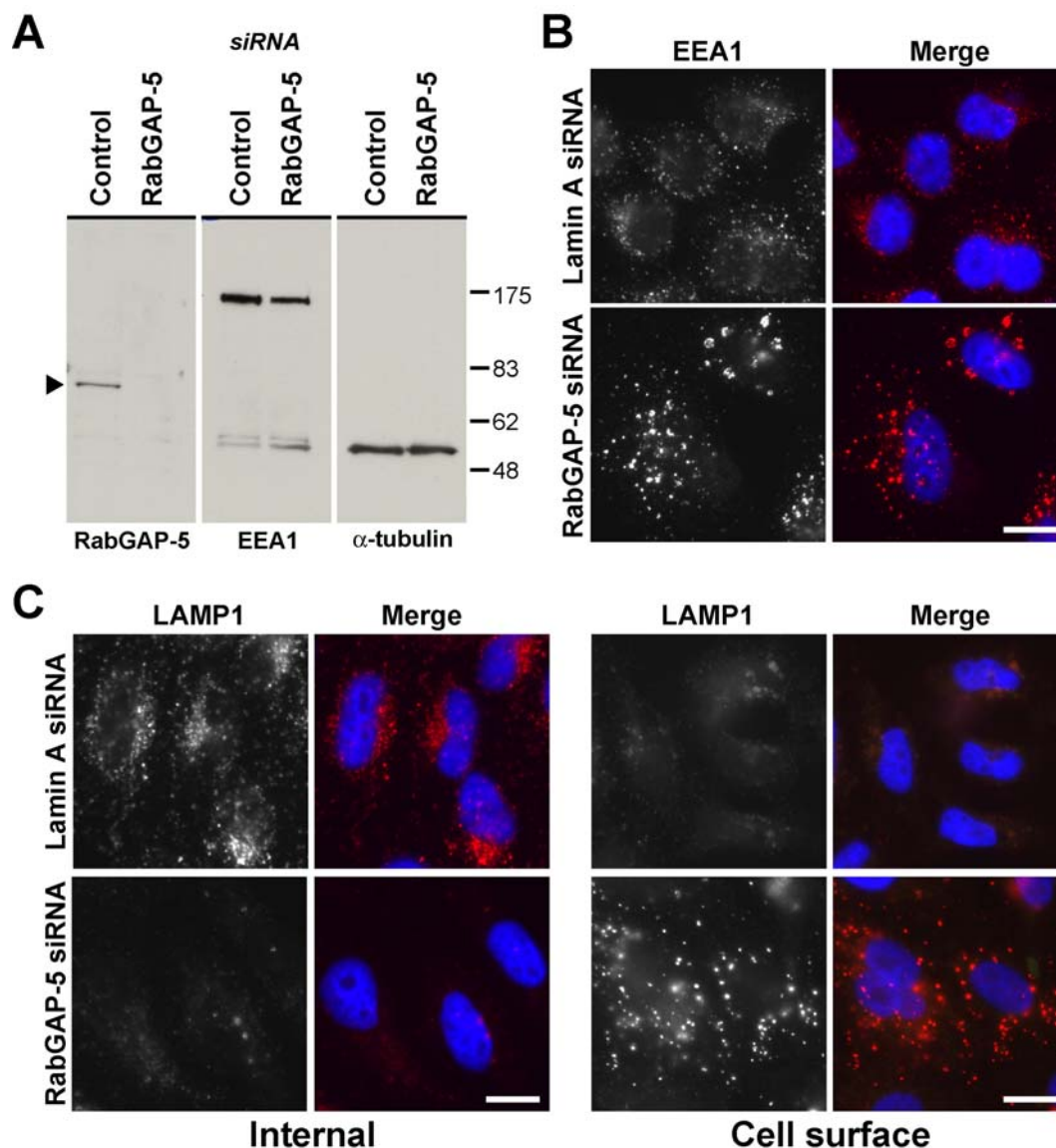


Figure 2-16 RabGAP-5 depletion causes enlarged endosomes and sorting defects. HeLa cells treated with control Lamin A or RabGAP-5 siRNA duplexes for 72 hours were (A) analysed by western blot with antibodies against RabGAP-5 (marked by an arrowhead), α-tubulin, or EEA1 and LAMP1 (note that EEA1 runs at 175 kDa while LAMP1 is a smeared band in the 83 kDa region). (B) Cells treated equally were fixed and then stained for EEA1 (red), or (C) fixed and then stained for LAMP1 (red) either with (Internal) or without detergent extraction (Cell surface). Bars indicate 10 μm.

2.2.12 Elevated levels of Rab5 cause a phenotype resembling RabGAP-5 depletion

If the enlarged endosomes caused by depletion of RabGAP-5 are due to elevated levels of endogenous active Rab5, then an elevation of the levels of GTP Rab5 by other means should cause the same phenotype.

The size of endosomes was increased in cells expressing the GTP restricted mutant Rab5^{Q79L} (Figure 2-17). Cells expressing Rabex-5 (Figure 2-17), the GEF for Rab5 (Horiuchi et al., 1997), also showed enlarged endosomes.

These results indicate that elevated levels of active Rab5 cause the phenotype observed after depletion of RabGAP-5.

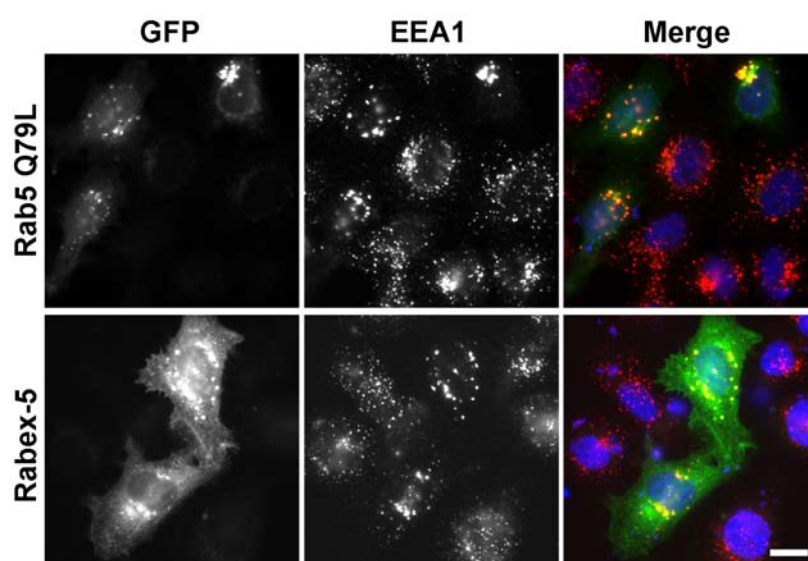


Figure 2-17 Elevated Rab5 GTP levels cause enlarged endosomes. HeLa cells were transfected with GFP-tagged Rab5^{Q79L} or GFP-tagged Rabex-5 for 24h. The Cells were fixed and stained for EEA1 (red). The bar indicates 10µm.

2.2.13 Depletion of RabGAP-5 blocks trafficking through early endosomes

The depletion of RabGAP-5 probably led to miss-localisation of LAMP1 because of defective endosomal trafficking (Figure 2-16C). To further investigate this defect, the trafficking of EGF was analysed in cells depleted of RabGAP-5. Again, fluorescent EGF was followed as readout for receptor trafficking. HeLa L cells were treated with control or RabGAP-5 specific siRNA duplexes for 72 hours. Then they were incubated at 4°C in the presence of labelled EGF to allow binding to the EGF receptor. The cells were then shifted to 37°C to initiate endocytosis of the activated receptor and fixed at the indicated time points.

Both binding of EGF to the receptor at the PM and internalisation of EGF after 10 minutes into EEA1 positive structures were not altered by depletion of RabGAP-5 in comparison to control siRNA (Figure 2-18). This indicates that the uptake of EGF into clathrin-coated vesicles and their trafficking to early endosomes is not affected by depletion of RabGAP-5.

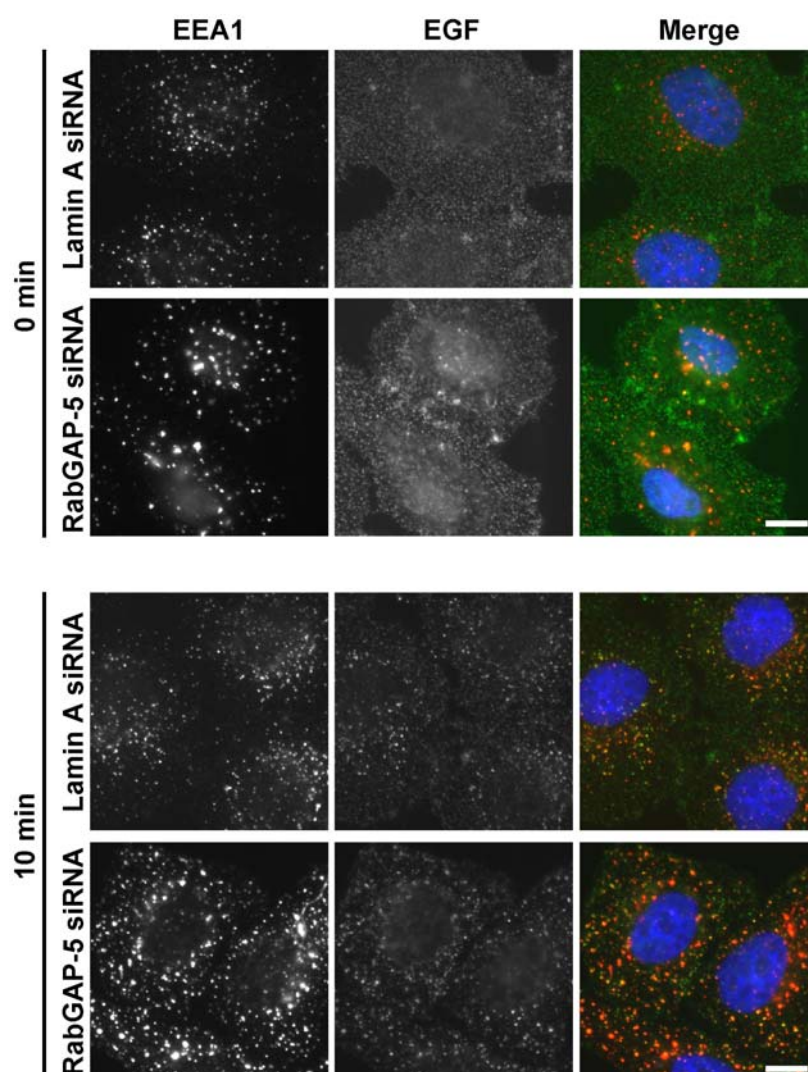


Figure 2-18 Depletion of RabGAP-5 doesn't block the uptake of EGF. Uptake of EGF (green) was followed in HeLa cells treated with control Lamin A or RabGAP-5 specific siRNA oligonucleotides for 72 hours. After 0 and 10 minutes of uptake, cells were fixed and stained for EEA1 (red). Bars indicate 10 μ m.

EGF started to separate from EEA1 positive structures 30 minutes after internalisation in cells treated with control siRNA. After 60 minutes the EGF signal was lost from early endosomes in these cells (Figure 2-19). The reduction of the red EGF signal suggests that the EGF receptor was properly sorted into the degradative pathway. In cells

depleted of RabGAP-5 EGF accumulated in enlarged early endosomes after 30 minutes. It was still retained in these structures after 60 min (Figure 2-19) and did not enter the degradative pathway. This is clearly seen in the enlarged merged images where the yellow colour indicates an overlap of EGF and EEA1.

Trafficking through early endosomes, which depends on Rab5, is therefore blocked in the absence of RabGAP-5 and endocytosed material is not sorted for lysosomal degradation. This shows that endogenous RabGAP-5 is an important regulator of Rab5 dependent traffic.

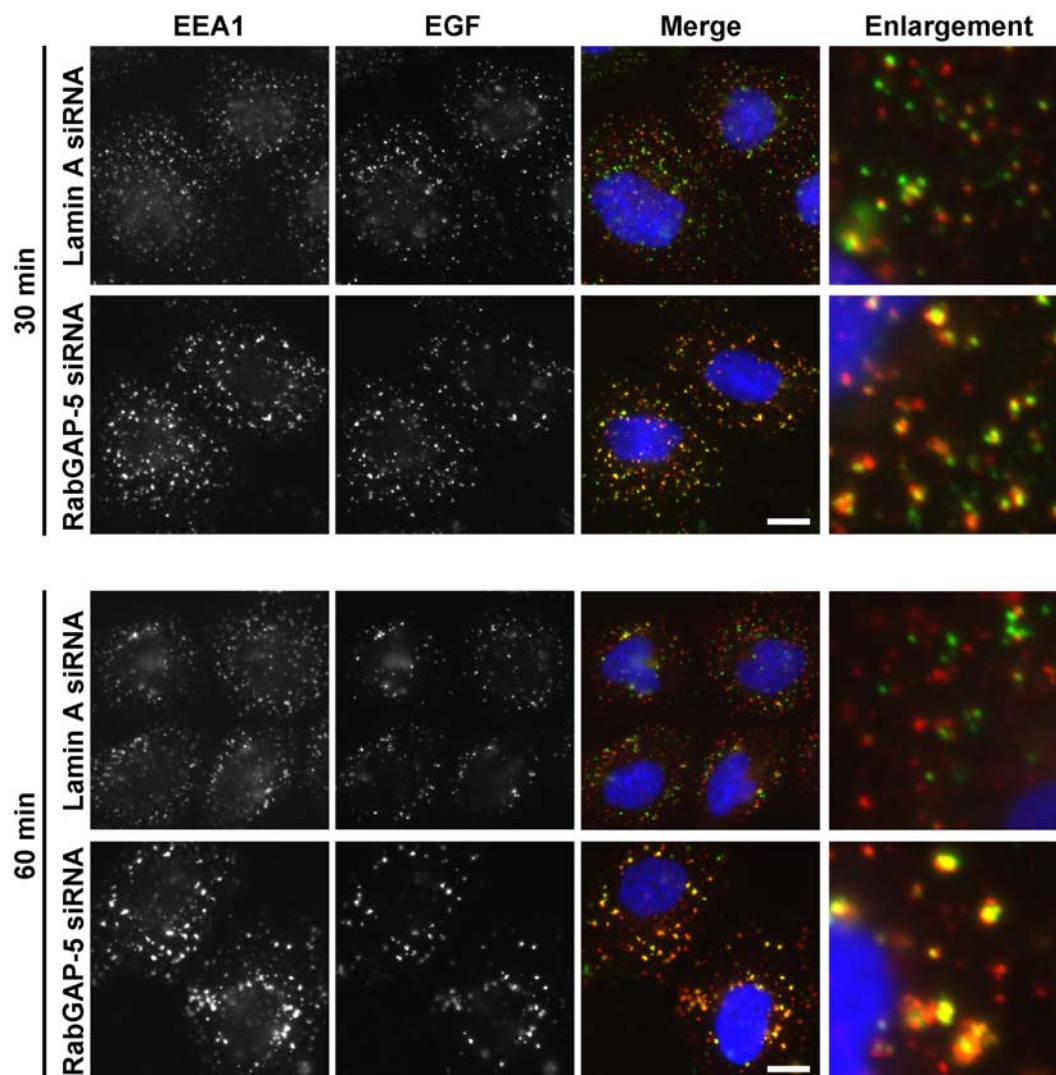


Figure 2-19 Depletion of RabGAP-5 blocks trafficking of EGF. Trafficking of EGF (green) was followed in HeLa cells treated with control Lamin A or RabGAP-5 specific siRNA oligonucleotides for 72 hours. The cells were fixed after 30 and 60 minutes and stained for EEA1 (red). An enlargement of the merged images is shown in the rightmost panel. Bars indicate 10 μm.

2.3 Summary

To identify GAPs regulating Rabs involved in endocytosis the human genome database was searched for proteins containing a TBC domain. These proteins are known from work in *S. cerevisiae* to function as RabGAPs. Forty proteins were identified, amplified by PCR from cDNA libraries and sub-cloned.

To identify pairs of Rabs and their regulatory GAPs, a reverse yeast two-hybrid screening system was established. In this system all TBC domain proteins were tested against a all human Rabs for their ability to interact. To gain the required specificity, this system required the introduction of two mutations: a conserved glutamine of the Rabs was mutated to alanine to restrict them in the GTP bound form; a conserved arginine of the GAPs was replaced by alanine to ensure correct substrate recognition. Using this screening method, a GAP for Rab5 termed RabGAP-5 was identified. This novel RabGAP stimulated GTP hydrolysis by Rab5 *in vitro* dependent on its catalytic arginine¹⁶⁵. The TBC domain was mapped to aa 1-451. Expression of RabGAP-5 in human cells redistributed the Rab5 effector EEA1 to the cytoplasm. Co-transfected Rab5 was relocated to the Golgi apparatus by the expression of RabGAP-5. Structures independent of Rab5 such as the Golgi apparatus were not affected. Expression of RabGAP-5 blocked the uptake of both EGF and transferrin. It also altered the steady state distribution of the endogenous transferrin receptor.

When RabGAP-5 was depleted by siRNA the size of endosomes was increased. Similar phenotypes were observed in cells with elevated levels of GTP bound Rab5. In cells depleted of RabGAP-5 trafficking through endosomes was blocked. This was shown by distribution of lysosomal LAMP1 to the plasma membrane and the inability of endocytosed EGF to exit from endosome into the degradative pathway.

Taken together, these data strongly suggest that RabGAP-5 is a novel and specific GAP for Rab5, and an essential regulator of endocytosis.

RN-tre, which was previously reported to act as a Rab5 GAP interacted with the closely related Rab43 and Rab30 in the yeast two-hybrid screen but failed to interact with Rab5. When tested *in vitro*, RN-tre strongly stimulated GTP hydrolysis by Rab43. Rab43 was found to localise to the Golgi apparatus. RN-tre furthermore failed to cause Rab5 dependent phenotypes. This suggests that RN-tre does not act as a GAP for Rab5 *in vivo*, and that it is a novel Rab43 GAP.

3 Regulation of secretion by TBC1D20

3.1 Aim of this Work

Like endocytosis, secretion is a highly regulated process (Bonifacino and Glick, 2004). Many steps in the secretory pathway involve Rab GTPases (Zerial and McBride, 2001). The early secretory pathway from the ER to the Golgi apparatus (Duden, 2003) is regulated by the sequential activities of Rab1 (Allan et al., 2000; Segev, 1991) and Rab2 (Short et al., 2001; Tisdale and Balch, 1996).

Despite the fact that numerous Rabs are involved in the control of the secretory pathway, little is known about their regulation. It is also not known which Rabs are essential for these processes. To identify both GAPs and Rabs involved in the regulation of early secretory trafficking at the same time, a novel screening method had to be established. Using this method not only regulatory GAPs, but also the Rabs essential for secretion should be identified.

3.2 Results

3.2.1 Rab inactivation screening

When a Rab is inactivated by its GAP it no longer recruits its effectors to the membrane. Trafficking processes dependent on these effectors are therefore blocked. The expression of RabGAP-5 redistributed the Rab5 effector EEA1 to the cytoplasm (Figure 2-8) but did not affect Rab5 independent organelles. RabGAP-5 also blocked the Rab5 dependent trafficking of EGF (Figure 2-12). All phenotypes caused by RabGAP-5 expression were dependent on its catalytic activity.

Based on these initial studies on Rab5 it was proposed that the expression of a library of human RabGAPs and the analysis of the resulting phenotypes could be used to identify the GAPs involved in the regulation of a specific trafficking step. This screening technique uses three steps to define specificity: First, the catalytically inactive GAPs must not give rise to the same phenotype as the wild-type proteins. This ensures that the phenotypes observed are due to catalytic Rab inactivation. Second, the GAPs that cause activity dependent phenotypes have to be tested for their ability to promote hydrolysis against all Rabs. This ensures full specificity in the identification of the target Rab. Third, siRNA mediated depletion and expression of dominant negative putative target Rabs should recapitulate the phenotypes of GAP expression.

With this approach it is possible to identify GAPs and Rabs regulating specific trafficking steps at the same time. This screening method, as it does not postulate that any given Rab or GAP is involved, is a non-biased approach.

3.2.2 A Rab inactivation screen for Golgi fragmentation

The structure and integrity of the Golgi apparatus depends on multiple Rab effector proteins. To identify GAPs and Rabs involved in the regulation of the early secretory pathway a screen for Golgi fragmentation was performed. In this screen 38 human GFP-tagged TBC-domain proteins were expressed in HeLa L cells. The cells were fixed after 24 hours and stained for the *cis*-Golgi marker GM130 (Nakamura et al., 1995) and the *trans*-Golgi protein TGN46 (Prescott et al., 1997).

For each RabGAP, n=100 cells were examined for changes in their Golgi morphology in comparison to neighbouring non-expressing cells. Based on Golgi fragmentation in 10% of control cells, only a RabGAP causing a fragmentation in more than 40 % of the cells was rated as positive to gain a signal to noise ratio of four to one.

Out of 38 TBC domain proteins tested only seven (Figure 3-1A) showed significant effects on the Golgi morphology. These were TBC1D20, TBC1D22A, TBC1D22B, XM_37557, TBC1D14, RN-tre and PRC17, a protein involved in prostate cancer (Pei et al., 2002) (Figure 3-1A, B). Five of these proteins caused Golgi fragmentation dependent on their catalytic activity (Figure 3-1B). This suggests that the phenotypes were due to inactivation of endogenous Rabs. TBC1D14 and PRC17 were classified as false positives since the expression of their inactive mutants showed equivalent or increased effects on Golgi morphology. The expression of both wild-type and inactive mutant PRC17 caused apoptosis. As Golgi fragmentation occurs in apoptosis (Lane et al., 2002) the phenotype caused by expression of PRC17 appears to be indirect.

The closely related proteins TBC1D22A and B partially localised to the Golgi (Figure 3-1B). The *S.cerevisiae* homologue of TBC1D22B, GYP1, has GAP activity towards human Rab33b (Pan et al., 2006), which is involved in trafficking steps at the Golgi apparatus (Valsdottir et al., 2001; Zheng et al., 1998). RN-tre is a GAP for Rab43 (Figure 2-7) and Rab43 localises to the Golgi (Figure 2-11). XM_37557 is a GAP specific for Rab8a (Yoshimura et al., 2007). Rab8a is required for the formation of primary cilia in quiescent cells and is localised at the Golgi in proliferating cells. TBC1D20, which has no known target Rab, caused the apparent loss of the Golgi apparatus and showed a distinct reticular localisation (Figure 3-1 B).

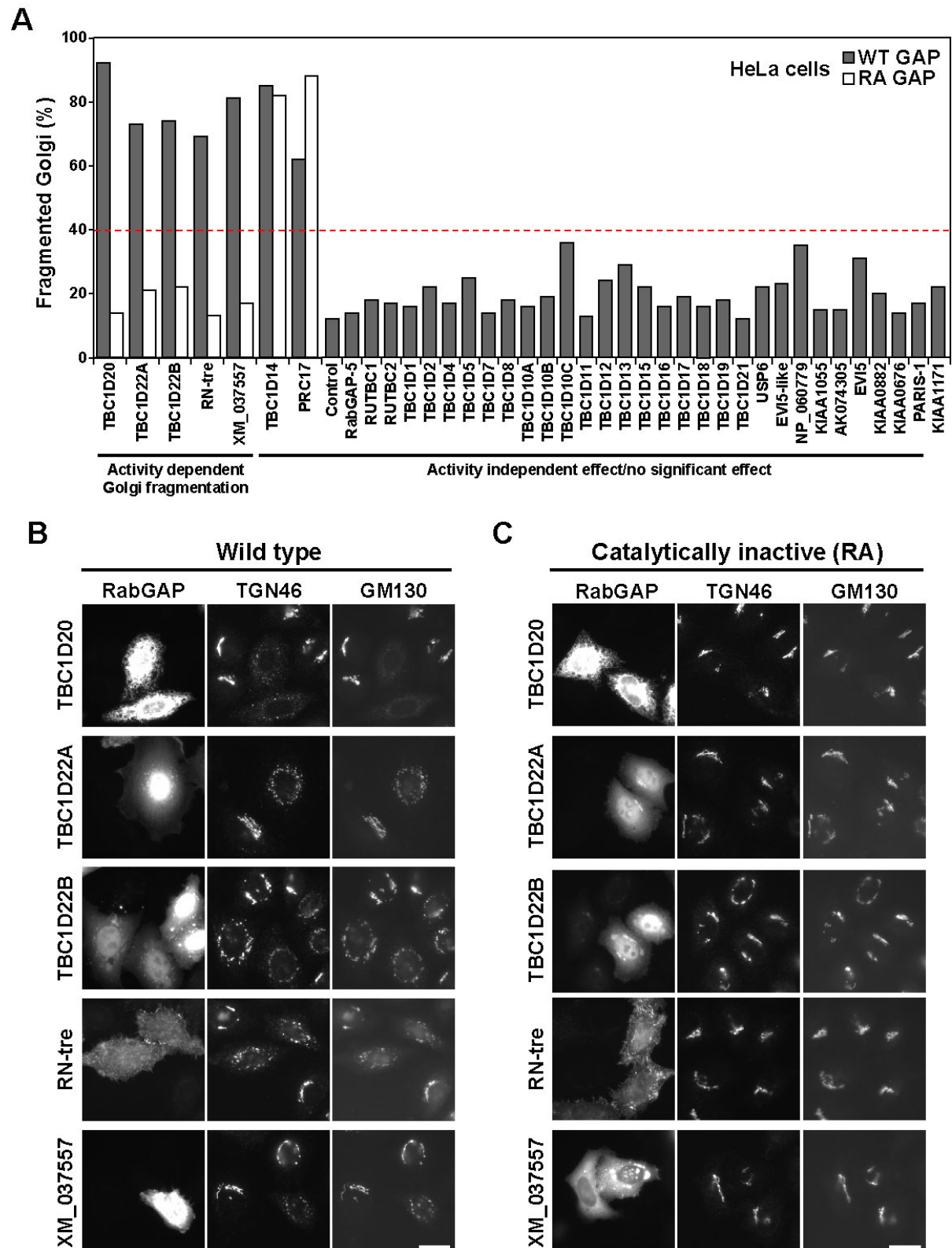
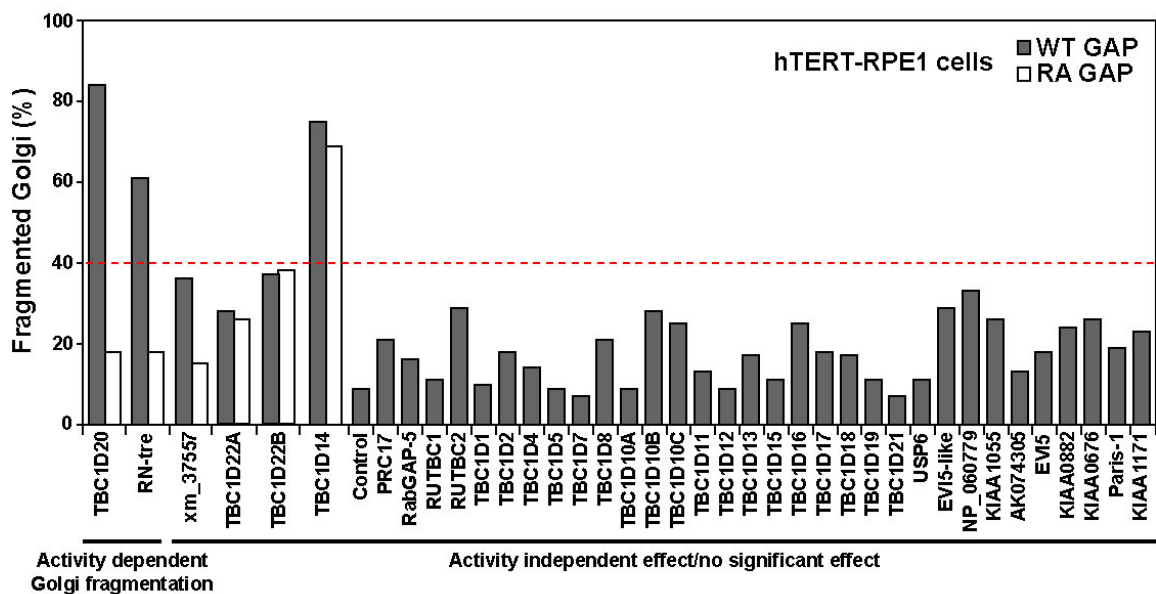


Figure 3-1 Golgi fragmentation in HeLa cells. HeLa cells were transfected with GFP-tagged TBC domain proteins for 24 hours. The cells were then fixed and stained with antibodies against GM130 and TGN46. (A) $n=100$ cells for each TBC domain protein were analysed and their Golgi was rated as fragmented or not fragmented compared to neighbouring non-expressing control cells. (B) GFP tagged TBC domain proteins scoring Golgi fragmentation in more than 40% of the cells are depicted as both wild-type and inactive (RA) mutants. Bars indicate $10\mu\text{m}$.

Next, the same screen was carried out in telomerase immortalized human retinal epithelial (hTERT-RPE1) cells to identify ubiquitously expressed essential Rabs and GAPs and to eliminate cell-type specific proteins. This second screen also helps to validate the screen in HeLa cells.

In hTRET-RPE1 cells only three TBC domain-containing proteins caused significant alterations of the Golgi morphology: TBC1D20, RN-tre and TBC1D14 (Figure 3-2A). In the case of TBC1D14, the phenotype again did not depend on the catalytic activity (Figure 3-2A) of the protein.

A



B

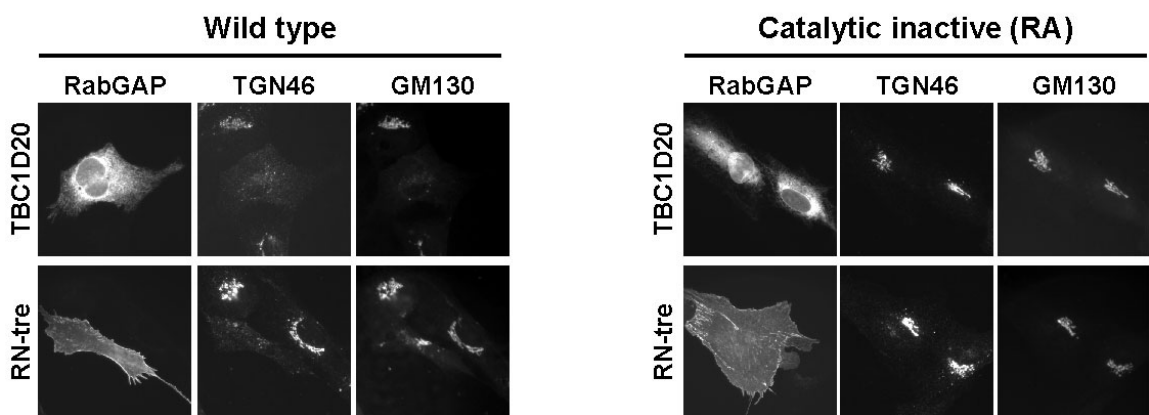


Figure 3-2 Golgi fragmentation in hTERT-RPE1 cells. The cells were transfected with GFP-tagged TBC domain proteins for 24 hours. The cells were then fixed and stained with antibodies against GM130 and TGN46. (A) $n=100$ cells for each TBC domain protein were analysed and their Golgi morphology was rated as fragmented or not fragmented compared to non-expressing neighbouring cells. (B) GFP-tagged TBC domain proteins causing Golgi fragmentation in more than 40% of the cells are depicted both as wild-type and inactive (RA) mutants. Bars indicate 10µm.

The only GAPs positive in both screens were TBC1D20 and RN-tre (Figure 3-1A, Figure 3-2A). This indicates that these GAPs regulate ubiquitously expressed Rabs that are essential for structuring the Golgi apparatus in the cells tested. The GAPs that caused Golgi fragmentation in only one of the screens are unlikely to regulate ubiquitously essential Rabs.

TBC1D20 again caused an apparent loss of the Golgi apparatus, affecting both the *cis*-Golgi stained by GM130 and the *trans*-Golgi stained by TGN-46 (Figure 3-2B, Figure 3-3) equally. This indicates that the target Rab of TBC1D20 has an essential function for the integrity of the Golgi apparatus.

RN-tre on the other hand showed a markedly stronger effect on TGN46 than on GM130 (Figure 3-2B, Figure 3-3) in hTERT-RPE1 cells. It was also the only GAP in both screens that showed a differential effect on the *cis*- and *trans*-Golgi compartments. This indicates that RN-tre may regulate a Rab involved in trafficking steps at the TGN.

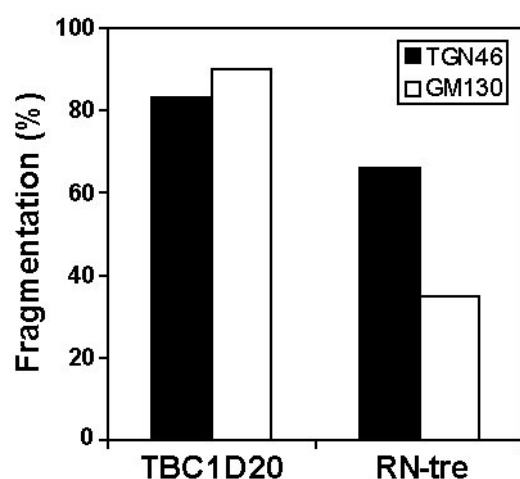


Figure 3-3 RN-tre shows more TGN fragmentation in hTERT-RPE1 cells. The cells were transfected with of GFP-tagged RN-tre and TBC1D20 for 24 hours. The cells were then fixed and stained with antibodies against GM130 and TGN46. n=100 transfected cells for each TBC domain protein were analysed by microscopy and scored as fragmented or not fragmented for both TGN46 and GM130 independently.

3.2.3 A Rab inactivation screen for changes in ERGIC morphology

To further define which trafficking process the different GAPs regulate, the effect of their expression on the ER-Golgi intermediate compartment (ERGIC) was examined. A RabGAP that causes Golgi fragmentation and has an effect on the ERGIC is likely to be a regulator of the early secretory pathway. On the other hand, a TBC domain protein that gives rise to Golgi fragmentation, but has no effect on the ERGIC, most likely regulates trafficking between the Golgi cisternae or at the TGN.

ERGIC-53, a mannose-specific transmembrane lectin was used as a marker for this screen. This protein predominantly localises to the ERGIC, but a small fraction is found in the ER and on ERES (Hauri et al., 2000). It directly recycles between the ERGIC and the ER, and only little ERGIC-53 recycles from the Golgi to the ER (Klumperman et al., 1998).

HeLa cells were transfected with 38 GFP-tagged TBC domain proteins independently and fixed after 24 hours. The cells were stained with an antibody against ERGIC-53. They were analysed and the morphology of their ERGIC was scored as either normal or altered in comparison to neighbouring non-expressing cells. Based on an altered ERGIC morphology in 10% of control cells, a cut-off of 40% was chosen.

TBC1D20 fragmented the ERGIC (Figure 3-4A) dependent on its catalytic activity (Figure 3-4B). Interestingly, ERGIC-53 did not stain small punctate structures in the periphery of the cell, most likely ERES, in cells expressing TBC1D20 (Figure 3-4B). TBC1D22B, but not TBC1D22A, disrupted the ERGIC dependent on its catalytic activity (Figure 3-4A). The perinuclear pool of ERGIC-53 was distributed into fragments in cells expressing TBC1D22B, but in contrast to TBC1D20 expressing cells the small peripheral structures were still present (Figure 3-4B). RN-tre and XM_037557 only caused subtle changes to the ERGIC (Figure 3-4A, B).

A

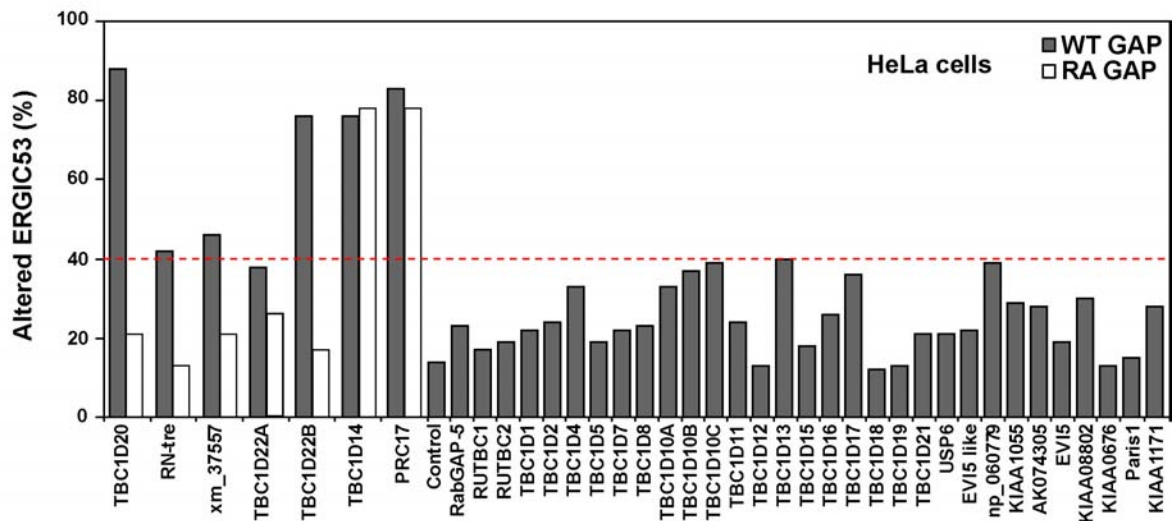
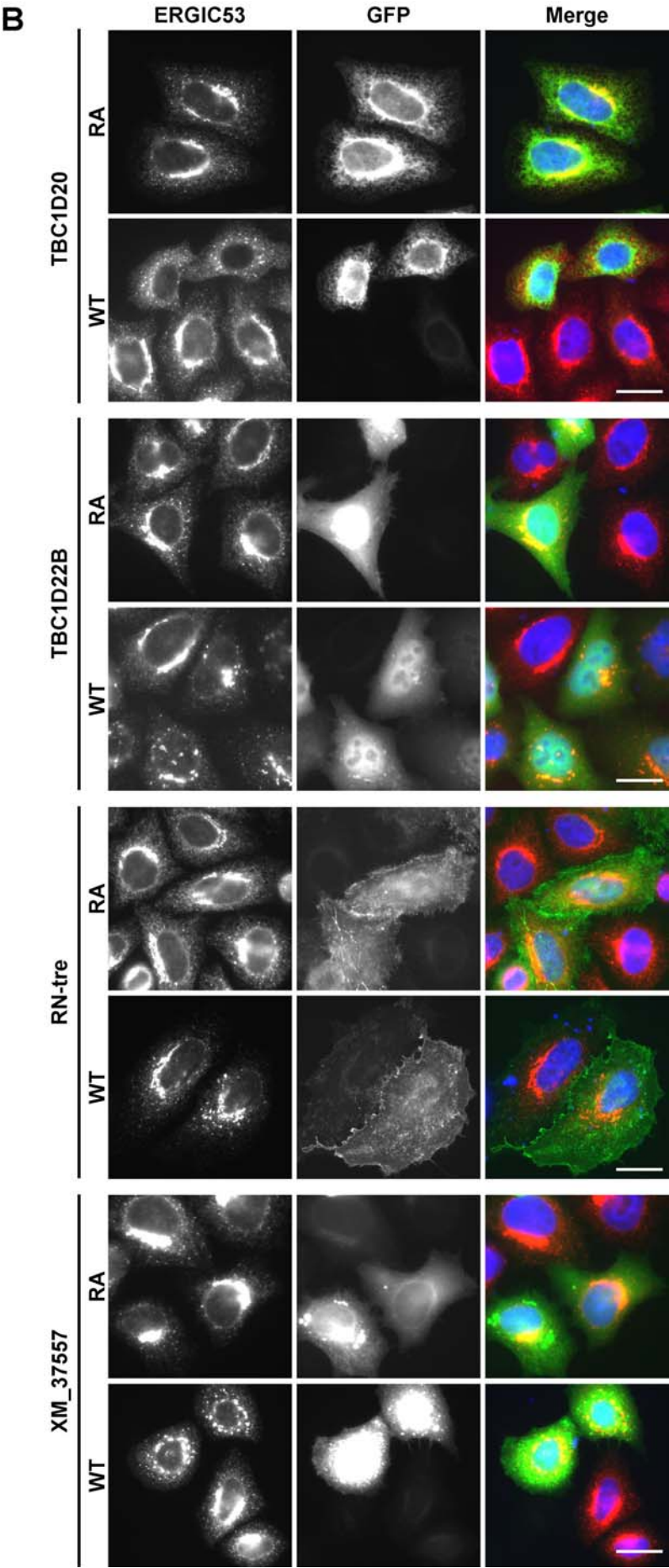


Figure 3-4 A screen for TBC domain proteins altering ERGIC structure. HeLa cells were transfected with GFP-tagged TBC domain proteins for 24 hours. The cells were then fixed and stained for ERGIC-53 (red). (A) $n=100$ cells for each TBC domain protein were analysed by microscopy and scored as fragmented or not fragmented. (B, [see next page](#)) GFP-tagged TBC domain proteins that caused ERGIC fragmentation in more than 40% of expressing cells are depicted both as wild-type (WT) and inactive (RA) mutants. Bars indicate $10\mu\text{m}$.



3.2.4 A Rab inactivation screen for a block of VSV-G trafficking

To further analyse which of the human GAPs regulates secretion, the trafficking of a protein from the ER through the secretory pathway to the plasma membrane was followed in cells expressing these GAPs. As a model cargo a temperature sensitive mutant of a type-I transmembrane glycoprotein of the vesicular stomatitis virus (VSV), ts-O45-G (VSV-G) was used. VSV-G misfolds and accumulates in the ER at the non-permissive temperature of 39.5°C. It refolds at 4°C and is then transported to the cell surface at 31.5°C (Presley et al., 1997; Scales et al., 1997). A GFP tag is fused to the C-terminus of VSV-G that faces the cytoplasm. A specific antibody detects the luminal domain of VSV-G. When used on cells without prior detergent extraction of the plasma membrane, this antibody only stains VSV-G at the cell surface and therefore provides readout for successful trafficking.

Similar to the previous screens (see 3.2.2 and 3.2.3), 38 myc-epitope-tagged human TBC domain proteins were transfected in parallel into HeLa cells. A VSV-G encoding plasmid was co-transfected, and the cells were incubated for 2 hours at 37°C. Then the cells were incubated for 12 hours to 39.5°C to accumulate misfolded VSV-G in the ER. The cells were shifted to 4°C for 30 minutes to stop trafficking and promote proper folding of VSV-G. After these 30 minutes a sample, which corresponds to the $t=0$ time point, was immediately fixed. The cells were then incubated at 31.5°C to allow pulse secretion of VSV-G. After 60 minutes the cells were fixed without detergent extraction of the plasma membrane to stain VSV-G at the plasma membrane. Afterwards the cells were permeabilised and stained for the myc-epitope-tag to identify GAP expressing cells. Co-transfected cells were identified by microscopy and dependent on the presence of VSV-G at the plasma membrane cells that block transport were identified. As in the previous screens for Golgi fragmentation or changes in the ERGIC morphology, a cut-off of 40% was chosen.

Strikingly, out of all TBC domain proteins only TBC1D20 was able to prevent the appearance of the VSV-G at the cell surface after 60 minutes (Figure 3-5A). This block of transport was dependent on the catalytic arginine¹⁰⁵ of TBC1D20 (Figure 3-5B). This indicates that this effect on VSV-G trafficking was due to specific inactivation of a Rab. The other RabGAPs that fragmented the Golgi or affected the morphology of the ERGIC did not block VSV-G transport (Figure 3-5A). They also didn't show any significant difference in VSV-G trafficking between wild-type and catalytically inactive mutants (Figure 3-5B). This shows that out of all human RabGAPs only TBC1D20 inactivates a Rab that is essential for the secretion of VSV-G.

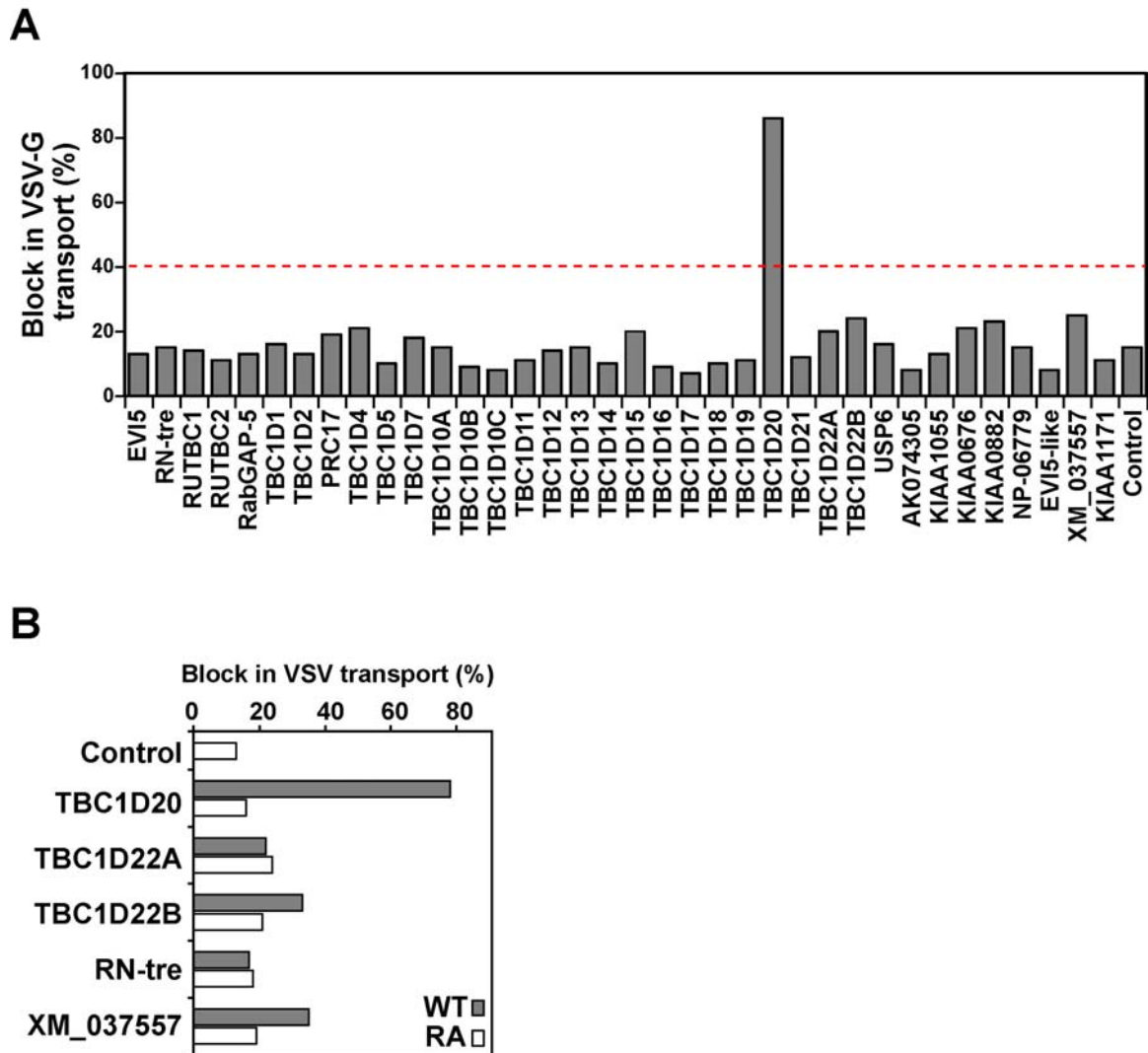


Figure 3-5 TBC1D20 is the only TBC domain protein that blocks VSV-G trafficking. VSV-G transport assays were performed for a total time of 15 hours in HeLa cells expressing myc-epitope-tagged TBC domain proteins (A) HeLa cells co-transfected with VSV-G and wild-type TBC domain proteins were stained for surface VSV-G and the myc-epitope tag. n=100 cells were analysed by microscopy for each GAP and were scored as either block or no block of trafficking. (B) HeLa cells were co-transfected with VSV-G and wild-type (WT) or catalytically inactive (RA) mutant TBC domain proteins that fragment the Golgi. They were stained for surface VSV-G and the myc-epitope tag. n=100 cells were analysed for each GAP and were scored as either block or no block of trafficking.

The over-expression of TBC1D20 caused a strong effect on Golgi morphology in all cell lines analysed. It also perturbed the organisation of the ERGIC in a unique way. Out of all TBC domain proteins it was the only one that blocked the secretion of VSV-G. TBC1D20 is therefore the most likely candidate for a GAP that regulates an essential Rab involved in the regulation of the early secretory pathway. This TBC domain protein and the phenotypes caused by its over-expression were therefore studied in more detail.

3.2.5 TBC1D20 is a highly conserved TBC domain protein

To investigate the evolutionary conservation of TBC1D20 the genomes of several vertebrates and yeast were searched. TBC1D20 homologues were identified using online database search engines at BLAST (<http://www.ncbi.nlm.nih.gov/blast/>).in macaque, mouse, rat, dog, cow, zebrafish, African clawed toad, and the three yeasts *Saccharomyces cerevisiae*, *Schizosaccharomyces pombe*, and *Kluyveromyces lactis*. Partial sequences of homologue proteins were also found in other species but omitted for simplicity. The protein sequences of the homologue proteins were aligned to the human TBC1D20 protein sequence using the Vector NTI® software (Figure 3-6).

This alignment showed that TBC1D20 is a highly conserved protein. It is almost identical in all mammals, and the similarity is very striking even to lower vertebrate sequences. The similarity to the yeast proteins appears less pronounced. But even in yeast, the consensus sequences that identify the TBC domain (1.3.1) and the catalytically relevant residues arginine¹⁰⁵ and glutamine¹⁴⁴ (Pan et al., 2006) are conserved.

TBC1D20 is a rather small member of the family of TBC domain containing proteins with 403 aa for the human protein. In contrast to most other RabGAPs (Figure 2-2) it does not contain additional conserved protein domains. The only other component identified in the sequence of all homologue proteins is a hydrophobic stretch close to the C-terminus of TBC1D20 (Figure 3-6). Further analysis with the PSORTII prediction algorithms (<http://psort.nibb.ac.jp/form2.html>) suggested that this hydrophobic stretch might form a transmembrane domain (TMD) or membrane anchor. This indicates that TBC1D20 might be localised to membranes via its C-terminus.

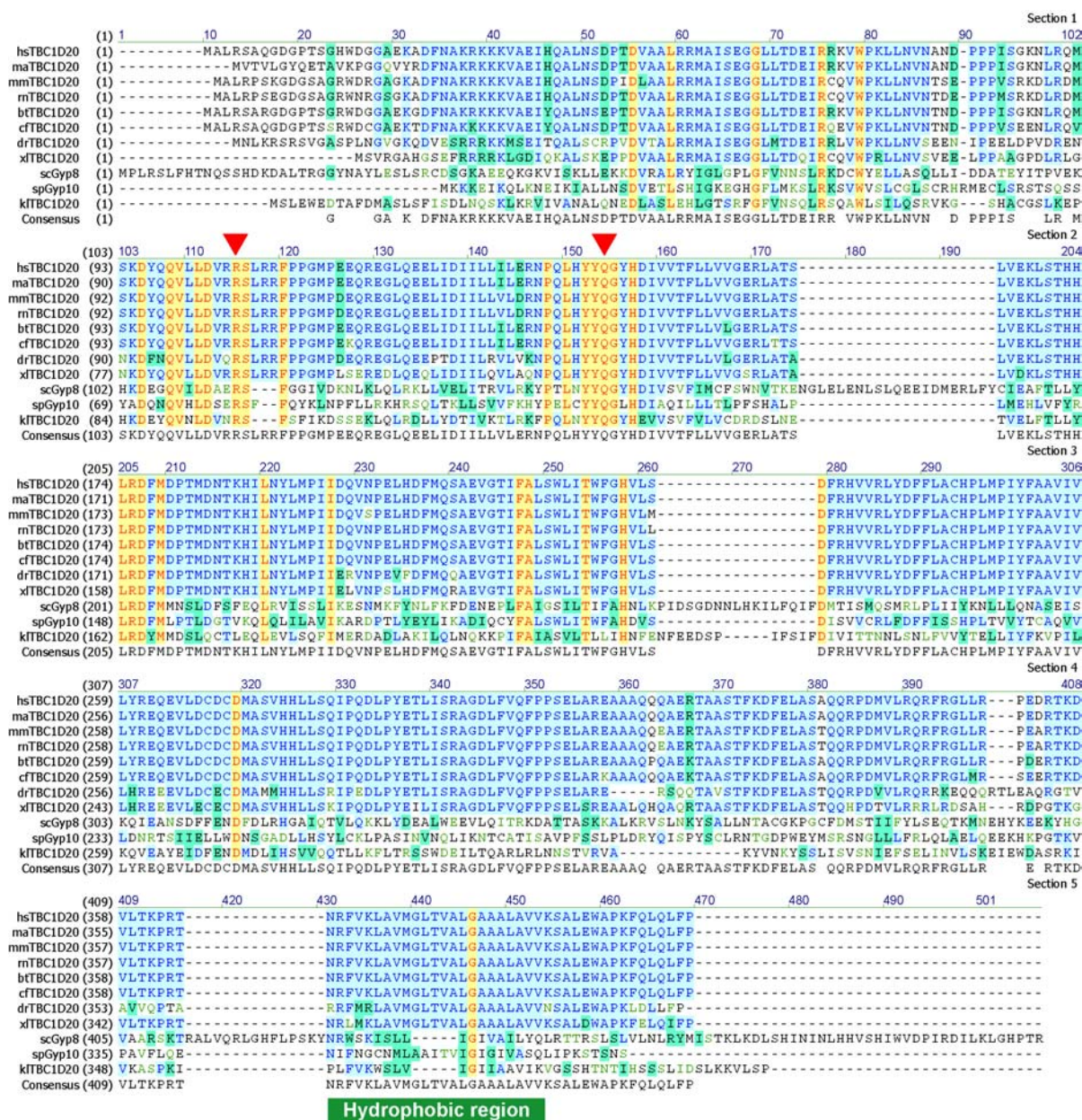


Figure 3-6 Alignment of TBC1D20 sequences. Proteins were identified in human (hs), macaque (ma), mouse (mm), rat (rn), dog (cf), cow (bt), zebrafish (dr), African clawed toad (xl), *Saccharomyces cerevisiae* (scGyp8), *Schizosaccharomyces pombe* (spGyp10), and *Kluyveromyces fragilis* (KITBC1D20). Only full length sequences were included. Identical amino acids are coloured in red on a yellow background. Dark blue letters on a light blue background indicate a high degree of conservation. Dark blue letters on a green background show similar amino acids. Red arrowheads indicate the conserved arginine and glutamine residues required for GTP hydrolysis.

3.2.6 Over-expression of TBC1D20 causes a unique “loss of Golgi” phenotype

TBC1D20 was unique amongst the GAPs that caused Golgi fragmentation since it triggered a complete loss of defined Golgi structures. To further investigate this “loss of Golgi” phenotype, markers for different Golgi sub-compartments were analysed in cells over-expressing TBC1D20: the Rab1 effector p115 (Alvarez et al., 1999) that localises to the cis-Golgi and ERGIC; the cis-Golgi transmembrane protein Golgin84 (Bascom et al., 1999; Diao et al., 2003); and Golgin97, which localises to the TGN via its ARF1 interacting GRIP domain (Barr, 1999; Griffith et al., 1997; Lu and Hong, 2003).

The expression of TBC1D20 resulted in the loss of recognizable Golgi or punctate vesicular staining for all of these markers (Figure 3-7A). The specific staining was barely detectable by immunofluorescence and appeared as a haze distributed throughout the cytoplasm. On the other hand, the expression of TBC1D20 did not alter the staining of the endosomal Rab5 effector EEA1 (Figure 3-7A). The morphology of the Golgi apparatus was not affected by the expression of catalytically inactive TBC1D20^{R105A} (Figure 3-7B) although a similar expression level and distribution was observed.

These data show that TBC1D20 specifically perturbs all compartments of the Golgi, but doesn't have an effect on other sub-cellular compartments like early endosomes. Taken together with the observation that catalytically inactive TBC1D20 did not have an effect on the morphology of the Golgi apparatus, these data suggest that the “loss of Golgi” phenotype is due to inactivation of a Rab involved in regulation of trafficking events at the Golgi.

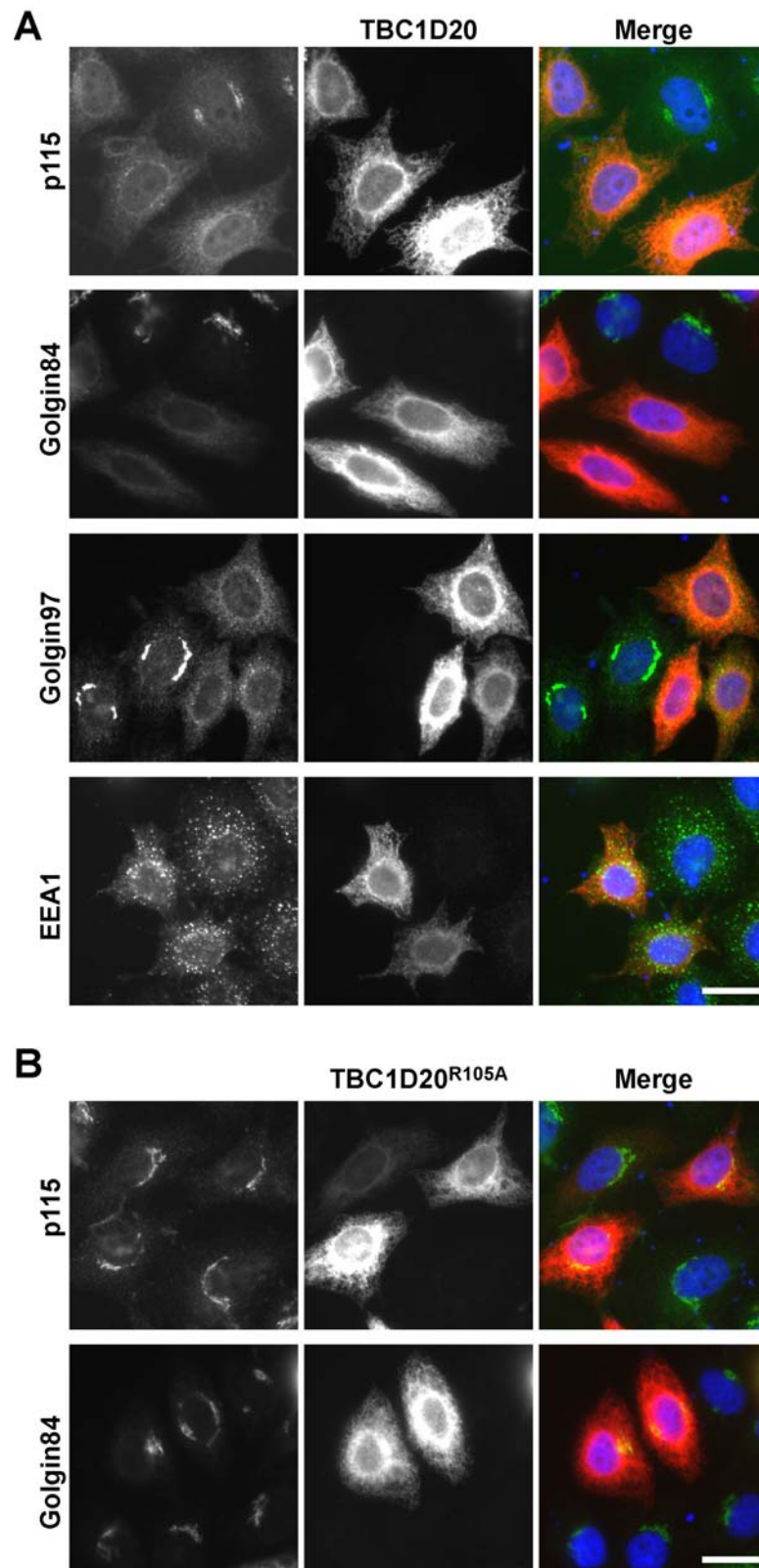


Figure 3-7 TBC1D20 causes a “loss of Golgi” phenotype. HeLa cells were transfected with myc epitope-tagged (A) wild type or (B) catalytically inactive TBC1D20^{R105A} for 24 hours. The cells were then fixed and stained with antibodies against the myc epitope tag (red), p115 (green), Golgin84 (green), Golgin97 (green) or EEA1 (green). Bars indicate 10 μ m.

The “loss of Golgi” phenotype in cells expressing TBC1D20 raised the question of the fate of the Golgi proteins. Various fates are conceivable: integral membrane proteins such as Golgi enzymes might be redistributed to other membrane compartments or become degraded by missorting to lysosomes; peripheral membrane proteins such as GM130 or p115 might be degraded by the proteasome or might be relocated to the cytosol; the Golgi proteins might also reside on or in membrane structures that are too small to be resolved by immunofluorescence. To test these possibilities a series of experiments was performed.

First, the fate of a Golgi-enzyme was studied. N-acetylglucosaminyltransferase-I (NAGT-I) is a protein of the *medial*- and *trans*-Golgi (Nilsson et al., 1993). It is specifically retained in these Golgi cisternae by its transmembrane domain and stalk region (Nilsson et al., 1996) and initiates the conversion of N-linked oligosaccharides to the complex type (Dunphy et al., 1985).

HeLa cells were transfected with GFP-tagged NAGT-I. The cells were then incubated for 10 hours to start the expression of NAGT-I and to localise it to the *medial*- and *trans*-Golgi. After 10 hours the cells were transfected with myc-epitope-tagged wild-type or catalytically inactive TBC1D20^{R105A}. After a total time of 22 hours the cells were fixed and stained with the antibodies indicated.

NAGT-I localised to the Golgi in cells that only expressed the GFP-tagged protein (Figure 3-8). In cells co-expressing wild-type TBC1D20 NAGT-I failed to co-localise with the Golgi marker GM130 (Figure 3-8), which was diffusely dispersed throughout the cytoplasm. Instead, it was found to localise to a reticular structure. When cells were stained for the ER marker calnexin, NAGT-I was found to co-localise with calnexin (Figure 3-8) in cells expressing wild-type TBC1D20. This shows that NAGT was redistributed to the ER. In cells expressing catalytically inactive TBC1D20^{R105A}, NAGT-I was found in the Golgi and did not redistribute to the ER (Figure 3-8). The redistribution of NAGT-I was therefore due to the specific inactivation of a Rab GTPase by TBC1D20.

These data show that Golgi enzymes such as NAGT-I are redistributed to the ER in cells over-expressing TBC1D20.

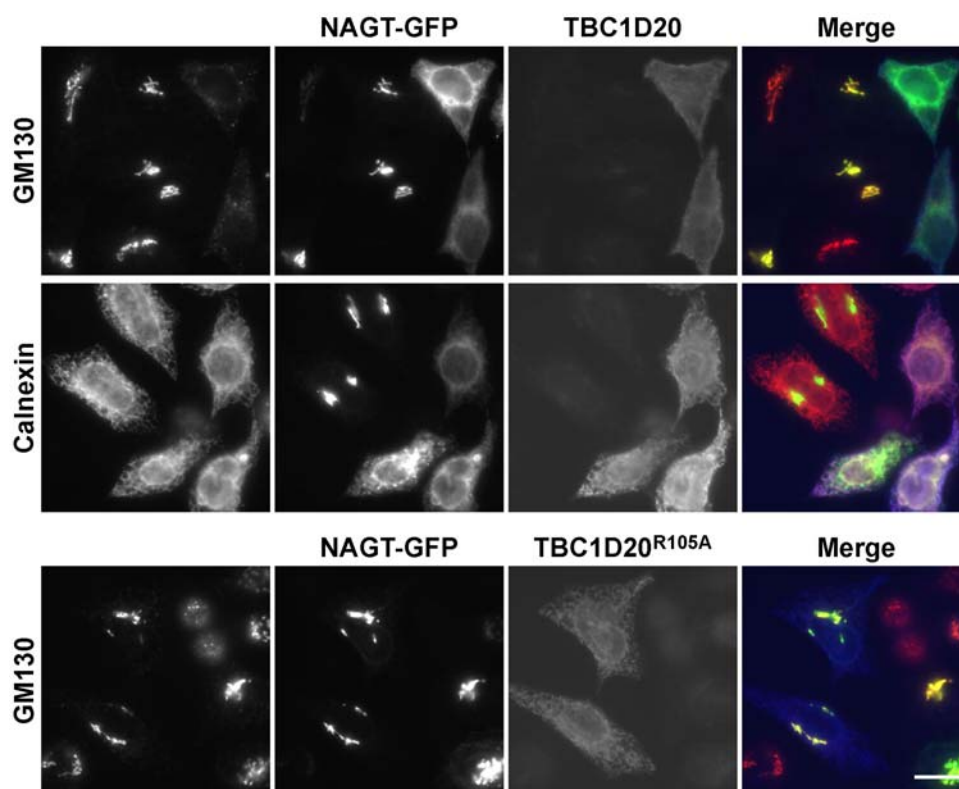


Figure 3-8 Expression of TBC1D20 redistributes Golgi enzymes to the ER. HeLa cells were transfected with GFP-tagged NAGT-I (green) for 10 hours. Then they were transfected with Myc-tagged wild-type or catalytically inactive TBC1D20^{R105A} for further 12 hours. The cells were then fixed and stained for GM130 (red) or Calnexin (red) and the myc-epitope tag (blue). The bar indicates 10μm.

To test whether or not peripheral Golgi proteins are degraded in cells over-expressing TBC1D20 several western blot experiments were carried out. HeLa cells grown on 10 cm cell culture dishes were transfected for 24 hours with myc-epitope-tagged wild-type or catalytically inactive TBC1D20^{R105A}. The cells were then harvested, lysed in mammalian lysis buffer, and the lysate was cleared by centrifugation, and 20μg of these extracts were western blotted. The blots were probed with antibodies against the myc-epitope-tag, p115, GM130, and to tubulin as a loading control. Noticeably, the expression of wild-type and catalytically inactive TBC1D20^{R105A} reached similar levels (Figure 3-9A). Despite the high transfection efficiency, over 50% estimated by immunofluorescence, no change was observed in the levels of either GM130 or p115 in cells expressing TBC1D20 (Figure 3-9A). This finding shows that these Golgi proteins were not degraded in cells over-expressing wild-type TBC1D20.

To analyse whether or not the Golgi proteins were still membrane bound, a set of membrane fractionation experiments were carried out. For these experiments a 10 cm dish of HeLa cells was transfected with myc-epitope-tagged wild-type TBC1D20 for 24 hours. To

compare the TBC1D20 phenotype to other factors that cause Golgi fragmentation, another dish of HeLa cells was transfected with constitutive active Sar1^{H79G}. Expression of Sar1^{H79G} prevents un-coating of COPII and causes a phenotype similar to TBC1D20. (Ward et al., 2001; Yoshimura et al., 2004). Another dish of cells was not transfected but incubated with Brefeldin A (BFA) for 30 minutes prior to harvesting. BFA treatment also fragments the Golgi and blocks secretion (Lippincott-Schwartz et al., 1989). As a control a dish of non-transfected and non-treated cells was used.

The cells were harvested and broken open by passing them 40 times through a 27G needle. Nuclei and cell debris were removed by centrifugation for 5 min at 1000x g and 4°C. This post-nuclear supernatant was split into two equal halves. One of them was kept on ice and represents the total material. The other half was spun for 30 min at 100,000x g. The supernatant of this centrifugation contains all the cytosolic proteins. Membranes and membrane bound proteins are found in the pellet fraction. The distribution of proteins between membranes and the cytoplasm can be analysed by western blotting these fractions.

The peripheral membrane protein GM130 and the integral membrane protein Golgin84 remained associated with the membranes to the same extent in control cells and in cells expressing wild type TBC1D20 (Figure 3-9B). The same was true in cells expressing Sar1^{H79G} or treated with BFA (Figure 3-9B). Under the same conditions, the membrane-associated pool of the Rab1 effector p115 was lost in cells expressing TBC1D20 (Figure 3-9B). This loss was not due to Golgi fragmentation, as BFA treatment and Sar1^{H79G} expression did not have an effect on the distribution of p115 (Figure 3-9B). The fractionation experiments also showed that TBC1D20 is associated with membranes (Figure 3-9B)

Taken together, these results show that Golgi proteins have different fates in cells expressing TBC1D20. Golgi enzymes are redistributed to the ER. Golgi matrix proteins such as GM130 or Golgin84 remain associated with membranes. They appear as a haze in immunofluorescence and are therefore likely to be associated with vesicles that are too small to be resolved by the light microscope. This suggests that the Golgi apparatus is vesiculated in the “loss of Golgi” phenotype. The Rab1 effector p115 was lost from the membrane fraction in TBC1D20 expressing cells. This indicates that the phenotypes observed in cells over-expressing TBC1D20 might be due to defects in the Rab1-p115 dependent COPII vesicle-tethering pathway. It also suggests that TBC1D20 may act as a GAP for Rab1, as p115 requires active Rab1 for its membrane association (Allan et al., 2000).

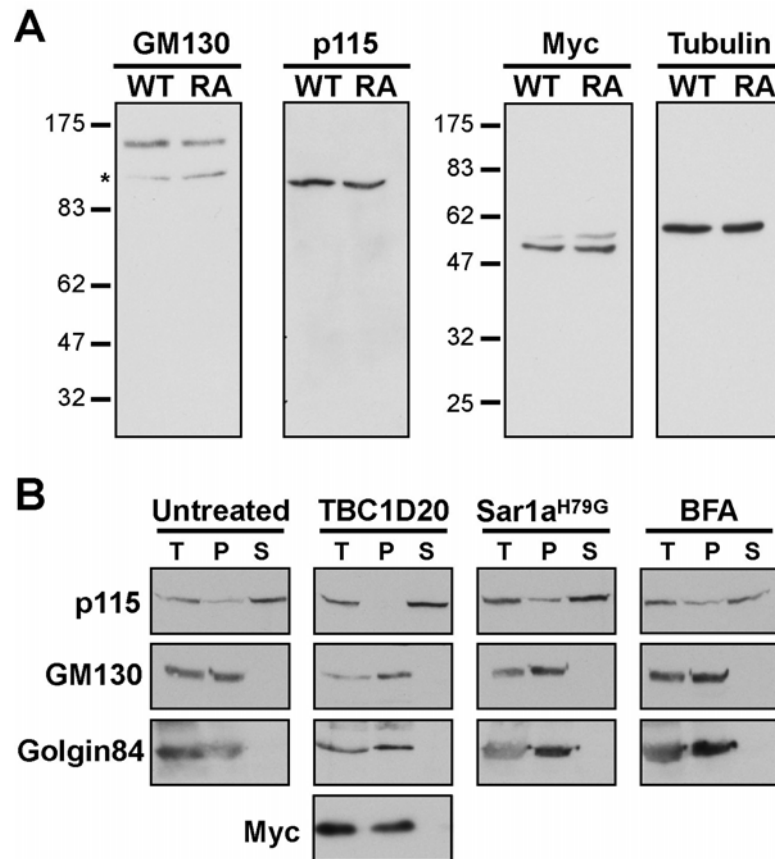


Figure 3-9 TBC1D20 displaces p115 from membranes. (A) HeLa cells were transfected with either wild-type (WT) or catalytically inactive TBC1D20^{R105A} (RA) for 24 hours. 20µg of cell extracts were western blotted and probed for GM130 and p115. The myc-epitope shows the expression of TBC1D20, and α -tubulin acts as a loading control. The asterisk indicates a GM130 breakdown product. (B) HeLa cells left untreated, expressing myc-tagged TBC1D20 or Sar1^{H79G} for 24 hours, or treated with BFA for 30 minutes were harvested and fractionated. Equivalent amounts of the total lysate (T), the membrane pellet (P), or the soluble cytosolic fraction (S) were western blotted and probed for p115, GM130, Golgin84 and the myc-epitope-tag, respectively.

3.2.7 TBC1D20 blocks exit of VSV-G from the ER

Next, the block of VSV-G trafficking in cells over-expressing TBC1D20 was studied in more detail. Wild-type or catalytically inactive TBC1D20^{R105A} were co-transfected with a plasmid encoding VSV-G into HeLa cells. The experimental setup was as described in 3.2.4. COPII positive structures were stained with antibodies against Sec31 and the Golgi was stained for GM130. After 60 minutes cells were fixed without detergent extraction to stain VSV-G at the plasma membrane.

At $t=0$ VSV-G accumulated in the ER (Figure 3-10) independent of TBC1D20. The amount of VSV-G was the same in cells transfected with either wild-type or catalytically inactive TBC1D20^{R105A} as judged by immunofluorescence. This indicates that the absence of

VSV-G at the cell surface (Figure 3-5A, B) was not simply due to the lack of synthesised viral protein. VSV-G did not co-localise with COPII positive structures at this time point.

After 10 minutes VSV-G started to leave the ER in cells expressing TBC1D20^{R105A} as well as in cells expressing only VSV-G (Figure 3-10). The GFP-tagged VSV-G co-localised with COPII positive structures at this time point. This shows that a wave of folded VSV-G started to exit the ER. In cells expressing wild type TBC1D20 however, the viral protein was retained in the ER (Figure 3-10).

After 30 minutes of transport, the majority of VSV-G was found at the Golgi in cells expressing only VSV-G or both VSV-G and TBC1D20^{R105A} (Figure 3-10). In cells expressing wild-type TBC1D20 it was still retained in the ER (Figure 3-10).

At t=60 VSV-G reached the cell surface in cells expressing TBC1D20^{R105A} (Figure 3-10). The same was true for cells only expressing VSV-G. Even after 60 minutes VSV-G did not exit the ER in wild-type TBC1D20 expressing cells (Figure 3-10). VSV-G did not accumulate at any structures at the ER. This shows that VSV-G was not recruited to ERES in cells expressing wild-type TBC1D20.

These data show that TBC1D20 blocks trafficking of VSV-G dependent on its catalytic activity. Importantly, VSV-G is retained in the ER and does not accumulate in COPII positive structures or at ERES. These data suggest a role for TBC1D20 and the Rab it regulates at the level of the ER.

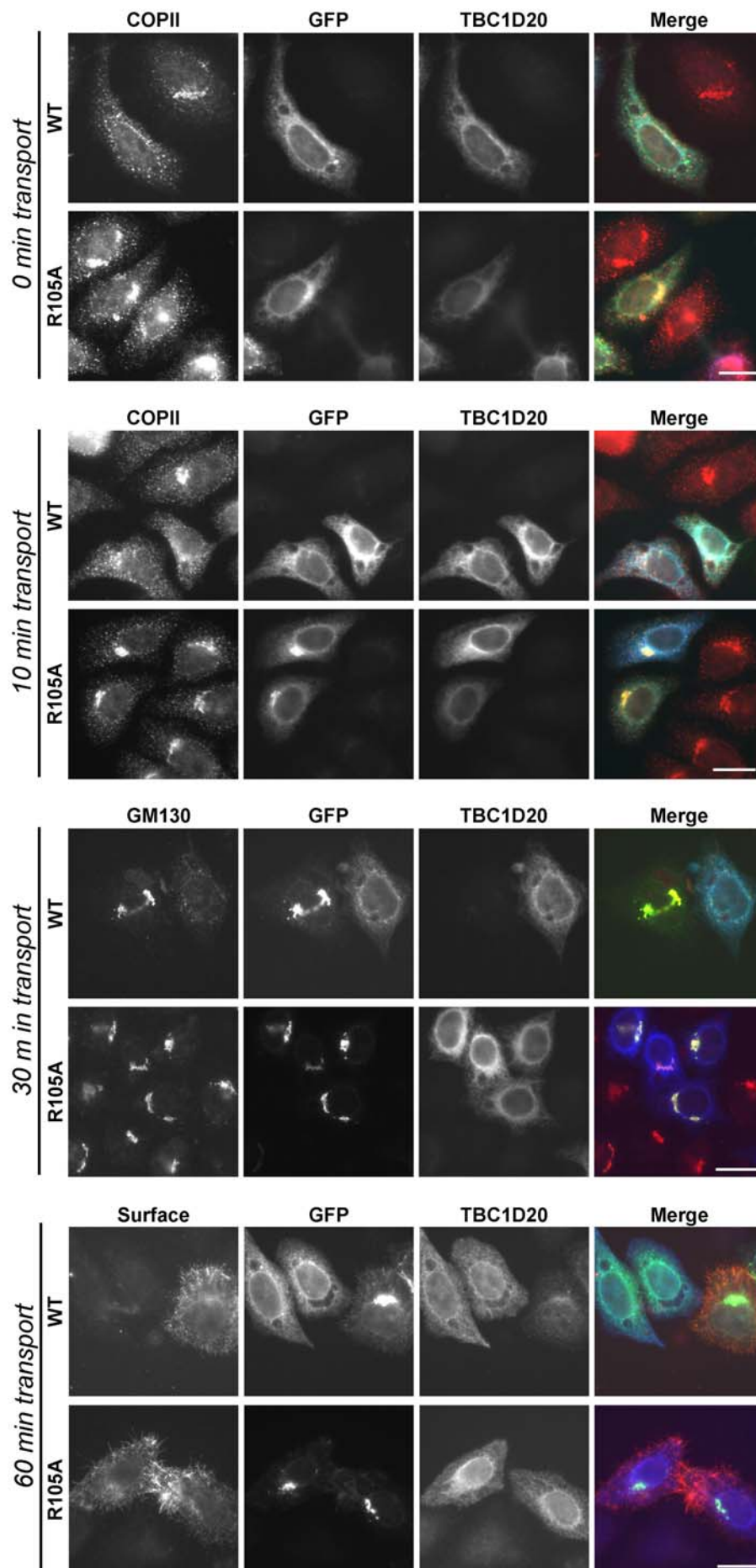


Figure 3-10 TBC1D20 blocks VSV-G trafficking at the ER. VSV-G transport assays were performed for a total time of 15 hours in HeLa cells expressing myc-epitope-tagged wild-type (WT) or catalytically inactive TBC1D20^{R105A} (RA). The cells were fixed at the time points indicated and stained for the myc-epitope-tag (blue), Sec31 (red at t=0, t=10), GM130 (red at t=30) or surface VSV-G (red at t=60). GFP shows total VSV-G. The bars indicate 10 μ m.

3.2.8 TBC1D20 expression causes scattering of COPII

Budding of vesicles from the ER and trafficking between the ER and the Golgi depends on the COPII coat. The block of ER to Golgi transport in cells expressing TBC1D20 might therefore be linked to defective COPII function.

COPII vesicles are formed at ERES (Hammond and Glick, 2000). The activation of the small GTPase Sar1 leads to the consecutive stepwise recruitment of the heterodimeric COPII subunits Sec23/24 and Sec13/31 (Barlowe et al., 1994). The curvature of the sub-complexes deforms the membrane and leads to abscission of the vesicles (Bonifacino and Glick, 2004). COPII vesicles form clusters, and consequently the ERGIC, dependent on the Rab1-p115 tethering pathway (Allan et al., 2000).

HeLa cells were transfected with myc-epitope-tagged wild-type or inactive TBC1D20^{R105A} for 24 hours to study COPII in more detail. The cells were then fixed and stained for Sec31 or Sec24C, respectively. In control cells COPII positive structures accumulated in the perinuclear region (Figure 3-11 A). In cells expressing wild-type TBC1D20 no perinuclear accumulation of COPII positive structures was observed (Figure 3-11 A) in cells were stained for Sec31 or Sec24 (Figure 3-11 B). The peripheral COPII structures on the other hand were not affected. This indicates that COPII clustering but not COPII vesicle formation is defective in cells over-expressing wild-type TBC1D20. In cells expressing catalytically inactive TBC1D20^{R105A} no scattering of COPII positive structures was observed (Figure 3-11A, B). The COPII positive structures observed in these cells were comparable to non-expressing control cells. This shows that the phenotype is due to the specific inactivation of a target Rab.

TBC1D20 therefore interferes with the clustering of COPII vesicles that depends on the Rab1 effector p115. This finding fits with the observation that p115 is lost from membranes in cells over-expressing wild-type TBC1D20.

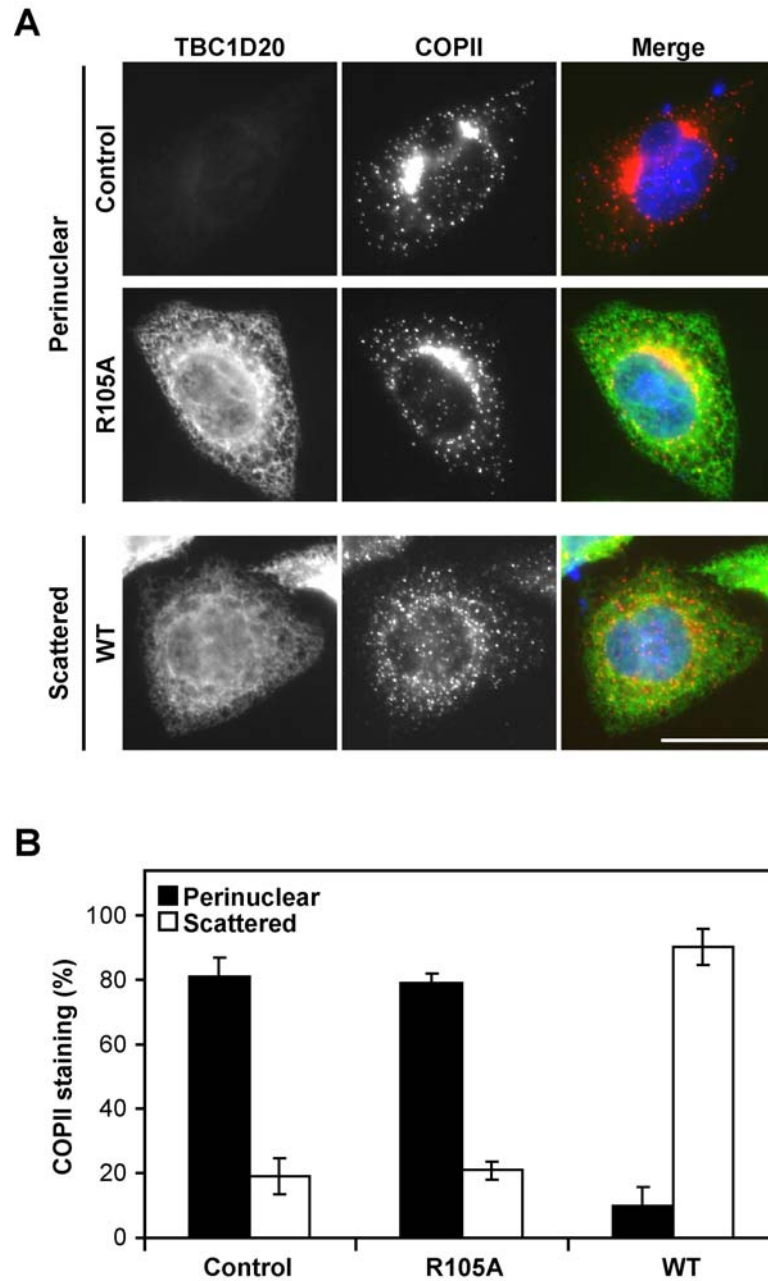


Figure 3-11 TBC1D20 expression causes COPII scattering. HeLa cells were transfected with myc-epitope-tagged wild-type (WT) or catalytically inactive TBC1D20R^{105A} (R105A) for 24 hours before fixation. (A) The cells were stained for the myc-epitope (green) and Sec31 (red). Bar corresponds to 10 μ m. (B) n=100 cells stained for Sec31 or Sec24C were analysed and the COPII staining was scored as either scattered or perinuclear as compared to neighbouring non-expressing cells.

3.2.9 TBC1D20 expression does not interfere with COPII dynamics

To analyse if over-expression of TBC1D20 blocks transport of cargo in the ER by interfering with the assembly of the COPII vesicle coat, the dynamics of COPII vesicle formation were analysed.

Fluorescence recovery after photobleaching (FRAP) was used in collaboration with Dr. David Stephens in the University of Bristol to study the dynamics of COPII vesicle formation in cells over-expressing TBC1D20. FRAP is a widely used technique (Presley, 2005; Reits and Neefjes, 2001) that exploits the fact that chromophores can be bleached in a defined area by a laser pulse of an appropriate wavelength. The fluorescence of the bleached area is then measured over time. By measuring the time needed to regain the fluorescence intensity after the laser pulse, the dynamics of a system can be studied.

As the COPII coat component Sec23 has GAP activity towards the small GTPase Sar1 required for COPII coat formation, it causes destabilisation and dissociation of the coat (Bickford et al., 2004). Therefore the COPII coat undergoes a cycle of disassembly and reassembly until the vesicle buds of the ERES. If TBC1D20 blocks ER exit by interfering with COPII dynamics, the FRAP kinetics of COPII should be different in cells over-expressing TBC1D20. The fluorescence of the COPII component Sec16 (Connerly et al., 2005; Watson et al., 2006) in cells expressing TBC1D20 was regained 50 seconds after bleaching (Figure 3-12A). Compared to the turnover of COPII components in control cells no change in the fluorescence recovery kinetics was observed (Figure 3-12B, C). This shows that TBC1D20 does not interfere with the dynamics of COPII vesicle formation.

This finding indicates that the block of ER exit and the altered distribution of COPII positive structures in cells expressing TBC1D20 cannot be explained by alteration in the dynamics of COPII coat assembly. These effects are therefore likely to be caused by the inactivation of a Rab required for both COPII vesicle clustering or cargo exit from the ER.

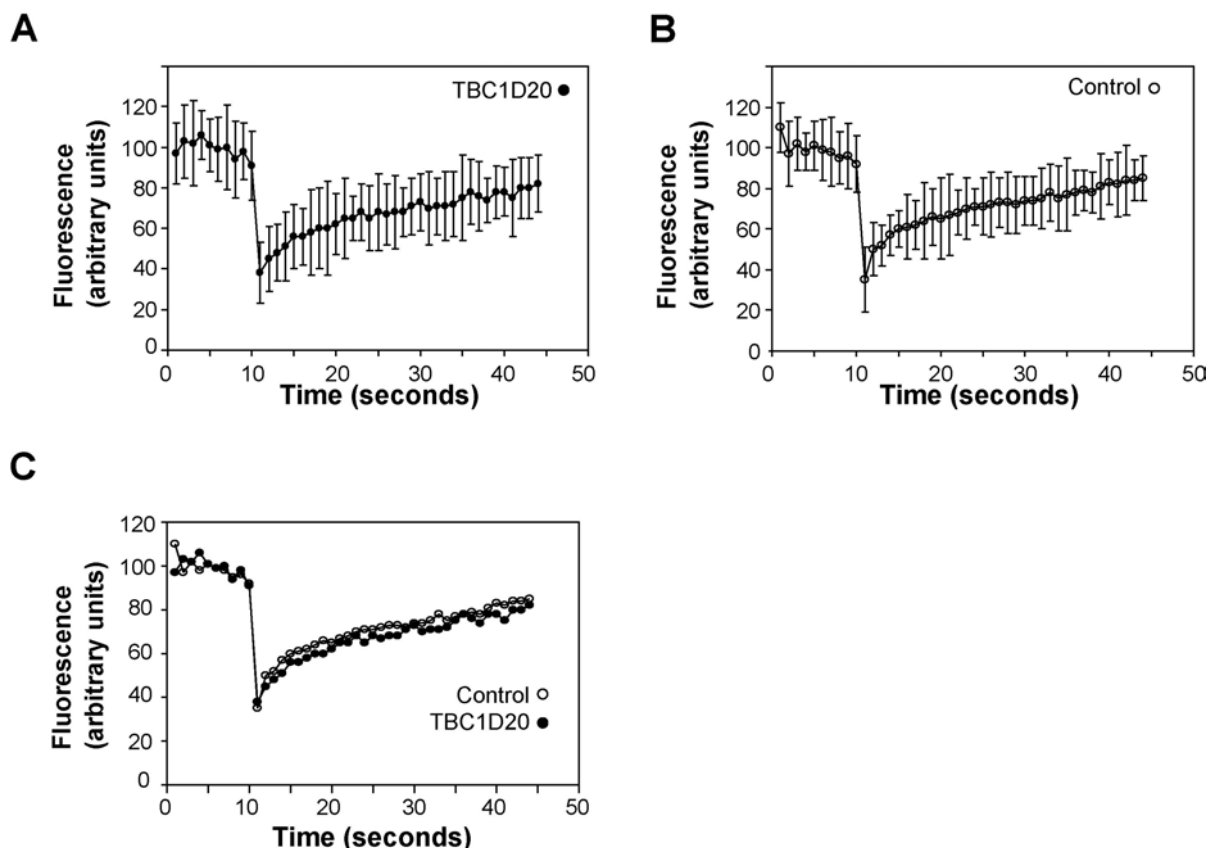


Figure 3-12 COPII dynamics are not affected by TBC1D20 expression. FRAP was performed on cells expressing (A) myc-epitope-tagged TBC1D20 and Venus- Sec16 or (B) in control cells only expressing Venus- Sec16. A Leica TCS SP3 AOBS scanning confocal microscope with a pinhole size of 2 Airy units, eightfold line averaging, was used at 1 frame per second, and region-of-interest bleaching with 10 iterations of the 514 nm laser at 100% AOTF power. Cells used for photobleaching were confirmed to express myc-epitope-tagged TBC1D20 by subsequent immunofluorescence; 95% of all cell transfected with Venus-Sec16 were found to be transfected with myc-epitope tagged TBC1D20. Plots are of the average intensity of individual structures over time; error bars indicate the standard deviation (five cells per experiment, $n=3$).

3.2.10 The cargo receptor p24 reveals a sorting defect caused by TBC1D20

As the expression of TBC1D20 did not alter COPII dynamics, defective cargo selection as a reason for the block of ER exit was investigated.

Both ERGIC-53, which recycles between the ERGIC and the ER, and p24, which recycles between the ER, the ERGIC and the Golgi were analysed. p24, a protein of a family of type-I membrane proteins, binds both COPI (Sohn et al., 1996) and COPII (Dominguez et al., 1998) to mediate its cycling. p24 proteins form oligomeric complexes (Denzel et al., 2000) and function as receptors for various cargo molecules (Fiedler et al., 1996), which are proposed to be enriched in budding vesicles by p24 (Schimmoller et al., 1995).

To analyse the effect of TBC1D20 over-expression on these molecules, HeLa cells were transfected with GFP-tagged p24 for 6 hours. Then the cells were transfected with

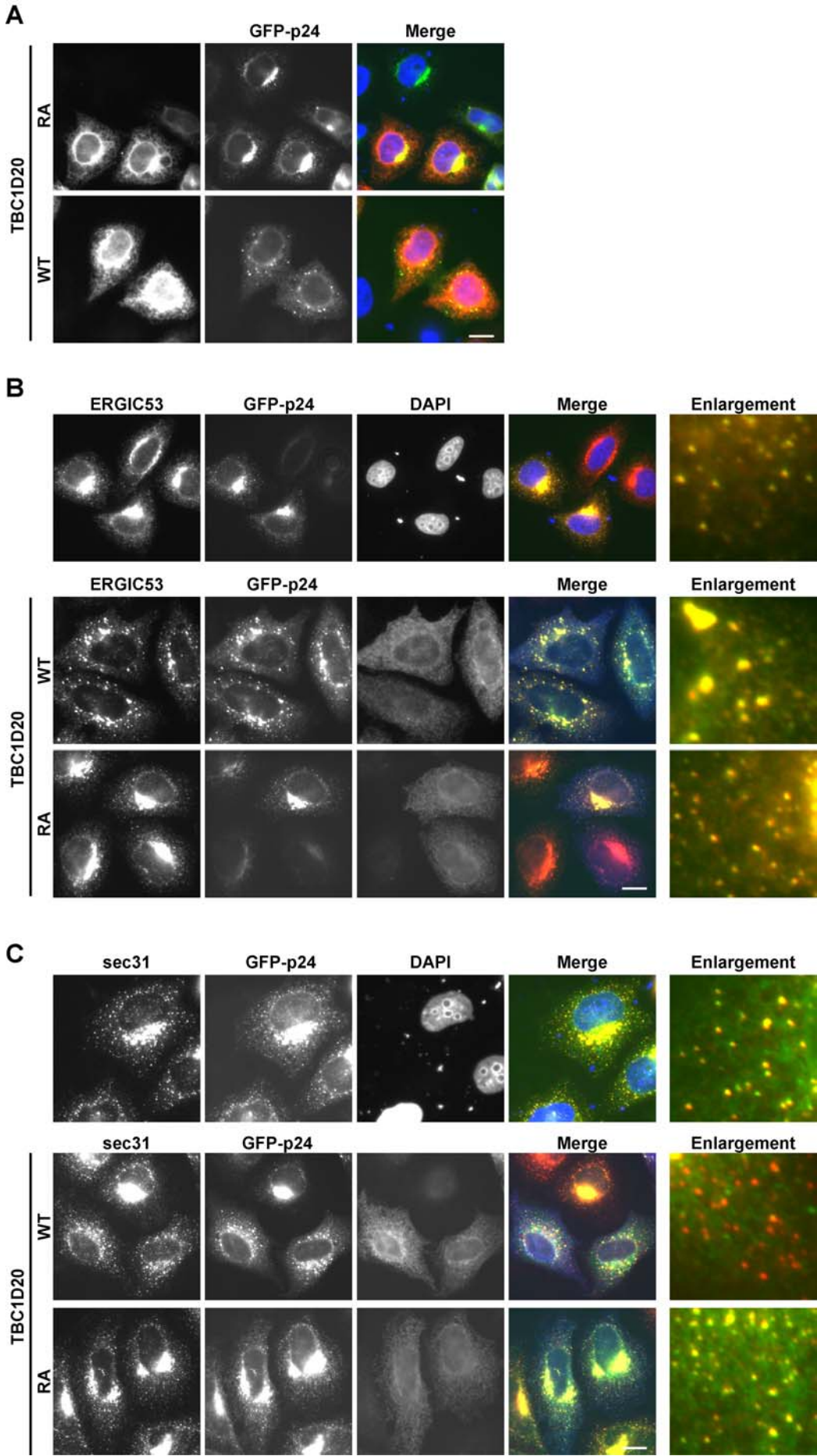
myc-epitope-tagged wild-type or catalytically inactive TBC1D20^{R105A} for a further 12 hours. The cells were then fixed and stained for ERGIC-53 or Sec31, respectively.

GFP-p24 localised to the ER, to ERES, the ERGIC and the Golgi apparatus in control cells. GFP-tagged p24 largely co-localised with ERGIC-53 (Figure 3-13B) and did not alter the distribution of ERGIC-53 positive structures. Their co-localisation on small punctate structures, most likely ERES, is shown more clearly in the enlargement. In cells expressing wild-type TBC1D20 GFP-p24 localised to large punctate structures (Figure 3-13A). When cells expressing both wild-type TBC1D20 and GFP-tagged p24 were stained for ERGIC-53, both p24 and ERGIC-53 localised to the same large punctate structures (Figure 3-13B). Notably, the small punctate structures resembling ERES were no longer observed under these conditions. This can be seen more clearly in the enlargements.

When cells expressing GFP-tagged p24 were stained for Sec31 as a COPII marker, a large extent of co-localisation was observed, especially on small punctate ERES (Figure 3-13C). This is seen more clearly in the enlargement. In cells over-expressing wild-type TBC1D20 (Figure 3-13C), GFP-p24 localised to large structures whereas Sec31 was scattered throughout the cell as previously observed (Figure 3-11). Sec31 was also found on small punctate structures resembling ERES under these conditions. GFP-p24 did not co-localise with Sec31 in these structures in cells expressing wild-type TBC1D20. This is more clearly seen in the enlargement that shows red punctate structures stained for Sec31, which lack green GFP-p24 signal (Figure 3-13C). The expression of TBC1D20^{R105A} did not result in changes in the distribution of p24, ERGIC-53 or Sec31 in comparison to control cells (Figure 3-13A, B, C). This shows that the phenotypes observed are due to the catalytic activity of TBC1D20.

These data show that cargo receptors such as ERGIC-53 and p24 are absent from ERES in cells over-expressing TBC1D20. This finding might provide an explanation for the defect in trafficking of cargo from the ER under these conditions. These findings also show that the ERGIC is a functionally separate compartment that reacts distinct from the Golgi and COPII positive structures to the over-expression of TBC1D20.

Figure 3-13 Recycling ERGIC markers are lost from ERES in TBC1D20 expressing cells. See next page. HeLa cells were transfected with GFP-tagged p24 for 6 hours. Then they were transfected with wild-type (WT) or catalytically inactive (RA) myc-epitope-tagged TBC1D20 (blue). The cells were fixed after further 18 hours and stained for (A) the myc-epitope-tag (red), (B) ERGIC-53 (Red) and the myc-epitope-tag (blue) or (C) Sec31 (red) and the myc-epitope-tag (blue). GFP was visualized (A, B, C) directly (green). The enlargements correspond to 10x10 μm and only show red and green colour. The bars indicate 10 μm .



3.2.11 TBC1D20 is a GAP for Rab1 and Rab2 *in vitro*

To identify the target Rab of TBC1D20, a series of *in vitro* GTP-hydrolysis assays similar to the ones used to identify Rab5 as the target of RabGAP-5 was performed.

TBC1D20 could not be produced as a full-length recombinant protein in the same vector used for the production of RabGAP-5, probably due to the hydrophobic stretch (Figure 3-6). Without this stretch TBC1D20 was successfully produced in *E. coli* as a recombinant protein with a N-terminal MBP-tag and a C-terminal 6x His tag. Recombinant TBC1D20 was then tested for its ability to stimulate GTP hydrolysis by all human Rabs. For simplicity some Rab isoforms were omitted. The basal GTPase activity of the Rabs was subtracted from the activity stimulated by TBC1D20, so that only GAP mediated hydrolysis is shown.

TBC1D20 strongly stimulated GTP hydrolysis by Rab1 and Rab2 (Figure 3-14A). Some additional activity of TBC1D20 was observed towards Rab8A, Rab13, Rab18, and Rab35 (Figure 3-14A). All these Rabs are closely related members of the Rab1/Sec4 group (Figure 1-5). This might explain why TBC1D20 can activate them *in vitro*. TBC1D20 did not display GAP activity towards Sar1 and ARF1 (Figure 3-14 A). Both these non-Rab GTPases also belong to the Ras superfamily and are required for protein trafficking and the maintenance of normal Golgi structure (Bonifacino and Glick, 2004).

The minimal predicted TBC domain TBC1D20 aa 1-317 stimulated GTP hydrolysis by Rab1 to a similar extent as TBC1D20 aa 1-364 (Figure 3-14B). The catalytic activity of both the longer version of the protein and the minimal TBC domain was abolished when the catalytic arginine 105 of the TBC-domain was mutated to alanine (Figure 3-14B). When the glutamine 67 of Rab1 was mutated to leucine to restrict it in the GTP bound state the basal hydrolysis rate was strongly reduced (Figure 3-14B). TBC1D20 did not stimulate GTP hydrolysis by Rab1^{Q67L} (Figure 3-14B).

To investigate if TBC1D20 is the only GAP for Rab1 or Rab2, the five TBC domain proteins, which were able to disrupt the Golgi (see Figure 3-1 and Figure 3-2) or alter the structure of the ERGIC (see Figure 3-4), were produced in the same way as TBC1D20 and tested for their ability to stimulate GTP hydrolysis by Rab1 or Rab2. These assays showed that only TBC1D20, but none of the other GAPs was able to stimulate GTP-hydrolysis by Rab1 or Rab2 to a significant extent (Figure 3-14C). This finding is consistent with publications showing that the TBC1D22 family acts on Rab33 (Pan et al., 2006), and that

XM_037557 is a GAP for Rab8a (Yoshimura et al., 2007). RN-tre was already shown to be a GAP for Rab43 (Figure 2-11).

These experiments show that TBC1D20 is a GAP for Rab1 and Rab2 *in vitro*. They also show that TBC1D20 is the only GAP that causes Golgi fragmentation or changes in the ERGIC morphology that acts on Rab1 or Rab2.

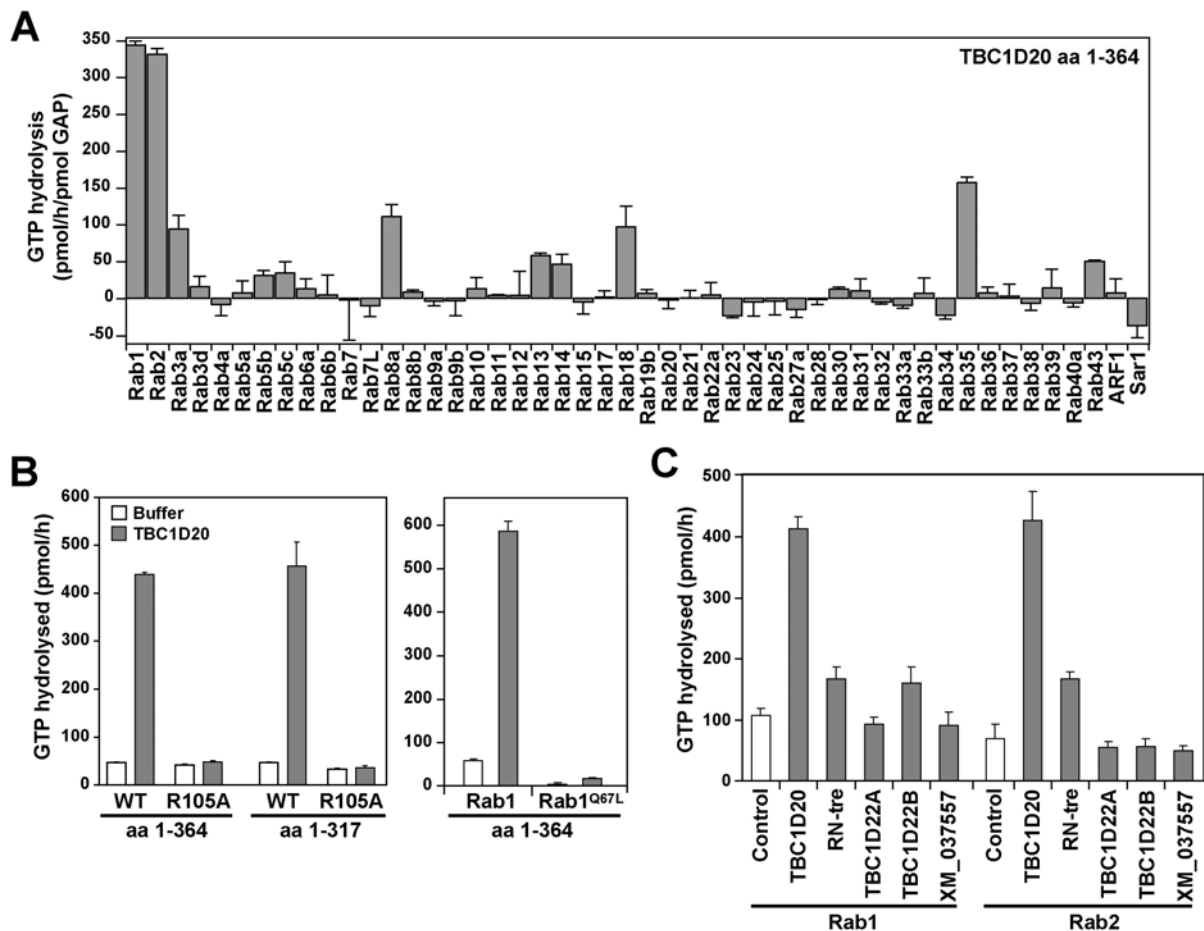


Figure 3-14 TBC1D20 is a GAP for Rab1 and Rab2 *in vitro*. All reactions were carried out for 60 minutes. (A) To determine the specific activity towards a wide range of GTPases, 0.5 pmoles TBC1D20 aa1-364 were tested against 100 pmoles of the GTPases indicated. The basal GTP hydrolysis with a buffer control was subtracted from TBC1D20 stimulated hydrolysis in each case. (B) 5 pmoles of wild-type and TBC1D20^{R105A} aa1-364 or the minimal TBC-domain aa 1-317 were tested against 100 pmoles of either wild-type Rab1 or Rab1^{Q67L}. Basal GTP hydrolysis with buffer is plotted as open bars and GAP-stimulated GTP hydrolysis as grey bars. (C) Buffer (control) or 0.5 pmoles of the GAP indicated were tested against 100 pmoles of Rab1 or Rab2. Basal GTP hydrolysis with buffer is plotted as open bars and GAP-stimulated GTP hydrolysis as grey bars.

3.2.12 Dominant negative Rab1^{N121I} mimics the TBC1D20 phenotype

To narrow down the target of TBC1D20 *in vivo*, the phenotypes caused by expression of dominant-negative Rabs were compared to the phenotypes caused by the over-expression of

TBC1D20. Dominant negative Rabs are generated by mutations that either keep the Rab in a nucleotide free state or prevent GEFs from reloading them with GTP. HeLa cells were transfected with dominant negative GFP-tagged Rabs for 24 hours. The cells were then fixed, and stained for the Golgi marker GM130 or the COPII marker Sec31, respectively. Dominant-negative Rab43^{T32N} was used as a positive control (Fuchs et al., 2007).

When n=100 cells were analysed only Rab43^{T32N} and Rab1^{N121I} fragmented the Golgi and scattered COPII positive structures (Figure 3-15A). None of the other Rabs that were activated by TBC1D20 *in vitro* caused significant changes to either structure.

In cells expressing Rab43^{T32N} small COPII clusters were observed that probably localised to the Golgi fragments that were observed under these conditions (Figure 3-15B). Dominant negative Rab1^{N121I} on the other hand caused a “loss of Golgi” phenotype and scattered COPII into evenly sized structures throughout the cell (Figure 3-15B). These phenotypes mimic the phenotypes observed in cells over-expressing wild-type TBC1D20 (Figure 3-7, Figure 3-11). The expression of neither wild-type nor constitutive active Rab1^{Q67L} had an effect on the Golgi morphology or the distribution of COPII (Figure 3-15A, B). This shows that the phenotypes observed were not simply due to elevated Rab1 levels. These findings indicate that TBC1D20 acts as a specific Rab1 GAP *in vivo*.

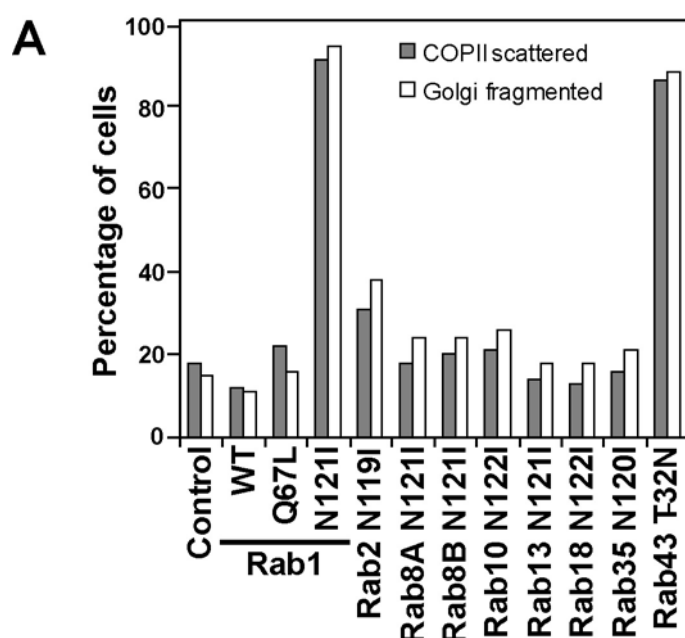
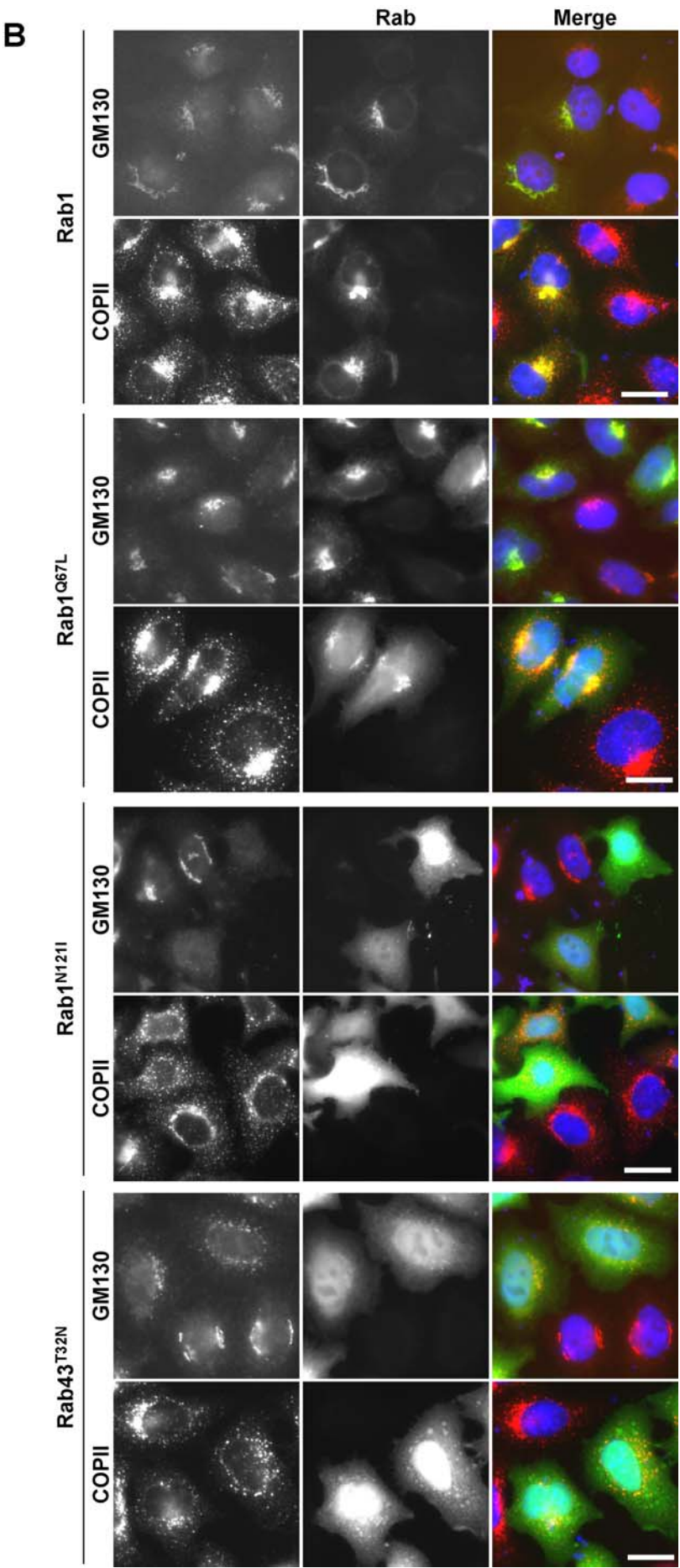


Figure 3-15 Dominant negative Rab1 causes a “loss of Golgi” phenotype. HeLa cells were transfected with GFP-tagged Rabs for 24 hours. The cells were then fixed and (B, **see next page**) stained for GM130 (red) or Sec31 (red), respectively. (A) In n=100 cells the Golgi morphology was scored as either normal or fragmented in comparison to non-expressing neighbouring cells. The COPII distribution was scored as either perinuclear or scattered in comparison to neighbouring non-expressing cells. The bar indicates 10µm.



3.2.13 Depletion of Rab1 causes Golgi fragmentation

To further narrow down the *in vivo* target of TBC1D20, both Rab1 and Rab2 were depleted by siRNA. The expression of a dominant negative Rab or the specific GAP diminishes the amount of active Rab and thus inhibits processes dependent on active Rab. The same should be achievable by diminishing the endogenous Rab by siRNA.

To deplete HeLa cells of endogenous Rab1 or Rab2, respectively, cells were treated with specific siRNA duplexes or control siRNA for 72 hours. To check mRNA degradation, the cells were transfected with GFP-tagged wild-type Rabs for the last 24 hours. The cells were then fixed and stained for the Golgi marker GM130. Cell extracts were generated and 10µg were analysed by western blot and probed for the GFP tag. This method is proven to be an effective readout for mRNA depletion in the case of other Rabs (Fuchs et al., 2007).

Western blotting showed the depletion of the messages for Rab1 and Rab2 (Figure 3-16A). No GFP signal was observed by immunofluorescence for Rab1 and Rab2 as compared to control siRNA (Figure 3-16B,C).

Depletion of Rab2 caused scattering of the Golgi apparatus (Figure 3-16B). Remarkably, these Golgi fragments remained clustered in the perinuclear region. On the other hand, in cells depleted of Rab1 the Golgi apparatus was massively fragmented and vesiculated (Figure 3-16C). These fragments, in contrast to cells depleted of Rab2, were evenly distributed throughout the cytoplasm.

In contrast to expression of dominant negative Rab1^{N121I} or TBC1D20, in cells depleted of Rab1 the Golgi was only fragmented and no “loss of Golgi” phenotype was observed. The phenotype of Rab1 depletion, however, still resembles the TBC1D20 phenotype better than depletion of Rab2. This again suggests that Rab1 is the primary target of TBC1D20 *in vivo*.

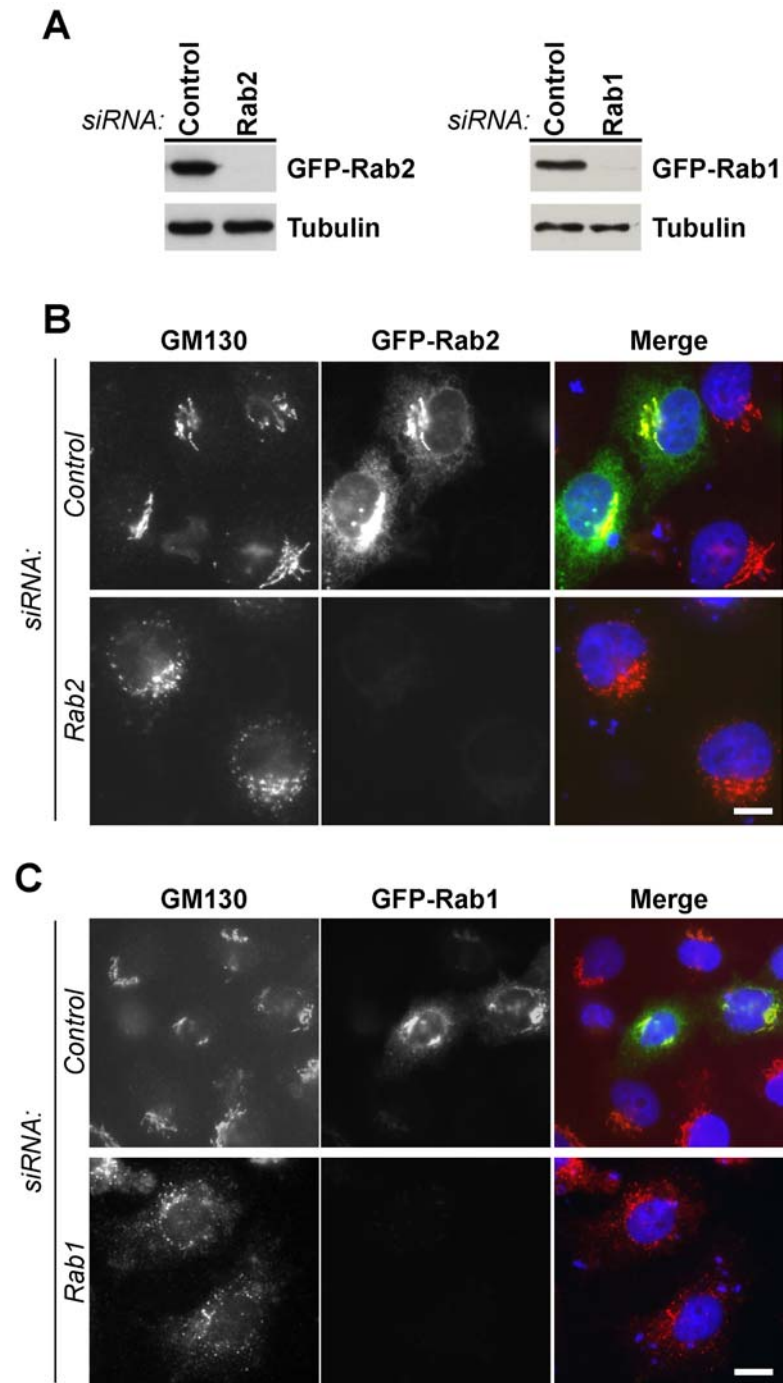


Figure 3-16 Rab1 depletion causes Golgi fragmentation. HeLa cells were treated with control, Rab1 or Rab2 siRNA duplexes for 72 hours were transfected for 24 hours with GFP-tagged Rab1 or Rab2, respectively. The cells were lysed and (A) analysed by western blot with antibodies against the GFP-tag to show mRNA depletion and α -tubulin as a loading control. (B) Cells treated equally with Rab2 specific or control siRNA duplexes were fixed and stained for GM130 (red). (c) Cells treated equally with Rab1 specific or control siRNA duplexes were fixed and stained for GM130 (red). The bars indicate 10 μ m.

3.2.14 Depletion of Rab1 but not Rab2 blocks VSV-G transport

To further narrow down the *in vivo* target Rab of TBC1D20, the trafficking of VSV-G was analysed in cells depleted of Rab1 or Rab2. The effects of depleting the Rab1 key effector p115 and the Rab1 and p115 interacting golgin GM130 on VSV-G trafficking were investigated as well. After 60 hours of depletion, HeLa cells were transfected with VSV-G and treated as previously described (see 3.2.7).

The depletion of Rab1 resulted in a block of VSV-G trafficking at the level of the ER (Figure 3-17B). The phenotype observed was similar to expression of TBC1D20 (Figure 3-10). Depletion of Rab2 on the other hand did not block anterograde transport of VSV-G from the ER to the cell surface, even though the Golgi was fragmented (Figure 3-17B). This shows that Rab1 but not Rab2 is essential for VSV-G trafficking.

The effects of depleting the Rab1 effector p115 and GM130 on VSV-G transport were then analysed. Western blotting showed that these proteins were specifically depleted by siRNA (Figure 3-17A). In cells depleted of p115 VSV-G left the ER and accumulated in a collapsed punctate structure. VSV-G didn't reach the cell surface after 60 minutes (Figure 3-17B). This finding demonstrates the importance of p115 in the regulation of trafficking steps between the Golgi and the ER. Even though GM130 is required for normal Golgi-ribbon and COPII vesicle organization (Puthenveedu et al., 2006), it was not required for VSV-G transport (Figure 3-17B). The Golgi was disrupted in cells depleted of GM130, but VSV-G was transported the plasma membrane after 60 minutes.

These data show that the block of VSV-G trafficking observed in cells over-expressing wild-type TBC1D20 is due to the inactivation of endogenous Rab1. They also show that Rab1 is the primary target of TBC1D20 *in vivo*. Although Rab1 binding proteins, such as its effector p115 and GM130 may contribute to the phenotypes caused by TBC1D20 overexpression, they can't explain why secretory cargo is blocked in the ER. This indicates that TBC1D20 and Rab1 have a function independent of these Rab1 binding proteins at the level of the ER.

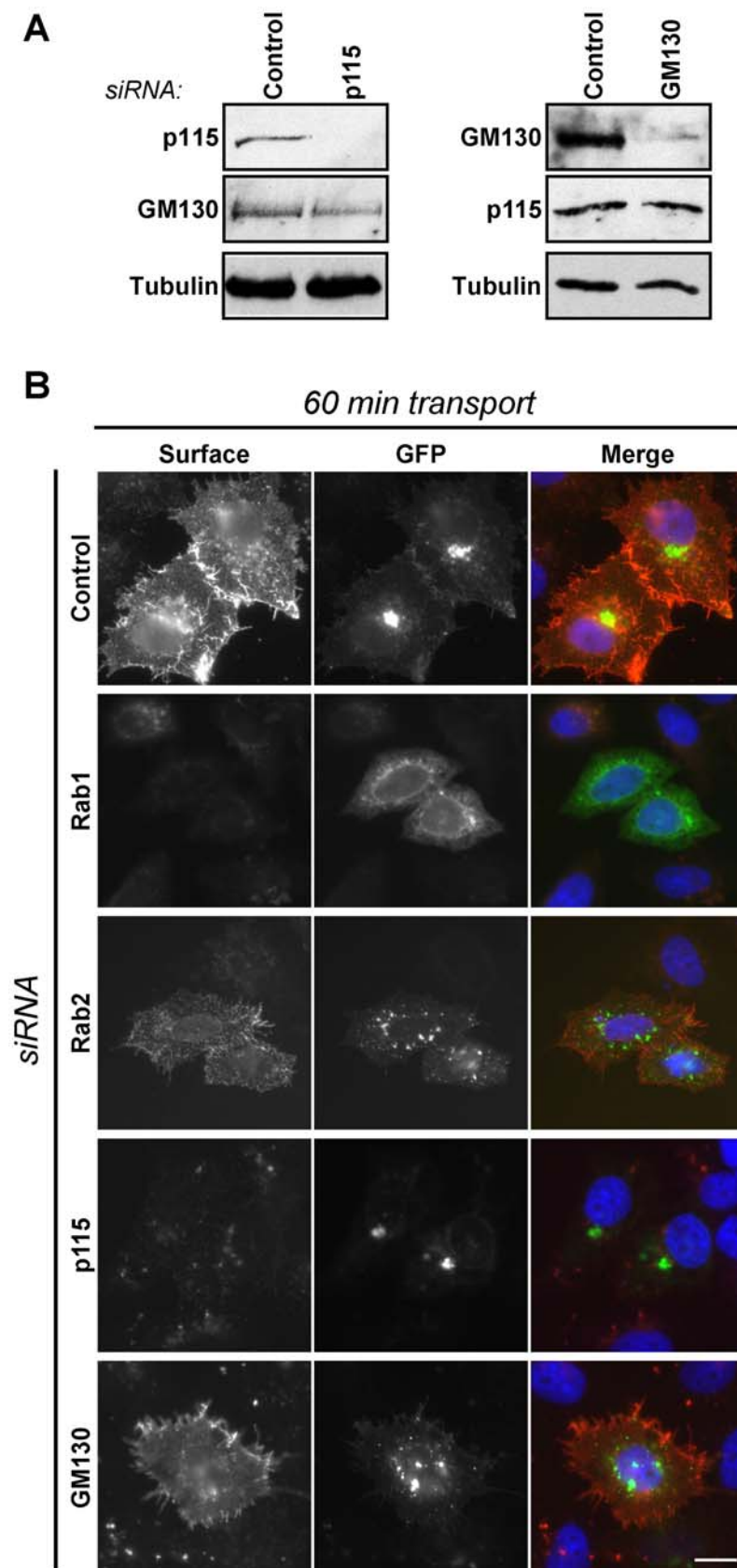


Figure 3-17 Depletion of Rab1 blocks VSV-G trafficking at the ER. VSV-G transport assays were performed for a total time of 15 hours in HeLa cells depleted of Rab1, Rab2, p115 or GM130. (A) GM130 and p115 were specifically depleted as shown by western blot. (B) Cells were fixed after 60 minutes and stained for surface VSV-G (red). GFP shows total VSV-G. The bar indicates 10 μ m.

3.2.15 Dominant negative Rab1^{N121I} blocks VSV-G transport

To consolidate that the block of VSV-G trafficking seen in cells expressing TBC1D20 is due to inactivation of Rab1, the effect of various Rab1 mutants on the trafficking of VSV-G was investigated.

HeLa cells were transfected with myc-epitope-tagged wild-type Rab1, constitutive active Rab1^{Q67L} or dominant negative Rab1^{N121I} and incubated at 37°C for 10 hours. Subsequently, the cells were transfected with a plasmid encoding VSV-G and treated as previously described (see 3.2.4).

For each Rab1 variant n=100 cells were analysed and dependent on the presence of VSV-G at the plasma membrane after 60 minutes they were scored as either block or transport. Only the expression of Rab1^{N121I} caused a block of VSV-G trafficking (Figure 3-18A). It blocked the exit of VSV-G from the ER (Figure 3-18B), similar to the phenotype in cells depleted of Rab1 or over-expressing wild-type TBC1D20. Cells expressing wild-type Rab1 did not show significant differences in transport when compared to non-expressing control cells (Figure 3-18A, B). The hydrolysis deficient (Figure 3-14B) Rab1^{Q67L} mutant did not cause a block of VSV-G transport to the plasma membrane (Figure 3-18A,B).

These findings support the idea that the ER exit of VSV-G depends on active Rab1. The depletion of endogenous Rab1 by siRNA or the over-expression of TBC1D20 showed the same phenotype as the expression of dominant negative Rab1^{N121I}. Surprisingly, the hydrolysis deficient Rab1^{Q67L} did not affect the transport of VSV-G as compared to control cells. According to the standard model, in which the GAP regulates the lifetime of active Rab, VSV-G should accumulate in COPII positive structures under these conditions, similar to EGF accumulating in early endosomes in Rab5^{Q79L} expressing cells (Fuchs et al., 2007). This suggests that in the case of Rab1 another regulatory mechanism is used.

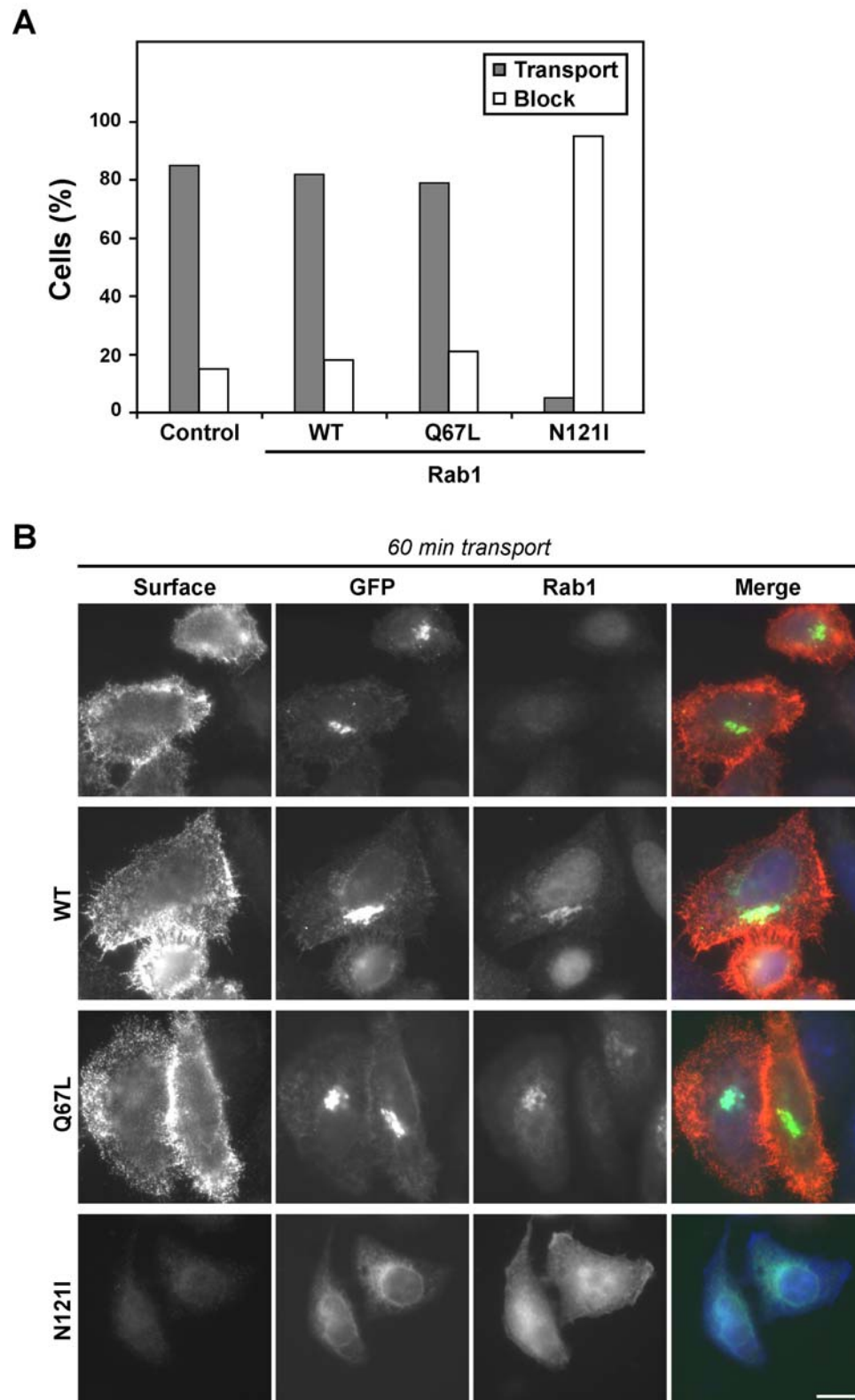


Figure 3-18 Dominant negative Rab1 blocks ER exit of VSV-G. VSV-G transport assays were performed for a total of 15 hours in HeLa cells expressing myc-epitope-tagged wild-type (WT) constitutive active (Q67L) or dominant negative (N121I) Rab1 (A) HeLa cells co-transfected with VSV-G and Rab1 were stained for surface VSV-G and the myc-epitope tag. $n=100$ cells were scored as either block or no block of trafficking. (B) Cells treated equally were fixed after 60 minutes and stained for surface VSV-G (red) and the myc-epitope-tag (blue). GFP indicates total VSV-G. The bar indicates 10 μm .

3.2.16 TBC1D20 depletion causes increased p115 clustering

To test whether or not endogenous TBC1D20 is required to regulate Rab1 in HeLa and hTERT-RPE1 cells it was depleted using specific siRNA oligonucleotides.

Various attempts with recombinant protein or synthetic peptides were made to generate an antibody against TBC1D20. None of these antibodies had high enough affinity to detect endogenous TBC1D20. To check the depletion of TBC1D20 therefore an approach similar to the one used for determining the depletion of Rabs (Figure 3-16) was used. HeLa cells were treated with specific siRNA duplexes to target TBC1D20 in parallel with control siRNA duplexes for 72 hours. For the last 24 hours, the cells were transfected with GFP-tagged TBC1D20^{R105A}. The inactive mutant was used to avoid the phenotype of TBC1D20 over-expression to interfere with the analysis of the siRNA-mediated depletion. The cells were fixed and stained for various markers of the early secretory pathway. Cells treated equally were lysed and 10µg were analysed by western blot.

Probing the western blot for with antibodies against GFP showed that TBC1D20 was efficiently silenced (Figure 3-19B). The intensity of the p115 staining was increased in cells depleted of TBC1D20 when compared to control cells (Figure 3-19A). The Golgi stained by p115 was also more compact. The staining pattern of GM130 was more compact in cells depleted of TBC1D20 as well, but it did not increase in its intensity (Figure 3-19A). COPII, stained with an antibody against Sec31, partially lost its perinuclear organization and was scattered in cells depleted of TBC1D20 (Figure 3-19A). More and smaller clusters compared to control cells were observed under these conditions.

These data show that endogenous TBC1D20 contributes to the organization of COPII vesicles, the formation of VTCs and the morphology of the Golgi complex. They furthermore agree that TBC1D20 functions as a Rab1 GAP *in vivo* as the observed phenotypes can be explained by elevated levels of active Rab1. More active Rab1 recruits more of its effector p115 to membranes. Rab1 binds GM130 (Moyer et al., 2001) but does not recruit it to Golgi membranes. The compaction observed is consistent with the idea that p115 is required for the clustering of pre- Golgi compartments. The formation of COPII clusters also depends on p115; therefore an increase in active Rab1 might cause the formation of too many independent structures.

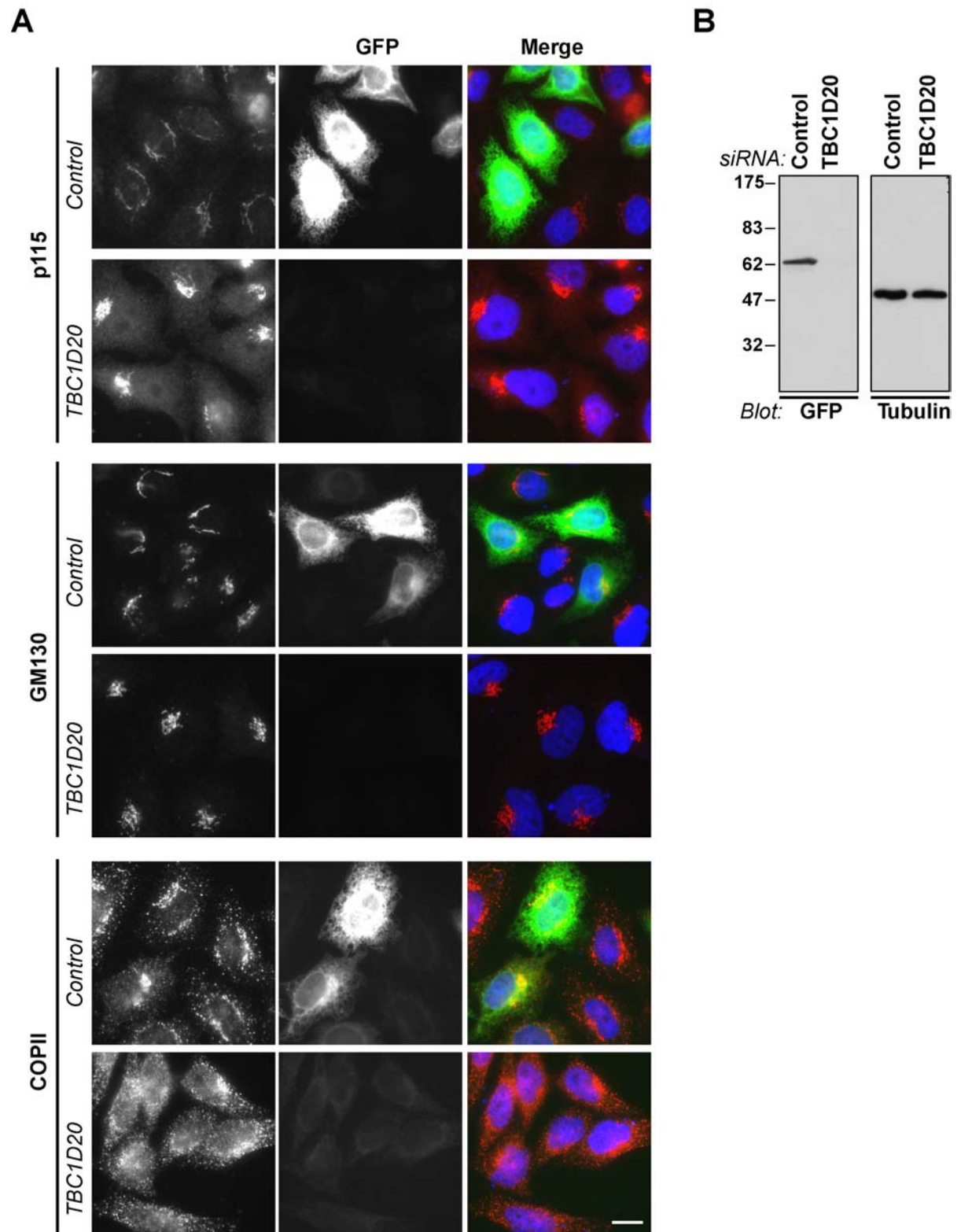


Figure 3-19 Depletion of TBC1D20 increases p115 staining and changes COPII distribution. HeLa cells treated with control (*Control*) or specific TBC1D20 siRNA duplexes (*TBC1D20*) for 72 hours were transfected with GFP-tagged TBC1D20^{R105A} for 24 hours and (B) analysed by western blotting with antibodies against the GFP-tag to show depletion and α -tubulin as a loading control. (A) Cells treated equally were fixed and stained for p115, GM130 or Sec31 (all red). Bars indicate 10 μ m.

Next, TBC1D20 was depleted in hTERT-RPE1 cells in the same way as in HeLa cells. The cells were stained for COPII using Sec31 as a marker.

In control hTERT-RPE1 cells the staining of COPII positive structures did not accumulate in the perinuclear region like in HeLa cells. Instead, the COPII positive structures were evenly distributed (Figure 3-20). In cells depleted of TBC1D20, an accumulation of these structures in the perinuclear region was observed (Figure 3-20). This clustering depends on the Rab1 effector p115. It indicates that there is more active Rab1 in cells depleted of TBC1D20, which recruits more p115 and thus causes increases clustering of COPII positive structures.

The data obtained by depleting TBC1D20 in different cell lines strongly suggest that it acts as the GAP for Rab1 *in vivo*. Its depletion led to increased p115 staining and amplified p115 dependent COPII clustering. Both of these effects are most likely due to elevated levels of active endogenous Rab1.

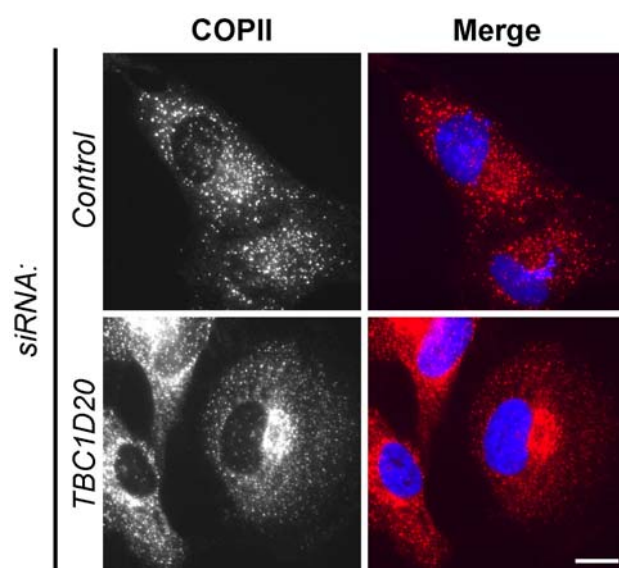


Figure 3-20 Depletion of TBC1D20 causes increased clustering of COPII. hTERT-RPE1 cells treated with control or specific TBC1D20 siRNA duplexes for 72 hours were fixed and stained with antibodies against Sec31 (red). The bar indicates 10 μ m.

3.2.17 The depletion of TBC1D20 does not block VSV-G trafficking

Surprisingly, the expression of Rab1^{Q67L} did not block VSV-G transport. Therefore the effect of the depletion of TBC1D20 on VSV-G trafficking was analysed. Both expression of Rab1^{Q67L} and depletion of TBC1D20 increase the amount of active Rab1 and should therefore cause the same phenotype.

TBC1D20 was depleted for 72 hours as previously (see 3.2.16). 14 hours prior to the fixation the cells were transfected with a plasmid encoding VSV-G and treated as described previously (see 3.2.4).

At the t=0 time point, equal amounts of VSV-G were found at the ER in both control and TBC1D20 depleted cells (Figure 3-21) as judged by microscopy. This shows that depletion of TBC1D20 did not affect the expression of VSV-G. After 5 minutes VSV-G was predominantly localised in COPII positive structures and after 30 minutes in the Golgi (Figure 3-21). Neither the disorganisation of COPII nor the compaction of the Golgi apparatus in cells depleted of TBC1D20 (see Figure 3-20) caused changes in VSV-G trafficking. In both the control and TBC1D20 depleted cells VSV-G was trafficking with similar kinetics. When the cell surface was stained for VSV-G after 60 minutes, in both control and TBC1D20 depleted cells VSV-G reached its destination.

These data show that depletion of TBC1D20 does not cause a block of the trafficking of VSV-G. This observation fits with the finding that Rab1^{Q67L} does not block VSV-G trafficking and is in contrast to the observations on EGF trafficking in the case of RabGAP-5 depletion (Figure 2-19) and Rab5^{Q79L} expression (Fuchs et al., 2007). Therefore, the regulation of Rab1 must differ from the regulation of Rab5 and does not fit the classical Rab cycle.

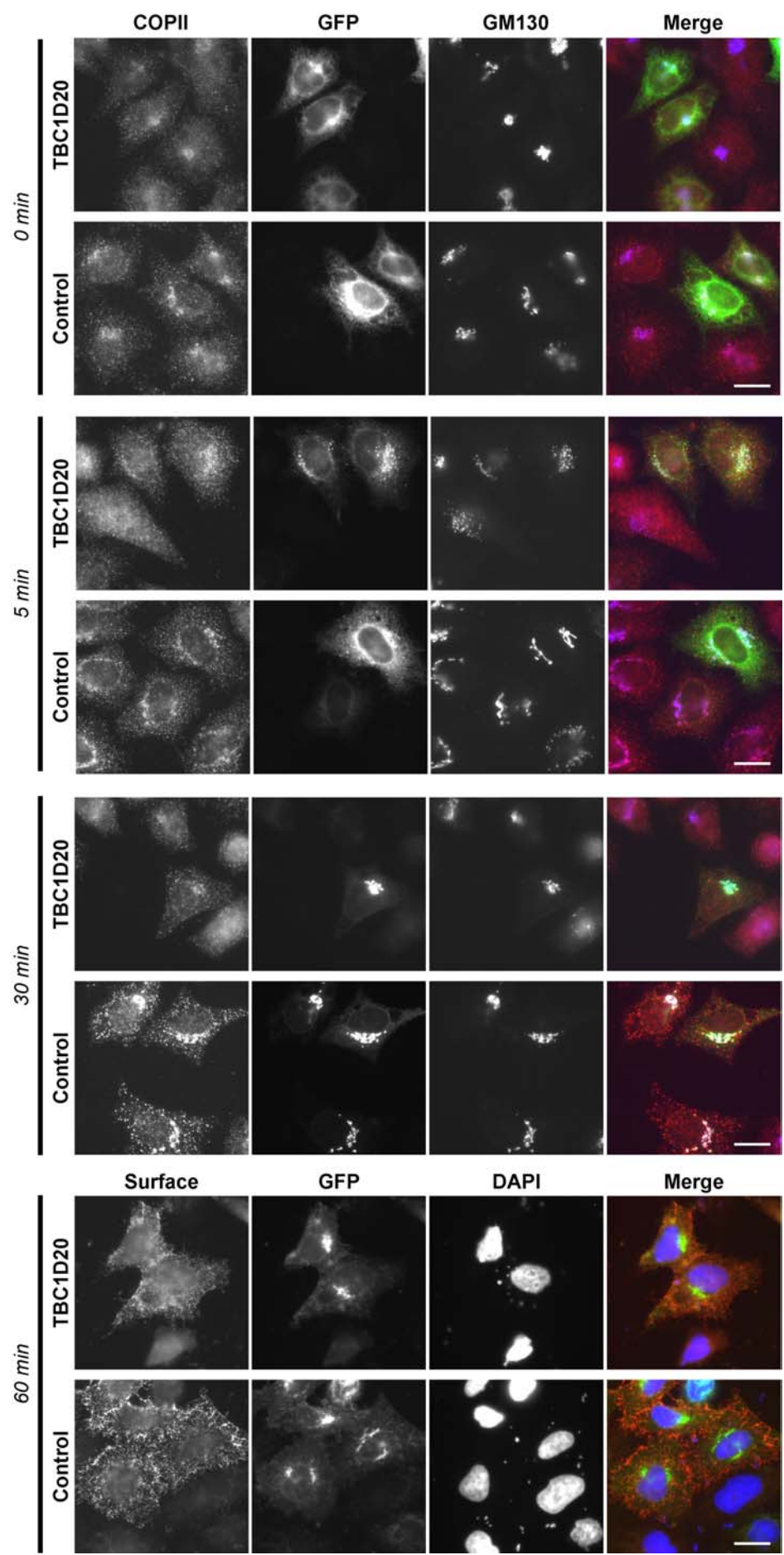


Figure 3-21 Depletion of TBC1D20 does not block VSV-G trafficking. HeLa cells were treated with TBC1D20 specific siRNA duplexes (TBC1D20) or control siRNA duplexes (Control) for 72 hours. VSV-G transport assays were performed for a total time of 15 hours. The cells were fixed at the time points indicated and stained for GM130 (blue, t=0,5,30) and Sec31 (red t=0,5,30) or surface VSV-G (red t=60). GFP indicates total VSV-G. The bars indicate 10 μ m.

3.2.18 TBC1D20 is a RabGAP localising to the ER

The results presented so far show that TBC1D20 controls the activity of Rab1. Inactivation of Rab1 blocked the exit of cargo molecules from the ER, but the depletion of the Rab1 effector p115 did not block ER exit. Therefore the question arose whether TBC1D20 and Rab1 have a function on the ER independent of p115.

HeLa cells were transfected with wild-type or catalytically inactive TBC1D20^{R105A}. After 24 hours the cells were fixed and stained for the ER marker Calnexin. TBC1D20 co-localised with calnexin independent of its catalytic activity (Figure 3-22). It localised to the tubulated portions of the ER and also to the ring like structure characteristic of the nuclear envelope. Even though expression of TBC1D20 causes a “loss of Golgi” phenotype and blocks trafficking at the ER, no change of the ER morphology was observed.

These data show that TBC1D20 is an ER localised RabGAP. As TBC1D20 regulates Rab1, they furthermore suggest the presence of Rab1 dependent processes on the ER.

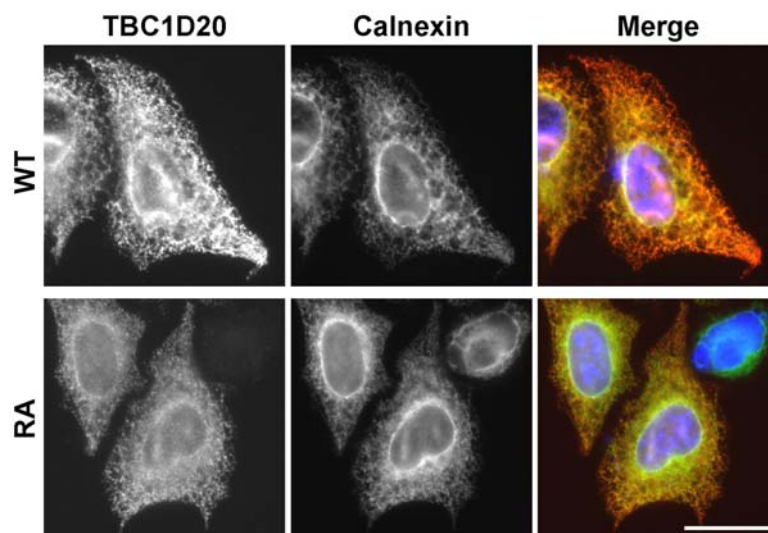


Figure 3-22 TBC1D20 localises to the ER. HeLa cells were transfected with myc-epitope-tagged wild-type (WT) or catalytically inactive TBC1D20^{R105A} (RA) for 24 hours and then fixed with PFA. The cells were stained with antibodies against the myc-epitope-tag (red) and Calnexin (green). The bar indicates 10 μ m.

3.2.19 TBC1D20 localises to the ER via a C-terminal TMD

Next, the ER localisation and the membrane association (Figure 3-9) of TBC1D20 were analysed in more detail. TBC1D20 has a hydrophobic stretch at its C-terminus (Figure 3-6).

To analyse whether or not TBC1D20 is an integral membrane protein a series of carbonate extraction experiments was carried out (Fujiki et al., 1982). These experiments use Na_2CO_3 to break open membrane bound compartments. This releases their content and removes peripheral membrane proteins. Integral membrane proteins on the other hand remain associated with membranes. A 15 cm dish of HeLa cells was transfected with GFP-tagged TBC1D20 for 24 hours. The cells were then harvested and broken open by passing them 40 times through a 27G needle. Nuclei and cell debris were removed by centrifugation for 5 min at 1000x g and 4°C to generate a post-nuclear supernatant (PNS). An aliquot of the PNS was split in two halves. One half was kept on ice as the total material (T), while the other was spun at 100,000-x g to generate a membrane pellet. The membrane pellet was resuspended in 100 mM Na_2CO_3 and incubated on ice for 30 min. To recover the membranes, the sample was spun at 100,000-x g again. The supernatant was precipitated with TCA and the pellet was resuspended in sample buffer. Equal amounts of the total (T), the carbonate extracted supernatant (SN) and the membrane pellet (P) were analysed by western blot.

TBC1D20 was found in the in the membrane fraction, but was absent from the supernatant (Figure 3-23A). The type-II transmembrane protein Golgin-84 (Bascom et al., 1999) behaved equally (Figure 3-23A). The peripheral membrane protein GM130 on the other hand was not found in the membrane fraction, but was precipitated from the supernatant (Figure 3-23A). These data show that TBC1D20 behaves like an integral membrane protein.

To analyse the topology of TBC1D20 in the membrane a series of proteinase K digestion experiments (Tarone et al., 1982) was carried out. Proteinase K digests proteins, but cannot penetrate through intact membranes. Therefore portions of proteins inside the lumen of organelles are only accessible to proteinase K digestion after detergent treatment. A 15 cm dish of HeLa cells was transfected with N-terminally GFP-tagged TBC1D20 for 24 hours. The cells were harvested and broken open. The cell suspension was cleared by centrifugation. The PNS was split into three equal aliquots: one was left untreated on ice; one was incubated in the presence of proteinase K on ice; the third was incubated in the

presence of both proteinase K and the detergent TritonX-100. All three aliquots were precipitated in TCA, and equal amounts were analysed by western blot.

These experiments showed that TBC1D20 was degraded by proteinase K independent of the presence of detergent (Figure 3-23B). Therefore, the N-terminus of TBC1D20 tagged with GFP faces the cytoplasm. The type-II transmembrane protein Golgin84, which has a large cytosolic domain behaved like TBC1D20 (Figure 3-23B). TGN46 on the other hand, which has a large heavily glycosylated luminal domain, was only accessible to proteinase K digestion in the presence of detergent (Figure 3-23B).

These findings show that TBC1D20 is an ER associated type-II transmembrane protein and that its N-terminal TBC domain is oriented towards the cytoplasm (Figure 3-23C).

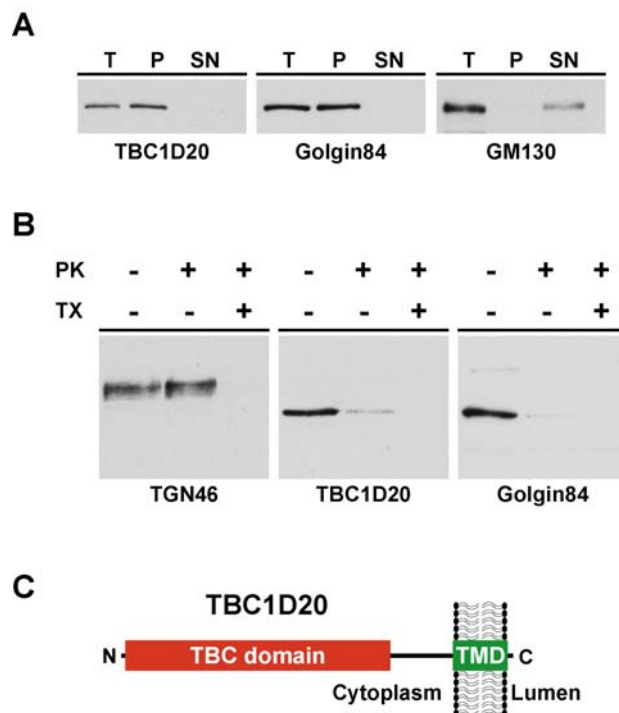


Figure 3-23 TBC1D20 is a type-II-transmembrane protein. (A) Carbonate extraction experiments were performed to investigate the membrane association of GFP-tagged TBC1D20. Golgin84 and GM130 were taken as representative integral and peripheral membrane proteins, respectively. Total (T) refers to the input, Pellet (P) indicates the membrane bound fraction and the supernatant (SN) shows the membrane free fraction. (B) The topology of TBC1D20 was analysed by proteinase K (PK) digestion experiments in the presence (+) or absence (-) of Triton X-100 (TX). TGN46 and Golgin84 were taken as representative proteins with large luminal or cytosolic domains, respectively. As TGN46 is glycosylated, a smear is observed. (C) A schematic shows the topology of TBC1D20. Lumen refers to ER lumen.

3.2.20 The TMD of TBC1D20 is required for its ER localisation

To further analyse the targeting of TBC1D20, a series of truncations were generated. HeLa cells were transfected with these truncations for 24 hours. The cells were then fixed and stained for the Golgi marker GM130.

Myc epitope tagged C-terminal truncations of wild-type TBC1D20 were used to determine the minimal TBC domain. Full length wild-type TBC1D20 localised to the ER and caused the “loss of Golgi” phenotype (Figure 3-24). TBC1D20 aa 1-337 and aa 1-317 were catalytically active (Figure 3-24) but did not localise to the ER. The “loss of Golgi” phenotype was not observed in cells expressing TBC1D20 aa 1-301 (Figure 3-24). These data are consistent with the biochemical data (Figure 3-14B) and show that the ER localisation of TBC1D20 is dispensable for its activity.

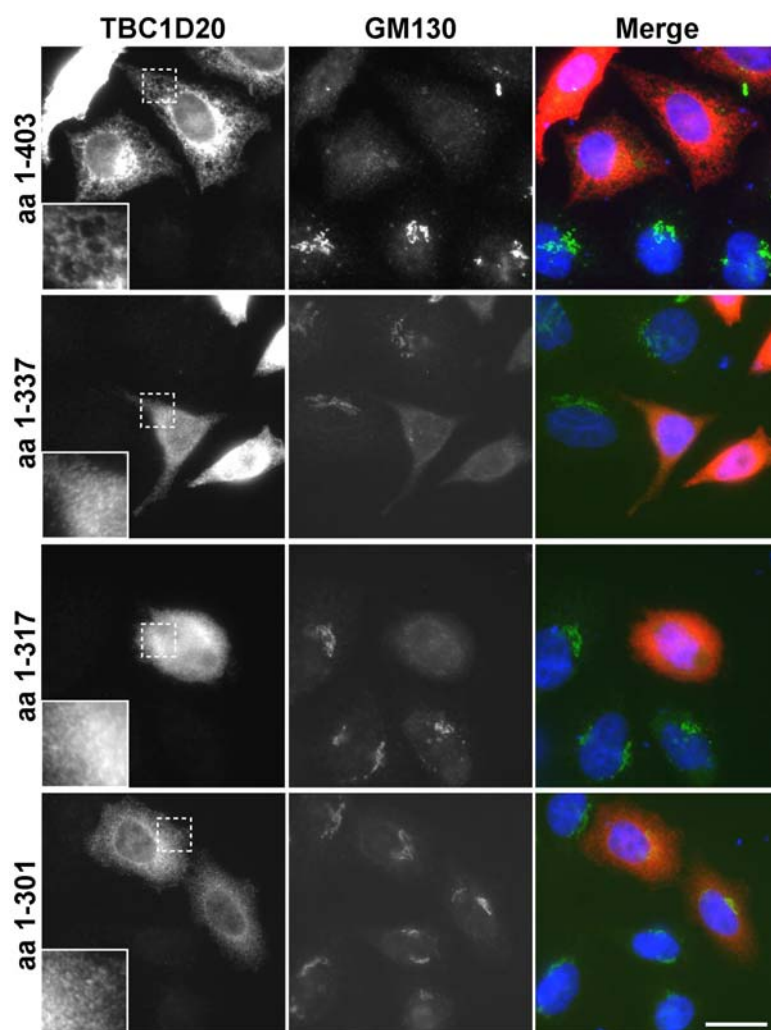


Figure 3-24 The activity of TBC1D20 is independent of its ER localisation. HeLa cells were transfected with wild-type myc-epitope-tagged TBC1D20 full length and truncation constructs. The cells were fixed after 24 hours and stained for the myc-epitope-tag (red) and GM130 (green). The enlargements to clarify TBC1D20 localisation correspond to 10x10 μm . The bar indicates 10 μm .

To analyse the ER targeting of TBC1D20 GFP-tagged N-terminal deletion constructs were generated. Full-length TBC1D20^{R105A} localised to the ER and nuclear envelope (Figure 3-25). The N-terminal deletions aa 301-403 and aa 336-403 showed a similar localisation (Figure 3-25). The shortest localising sequence was encoded in aa 364-403 (Figure 3-25). This amino acid stretch, which only consists of the TMD and the luminal amino acids, showed a slightly altered distribution and localised more strongly to the nuclear envelope and less to the reticular ER. It localised to the Golgi as well. This is more obvious in cells expressing low levels of TBC1D20 aa 364-403.

These findings show that the C-terminal TMD is required for the localisation of TBC1D20 to the ER. They furthermore indicate that a stretch of amino acids N-terminally adjacent to the TMD might be required to fine-tune the localisation of TBC1D20.

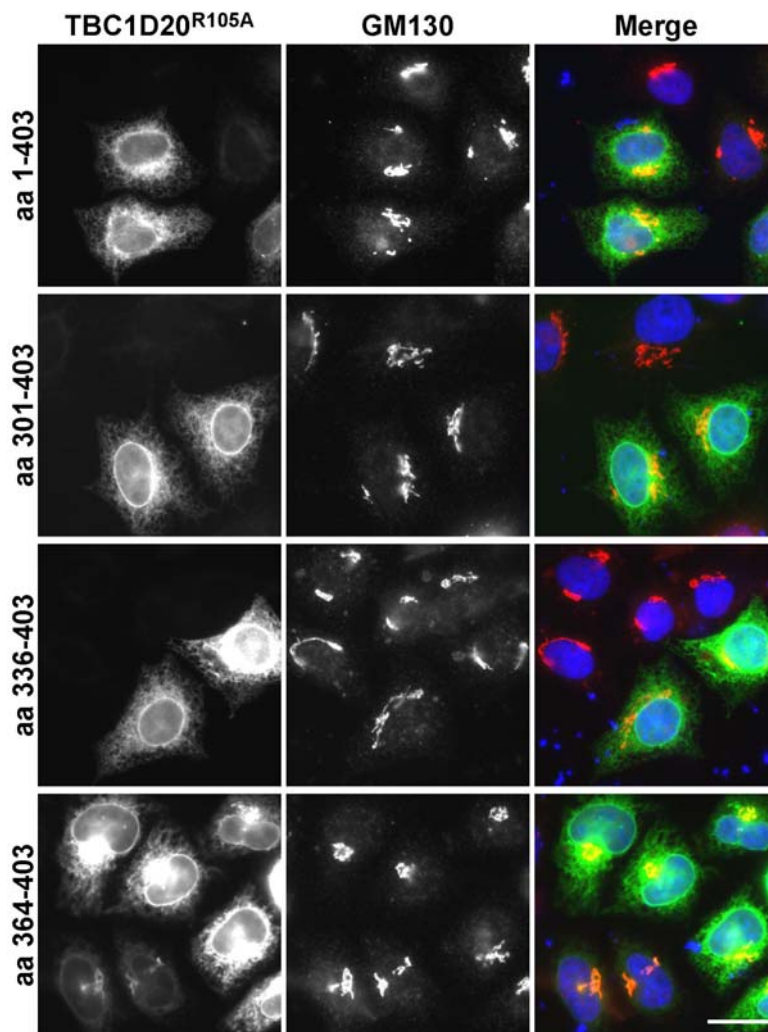


Figure 3-25 TBC1D20 localises to the ER via its TMD. HeLa cells were transfected with catalytically inactive GFP-tagged TBC1D20^{R105A} full length and truncation constructs. The cells were fixed after 24 hours and stained for GM130 (red). GFP was visualized directly (green). The bar indicates 10µm.

A schematic representation of these experiments is added (Figure 3-26) for clarity. The minimal TBC domain is encoded by aa 1-317, consistent with the data obtained by *in vitro* GAP assays. The localisation of TBC1D20 depends on the TMD on its C-terminus, and is encoded by the aa 364-403.

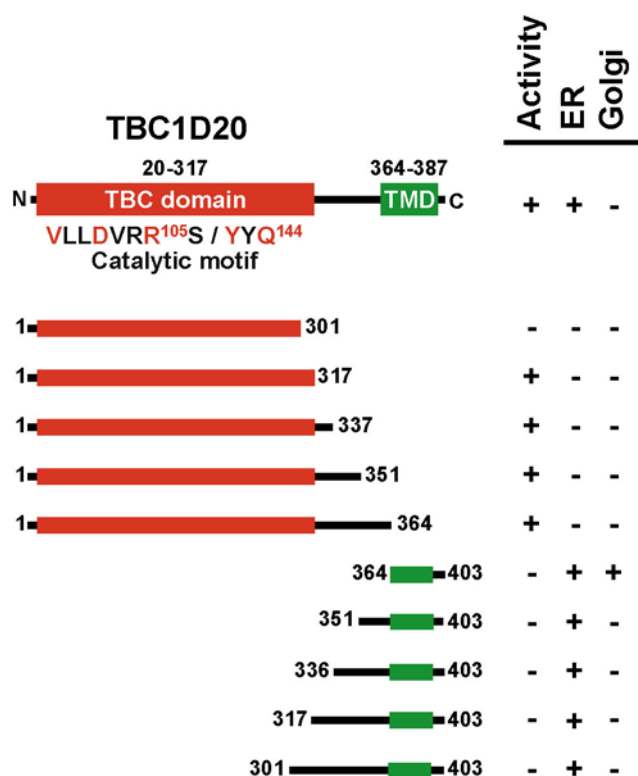


Figure 3-26 Schematic representation of TBC1D20 mapping experiments. The red of the TBC domain represents myc-epitope-tagged constructs; GFP-tagged constructs are indicated by the green colour of the TMD. Drawings are not to scale.

3.2.21 TBC1D20 interacts with Reticulon 1 variant 2

The localisation of TBC1D20 to the ER raised the question of whether this targeting is mediated by the interaction of TBC1D20 with ER associated proteins.

To identify interactors of TBC1D20 that could help its localisation to the ER, two yeast two-hybrid screens were performed. Full-length TBC1D20 and TBC1D20 aa 364-403 was used as bait, respectively. A cDNA library generated from human testis was chosen as prey for these screens. The screen of TBC1D20 aa 364-403 covered 875,000 clones but failed to identify interactors. This indicates that this part of TBC1D20 might not be sufficient to interact with other proteins. The screen with full length TBC1D20 however, which covered 1,780,00 clones, revealed two interactors.

One of these interactors was a full-length clone of an ER resident protein called BAP31. This protein is involved in the regulation of ER exit and the quality control of MHC molecules (Ladasky et al., 2006) and IgD (Schamel et al., 2003). This protein is very interesting in the aspect of the role TBC1D20 plays in the regulation of ER exit. The second positive clone was the C-terminus of Reticulon 1 variant 2 (RTN-1). Reticulons are a group of 4 proteins, each of which has multiple isoforms (Yan et al., 2006). They are associated with the ER by four C-terminal hydrophobic regions (Iwahashi et al., 2007). RTNs were shown to be involved in ER-Golgi trafficking (Wakana et al., 2005), bind to SNAREs (Steiner et al., 2004) and shape sub-domains of the ER (Voeltz et al., 2006). A *S. cerevisiae* RTN homologue has been shown to interact with Ypt1, the yeast Rab1 (Geng et al., 2005). As TBC1D20 functions as a GAP for Rab1, the interaction of RTN-1 and TBC1D20 was analysed in more detail.

First, a series of directed yeast two-hybrid assays was performed. These showed that the TMD of TBC1D20 is necessary but not sufficient for the interaction with RTN-1 (Figure 3-27A). The minimal RTN-1 interacting region included the TMD and an adjacent cytoplasmic stretch. This is the shortest fragment that showed the same localisation as full-length TBC1D20 when expressed in cells (Figure 3-25). This suggests that the interaction with RTN-1 might be required for the proper localisation of TBC1D20.

To confirm these results at the protein level, immunoprecipitation experiments were performed. The cells were lysed in digitonin as this mild detergent was previously shown to preserve RTN membrane complexes (Voeltz et al., 2006). 10 cm dishes of HeLa cells were co-transfected with one of the myc-epitope-tagged TBC1D20 constructs indicated and GFP-tagged RTN-1 for 24 hours. The cells were then harvested, lysed and cleared by centrifugation. 1 µg of purified anti-GFP antibody and protein-G sepharose were added and the slurry was incubated for 2 hours. The slurry was then washed to remove non-bound proteins and boiled in SDS sample buffer. These experiments showed that RTN-1 interacts with full-length TBC1D20 irrespective of its catalytic activity (Figure 3-27B). The first 337 amino acids of TBC1D20, which lack the ER-targeting region that interacted with RTN-1 in direct yeast two-hybrid, did not show any significant binding to RTN-1 under the same conditions (Figure 3-27B). These findings show that TBC1D20 forms a complex with RTN1.

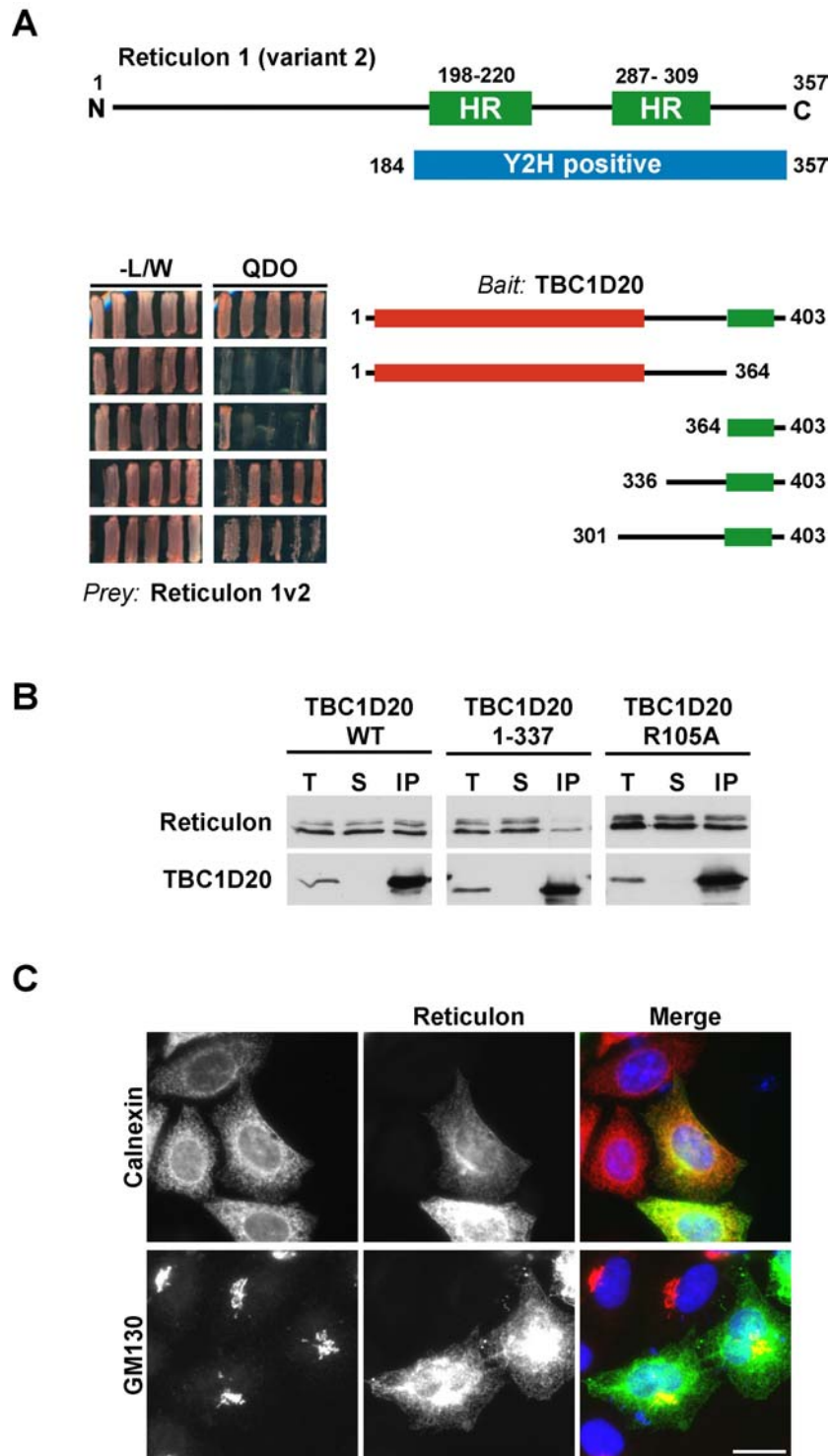


Figure 3-27 TBC1D20 interacts with RTN-1. (A) A schematic of RTN-1 showing the two hydrophobic regions (HR). The minimal TBC1D20 binding fragment identified by yeast two-hybrid (Y2H) screening is shown in blue. Drawing is not to scale. Directed yeast two-hybrid assays were performed using RTN-1 as prey and the TBC1D20 truncations indicated. Growth on selective medium (QDO) indicates interaction. (B) GFP-immunoprecipitations were performed from HeLa cells co-transfected with myc-epitope-tagged RTN-1 and GFP-tagged TBC1D20 as indicated. The immunoprecipitates were probed with antibodies against GFP or Myc to detect TBC1D20 and RTN-1, respectively. Total (T) corresponds to the input, supernatant (S) to the non-bound and (IP) to precipitated material. (C) HeLa cells were transfected with GFP-tagged RTN-1 for 24 hours, fixed and stained for GM130 (red) or Calnexin (red). GFP was visualized directly (green). The bar indicates 10 μ m.

HeLa cells were then transfected with RTN-1 to analyse its localisation. The cells were fixed after 24 hours and stained for GM130 or calnexin, respectively. RTN-1 co-localised with calnexin (Figure 3-27C) but not with GM130 (Figure 3-27C). Notably, the morphology of the Golgi apparatus was not affected by the over-expression of RTN-1.

Taken together, these data show that TBC1D20 contains a specific ER-targeting motif that interacts with a member of a family of known ER proteins. This interaction appears to be required for the proper ER localisation of TBC1D20. The interaction requires the TMD of TBC1D20 together with an adjacent cytoplasmic stretch and the hydrophobic regions of RTN-1. This suggests that these proteins form a complex in the ER membrane.

3.2.22 RTN-1 modulates the activity of TBC1D20 *in vivo*

The interaction of TBC1D20 with RTN-1 suggests that RTN-1 might be important to control the activity of TBC1D20. As over-expression of TBC1D20 causes a “loss of Golgi”, this phenotype was used as readout of the activity of TBC1D20. HeLa cells were either transfected with myc-epitope-tagged TBC1D20 alone, or co-transfected with GFP-tagged RTN-1 for 24 hours. The cells were then fixed and stained for the Golgi marker GM130.

The over-expression of wild-type TBC1D20 caused a loss of the Golgi (Figure 3-28). This effect was antagonized by the co-expression of RTN-1, as judged by the recovery of GM130 staining into a fragmented perinuclear ribbon structure in cells expressing both wild-type TBC1D20 and RTN-1 (Figure 3-28). The “loss of Golgi” phenotype was therefore reduced in these cells to a Golgi fragmentation phenotype. The expression of TBC1D20^{R105A} did not cause a “loss of Golgi” phenotype (Figure 3-28). When co-expressed, RTN-1 and TBC1D20^{R105A} co-localised in the ER, and the Golgi appeared normal as compared to non-expressing control cells (Figure 3-28). The expression of TBC1D20 aa 1-337 caused a “loss of Golgi” phenotype. If the antagonising effect of RTN-1 on TBC1D20 is specific, then it should require the RTN-1 interacting part of TBC1D20. As predicted, TBC1D20 aa 1-337, which does not interact with RTN-1 (Figure 3-27) caused the “loss of Golgi” phenotype independent of the presence of RTN-1 (Figure 3-28).

These findings show that the interaction of RTN-1 with TBC1D20 not only serves to localise TBC1D20 to the ER, but also modulates its activity. This modulation might be linked to the properties of RTNs to define sub-compartments of the ER and thus restrict the distribution of TBC1D20 in the ER.

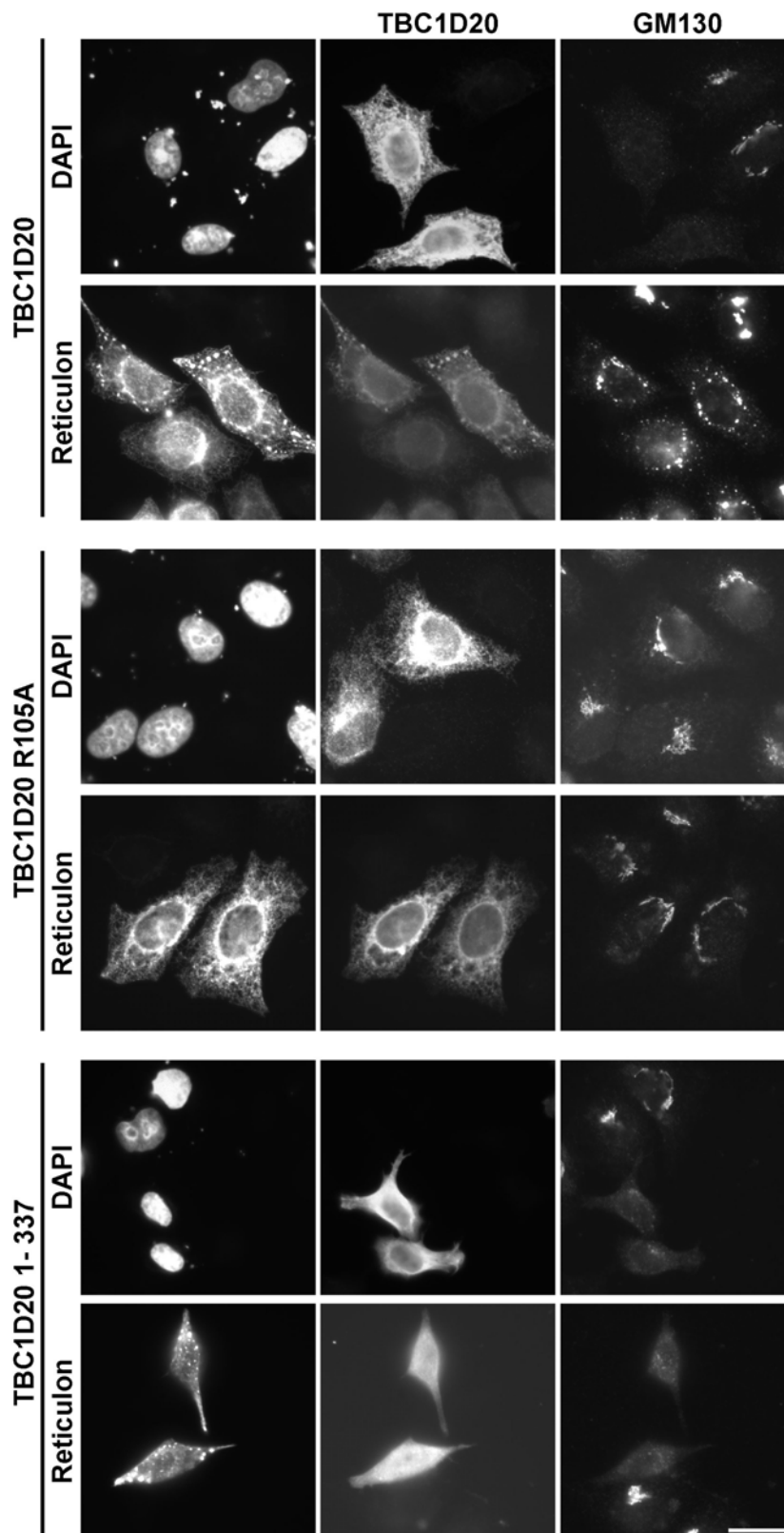


Figure 3-28 RTN-1 expression antagonises the “loss of Golgi” phenotype. HeLa cells were transfected with myc-epitope-tagged wild-type, catalytically inactive TBC1D20^{R105A}, or TBC1D20 aa 1-337 in the absence or presence of GFP-tagged RTN-1 (Reticulon) for 24 hours. The cells were fixed and stained for GM130 and the myc epitope. In single transfection panels DNA was stained with DAPI. The Bar indicates 10µm.

To show the distribution of these phenotypes the Golgi morphology in $n=100$ cells was analysed for each condition. The Golgi morphology was scored as intact, when it was comparable to neighbouring non-expressing cells. It was scored as fragmented, when GM130 stained a fragmented perinuclear ribbon structure. The cells were scored to have a “loss of Golgi” phenotype when these structures were not observed.

This analysis showed that the co-expression of RTN-1 with wild-type full length TBC1D20 strongly reduced the percentage of cells with a “loss of Golgi” phenotype while the percentage of cells with fragmented Golgi was equivalently increased (Figure 3-29). In the case of TBC1D20 aa 1-337, the co-expression of RTN-1 did not significantly alter the distribution of the phenotypes (Figure 3-29). Expression of TBC1D20^{R105A} showed the same distribution of phenotypes as control cells independent of the presence of RTN-1 (Figure 3-29). The over-expression of RTN-1 alone did not alter the distribution of phenotypes compared to non-expressing control cells (Figure 3-29).

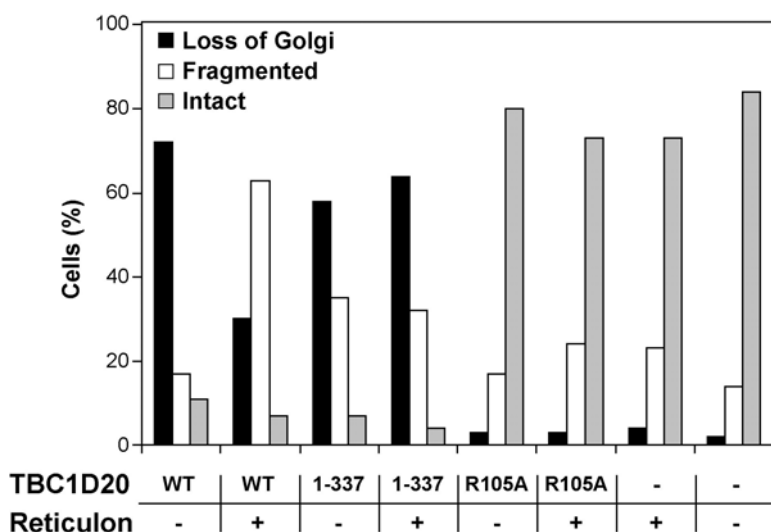


Figure 3-29 Distribution of phenotypes in cells expressing RTN-1 and TBC1D20. HeLa cells were transfected with myc-epitope-tagged wild-type, catalytically inactive TBC1D20^{R105A}, or TBC1D20 aa 1-337 in the absence (-) or presence (+) of GFP-tagged RTN-1 (Reticulon) for 24 hours. The cells were fixed and stained for GM130 and the myc-epitope tag. $n=100$ cells were analysed for each condition and the Golgi was scored as normal, fragmented or lost in comparison to non-expressing control cells.

To exclude that the modulatory effect of RTN-1 on the activity of TBC1D20 is due to altered expression levels a series of western blots was performed. HeLa cells were transfected with myc-epitope-tagged TBC1D20 constructs alone or co-transfected with GFP-tagged RTN-1 for 24 hours. The cells were then lysed and equal amounts were analysed by western blot. The blots were probed with antibodies against GFP and the myc-epitope-tag to

show RTN-1 and TBC1D20, respectively. These experiments showed that the co-expression of RTN-1 did not alter the expression levels of TBC1D20 (Figure 3-30), independent of their physical interaction. The modulatory effect of RTN-1 is therefore not due to decreased expression levels of TBC1D20.

Taken together, these findings indicate that the interaction of RTN-1 with TBC1D20 not only ensures the proper localisation of TBC1D20 to the ER, but also serves as a way to regulate the activity of TBC1D20. They furthermore suggest that RTN-1 helps to compartmentalize the ER not only by shaping ER sub-domains (Voeltz et al., 2006), but also by controlling the activity of TBC1D20, which is probably mediated by restricting TBC1D20 to specific ER sub-domains.

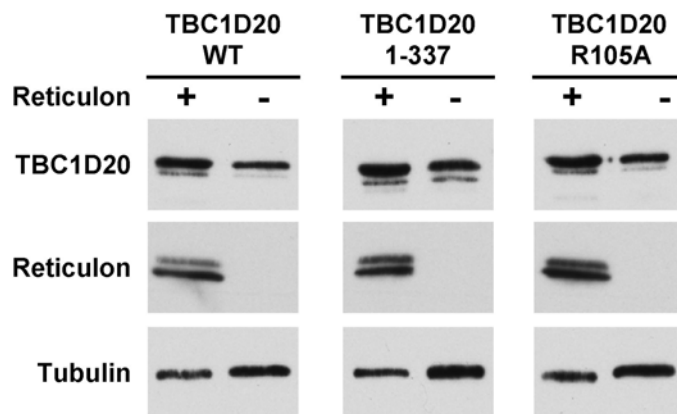


Figure 3-30 Expression of RTN-1 does not alter TBC1D20 expression levels. HeLa cells were transfected with myc-epitope-tagged wild-type, catalytically inactive TBC1D20^{R105A}, or TBC1D20 aa 1-337 in the absence (-) or presence (+) of GFP-tagged RTN-1 (Reticulon) for 24 hours. The cells were harvested and lysed. Western blots were probed with antibodies against GFP to show RTN-1 and against the myc-epitope-tag to show TBC1D20. The blots were probed with α -tubulin antibodies as a loading control.

3.3 Summary

To identify GAPs and Rabs involved in the regulation of early secretory traffic a novel screening method was established. This method uses the over-expression of RabGAPs to inactivate endogenous target Rabs. This inactivation causes phenotypes that help to identify which Rabs and GAPs are involved in the regulation of the process of interest. Screening for changes in the morphology of both the Golgi apparatus and the ERGIC as well as the ability of RabGAPs to block secretion resulted in only one candidate among all 38 RabGAPs tested, the highly conserved protein TBC1D20.

The over-expression of the ER localised TBC1D20 caused a unique “loss of Golgi” phenotype. When the fate of Golgi proteins was analysed by western blot, they were found to remain associated to membranes, with the exception of the Rab1 effector p115. Golgi enzymes redistributed to the ER. The exit of VSV-G from the ER was blocked in cells expressing TBC1D20. When TBC1D20 was tested in a biochemical assay against a broad selection of Rabs, it stimulated GTP hydrolysis by Rab1 and Rab2. Subsequent analysis of dominant negative mutant Rabs and specific siRNA showed that Rab1 is the primary *in vivo* target of TBC1D20. The expression of TBC1D20 scattered COPII positive structures, but did not interfere with the dynamics of the COPII coat. Under these circumstances cargo receptors such as p24 were absent from ERES, which possibly explains the block of secretion. Using truncations of TBC1D20 the minimal TBC domain was mapped to aa 1-317, consistent with biochemical data. Truncations and biochemical analysis also showed that the ER localisation of TBC1D20 depends on the presence of a TMD on its C-terminus. These experiments showed that TBC1D20 a type-II transmembrane protein.

The localisation of TBC1D20 depends on RTN-1, an interactor identified by a yeast two-hybrid screen. RTN-1 modulates the activity of TBC1D20 dependent on the physical interaction of both proteins. This suggests a model where TBC1D20 is localised to ER sub-domains by RTN-1.

These findings indicate a novel function of Rab1 at the level of the ER. They furthermore show that the activity of Rab1 is controlled at the level of the ER. Furthermore, the classical view of RabGAPs as the limiting factors of the lifetime of active Rab is challenged as both the depletion of TBC1D20 and the expression of constitutive active Rab1 failed to block trafficking at the level of COPII vesicles. This suggests a novel mode of Rab regulation at least in the case of Rab1.

4 Discussion

4.1 RabGAPs are a highly diverse protein family

Work in yeast has shown that RabGAPs contain a TBC domain (Albert et al., 1999; Strom et al., 1993; Vollmer et al., 1999). However, only very few members of this protein family were identified in the human genome prior to this work. A search of the human genome identified 40 proteins containing a TBC domain, some of which also give rise to splicing variants. Sequence analysis revealed that the TBC domain and the catalytic site signature sequence IxxDxxR (T/S) in motif B are variable. The arginine in this signature sequence, which is involved in GTP hydrolysis, is highly conserved, but not invariant. In some of the TBC domain proteins the arginine is shifted, in others the arginine is replaced by other amino acids. These findings might reflect differences in the Rabs that these GAPs regulate. Rab20, Rab24 and Rab25 for example do not have a conserved glutamine in the DxxGQ motif in G3 (1.2.1), and are therefore unlikely to hydrolyse GTP in the same way as the rest of the Rab family (Pan et al., 2006). Variations in the catalytic mechanism to hydrolyse GTP are reported for other members of the Ras superfamily. For example, RanGAP has an asparagine instead of an arginine, and the small GTPases Sar1 contributes as histidine instead of a glutamine to the reaction (Bos et al., 2007; Daumke et al., 2004; Seewald et al., 2002). It is therefore possible that in the largest group of the Ras super-family not only one catalytic mechanism is used to hydrolyse GTP.

Most human TBC domain proteins are multi-domain proteins. Many different domains are found in these proteins, for example: PTB domains, PH domains, GRAM domains, ubiquitin ligase domains and SH3 domains to name only a few. The GAPs of other small GTPases of the Ras super-family are also multi-domain proteins (Bos et al., 2007). All these GAPs function as integrators of signals onto the activity of a GTPase. Their composition of multiple domains therefore appears to be critical for their function.

4.2 Novel methods to study the interactions of Rabs and their GAPs

4.2.1 A novel yeast two-hybrid system to identify Rab-GAP pairs

To match the GAPs identified using a bioinformatic approach to the Rabs they regulate, a series of novel methods had to be established. First, a yeast two-hybrid based screen was established. Initial tests showed that wild-type GAPs do not interact with wild-type Rabs.

This finding is consistent with data that show that the interaction of a GAP and its target GTPase is only transient (Allin et al., 2001). After GTP hydrolysis has occurred, the GAP no longer interacts with its target and is released. It is also consistent with previous studies of yeast showing that the affinity of TBC domain proteins for their substrates is very low (Albert et al., 1999). To strengthen the interaction between the GAP and its target Rab a conserved glutamine of the Rabs was mutated to leucine to restrict them in their GTP bound active conformation. When wild-type GAPs were tested against these mutant Rabs interactions were observed but only partial specificity was achieved. It is likely that the introduction of the bulky hydrophobic leucine into the nucleotide-binding cleft of the Rab prevents the insertion of the arginine of the GAP into this cleft. This steric hindrance might explain why the GAPs showed reduced substrate specificity and interacted with groups of related Rabs under these circumstances. The arginine of the B motif of the GAPs was therefore replaced by alanine. When the mutant GAPs were tested against the constitutive active Rabs, specific interactions were observed. As shown for RabGAP-5 and RN-tre, the Rabs that interacted with the GAPs in this double mutant screen are their biochemical target. When RN-tre and RabGAP-5 were later tested against all human Rab GTPases, it was shown that these GAPs only activated GTP hydrolysis by the Rabs that they interacted with in the double mutant screen (Fuchs et al., 2007). These observations therefore validate the double mutant yeast two-hybrid approach.

The yeast two-hybrid data are also consistent with the recently solved structure of a Rab bound to a GAP (Pan et al., 2006). The glutamine of the Rab forms hydrogen bonds to the polypeptide backbone of a loop of the GAP that is inserted into the nucleotide-binding cleft. It is likely that this loop of the GAP cannot be inserted into the cleft if the glutamine of the Rab is mutated to leucine. As the GAP also interacts with the switch regions of the Rab, some interaction is still maintained, but might not be sufficient to ensure full specificity. When the positively charged arginine of the GAP is replaced by alanine, the truncated loop might fit into the nucleotide-binding cleft and the GAP can bind to its specific target. Therefore, this double mutant screen turns the GAP into an effector of the Rab and generates a stable interaction.

The data presented in this work also shed new light on the GTP restriction of constitutive active Rab mutants. The introduction of mutations in the conserved glutamine of Rabs was previously thought to prevent the glutamine from coordinating a water molecule for a nucleophilic attack at the γ -phosphate and thus keeps the Rabs GTP bound. According

to the recently solved structure discussed above (Pan et al., 2006) this glutamine interacts with a loop contributed by the GAP and is not directly involved in the catalysis of GTP hydrolysis. The findings that wild-type GAPs do not interact, or have reduced specificity for GTP restricted Rab mutants, suggests that the restriction is due to steric hindrance. This is illustrated by the finding that wild-type RN-tre does not interact with GTP restricted Rab43, and that RabGAP-5^{R165A} interacts more strongly with Rab5^{Q79L} than wild-type RabGAP-5 does. It was shown in the case of Rab1 and Rab5 that the GTP restricted mutants indeed have a reduced basal GTP hydrolysis rate, but are not completely hydrolysis deficient. This reduced basal hydrolysis rate however was resistant to RabGAP-5 or TBC1D20 mediated stimulation of GTP hydrolysis. These findings suggest that constitutive active Rabs are kept in their active conformation because they fail to properly interact with their cognate GAPs.

4.2.2 Rab inactivation screening as a novel method to analyse trafficking

The yeast two-hybrid screening method established in this work is a potent tool to identify pairs of Rabs and their regulatory GAPs. This method however, has numerous limitations. First, this method might not work in all cases, due to the structural differences between the various GAPs and their target Rabs and thus generate false negative results. Second, and most important, the organelles and trafficking processes regulated by particular Rabs and their GAPs are largely unknown. To gain more information about both partners and the processes they regulate another novel screening approach was established. Based on the fact that an inactivated Rab does not recruit effector molecules onto the membrane it provides identity to, a novel method called Rab inactivation screening was established. It was proposed that the expression of all human GAPs and analysis of the resulting phenotypes should identify GAPs involved in the regulation of a specific trafficking step.

To ensure that the phenotypes observed in the screen are due to the catalytic inactivation of a Rab, the catalytically inactive mutants of GAPs have to be examined in a next step. If a GAP causes a phenotype due to catalytic Rab inactivation, the inactive mutant GAP should not cause such an effect. RabGAP-5^{R165A} and RN-tre^{R150A} interacted with their specific target in yeast two-hybrid, which shows that the secondary structure of these proteins was maintained. The R-A mutation however efficiently abolished their activity to stimulate GTP hydrolysis by their target Rabs *in vitro*. These findings show that the arginine to alanine mutation specifically inactivates the TBC domain proteins without effects on their secondary structure. Therefore these R-A mutant GAPs are valid controls to show the specificity of a phenotype that is caused by the inactivation of an endogenous Rab.

In a consequent step, the candidate GAPs have to be tested against all Rabs for their ability to promote hydrolysis to identify their target Rab. To consolidate that the Rab identified by *in vitro* experiments is the *in vivo* target of the GAP, the expression of the dominant negative mutant of the Rab and its depletion should mimic the phenotypes caused by the over-expression of the GAP.

Proving the generality of this screening procedure, other researchers in the group used this method and successfully identified Rabs and their GAPs (Figure 4-1) involved in the formation of primary cilia and the regulation of clathrin independent endocytosis (Fuchs et al., 2007; Yoshimura et al., 2007). This technique was also used to prove that RabGAP-5 is the only GAP that regulates clathrin dependent endocytosis of EGF (Fuchs et al., 2007).

Not only Rabs, but also the other small GTPases of the Ras superfamily are controlled by GAPs and GEFs in their activity. The GAP mediated inactivation approach might therefore be useful to study the processes regulated by these GTPases as well.

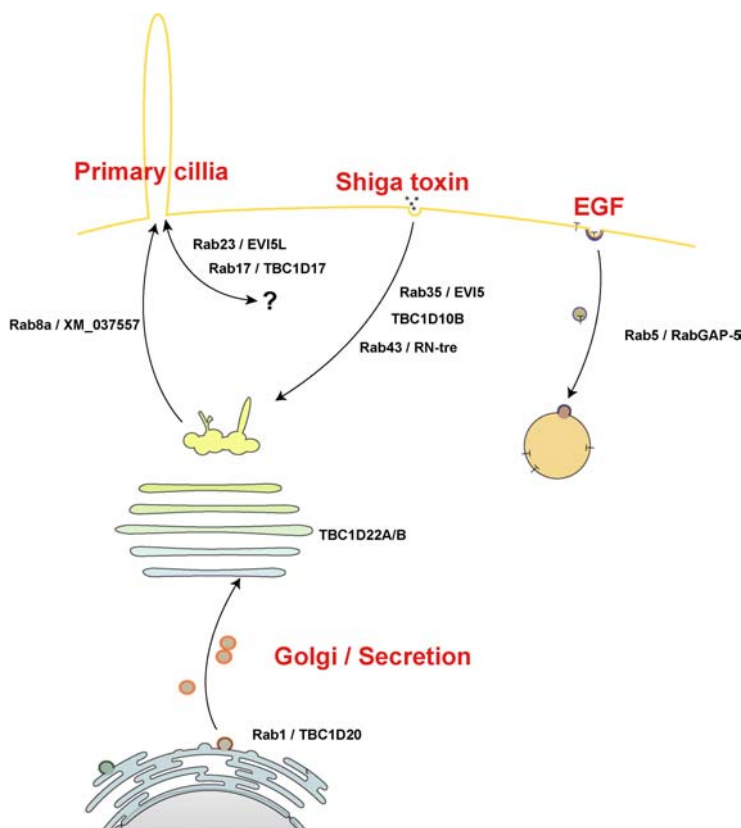


Figure 4-1 Rab inactivation screening results. Rab inactivation screening is a proven method to identify Rabs involved in a specific trafficking pathway and their regulatory GAPs. Figure layout is based on Figure 1-1.

4.3 RabGAP-5 is a specific Rab5 GAP

Many evolutionary conserved proteins tightly control endocytosis. One of the key Rabs involved in the regulation of clathrin dependent endocytosis is Rab5 (Zerial and McBride, 2001). In order to identify a Rab5 specific GAP out of forty human TBC domain proteins, the double mutant yeast two-hybrid screen was used. Only one out of all human TBC domain proteins was found to interact with Rab5, a protein later called RabGAP-5.

Like many other TBC domain proteins, RabGAP-5 is a multi domain protein. According to own observations and data from a later publication (Lan et al., 2005), the minimal TBC domain of RabGAP-5 ranges from aa 13 to aa 411 and is followed by a short coiled-coil stretch. It in the case of the TBC domain protein GAPCenA, a coiled-coil C-terminally of the TBC domain contributes to specific Rab binding (Fuchs et al., 2007). This coiled coil of RabGAP-5 might therefore contribute to specific substrate recognition as well. The TBC domain tested in the *in vitro* GAP assays and used in further experiments therefore contains this coiled-coil and ranges from aa 1 to aa 451. RabGAP-5 contains an Src-homology-3 (SH3) domain C-terminal of the TBC domain. This domain recognizes proline-rich sequences (Mayer, 2001) and is mostly found in proteins involved in signal transduction. This is an interesting finding for a regulator of Rab5 since this Rab is involved in the regulation of endocytosis of activated growth-factor receptors that follow the clathrin dependent pathway (Carpenter, 2000). The third domain of RabGAP-5 is a RUN domain at its C-terminus. The RUN domain was named after RPIP8, UNC-14 and NESCA (Callebaut et al., 2001). It is present in several proteins that are linked to GTPases of both the Rab and the Rap families. Its actual molecular function is not known. The C-terminus of RabGAP-5 including the RUN domain has been previously shown to be required for the interaction of RabGAP-5 with other molecules, which will be discussed later in more detail (Ichioka et al., 2005; Lee et al., 2004).

When the ability of RabGAP-5 to stimulate GTP hydrolysis by Rabs was analysed *in vitro*, it was found to specifically activate GTP hydrolysis by the three Rab5 isoforms. It was shown later (Fuchs et al., 2007), when RabGAP-5 was tested against all human Rabs, that it only stimulates GTP hydrolysis by the same three Rab5 isoforms.

To confirm that RabGAP-5 is a GAP for Rab5, the effects of over-expressing it in cells were analysed. RabGAP-5 over-expression redistributed the Rab5 effector EEA1 to the cytoplasm and inactivated co-expressed Rab5. Other sub-cellular organelles remained unaffected by the expression of RabGAP-5, which shows the specificity of these phenotypes.

These observations are consistent with previous publications that show that active Rab5 is required to recruit EEA1 to early endosomes (Christoforidis et al., 1999a; Lawe et al., 2000; McBride et al., 1999). EGF trafficking, which depends on Rab5 (Carpenter, 2000), was blocked by the over-expression of RabGAP-5. The recycling of the transferrin receptor was blocked under these circumstances as well. Remarkably, when all three isoforms of Rab5 were depleted by siRNA (Fuchs et al., 2007), the phenotypes observed resembled the phenotypes observed in cells over-expressing RabGAP-5. This shows that diminishing the endogenous pool of active Rab5 caused these phenotypes.

To analyse whether RabGAP-5 is an essential regulator of endocytic traffic, it was depleted by specific siRNA duplexes. The size of early endosomes was increased in cells depleted of RabGAP-5. This phenotype is also observed in cells that have elevated levels of active Rab5 (Stenmark et al., 1994). This shows that RabGAP-5 is required to control the activity of endogenous Rab5 and functions as a Rab5 specific GAP. When the trafficking of EGF was analysed in cells depleted of RabGAP-5, it was found that EGF is trapped in early endosomes and was not trafficked to lysosomes for degradation. This shows that RabGAP-5 is required to inactivate Rab5 on early endosomes in order to allow the maturation events required for the late stages of the endocytic pathway. This observation is consistent with another study, which showed that Rab7 replaces Rab5 on early endosomes as they mature (Rink et al., 2005). It furthermore shows the essential role for RabGAP-5 in the control of trafficking through early endocytic compartments.

Taken together, these data show that RabGAP-5 has all the characteristics expected of a GAP specific for Rab5. Evidence that RabGAP-5 in fact is the only human Rab5 GAP comes from a subsequent study (Fuchs et al., 2007), which showed that out of all human TBC domain proteins only RabGAP-5 blocks the Rab5 dependent endocytosis of EGF.

4.3.1 RabGAP-5 links signalling to membrane traffic

As RabGAP-5 is essential for sorting events at the early endosome and for the regulation of Rab5, the question raises of how RabGAP-5 might be controlled.

RabGAP-5 has been shown to interact with the tumour-suppressor Merlin (Lee et al., 2004) also known as Schwannomin, the gene product of NF2 (Okada et al., 2007). Merlin is an interaction partner of Hrs, which is an early endosome-associated adaptor molecule required for the sorting of growth-factor-receptors to late endosomes and lysosomes (Clague and Urbe, 2001). Hrs is recruited to the endosome by a complex of Eps15 (Komada and Kitamura, 2001) and the signal transducing adaptor molecule (STAM) (Row et al., 2005).

This complex is recruited to the endosome by activated growth factor receptors (Clague and Urbe, 2001). Therefore, RabGAP-5 may provide a link between growth-factor-receptor signalling and the regulation of endosomal trafficking by modulating the activity of Rab5.

Based on these findings it can be proposed that activated growth-factor-receptors control their own degradation and the termination of their signalling in a feedback loop (Figure 4-2). Activated growth-factor-receptors are endocytosed and traffic to Rab5 positive early endosomes where they recruit adaptor molecules like Hrs. Hrs and its binding partner Merlin could recruit RabGAP-5, which inactivates Rab5. Recent findings show that the inactivation of Rab5 is required to mature Rab5 positive endosomes into Rab7 positive late endosomes to enter the degradative pathway (Rink et al., 2005). It was also proposed that the probable Rab7 GEF C-VPS/HOPS or CORVET (Peplowska et al., 2007; Wurmser et al., 2000) is a Rab5 effector. Rab5 might therefore indirectly activate Rab7. The inactivation of Rab5 by RabGAP-5 can thus promote the maturation of early endosomes into late endosomes and MVBs, and thus stimulate the degradation of signalling molecules. Interestingly, another RabGAP-5-interacting protein (Ichioka et al., 2005) called Alix is required for formation of the multivesicular body and endosome organization (Cabezas et al., 2005; Matsuo et al., 2004).

Consistent with the proposed model, the depletion of RabGAP-5 did not have an effect on the Rab5 dependent uptake of EGF, but trapped EGF in early endosomes and prevented its degradation. RabGAP-5 therefore seems to be required to terminate the activity of Rab5 to allow the initiation of consecutive trafficking steps. On the other hand, Rab5 activity is also required for CCV formation (McLauchlan et al., 1998). According to this role of Rab5, the expression of RabGAP-5 and the depletion of Rab5 (Fuchs et al., 2007) blocked EGF trafficking at this early stage.

A recent publication shows that RabGAP-5 binds directly to TrkA and TrkB (Liu et al., 2007) and suggests a different model for the regulation of endosomal signalling. These authors propose that early recruitment of RabGAP-5 by TrkA/B prevents Rab5 from being activated and thereby results in long-lived signalling endosomes. Activation of Rab7 would therefore be prevented and the signalling molecules would therefore not enter the degradative pathway.

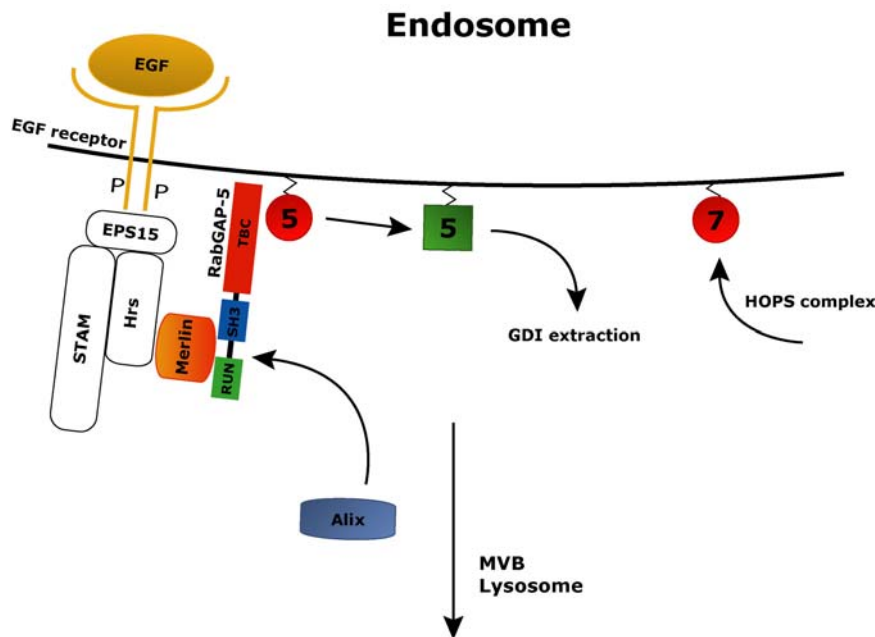


Figure 4-2 RabGAP-5 provides a link between signalling and Rab5 regulation. Activated growth factor receptors recruit protein complexes onto the early endosome that recruit RabGAP-5. RabGAP-5 inactivates Rab5 and the early endosome matures into a Rab7 positive late endosome. The number 5 indicates Rab5, Rab7 is indicated by the number 7. Active, GTP bound Rab is symbolised by a red sphere, inactive Rab by a green square.

4.3.2 RabGAP-5 and Merlin

Of special interest for future research into RabGAP-5 function is its interaction with the tumor suppressor Merlin (Lee et al., 2004). Merlin switches between an active and an inactive conformation dependent on the phosphorylation of its C-terminus by the p21-activated kinase (PAK). Merlin accumulates at adherence junctions (Lallemand et al., 2003) and is essential for cell-cell contact mediated cell cycle arrest (Lallemand et al., 2003; Morrison et al., 2001; Okada et al., 2005). The ability of PAK to release cells from contact inhibition is blocked by a form of Merlin that lacks the PAK phosphorylation site, which suggests that PAK promotes cell proliferation by phosphorylating and thus inactivating Merlin (Lallemand et al., 2003; Okada et al., 2005).

Recent findings show that Merlin inhibits cell proliferation by stabilising adherence junctions and negatively regulates EGF receptor signalling and internalization (Curto et al., 2007). The block of EGF endocytosis in cells over-expressing RabGAP-5 suggests an interesting link to these observations. Merlin might recruit RabGAP-5 to block Rab5 dependent EGF uptake and thus stop cell proliferation. Further support for this idea comes from the finding that Connexin43, a component of gap junctions that interacts with cadherins (Giepmans, 2006), binds RabGAP-5 (Lan et al., 2005). RabGAP-5 might therefore be

recruited to cell-cell contacts by the combined action of Merlin and Connexin43 and block Rab5 dependent endocytosis at these sites.

This model implies a role for RabGAP-5 not only in terminating Rab5 activity on the early endosome but also points to a role of RabGAP-5 in the regulation of cell proliferation and cell polarity.

4.4 RN-tre is a GAP for Rab43

The TBC domain protein RN-tre was reported to act as a GAP for Rab5 (Lanzetti et al., 2004; Lanzetti et al., 2000). The data presented in this work show that RN-Tre acts as a weak Rab5 GAP *in vitro*, and that RN-tre is in fact a GAP for Rab43. The weak activity of RN-tre towards Rab5 is unlikely to be physiologically relevant for multiple reasons.

RN-Tre was found to bind to Rab43 and Rab30 but not Rab5 in the yeast two-hybrid screen. These interactions were only observed when both the Rabs and RN-tre were mutated. This indicates that this interaction is due to a GAP-Rab interaction and not due to the fact that RN-tre as a Rab5 GAP is an effector for Rab43 or Rab30.

RN-tre strongly activated GTP hydrolysis by Rab43 *in vitro*, and only weakly by Rab5. When RN-tre was later tested against all human Rab GTPases it was shown to have specific activity towards Rab43 (Fuchs et al., 2007). This indicates that the activation of Rab5 by RN-tre is most likely a consequence of using purified proteins at high concentrations *in vitro*. Remarkably, despite its high degree of similarity to Rab43, no significant activation of GTP hydrolysis by Rab30 was observed in the presence of RN-tre. This shows that the yeast two-hybrid system can identify interacting Rabs, but final specificity can only be provided by biochemical *in vitro* GAP assays with recombinant proteins.

In contrast to RabGAP-5, the over-expression of RN-Tre failed to redistribute the Rab5 effector EEA1 or Rab5 *in vivo*. When tested in hTERT-RPE1 cells, the TGN marked by TGN46 was more affected by the expression of RN-tre than the *cis*-Golgi marked by GM130. Consistent with this, the target of RN-tre is present at the Golgi apparatus. This observation is consistent with the finding that RN-tre and Rab43 are regulators of retrograde transport from the PM to the TGN by a clathrin independent trafficking route exploited by Shiga toxin (Fuchs et al., 2007).

The observation that RN-tre regulates an endocytic retrograde trafficking step helps to explain why it was previously found to interfere with EGF uptake (Lanzetti et al., 2000).

With low doses of EGF, the EGF receptor is almost entirely transported via the clathrin dependent pathway. At higher or saturating doses it spills over into the clathrin independent pathway (Sigismund et al., 2005). With saturating amounts of EGF, RN-tre would prevent transport of the pool of EGF receptor entering via the clathrin-independent pathway, and thus show a reduction in EGF uptake. It will therefore be interesting to investigate the role of the RN-tre and RabGAP-5 regulated pathways under true physiological conditions in tissues where EGF signalling is critical for normal growth and development.

4.5 TBC1D20 regulates secretion by inactivating Rab1

4.5.1 The Rab1 GAP TBC1D20 regulates Golgi morphology and ER exit

Out of 38 human TBC domain proteins tested in a Rab inactivation screen only the GAPs TBC1D20, TBC1D22A, TBC1D22B, XM_037557 and RN-tre caused Golgi fragmentation in HeLa cells dependent on their catalytic activity. When the fragmentation of the Golgi apparatus was analysed in hTERT-RPE1 cells, only TBC1D20 and RN-tre caused a phenotype dependent on their catalytic activity. This finding suggests, that the GAPs that were not positive in both screens either do not regulate ubiquitously essential Rabs or that HeLa cells lack Rabs that can redundantly fulfil the role of the Rabs inactivated by these GAPs.

TBC1D22A and TBC1D22B most likely regulate the Rab33 family (Pan et al., 2006) that regulates trafficking at the Golgi apparatus (Valsdottir et al., 2001; Zheng et al., 1998). RN-tre has GAP activity towards Rab43, which localises to the TGN and regulate a clathrin independent pathway from the PM to the TGN (Fuchs et al., 2007). XM_037557 is a GAP specific for Rab8a, which is required for the formation of primary cilia in serum-starved cells and localises to the Golgi in proliferating cells (Yoshimura et al., 2007). All these GAPs therefore regulate Rabs that are involved in trafficking associated to the Golgi. This validates the screening approach, and proves that in fact the GAPs associated with a trafficking step or organelle of interest are specifically identified by this method.

When the ability of human GAPs to cause morphological changes to the ERGIC was analysed in a Rab inactivation screen, only TBC1D20 and TBC1D22B caused a phenotype. This indicates, that the Rabs regulated by these two GAPs are involved in the regulation of trafficking processes between the Golgi and the ER. However, out of all human GAPs only TBC1D20 blocked the trafficking of VSV-G. The role of the Rab regulated by TBC1D22B therefore appears less critical.

Based on the results of these screens, TBC1D20 was analysed in more detail. The expression of this highly conserved GAP resulted in the apparent loss of *cis*-, *medial*-, and *trans*-Golgi markers, a so-called “loss of Golgi” phenotype. Further investigation revealed that TBC1D20 blocked the exit of VSV-G from the ER. TBC1D20 is unique amongst the TBC-domain proteins in that it possesses a transmembrane domain. This domain is required to target TBC1D20 to the ER. When tested in a biochemical GAP assay against all human Rabs, TBC1D20 showed specific activity towards Rab1 and Rab2. The other GAPs that caused Golgi fragmentation failed to stimulate GTP hydrolysis by Rab1 or Rab2, consistent with their reported target Rabs.

To narrow down the *in vivo* target of TBC1D20, the phenotypes of dominant negative Rabs were compared to phenotypes caused by over-expression of TBC1D20. These experiments showed that only dominant negative Rab1^{N121I} recapitulates these phenotypes. When Rab1 and Rab2 were depleted by siRNA, both gave rise to Golgi fragmentation. The Golgi fragments in cells depleted of Rab2 were forming a cluster whereas the Golgi fragments in cells depleted of Rab1 appeared more vesiculated and spread throughout the cell. This is consistent with the idea that the Rab1 effector p115 is required for clustering of pre-Golgi structures (Alvarez et al., 1999). In the case of Rab2 depletion the fragments were possibly still connected by the Rab1 effector p115 interacting with the GM130/ GRASP65/ Giantin complex on the Golgi (Short et al., 2005). In contrast to the expression of dominant negative Rab1^{N121I} or TBC1D20, in cells depleted of Rab1 the Golgi was only fragmented and no “loss of Golgi” phenotype was observed. This might be explained by the different kinetics of the Rab1 siRNA that takes 72 hours compared to 24 hours of expression. In contrast to the case of the depletion of Rab1, which removes both the active and the inactive pool of the Rab, expression of TBC1D20 or Rab1^{N121I} increase the pool of GDP bound Rab. This GDP-bound Rab might sequester the Rab1 GEF, and thus strengthen the phenotype. The phenotype of Rab1 depletion, however, still resembles the TBC1D20 phenotype more closely than the phenotype obtained upon depletion of Rab2. The depletion of Rab1 and Rab2 by siRNA furthermore showed that only the depletion of Rab1 completely blocked the trafficking of VSV-G at the ER. Therefore it was concluded that the phenotypes observed in cells over-expressing TBC1D20 are mainly due to the inactivation of endogenous Rab1. As predicted, the block of VSV-G trafficking was also observed in cells expressing dominant-negative Rab1^{N121I}. Consistent with the role of TBC1D20 as the GAP for Rab1, the Rab1 dependent clustering of COPII vesicles was strongly impaired in cells over-expressing

TBC1D20. Furthermore, p115, which is recruited by Rab1 to membranes, was lost from the membrane fraction in cells expressing TBC1D20.

The finding that TBC1D20 acts as a GAP for Rab1 is consistent with previous studies on budding yeast Gyp8, the homologue of human TBC1D20. Gyp8p has GAP activity towards Ypt1p, the homologue of human Rab1 (De Antoni et al., 2002). The yeast GAP activity towards Ypt1p is found in a particulate membrane fraction (Jena et al., 1992), which suggests that Gyp8 might have the same ER localisation as TBC1D20.

The finding that TBC1D20 blocks ER exit of cargo as a result of the inactivation of Rab1 is consistent with older observations that the membrane extraction of Rab1 by GDI prevents the ER exit of VSV-G (Peter et al., 1994) and that the ability to restore ER exit depends on the addition of recombinant Rab1. This argues that ER exit specifically depends on the presence of Rab1. In contrast to the inactivation of Rab1, the depletion of the Rab1 effector p115 did not cause a block of ER exit. Secretory cargo was able to exit the ER under these conditions and accumulated in a punctate cluster adjacent to the nucleus, but did not reach the plasma membrane. This supports the role of p115 in regulating SNARE mediated fusion of ER derived vesicles with early Golgi compartments (Allan et al., 2000). In contrast to TBC1D20 expression, Rab1 depletion or the expression of dominant negative Rab1^{N121I}, depletion of p115 does not alter the levels of active Rab1. These findings suggest that Rab1 has a p115 independent function in controlling the exit of secretory cargo from the ER.

To further consolidate that TBC1D20 acts as a GAP for Rab1 *in vivo*, it was depleted by siRNA. In cells depleted of TBC1D20 the intensity of the p115 staining and p115 dependent COPII clustering was increased. Both these findings are consistent with elevated Rab1 levels caused by the depletion of a GAP for Rab1.

Even though the data provided in this work strongly suggest that TBC1D20 acts predominantly on Rab1 *in vivo*, they cannot fully rule out the possibility that TBC1D20 is a GAP for Rab2 as well. Rab2 is only found in higher eukaryotic cells and does not have a counterpart in yeast. It is thought to act downstream of Rab1, and functions in tethering ER and ERGIC derived vesicle to the early Golgi (Tisdale and Balch, 1996). As TBC1D20 mediated inactivation of Rab1 occurs before Rab2 comes to act, effects caused by Rab2 inactivation will always be covered by phenotypes caused by Rab1 inactivation.

4.5.2 RTN-1 is an ER associated regulator of TBC1D20

To understand more about TBC1D20 function and ER, a yeast two-hybrid screen was carried out. This screen identified the Reticulon RTN-1 as an interaction partner of

TBC1D20, and this interaction was confirmed by immunoprecipitation. Reticulons are involved in the organisation and the shaping of the ER (De Craene et al., 2006; Voeltz et al., 2006) and in the regulation of ER to Golgi transport (Wakana et al., 2005). All members of the Reticulon family are characterised by a C-terminal domain that forms two hairpin loops in the membrane of the ER. TBC1D20 interacts with this membrane bound portion of RTN-1, which suggests that both proteins form a complex in the ER membrane. Four different Reticulons are known so far, all of which give rise to multiple splicing variants (Oertle and Schwab, 2003; Yan et al., 2006). The differences between the Reticulons are found in their variable N-termini, whereas their C-termini are very similar. TBC1D20 might therefore interact with multiple members of the Reticulon family.

The physical interaction of TBC1D20 with RTN-1 had a modulatory effect on the ability of TBC1D20 to cause a “loss of Golgi” phenotype. One possible explanation may relate to the proposed function of Reticulons in the compartmentalisation of the ER (De Craene et al., 2006; Voeltz et al., 2006). The interaction of TBC1D20 with RTN-1 seems to be necessary for its proper ER localisation: the TMD of TBC1D20, which was not sufficient to interact with RTN-1, localised to both the Golgi apparatus and the ER. The minimal part of TBC1D20 interacting with RTN-1 however localised similar to the full-length protein. RTN-1 might therefore also restrict the localisation of TBC1D20 within the ER. It is conceivable that RTN-1 keeps TBC1D20 away from ERES, and that this restriction is important to define or confine these sites to sub-domains of the ER. The over-expression of TBC1D20 might override the spatial restriction by endogenous RTN-1 and thus inactivate Rab1 and cause the “loss of Golgi” phenotype. The co-expression of RTN-1 counteracts this effect and therefore weakens the phenotype.

Work in budding yeast has shown that Rtn1p forms a complex with the GDF Yip3p (Geng et al., 2005). This complex precipitates Ypt1p, the yeast Rab1 homologue. This suggests that GDF mediated insertion of Rab1 into the ER is tightly controlled by the association of TBC1D20 with RTN-1 and the GDF.

4.5.3 Rab1 is the conserved key regulator of the early secretory pathway

Surprisingly, out of all human GAPs only TBC1D20 was able to block trafficking of VSV-G, which did not exit the ER in cells over-expressing wild-type TBC1D20. Both the depletion of Rab1 and the expression of dominant negative Rab1^{N121I} caused the same phenotype, which shows that this block is due to the inactivation of Rab1. This raises the question of why the inactivation of none of the other Rab blocks secretion.

First, simply analysing the appearance of VSV-G at the cell surface does not answer questions regarding changes in the kinetics of trafficking or in the route of transport. In the absence of one trafficking pathway it is possible that cargo might choose different, possibly redundant trafficking routes, which are regulated by other Rabs. Such routes are important for trafficking, for example in polarised apical and basolateral sorting. However, in a cultured non-polarised HeLa cell such different trafficking routes probably act redundantly.

Second, and most importantly, the fact that TBC1D20 was the only positive in this screen suggests that it regulates an essential early trafficking step. All cargo has to pass through this step before it is sorted to its final destinations. Inactivation of other Rabs by GAP expression did not block transport of VSV-G, despite the fact that a number of these caused Golgi fragmentation. This indicates that the Rabs regulated by these GAPs are important for a normal Golgi morphology, but none of them regulates a essential step in secretory trafficking.

These findings point to the fact that Rab1 is a key regulator of trafficking between the ER and the Golgi apparatus. In budding yeast although additional Rabs are needed for transport from the Golgi to the cell surface, the Rab1 homologue Ypt1 is the sole Rab required for ER to Golgi transport, and transport through the Golgi (Brennwald and Novick, 1993). Surprisingly, the results shown in this work reveal a similar picture in mammalian cells. Despite its greater size and morphological complexity, the mammalian Golgi apparatus therefore appears more similar to its budding yeast counterpart in terms of Rab function. Interestingly, unlike other *S.cerevisiae* Ypt proteins whose homologue proteins usually form a group of Rabs in the human genome, Ypt1 has only one related human protein, Rab1. This shows that trafficking between the ER and the Golgi is an evolutionary conserved pathway, which was not subject to diversification during the evolutionary expansion of trafficking routes. The necessity to establish a tight regulation of this step in secretion might be a possible explanation for this finding. Therefore, Rab1/Ypt1 is the conserved key regulator of the early secretory pathway.

4.5.4 TBC1D20 and the Rab cascade

The finding that trafficking of VSV-G is blocked at the level of the ER raises the question of why ER exit is defective in cells with inactive Rab1.

One explanation is that it may be important to couple the sorting of cargo into COPII vesicles with the activation of Rab1. Interestingly, a similar role has already been proposed for Ypt1 in *S.cerevisiae*, where it was found that Ypt1p regulates and couples sorting of cargo molecules in the ER to subsequent vesicle targeting (Morsomme and Riezman, 2002). The same proposal has also been made for Rab5 (McLauchlan et al., 1998). Such a coupling ensures that the newly formed vesicles recruit the correct tethering factors and therefore dock to and fuse with the correct target membrane. Therefore, a vesicle without Rab1 should not recruit any cargo. Consistent with this prediction, cargo receptors such as ERGIC53 or p24 do not accumulate at ERES in cells over-expressing TBC1D20 despite normal COPII dynamics. This shows that the block of ER exit is based on defective cargo sorting rather than on defective vesicle formation.

How such a coupling might occur is less clear, and will require investigation of further Rab1 effector molecules like the MICAL family of proteins, which also propose a link to the microtubule network (Fischer et al., 2005; Weide et al., 2003). The Rab1 GEF, TRAPPI (Wang et al., 2000), provides another possible explanation for this coupling. TRAPPI has recently been shown to directly bind to the Sec23 subunit of the COPII coat (Cai et al., 2007). At least one of the TRAPPI subunit is recruited to ERES (Yu et al., 2006). Thus, TRAPP provides a means to activate Rab1 at the forming vesicle when sufficient COPII components are recruited by cargo and cargo receptors.

The finding that in cells lacking active Rab1 ER exit is blocked, gains further importance in the light of a model called Rab cascade (Haas and Barr, 2007; Markgraf et al., 2007; Ortiz et al., 2002). This model is based on the finding that the Rab Ypt31/32 recruits Sec2, the GEF for the Rab Sec4, which acts downstream of Ypt31/32 (Ortiz et al., 2002). The Rab cascade model proposes that Rabs regulate the activity and recruitment of downstream Rabs by their effectors, which act as regulators of these Rabs. One question is how such a cascade is initiated. The observation that COPII recruits the Rab1 GEF TRAPPI shows that the vesicle coat itself can trigger the Rab cascade and provides a link between cargo recognition and the Rab cascade. Importantly, every cascade needs to be tightly controlled at the beginning. The ER associated Rab1 GAP TBC1D20 can provide a counterpart to the GEF activity of TRAPPI to ensure the specific initiation of this cascade.

4.5.5 Rab1 and Golgi biogenesis

In contrast to any of the other 38 RabGAPs tested, over-expression of TBC1D20 caused the apparent loss of *cis*-, *medial*-, and *trans*-Golgi markers. This “loss of Golgi” phenotype cannot be simply due to a block of trafficking, as the expression of Sar1^{H79G} (Yoshimura et al., 2004) or the treatment of cells with BFA (Lippincott-Schwartz et al., 1989) only cause a fragmentation of the Golgi apparatus despite their ability to block ER to Golgi trafficking. The difference of these to the over-expression of TBC1D20 is that they do not alter the level of active Rab1. Why does interfering with Rab1 function cause such an extreme phenotype?

Although debated for many years (Mironov et al., 1997; Pelham, 2001), most recent findings indicate that the Golgi stack is not formed of static cisternae with cargo shuttling from one to the next via vesicle carriers. Instead, the Golgi is now widely believed to consist of highly dynamic and continuously maturing cisternae that modify their cargo as they progress from the *cis*- to the *trans*- face of the Golgi stack (Bonfanti et al., 1998; Losev et al., 2006). The residing enzymes in turns, which grant sequential biochemical activity, recycle in vesicles to equip the Golgi cisternae as they progress. The steady state structure of the Golgi stack is according to this cisternal maturation model a representation of the dynamic balance between anterograde and retrograde trafficking. The mode of Golgi biogenesis is also a matter of discussion (Glick, 2002; Lowe and Barr, 2007). According to the cisternal maturation model, the question of how the Golgi is formed might be answered by the ability of cisternae to be formed *de novo* from ER derived material. Even though under some conditions the division of pre-existing structures forms the Golgi (Shima et al., 1998), there is good evidence that the Golgi can arise directly from the ER (Mironov et al., 2003). It was shown that the organization of ERES and COPII vesicle trafficking are paramount for normal Golgi biogenesis and function (Connerly et al., 2005). Furthermore, the availability of cargo such as Golgi enzymes is a key factor in determining the size of the resulting Golgi cisternae (Guo and Linstedt, 2006).

How do these findings correlate with the “loss of Golgi” phenotype? In the case of Rab1 inactivation, cargo and Golgi enzymes are trapped in the ER and thus prevent normal Golgi biogenesis, which depends on their availability. Inactivation of Rab1 also leads to the loss of p115 from membranes. This Rab1 effector is required for COPII clustering and the formation of Golgi precursors. Rab1 inactivation therefore combines defects in both cargo transport and vesicle tethering. This combination might cause a more severe defect in Golgi biogenesis than depletion of individual tethering factors or a block of cargo transport.

4.6 An additional model of GAP mediated Rab regulation

Surprisingly, the depletion of TBC1D20 and the expression of constitutive active Rab1^{Q67L} failed to cause a block of VSV-G trafficking. Consistent with these data, *S.cerevisiae* GYP8, which is the homologue of TBC1D20, is not essential for secretion (De Antoni et al., 2002). Furthermore, a yeast strain expressing constitutive active *Ypt1*^{Q67L} does not exhibit growth defects, shows normal rates of secretion, and normal membrane morphology (Richardson et al., 1998).

Since neither TBC1D20 in human cells nor GYP8 in yeast is essential for secretion, the regulation of GTP hydrolysis appears not to be critical for Rab1/Ypt1 function under laboratory conditions. On the other hand, the inactivation of Rab1 has a strong effect on Golgi morphology and secretion in both human and yeast (Bacon et al., 1989; Jedd et al., 1995). How can these observations be consistent with the classical model of GAPs (Fig 1.6) as determinants of the lifetime of active Rab (Novick and Zerial, 1997)? According to the classic model, the GAP is also expected to localise to the target membrane but TBC1D20 localises to the ER. Therefore an additional model of Rab control is proposed (Figure 4-3).

In this model, GDI bound Rab is inserted into the membrane with the aid of a GDF and is then activated by its GEF. The GAP localises in the same membrane and inactivates the Rab again. The inactive Rab can be extracted by GDI or, more likely, become reactivated by the GEF. The Rab therefore cycles between the active and the inactive conformation, until the activity of the GEF can override the activity of the GAP. This could be mediated by either inactivation of the GAP or increased GEF activity. The GEF then keeps the Rab active and capable of recruiting effectors until the target is reached where the GEF activity decreases. The Rab is inactivated by its own basal GTP hydrolysis, and effectors recycle to the pool of active Rab.

In support of this model, the Rab1 GEF TRAPPI is recruited by COPII coat components during vesicle formation at ERES (Cai et al., 2007; Yu et al., 2006). TRAPPI activates Rab1 on ERES when cargo accumulates and coat formation is initiated. The ER associated GAP TBC1D20 counteracts this activity. The GEF activity of TRAPPI might override TBC1D20 mediated Rab1 inactivation when COPII components recruit sufficient TRAPPI. Once sufficient COPII components are present on the vesicle to get Rab1 activated, the vesicle buds from the ER as COPII components mediate budding and abscission. TRAPPI then keeps Rab1 active on the vesicle until the vesicle reaches the Golgi. At the *cis*-Golgi TRAPPI is converted to TRAPP II, and loses GEF activity towards

Rab1 (Morozova et al., 2006; Wang et al., 2000). On the *cis*- Golgi active Rab1 is required and binds to various molecules like GM130 or Golgin84. (Diao et al., 2003; Moyer et al., 2001). In the absence of its GEF however, Rab1 inactivates itself by its basal GTP hydrolysis.

According to this model, increased levels of active Rab1 in the absence of TBC1D20 or in cells expressing Rab1^{Q67L} do not prevent a vesicle to form and transport is therefore not blocked. This vesicle then fuses with the Golgi in a process that does not require the presence of a GAP and is thus not blocked under these circumstances. The cargo is then released and traffics on in a process independent of Rab1. The active Rab1 inactivates itself by its basal GTP hydrolysis in the absence of the GEF TRAPPI, and Rab1^{Q67L} might just reside on the Golgi.

Why is such a “regulator GAP” like TBC1D20 needed? One possibility is, that the regulation of the initiation vesicle transport is coupled to recognition of properly folded cargo as a proofreading mechanism before the commitment is made to form and traffic the vesicle. Such a proofreading mechanism might be important in ER stress conditions. Support for this idea comes from a recent study on the mechanism of α -synuclein mediated toxicity (Cooper et al., 2006). Misfolding of α -synuclein is associated with several neurodegenerative diseases like Parkinson's disease, even though the exact mechanism is unknown. This study shows that α -synuclein creates an ER-stress situation that results in a block of ER to Golgi trafficking. A genomic screen in yeast revealed that only YPT1 was able to suppress α -synuclein toxicity and recover ER to Golgi trafficking. GYP8 significantly enhanced α -synuclein mediated toxicity presumably by inactivation of Ypt1. These findings suggest, that Ypt1/Rab1 activity is limiting for ER exit under stress conditions. The negative regulation of Ypt1/Rab1 by Gyp8/TBC1D20 might therefore function as a proofreading mechanism and prevent the exit of misfolded proteins from the ER. Interestingly, Reticulons are also involved in various neurodegenerative diseases, which points to a general role of the early secretory pathway for these diseases (Wildasin, 2004; Yan et al., 2006).

Another explanation for the need of a “regulator GAP” comes from the observation that the NS5A protein of the Hepatitis C virus binds to TBC1D20 (Sklan et al., 2007a; Sklan et al., 2007b). TBC1D20 might be required in virus infected cells to block trafficking of membrane bound viral proteins to the cell surface to prevent spreading of the virus. The

interaction with the viral protein might inhibit TBC1D20 to ensure the transport of viral components to the PM.

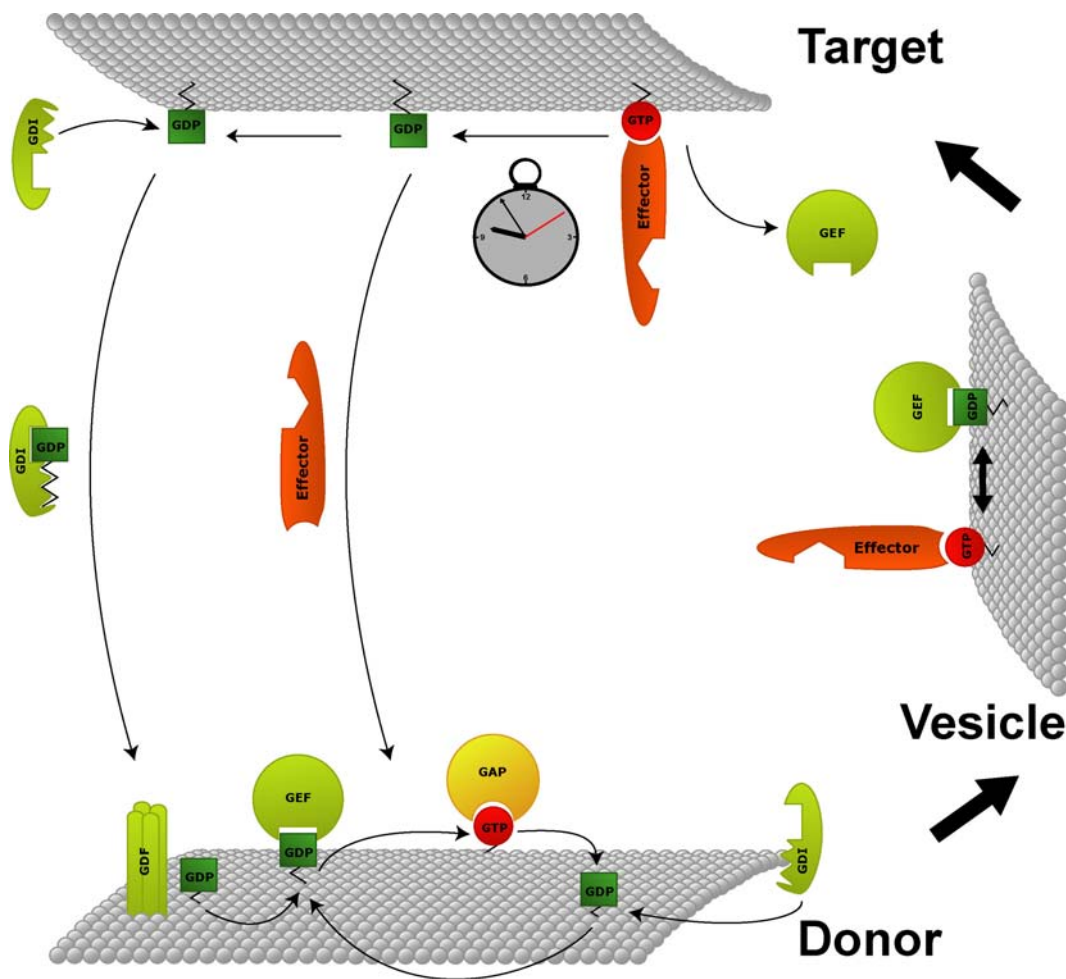


Figure 4-3 RabGAPs as regulatory factors of Rab cycle initiation. The small red sphere labelled “GTP” symbolises active Rab bound to GTP, a small green square labelled “GDP” indicates inactive Rab. Rab interacting molecules are identified by common abbreviations. A clock indicates the kinetic self-inactivation of Rabs. Drawing is not to scale.

The idea that activation of Rabs by GEFs and their inactivation by GAPs are closely linked seems counterintuitive at the first glance. However, using such a mechanism, the amount of active Rab can be tightly controlled dependent on the activity of GAPs and GEFs. A tight cycle of activation and inactivation is commonly used to regulate the activity of small GTPases. Sar1 for example, which is required for the COPII coat assembly is activated by Sec12 and inactivated by the coat subunit Sec23 it recruits. This allows the dynamic regulation of the coat assembly (Bonifacino and Glick, 2004). RhoA as another example is tightly regulated by its GAP and GEF at the same time during cytokinesis to generate a locally restricted pool of active RhoA (Yuce et al., 2005). Such a cycle of activation and

inactivation allows to respond to changes in conditions more precise and quickly and is a common feature amongst signalling molecules. Importantly, most GAPs are multi-domain proteins. This suggests that the activity of GAPs is regulated dependent on various signalling pathways.

TBC1D20 is the prime example of a “regulator GAP” as it is localised to the ER, the donor membrane, by its TMD. RabGAP-5 on the other hand acts as a prototypic “terminator GAP” in the regulation of the Rab5 to Rab7 transition. The depletion of RabGAP-5 leads to an accumulation of EGF in early endosomes, which shows the critical role of RabGAP-5 in terminating Rab5 activity. However, if RabGAP-5 is in fact recruited by Merlin to adherence junctions to prevent EGF uptake, this would turn the “terminator GAP” into a “regulator GAP”. This suggests that interacting proteins and signalling processes can alter the regulatory properties of GAPs.

Taken together, the observations made during the course of this work and data shown in recent publications indicate that RabGAP mediated inactivation of Rabs is a flexible and highly regulated process. This process requires further investigation to understand the basis and mechanics of the activity of these key regulators of Rab dependent membrane traffic.

4.7 The specificity of Rab-GAP interactions

The claim has been made based on findings in *S.cerevisiae*, that RabGAPs are promiscuous in the recognition of their substrates (Albert and Gallwitz, 1999). However, based on data presented in this work and in recent publications, this appears not to be the case.

The claim was based on GTP hydrolysis assays with truncated yeast TBC domain proteins (Albert and Gallwitz, 1999; Will and Gallwitz, 2001). However, we have recently shown (Fuchs et al., 2007) that in the case of the Rab4 GAP GAPCenA (Cuif et al., 1999) truncations lose their substrate specificity and interact with a wide range of Rab GTPases. The full-length protein on the other hand specifically interacted with its target Rab4. This illustrates that in order to observe specific interactions and activity the use of full-length TBC domain proteins is mandatory.

Another recent publication (Yoshimura et al., 2007) shows that the RabGAP XM_037557 stimulates GTP hydrolysis by Rab8a, but not by its isoforms Rab8b, reflecting the different properties of these very similar Rabs in the formation of the primary cilium. A promiscuous GAP certainly would not detect such small differences. Furthermore, if the

RabGAPs were in fact promiscuous in their substrate recognition, a Rab inactivation screen would not identify specific regulators of the organelles or trafficking processes of interest.

Taken together, the results presented in this work and other recent publications point to the fact, that RabGAPs actually have high substrate specificity, which is expected as they regulate proteins that provide membrane identity.

There are still much more GAPs not assigned to their target Rab than GAPs, which have been matched to their target. Furthermore, our knowledge about the mode of action and the regulation of the GAPs themselves is incomplete. With the tools and methods established in this work, further insights will certainly be provided. The RabGAP field therefore promises to generate many interesting findings in the coming years.

5 Material and Methods

5.1 Materials

5.1.1 Reagents

Reagents were obtained from Sigma-Aldrich (Seelze, Germany), Carl Roth (Karlsruhe, Germany) or VWR (Darmstadt, Germany) unless stated in the text.

5.1.2 Equipment

A list of commonly used equipment and its suppliers is given in the table below.

Equipment	Description and manufacturer
Benchtop centrifuge	Eppendorf Centrifuge 5417C
Benchtop refrigerated centrifuge	Eppendorf Centrifuge 5417R
Cell Culture Incubators	Heraeus HeraCell
Cell Culture Safety Hoods	Heraeus HeraSafe
Centrifuge	Heraeus Multifuge 3 L-R
Electroporation system	BioRad MicroPulser
Film Developer	Kodak X-OMAT 2000 Processor
Gel system	BioRad Mini-PROTEAN
Heating block/ mixer	Eppendorf Thermomix Compact
High pressure homogeniser	Avestin Emulsiflex C5
Incubators	Heraeus Function Line
Magnetic stirrer	IKA RET basic IKAMAG
PCR machines	Perkin Elmer Gene Amp 2400 Eppendorf Mastercycler Personal
pH meter	Beckman 340pH/Temp meter
Power pack	BioRad Power Pack 200 and 300
Scintillation counter	Packard Tri-carb 2900TR
Semi- dry blotter	BioRad Trans-blot SD
Shakers	Infors AG Multitron Grant Boeckel BFR25

SW28 rotor	Beckman
SW40 rotor	Beckman
Transilluminators	UVP 2UV Transilluminator UVP Gel Documentation System Fujifilm LAS3000
Ultracentrifuge	Beckman Optima LE-80K
UV/Visible Spectrophotometer	Amersham-Pharmacia Ultrospec 300pro
Vortex shaker	IKA MS3 basic
Waterbath	Haake DC10

5.1.3 Solutions

The composition of standard solutions not described in the respective methods chapter is given in the table below. Unless otherwise stated the solvent is water.

Solution	Composition
Assay Buffer (10x)	500 mM HEPES-NaOH, pH 6.8, 10 mg/ml purified BSA, freeze at -20°C, add DTT to 10 mM before using
DNA loading dye (6x)	0.25% (w/v) bromophenol blue, 40% (w/v) sucrose in TE
IMAC (5,20,200)	20 mM Tris-HCl pH8.0, 300 mM NaCl, (5, 20, 200) mM Imidazole
LB (Agar)	10 g/l Bacto-tryptone, 5 g/l Bacto-yeast extract, 10 g/l NaCl, (plus 15 g/l Agar)
LiPEG	100 mM LiOAc, 10 mM Tris-Cl, pH 8,0, 1mM EDTA, pH 8,0, 40 % PEG3350, sterile filtered, stored at 4°C
LiSorb	100 mM LiOAc, 10 mM Tris-Cl, pH 8,0, 1mM EDTA, pH 8,0, 1M Sorbitol, sterile filtered, stored at 4°C
Mammalian Lysis Buffer	20 mM Tris-HCl pH 7.4, 150 mM NaCl, 0.1% (w/v) Triton-X 100
Milk-PBS (blocking buffer)	4% milk powder in PBS , 0.2% (w/v) Tween-20
Moviol + DAPI	2.4 g Moviol 4-88 added to 6 g analytical grade glycerol while stirring, 6 ml of ddH ₂ O added and left for 2 hours

	at room temperature, 12 ml of 0.2 M Tris-HCl pH 8.5 added while stirring for 10 minutes at 50 °C , the solution was clarified by centrifugation at 3000 x g for 15 minutes and stored at – 20 °C
PBS	8 g/l NaCl, 0.2 g/l KCl, 1.44 g/l Na ₂ HPO ₄ , 0.24 g/l KH ₂ PO ₄ ,(pH 7.4)
Ponceau	0.2% Ponceau red in 1% acetic acid
SC (Agar)	6,7 g/l Yeast nitrogen base, 2 g/l appropriate “drop-out” mix, 20 g/l Glucose, 20 mM HEPES pH 6,5, (20 g/l Agarose)
SDS-PAGE lower buffer (4x)	181.72 g/l Tris base, 4 g/l SDS
SDS-PAGE running buffer (10x)	30.2 g/l Tris base, 188 g/l glycine, 10 g/l SDS
SDS-PAGE sample buffer (3x)	For 100 ml: 2.3 g Tris base, 9.0 g SDS, 30 ml glycerol, Adjust pH to 6.8 with HCl, adjust volume to 90 ml with dH ₂ O, 50 mg bromophenol blue, add 10% β-mercaptoethanol prior to use
SDS-PAGE transfer buffer	1x SDS-PAGE running buffer, 10% methanol
SDS-PAGE upper buffer (4x)	60.6 g/l Tris base, 4 g/l SDS
TAE (50x)	For 1 l: 242.4 g Tris base, 57.2 ml glacial acetic acid, 50 mM EDTA pH 8.0
TBS for dialysis	50 mM Tris, 150 mM NaCl, 2mM DTT
TE	10 mM Tris-HCl pH 8.0, 1 mM EDTA
Yeast lysis buffer	2,5% (w/v) SDS, 25 mM Tris-HCl pH 7,5 , 25 mM EDTA
Yeast S-Buffer	10mM K ₂ HPO ₄ , pH 7,2, 10mM EDTA, 50mM β-Mercaptoethanol, 50µg/ml Zymolyase

5.1.4 PCR primer

DNA primer to clone TBC domain proteins were designed according to 5.3.1, and obtained by Metabion (Martinsried, Germany).

Target Gene	Forward and reverse primer including restriction site (in capital letters)
EVI-5	GGGATCCCCatggccagtcaggtggcaagtc GCTCGAGtcagacagtgttgaatacgac
RN-tre/USP6NL	GAGATCTCCatgaattcagaccaggatgtagc GGTCGACtcacagcaacactgactcttgg
RUTBC1	GAGATCTCCatgggcagcgcagaggacgcagtc CGTCGACtcactgttctctatgagcatctg
RUTBC2	GAGATCTCCatggaggaggctgtgacacgcaag CGTCGACtcactgttctcaatcagagtctg
RUTBC3/RabGAP-5	GGGATCCCCatgtcaggaagccatacacctgcctgtggccc GGTCGACtcacccgtccacatcccagctgaag
TBC1D1	GAGATCTCCatggaaccaataacattcacagcaagg CGTCGACtcagtcgcccgtgggctcgggctgcg
TBC1D2	GGGATCCCatggaagcttaccggaccag GGTCGACtcaggcttccccctccacctcg
TBC1D3B/PRC17	GGGATCCCCatggacgtggtagaggctgcg GGTCGACctagaagcctggaggg
TBC1D4/AS160	GGGATCCCCatggagccgcccagctgcattcag GCTCGAGttatggcttatttctatcttggc
TBC1D5	GGGATCCCCatgtatcattccttatctgaaact GCTCGAGtcagatgtccaggggactcacaat
TBC1D6	GGGATCCCCatgcagcccgcgagcgctgcg CGTCGACctatgccactggtgcccgctctg
TBC1D7	GAGATCTCCatgactgaggactctcagagaaac GCTCGAGtcagcttgaatggaccgggggtcccag
TBC1D8	GGGATCCCCatgttctgaacctggatgagggtg GCTCGAGctacaagtactcagcttaagttc
TBC1D10A/EPI64	GGGATCCCCatggcgaagagcaacggagag GGTCGACttacaagtaggtgtcctcactctctt
TBC1D10B	GTGATCACCatgtctgggaccttggagtcctt CGTCGACtcagaagtaagcgtcctgccgggc
TBC1D10C	GGGATCCCCatggcccaggccctgggggaggac GCTCGAGtcagaagcgggtgtccaggaagga
TBC1D11/GAPCenA	GGGATCCCCatggatgacaaggcttctgttgaaaaatc GCTCGAGtcagcaagtcctttcccttgaacccccg
TBC1D12	GGGATCCCCatgggtcggggaatctccaggctc CGTCGACctagctttcaaagcaggactact
TBC1D13	GAGATCTCCatgtcaagtctgcacaagag GGTCGACctactttgagtcttgagctcctt
TBC1D14	GGGATCCCCatgactgatggaaaactctcc GGATCCtcagtgtcggagggatggactcc
TBC1D15	GGGATCCCCatggcggcggcgggtgtgtgagc GCTCGAGtcatgcagggtttaatctgcagac
TBC1D16	GAGATCTCCatgtctctgggccgctccttcgc GCTCGAGctatctgcggaagccgaagccgctc
TBC1D17	GAGATCTCCatggaaggagccggctacagggtg GCTCGAGttaggagtcggcgccctcgtcctc

TBC1D18	GTGATCACCCatggaggtcagagcttcattacag GGTCGACctacaaatatacaaaacttgatctatcc
TBC1D19	GGGATCCCCatgttgacaggaggagtcggacctc GCTCGAGtcagggtgacagtagcaaacagaaa
TBC1D20	GAGATCCTCCatggccctccggagtgcg GGTCGACtcagggaacagctgcagctgaacttag
TBC1D21	GGGATCCCCatgaccaccctctctcctgaaaac GCTCGAGtcagaggaagaaatcctttaatgt
TBC1D22A	GGGATCCCCatggccagcgcgaggggcccaggaag CGTCGACtcatttctgtagtattgggggc
TBC1D22B	GAGATCTCCatggccctccggagtgcg GGTCGACctatcggcggtagtatttg
USP6	GGGATCCCCatggacatggtagagaatgcagat CGTCGACttactgtaacatagagtacttttc
AK074305	GGGATCCCCatgtttcccctgaaggacgctgaa CGTCGACtcataattgaggagatgggatggt
KIAA1055	GAGATCTCCatgctcatggagaccatccaagcc CAGATCTcagggtatcctcctcctcgtcact
KIAA0676	GGGATCCCCatgtggctgagcccggaggaggtg GCTCGAGtcagccggaaactccaggctgctc
KIAA0882	GGGATCCCCatgtgggtgaaccggaggaggtg CGTCGACtcagccggacatggccgagatttc
NP_060222	GGGATCCCCatgtggctgaagcctgaggaagtg GCTCGAGttacatcttggttctagacctaa
NP_060779	GGGATCCCCatggcggaaggagaagatgtgccg GCTCGAGttaactttccaaagcatccaaaac
EVI5-like	GAGATCTCCatggcgagccccactctgagcccc GCTCGAGtcagttgtccagaccctggctgta
XM_037557	CGGATCCCCatgcggcaggacaagctgaccggg GCTCGAGtcacgttttttagtgccactgtttc
KIAA1171	GGGATCCCCatggactctccaggatacaactgc GCTCGAGtcactgggtgtcagggtcctggaa
Paris-1	GTGATCACCCatggagggcgctggggagaaacgccccgg GGTCGACtcaggcttccccctccacctcgtcctcgc

5.1.5 siRNA oligonucleotides

siRNA oligonucleotides for siRNA-mediated depletion of specific mRNAs were designed to a target sequence of NN(N19)dTdT using the *siDESIGN* Center on the Dharmacon homepage (www.dharmacon.com), or were obtained as preconfigured SMART- pools by Dharmacon. The siRNA oligonucleotides used in the course of this work are listed in the table below.

Target Gene	Target Sequence
GL2 (Control)	CGUACGCGGAAUACUUCGAUU
LaminA (Control)	CTGGACTTCCAGAAGAACATC
RabGAP-5	AACGGCCTGCGAGGCTGGTTT
TBC1D20 (SMART-Pool)	GGACUUGCCCUAUGAGACA
	GGACCAACCGCUUUGUGAA
	ACCCUCAGCUGCACUACUA
	ACGCAUGGCUAUCAGUGAA
p115	GCCGAGACGAUUCAAAAGCUU
	GGCAGCAGGUUUCUACAUUUU
GM130	CCCUGAGACAACCACUUCUUU
	GGCUGGCAUGCAGCUUAAACUU
	CCCCACUGCACAGCAGAUCUU
Rab1A (SMART-Pool)	GAACAAUCACCUCCAGUUAUU
	CAAUCAAGCUUCAAAUAUGUU
	GGAAACCAGUGCUAAGAAUUU
	CAGCAUGAAUCCCGAAUAUUU
Rab1B (SMART-Pool)	CCAGCGAGAACGUCAAUAAUU
	GCGCCAAGAAUGCCACCAAUU
	GACCAUGGCUGCUGAAAUCUU
	CAGCCAAGGAGUUUGCAGAUU
Rab2A (SMART-Pool)	GAAGGAGUCUUUGACAUAUU
	GAUAUUACACGGAGAGAUUU
	CGAAUGAUAACUAUUGAUGUU
	UGACCUUACUAUUGGUGUAUU
Rab2B (SMART-Pool)	GGACUUAUAUUCAUGGAAAUU
	GCGCCAAGAAUGCCACCAAUU
	GACCAUGGCUGCUGAAAUCUU
	CAGCCAAGGAGUUUGCAGAUU

5.1.6 Antibodies

The antibodies used in the course of this work are listed in the tables below, along with their typical dilutions used for western blotting (WB) and immunofluorescence (IF). The species indicated are M= Mouse, S= Sheep and R=Rabbit.

5.1.6.1 Primary antibodies

Name	Antigen	WB	IF	Source
M α Myc	c-myc, clone 9E10	1:1000	1:1000	Cancer Research
R α Myc	c-myc	---	1:1000	Santa Cruz
M α VSV-G	VSV-G luminal domain	---	1:20	Ira Mellman
M α EEA1	Human EEA1	1:50	1:50	BD Biosciences
S α GFP	His-GFP	1:2000	----	Barr laboratory
M α GM130	Human GM130	---	1:2000	BD Biosciences
S α GM130	His-rat GM130	1:1000	1:1000	Barr laboratory
M α Rab1b	Human Rab1b, clone 1E7	1:5		Weide lab
R α RabGAP-5	RabGAP-5 aa 1-451	1:250	----	Barr laboratory
M α Calnexin	Human cell lysate	1:1000	1:1000	Chemicon
S α Golgin-84	Human Golgin84	1:1000	1:2000	Martin Lowe
S α Golgin-97	Human golgin-97 aa 589-769	1:500	1:500	Barr laboratory
R α Golgin-160	Human golgin-160	1:1000	1:1000	Barr laboratory
S α p115	Rat p115 aa 772-959	1:2000	1:2000	Barr laboratory
R α sec24C	Human Sec24C	----	1:1000	David Stephens
M α sec31	Human Sec31	----	1:1000	BD Biosciences
M α ERGIC53	ERGIC53	----	1:1000	Alexis Biochemical
M α Lamp-1	Human Lamp1	1:1000	1:1000	BD Biosciences
M α TFnR	Human TFnR	1:1000	1:250	Chemicon
S α TGN46	Human TGN46	1:2000	1:2000	Serotech
M α Tubulin	Tubulin, clone DM1A	1:1000	1:1000	Sigma-Aldrich

5.1.6.2 Secondary antibodies

Name	Species	Antigen	WB	IF	Source
AMCA- α -M	Donkey	Mouse IgG	----	1:250	Jackson Labs
Cy2- α -M	Donkey	Mouse IgG	----	1:1000	Jackson Labs
Cy3- α -M	Donkey	Mouse IgG	----	1:1000	Jackson Labs
Cy2- α -R	Donkey	Rabbit IgG	----	1:1000	Jackson Labs
Cy3- α -R	Donkey	Rabbit IgG	----	1:1000	Jackson Labs
Cy2- α -S	Donkey	Sheep IgG	----	1:1000	Jackson Labs
Cy3- α -S	Donkey	Sheep IgG	----	1:1000	Jackson Labs
HRP- α -S	Donkey	Sheep IgG	1:10000	----	Jackson Labs
HRP- α -M	Sheep	Mouse IgG	1:2000	----	Amersham
HRP- α -R	Donkey	Rabbit IgG	1:2000	----	Jackson Labs

5.2 Bacterial methods

5.2.1 Growth and maintenance of *E. coli*

Bacteria were grown at 37 °C in LB medium containing an appropriate antibiotics for selection, either 100 µg/ml ampicillin, 50 µg/ml kanamycin, or 34 µg/ml chloramphenicol. Short-term storage was on LB-agar plates plus antibiotic at 4 °C.

5.2.2 Bacterial strains

The following *E. coli* strains were used in the course of this work.

Strain	Genotype	Use
XL1-blue	F ['] ::Tn10 <i>proA</i> + <i>B</i> + <i>lacI</i> q Δ (<i>lacZ</i>)M15/ <i>recA1</i> <i>endA1</i> <i>gyrA96</i> (<i>NaI</i> r) <i>thi</i> <i>hsdR17</i> (<i>rK-mK</i> +) <i>glnV44</i> <i>relA1</i> <i>lac</i>	General cloning applications
GM2163	F ⁻ <i>ara-14</i> <i>leuB6</i> <i>fhuA31</i> <i>lacY1</i> <i>tsx78</i> <i>glnV44</i> <i>galK2</i> <i>galT22</i> <i>mcrA</i> <i>dcm-6</i> <i>hisG4</i> <i>rfbD1</i> <i>rpsL136</i> <i>dam13</i> ::Tn9 <i>xylA5</i> <i>mtl-1</i> <i>thi-1</i> <i>mcrB1</i> <i>hsdR2</i>	Non-methylated DNA for digestion with Dam/ Dcm- sensitive enzymes

BL21(DE3)*	F ⁻ <i>ompT gal [dcm] [lon] hsdSB rB⁻ mB⁻</i> ; an <i>E. coli</i> B strain with DE3, a λ prophage carrying the T7 RNA polymerase gene	Recombinant protein expression
JM109*	F ⁺ <i>traD36 proA+B+ lacIq $\Delta(lacZ)M15/ \Delta(lac-proAB)$ glnV44 e14- gyrA96 recA1 relA1 endA1 thi hsdR17</i>	Recombinant protein expression
TOP10	F ⁻ <i>mcrA $\Delta(mrr-hsdRMS-mcrBC)$ $\Phi80lacZ\Delta M15 \Delta lacX74 recA1 deoR araD139 \Delta(ara-leu)7697 galU galK rpsL (StrR) endA1 nupG$</i>	TA-cloning of PCR products

*BL21(DE3) and JM109 strains carrying the pRIL plasmid (Stratagene) were used for recombinant protein expression. This plasmid encodes the tRNA genes for rare arginine, isoleucine, and leucine codons and conveys chloramphenicol resistance.

5.2.3 Preparation and transformation of chemically competent bacteria

To prepare chemically competent *E. coli*, a single colony was picked from a fresh plate and used to inoculate 50 ml of LB (with selection, if necessary) and grown overnight at 37 °C while shaking. 1 ml of overnight culture was then used to inoculate 100 ml of fresh LB and the cells were grown at 37 °C until an OD₆₀₀ of 0.5. The culture was then chilled on ice for 15 minutes before being transferred to a sterile centrifuge tube and centrifuged at 3000 x g for 10 minutes at 4 °C. The supernatant was discarded and the cell pellet resuspended in 0.4 total culture volume of TfbI (30 mM KOAc, 100 mM RbCl₂, 10 mM CaCl₂, 50 mM MnCl₂, 15% (v/v) glycerol, pH adjusted to 5.8 with dilute acetic acid). The cells were incubated on ice for 15 minutes and then pelleted as before. The cell pellet was then resuspended in 0.04 volumes TfbII (10 mM MOPS, 75 mM CaCl₂, 10 mM RbCl₂, 15 % (v/v) glycerol, pH adjusted to 6.5 with dilute NaOH). After storing on ice for 15 minutes, the cells were aliquoted into 50 μ l aliquots in sterile Eppendorf tubes, frozen in liquid nitrogen, and stored at – 80 °C until needed.

For transformation, aliquots were thawed on ice before adding the DNA. In general, 10 μ l of a ligation reaction was used for transformation of 50 μ l competent bacteria, or 1 μ l of plasmid DNA (approx. 200 ng). Cells and DNA were mixed and left on ice for 20 minutes before being heat-shocked in a 42 °C water bath for 90 seconds. Cells were placed back on

ice for 2 minute before the addition of 250 µl LB lacking antibiotics. The cells were allowed to recover for 60 minutes at 37 °C with shaking before being plated on LB-agar plates containing an appropriate selection antibiotic. All 250 µl of a ligation transformation were plated while only 50 µl of a plasmid transformation was plated. Plates were then incubated overnight at 37 °C.

5.2.4 Preparation and transformation of electrocompetent bacteria

To prepare electrocompetent *E. coli*, a single colony was picked from a fresh plate and used to inoculate 5 ml of LB and grown overnight at 37 °C with shaking. 2.5 ml of the overnight culture was then used to inoculate 500 ml of fresh LB and grown at 37 °C until an OD₆₀₀ of between 0.5 and 0.6. The culture was then chilled on ice for 15 minutes before being transferred to a sterile centrifuge tube and centrifuged at approximately 3000 x g for 10 minutes at 4 °C. The supernatant was removed and the cells resuspended in 10 ml sterile, ice-cold water. Centrifuge tubes were then filled with 500 ml ice-cold water and spun as before. The supernatant was removed and the volume adjusted to 50 ml with ice-cold 10 % (v/v) glycerol before centrifuging as above. The cell pellet was resuspended in an equal volume of ice-cold 10 % (v/v) glycerol and the cells were aliquoted into 40 µl aliquots in sterile Eppendorf tubes, frozen in liquid nitrogen, and stored at – 80 °C until needed.

For electroporation, sterile 2 mm electroporation cuvettes were placed on ice to chill during the cells thawed on ice. 2 µl of yeast miniprep DNA or 10ng plasmid DNA was added to the cuvette followed by 40 µl of electrocompetent cells. The cuvette was flicked to mix DNA and cells and left on ice for 15 minutes. The electroporator was set to 2.5 kV, 25 µFarads. Cuvettes were dried with a tissue wipe and placed into the chamber. The cells were electroporated, ideally with a time constant of 4.7. 250 µl of LB medium was added to the cuvette immediately and the cells were transferred to a sterile Eppendorf tube and incubated shaking at 37 °C for 1 hour before being plated on LB-agar plates containing an appropriate selective antibiotic and grown at 37 °C over night.

5.2.5 Plasmid DNA preparation from bacteria

Plasmid DNA was prepared using either miniprep or maxiprep kits (Qiagen, Hilden, Germany) according to the manufacturers instructions. Minipreps were prepared from 1.5 ml, maxipreps from 250 ml of overnight cultures grown in LB containing selective antibiotics at 37 °C.

5.2.6 Purification of 6xHis-tagged proteins from bacteria

A single colony was picked from a fresh plate of transformed *E. coli* and used to inoculate 25 ml of LB plus selective antibiotics and grown overnight at 37 °C with shaking. 10 ml of the overnight culture was then used to inoculate 1 l of fresh LB plus antibiotics and grown at 37 °C until an OD₆₀₀ of 0.5 – 0.6 was reached. Depending upon the protein being expressed, cultures were shifted to 18 °C for 30 minutes before being induced with 0.5 mM Isopropyl β -D-thiogalactoside (IPTG) from a 1 M stock or induced immediately at 37 °C. Cultures were then left for either 3 hours (37 °C) or overnight (18 °C). Bacteria were then harvested by centrifugation at 3000x g for 15 minutes at 4 °C and cell pellets were frozen on dry ice for 20 minutes.

For protein purification, cell pellets were thawed and resuspended by the addition of 20 ml IMAC5 buffer containing protease inhibitor tablets and 0,1% TX100 per litre of original culture. The resuspended bacteria pellet was homogenised using a chilled Emulsiflex C5 high-pressure homogeniser (Avestin Europe GmbH, Mannheim). The lysate was passed about 10 times through the homogeniser until the DNA was sheared and the lysate became much less viscous. The lysate was then centrifuged at 28000 rpm for 30 minutes at 4 °C in an SW28 rotor in a Beckman Optima LE-80K Ultracentrifuge (Beckman, USA) to pellet the cell debris. The cleared lysate supernatant was transferred into a clean falcon tube. 0.5 ml of Ni-NTA agarose (Qiagen) per litre of original culture, washed in the same buffer, was added to the cleared lysate and the tube was rotated for 2 hours at 4 °C to allow protein binding to occur. The resin was then pelleted by centrifugation at 1000 x g for 5 minutes at 4 °C and washed in 2 x 30 ml of IMAC20 containing 0.1 % TX100. The resin was then washed in a further 30 ml of IMAC20 without TX100 and bound protein was eluted by the addition of IMAC200. The eluate was collected in 1 ml fractions. After SDS-PAGE analysis of 10 μ l of these fractions, peak fractions containing recombinant protein were pooled and dialysed overnight at 4 °C TBS containing 2mM DTT. The recombinant protein was aliquoted, quickly frozen in liquid nitrogen and stored at -80°C. After quickly thawing the protein at 37°C with shaking the concentration was determined using a standard Bradford assay (5.4.3).

5.3 DNA methods

Enzymes for DNA modification were obtained from New England Biolabs (Ipswich, MA, USA), Promega (Madison, WI, USA), or Invitrogen (Carlsbad, CA, USA) and used according to the supplier's instructions.

5.3.1 "Shortway" cloning strategy

A standard cloning strategy, referred to as the "Shortway" system, was used when generating constructs, in order to make all inserts compatible with a wide range of different vectors. This involved generating inserts with a *Bam*HI, *Bgl*II, or *Bcl*I site at the 5' end and a *Sal*I or *Xho*I site at the 3' end. The overhanging ATC of the *Bam*HI/ *Bgl*II/ *Bcl*I site was designed to be in frame with the start codon of the insert.

GGG ATC CCC ATG (*Bam*HI)

GAG ATC TCC ATG (*Bgl*II)

GTG ATC ACC ATG (*Bcl*I)

The restriction site is bold and the start codon is in italics.

These restriction sites were added by PCR. The insert was TA-TOPO cloned into the vector pCRIITOPPO (Invitrogen, Carlsbad, CA, USA). Constructs were sequenced in pCRIITOPPO and then subcloned into the following vectors.

5.3.2 Compatible vectors

Yeast:

<i>DNA binding domain (n-term)</i>	pFBT9	BamHI-SalI
<i>Activation domain (N-term)</i>	pACT2	BamHI-XhoI

Bacterial expression:

<i>His-tagging (N-term)</i>	pQE32	BamHI-SalI
<i>GST-tagging (N-term)</i>	pFAT2	BamHI-XhoI
<i>MBP-tagging (N-term)</i>		
<i>with His-tag (C-term)</i>	pMalTEV-His	BamHI-SalI

Mammalian expression:

<i>GFP-tagging (N-term)</i>	pEGFP-C2	BglII-SalI
<i>GFP-tagging (C-term)</i>	pEGFP-N3	BglII-SalI
<i>Myc-tagging (N-term)</i>	pcDNA3.1/MycA	BamHI-XhoI

If a DNA stretch of interest contained internal XhoI and SalI sites it was cloned using 3' BamHI / BglII / BclI sites, and inserted into singly cut vectors using the indicated 5' end cutting enzyme. The vectors were treated with alkaline phosphatase for 15 min at 37° prior to loading on agarose gels. When all restriction sites required for “shortway –cloning” were found in the DNA stretch of interest, it was cloned, and one of the internal restriction sites was removed by a silent site directed mutagenesis.

5.3.3 Restriction digests and agarose gel electrophoresis of DNA

Analytical restriction digests were carried out in a total volume of 20µl using 0.5µl of each enzyme in the appropriate buffer to digest approximately 500 ng of DNA. Digests were carried out for 1.5 hour at the indicated temperature. The whole reaction was mixed with 4 µl DNA loading buffer and loaded for electrophoresis onto an agarose gel of concentrations between 0.5% and 2% depending on the expected size of the DNA fragments. To pour gels agarose of the desired concentration was dissolved in 1 x TAE by heating. Ethidium bromide was added to a concentration of 0.8 µg/ml for visualisation. The gel was run in 1 x TAE at a constant voltage of 80 V for 45 minutes. DNA was visualized on a UV transilluminator.

Preparative restriction digests were performed using 2.5 µg DNA. Vector DNA was treated with alkaline phosphatase at 37°C for 15 minutes by the addition of 1 µl enzyme to the digestion mix prior to loading on the gel.

After electrophoresis, appropriate bands were excised using a scalpel blade and purified using a gel extraction kit (Qiagen) according to the manufacturer's instructions.

5.3.4 Cloning digested DNA fragments

Ligations were performed in a total volume of 20µl using 1µl of T4 DNA ligase (NEB) in 1x ligase buffer (NEB). 100 ng of vector DNA was used along with enough insert DNA to make a 3:1 molar ratio of insert to vector DNA. Ligations were incubated for 2 hours at room temperature before transformation of bacteria with 10 µl ligation product.

5.3.5 cDNA synthesis

cDNA was generated by reverse transcription using the Advantage RT-for-PCR kit from BD Clontech (Franklin Lakes, NJ, USA). For this, 1 µg of total RNA was diluted to 12.5 µl in RNase-free water and, together with 1 µl of the oligo (dT)₁₈ primer (20 pmol/µl), heated for 2 minutes at 70 °C. After rapid cooling on ice the following components were added to the mixture: 4µl of 5x reaction buffer (250 mM Tris-HCl pH 8.3, 375 mM KCl, 15 mM MgCl₂),

1 µl of dNTP mix (10 mM), 0.5 µl of RNase inhibitor and 1 µl of MMLV reverse transcriptase. The reaction was incubated for 1 hour at 42 °C, and then heated for 5 minutes at 94 °C to stop the reaction and to terminate DNase activity. The reaction was diluted with RNase-free water to 100 µl total volume. 10 µl aliquots were frozen at -20°C.

5.3.6 PCR and cloning of PCR products

Oligonucleotides for PCR reactions were obtained from Metabion (Martinsried, Germany) pre-dissolved to 100 µM.

For all PCR reactions a GeneAmp PCR System 2400 thermocycler (Perkin-Elmer, Waltham, MA, USA) or a Benchtop Cycler (Eppendorf) was used. Reactions were carried out in a total volume of 50 µl and contained 1 x polymerase reaction buffer, 1.25 µM forward and reverse primers, 0.25 mM dNTPs, and 1 µl (2.5 U) *Pfu* turbo polymerase (Stratagene, La Jolla, CA, USA) or 1 µl (1 U) KOD hot start polymerase (Novagen, Madison, WI, USA). As a template either 10ng plasmid DNA, 5 µl marathon-ready cDNA library (Clontech, Palo Alto, CA, USA) or a HeLa cDNA library (see 5.3.5) was used.

For **Pfu** polymerase the following scheme was used:

- 2 min 95° C
- 15sec 95°
- 25 cycles of:
 - 30 sec 55°
 - 2 min / kb of DNA to be amplified 68°
- 2 min / kb of DNA to be amplified 68°
- Cooling to 4°C

For **KOD** polymerase normally the following scheme was used:

- 2 min 95° C
- 15sec 95°
- 25 cycles of:
 - 30 sec 60°
 - 30sec / kb of DNA to be amplified 72°
- 30sec / kb of DNA to be amplified 72°
- Cooling to 4°C

Dependent on the DNA stretch of interest elongation times and temperatures were altered. PCR products were then analysed by agarose gel electrophoresis.

For cloning from cDNA libraries, a nested approach was used. A first round of PCR was performed as described using primers matching sequences in the 3' UTR and in the 5' UTR. The product of this first round of PCR was purified using a PCR nucleotide removal kit (Qiagen, Hilden) according to the manufacturer's instructions. 5 µl of the purified PCR product were used in a second round of PCR. This time primers matching to the 3' and the 5' end of the ORF were used. The product of this second round of PCR was then analysed and purified by agarose gel electrophoresis.

Following gel extraction of PCR products using a Gel extraction kit (Qiagen, Hilden) according to the manufacturer's instructions, Adenosine overhangs were added to the ends of the PCR product by incubation with 1 µl *Taq* polymerase (Promega, Madison, WI, USA) at 72 °C for 30 minutes in the presence of 1x polymerase buffer and 0.25 mM dNTPs in a total volume of 50 µl. The product was inserted into the pCRIITOPPO vector using the TA-TOPO cloning system (Invitrogen, Carlsbad, CA, USA).

Two µl of TA- tailed PCR product was incubated with 0.5 µl TA-TOPO cloning mix for 5 minutes at room temperature. If the standard method wasn't successful 0.5 µl of salt mix was added and the mix was incubated for 30 minutes at room temperature. The entire mix was then used for transformation of TOP10 bacteria.

5.3.7 Site-directed mutagenesis

Point mutagenesis was carried out using a Quickchange method. Forward and reverse mutagenic primers were designed to be 33 bases long with the codon to be altered in the middle, 15 unchanged bases on either side. The quickchange reaction was set up in a total volume of 50 µl like in 5.3.6. The cycling parameters used were the same as for 5.3.6. After cooling to 4 °C, 1 µl of the restriction enzyme *DpnI* was added to the reaction and incubated for 1 hour at 37 °C to digest methylated parental DNA. 10 µl of the reaction mix was used to transform XL1-blue bacteria.

5.3.8 DNA sequencing

All insert DNAs generated by PCR or mutagenesis were sequenced commercially by Medigenomix (Martinsried, Germany), or in house by the Core Facility of the Max-Planck-Institute.

5.4 Protein methods

5.4.1 SDS-PAGE and Coomassie staining

Small (8 x 6.5 x 0.075 cm) SDS polyacrylamide gels were prepared. These consisted of a resolving, or upper gel and a stacking or upper gel. First the lower gel was cast in wide range of percentages dependent on the molecular size of the protein of interest.

Gel (%)	4	5	6	7	7.5	10	12	12.5	15
Lower buffer (4x)	2.5	2.5	2.5	2.5	2.5	2.5	2.5	2.5	2.5
AMBA (37.5:1)	1.3	1.7	2.0	2.3	2.5	3.3	4.0	4.2	5.0
Distilled water	6.2	5.8	5.5	5.2	5.0	4.2	3.5	3.3	2.5

To polymerise the minigel 10 µl TEMED and 100µl of 10% (w/v) APS were added and the gel was carefully overlaid with water. After the lower gel was fully polymerized the overlaying water was sucked of and an upper gel was cast on top.

Gel (%)	3	3.5	4	4.5
Upper buffer (4x)	2.5	2.5	2.5	2.5
AMBA (37.5:1)	1.0	1.2	1.3	1.5
Distilled water	6.5	6.3	6.2	6.0

To polymerise the minigel, 10µl TEMED and 100µl of 10% (w/v) APS were added. A comb was inserted immediately avoiding air bubbles.

Samples were prepared in SDS-PAGE sample buffer and boiled for 5 minutes at 95°C. Gels were run in a BioRad Mini-PROTEAN 3 gel chamber (BioRad, Germany) in SDS-PAGE running buffer at 180V, 30 mA per minigel.

Protein gels were stained by immersion in 0.01 % Coomassie Brilliant Blue R-250 in 50 % methanol, 10 % acetic acid for 20 minutes, while shaking. Gels were destained in 20 % isopropanol, 20 % acetic acid.

5.4.2 Western blotting

Proteins run on SDS-gels were transferred to 45 μ m Hybond-C Extra Nitrocellulose (Amersham-Pharmacia, UK) by semi-dry blotting in transfer buffer (1x SDS-PAGE running buffer plus 10 % methanol) using a Trans-Blot SD Transfer Cell (BioRad, Germany) at 15 V, 300 mA, for 45 minutes. Blots were then blocked in milk-PBS for 1 hour before addition of the primary antibody.

Blots were usually incubated with the primary antibody in milk-PBS for 1 hour at room temperature before being washed 3 x 5 minutes in milk-PBS. Secondary antibodies linked to horseradish peroxidase were subsequently incubated with the blot for 1 hour before the blots were washed for a further 3 x 5 minutes in milk. Bound antibodies were then detected by chemiluminescence using ECL Western blot detection reagents (Amersham-Pharmacia, UK) according to the manufacturer's instructions, exposed to Kodak X-Omat XAR-5 film for an appropriate length of time and developed in a Kodak X-OMAT 2000 Processor.

5.4.3 Determination of protein concentration

Protein concentrations were determined using the BioRad Protein Assay kit (BioRad, Germany), a modified version of the Bradford Assay. The dye reagent was diluted 1:5 in water and 1 ml 1x reagent was used per assay point. Known concentrations of bovine serum albumin (BSA) were used to generate a standard curve. The samples were mixed well with the dye reagent, and transferred to disposable cuvettes for measurement of the OD₅₉₅ in an Ultrospec 3000 Pro spectrophotometer (Amersham-Pharmacia). The Concentration of the protein samples was calculated according to the BSA standard curve.

5.4.4 Protein precipitation with TCA

From large volumes proteins were precipitated using trichloroacetic acid (TCA) for loading on SDS-PAGE gels. Sodium deoxycholate was added to a final concentration of 0.02 % and the sample vortexed. Next TCA was added to a final concentration of 12 %, the sample vortexed, and left on ice for 30 minutes. Precipitated proteins were then recovered by centrifugation at 20000 x g for 20 minutes at 4 °C. The supernatant was discarded and the pellet washed with ice-cold acetone before being centrifuged for a further 10 minutes. The supernatant was discarded and the pellet resuspended in an appropriate amount of 1.5x SDS-PAGE sample buffer with addition of 1 M Tris-HCl pH 8.0, to adjust the pH of the sample if necessary.

5.4.5 Antibody generation and purification

Polyclonal antibodies were generated by immunisation of rabbits with recombinant protein either in collaboration with Charles River Laboratories, L'Arbresle Cedex, France or the Max-Planck-Institute animal facility. Rabbits were immunised initially subcutaneously with 250 µg antigen mixed with Freund's complete adjuvant followed by four intramuscular boosts with 250 µg antigen mixed with Freund's incomplete adjuvant. All test bleeds and the final bleed out samples were tested on Western Blot for their ability to recognise recombinant antigen and the endogenous protein in cell extracts. Specific antibodies were purified from the bleed out via affinity chromatography.

In order to exclude antibodies against the tag- protein (MBP, GST, 6xHis) used to purify of original recombinant antigen, the tag- protein alone was coupled to Affigel-15 (BioRad, Germany). 4 ml of Affigel-15 beads were washed once with water to remove the isopropanol storage solution and added to 4 ml protein solution of 1 mg/ml recombinant tag protein. After 2 hours of incubation with shaking at 4 °C, the gel was spun for 2 minutes at 1000x g. Thereafter it was washed three times with 15 ml PBS, once with 15 ml of 0.2 M glycine pH 2.8 and again three times with 15 ml PBS to remove any uncoupled protein.

For purification of the antibody 15 ml of serum was filtered and incubated with 1 ml of the affinity matrix coupled to about 1 mg tag- protein rolling for 90 minutes at 4 °C. After this, the slurry was pelleted by centrifugation for 2 minutes at 1000x g. The supernatant contained the antigen- specific antibodies. Tag protein- specific antibodies remained bound to the matrix. The supernatant was then incubated rolling for 90 minutes at 4 °C with another equally prepared affinity matrix coupled to approx. 1 mg antigen to purify the antigen-specific antibodies. After this, the slurry was pelleted by centrifugation for 2 minutes at 1000x g. Following three washes with 15 ml PBS, bound antibodies were eluted using 0.2 M glycine pH 2.8 and collected as 1 ml fractions into Eppendorf tubes containing 200µl 1M Tris-HCl pH 8.0. Samples were immediately mixed to neutralise the acidic pH and stored on ice. After SDS-PAGE analysis antibody peak fractions were pooled, dialysed overnight against PBS, aliquoted and stored at – 80 °C or kept at 4 °C for immediate use.

5.5 Yeast methods

5.5.1 Strains, media and growth

The *S.cerevisiae* strain PJ69-4A was used for all two-hybrid experiments, the genotype of which is:

MATa, *trp1-901*, *leu2-3, 112*, *ura3-52*, *his3-200*, *gal4Δ*, *gal80Δ*, *LYS2::GAL1UAS-GAL1TATA-HIS3*, *GAL2UAS-GAL2TATA-ADE2*, *MEL1 met2::GAL7-lacZ*

Yeast was grown in either YPDA or SC dropout media selecting for appropriate plasmids at 30 °C. Short-term storage was on agar plates at 4 °C.

YPDA medium consisted of 20g/l peptone (Difco/Becton-Dickinson), 10 g/l yeast extract (Difco), and 20g/l glucose (plus 20 g/l Bacto-agar for YPDA-agar). The medium was then sterilised in an autoclave and, after cooling to approximately 55 °C, 6 ml 0.2 % sterile filtered adenine hemisulphate was added.

Synthetic complete (SC) dropout medium was prepared as follows: Amino acid base (-His/-Trp/-Leu/-Ura) was prepared by mixing 20 g alanine, arginine, asparagine, aspartic acid, cysteine, glutamine, glutamic acid, glycine, inositol, isoleucine, lysine, methionine, phenylalanine, proline, serine, threonine, tyrosine, and valine with 5 g adenine and 2 g para-aminobenzoic acid. To prepare dropout mixes, 36.7 g of amino acid base was mixed with either 2 g histidine, 4 g leucine, 2 g tryptophan, or 2 g uracil, as appropriate to form the correct dropout mix. The SC dropout medium was autoclaved and after cooling to approximately 55 °C, 6 ml 0.2 % sterile filtered adenine hemisulphate was added, unless the dropout medium should be without adenine.

5.5.2 Yeast transformation (frozen cell method)

To prepare frozen competent yeast cells, several colonies were picked from a freshly grown plate and grown overnight in YPDA or in SC –Trp for bait strains at 30 °C with shaking. The overnight culture was diluted to an OD₆₀₀ of 0.15 in fresh medium and grown at 30 °C to an OD₆₀₀ of 0.5 – 0.6 (1.2 – 1.5 x 10⁷ cells). The cells were then harvested at 3000 rpm for 2 minutes at room temperature in a Heraeus centrifuge. The cells were washed in one half culture volume sterile water and spun as before. The cells were then resuspended in 1/8th culture volume of LiSorb and incubated for 5 minutes at room temperature before being spun as before. The cell pellet was resuspended in 600 µl LiSorb per 100 ml original culture.

Single stranded carrier DNA was added (10 μ l /100 μ l yeast of 10 mg/ml Gibco salmon sperm DNA, heat-treated at 95 °C for 5 minutes). After aliquoting the cells were kept at -80°C.

To transform frozen competent yeast, the cells were thawed at room temperature. Per transformation 10 μ l of cells were used. About 100ng of plasmid DNA were added to the cells, followed by 150 μ l LiPEG and 17,5 μ l DMSO. The mixture was vortexed and incubated for 15 minutes at room temperature before heat-shocking for 15 minutes in a 42 °C waterbath. The cells were then pelleted at 400xg in a microfuge, the supernatant was removed, and the cells were resuspended in 200 μ l sterile water. 100 μ l were the plated onto appropriate selective plates and grown at 30 °C.

In the case of directed yeast two-hybrid experiments, transformed cells were originally grown on SC-Leu/-Trp plates to select for both the bait and prey plasmids. After 2 –3 days growth, colonies were picked and restreaked onto SC-Leu/-Trp and SC-QDO (SC-Leu/-Trp/-His/-Ade) plates to assess the two-hybrid interaction.

5.5.3 Plasmid DNA minipreps from yeast cells

To prepare plasmid DNA from yeast cells a matchhead-sized ball of cells scraped from a fresh plate into 1 ml water was pelleted at 400 g in a microfuge. The cell pellet was resuspended in 500 μ l buffer S. The cells were then incubated at 37 °C for at least 1 hour. Afterwards 100 μ l lysis buffer was added, vortexed, and the lysate incubated at 65 °C for at least 30 minutes until the mixture cleared. 166 μ l 3 M KOAc pH 5.5 was then added to stop the lysis reaction. The tubes were inverted to mix, and incubated on ice for 10 minutes. After centrifugation at 20000x g in a microfuge at 4 °C for 15 minutes the supernatant was transferred to a clean Eppendorf tube. 800 μ l cold ethanol was added and the tubes were inverted to mix. Following incubation on ice for 10 minutes the reaction was spun as before for a further 10 minutes. The supernatant was removed and the pellet washed in 1 ml 70% ethanol. The pellet was allowed to air dry before resuspending in 40 μ l sterile water.

5.5.4 Yeast two-hybrid screening

To screen human a cDNA library for potential interactors of a protein of interest, the protein was cloned into the pFBT9 vector. Next a competent bait strain containing this construct was generated as described in (5.5.2) using SC –Trp media as selection.

To determine the efficiency of transformation in the newly generated bait strain it was transformed using a cDNA library in pACT2 generated from human testis. It was then plated in different dilutions on SC -Leu/-Trp to select for co-transfected yeast. The

efficiency was calculated as [(number of colonies x volume of suspension (μl))/plated volume (μl) x dilution x amount of library DNA (μg)]. With this information a defined 1 million clones could be screened.

After transformation of the bait strain with sufficient cDNA library to ensure 1 million screened clones, the yeast was plated on 15 cm dishes on SC QDO to select for interaction. Plates were left at 30°C for up to seven days, before DNA was purified from the yeast as described in 5.5.3. The DNA was then transformed for amplification in *E. coli* using electroporation as described in 5.2.4 and subsequently purified as in 5.2.5. These plasmids were then re-transformed into the bait strain as in PJ 694A together with an empty pFBT9 plasmid. Using these two controls real positives could be distinguished from false positives and were then sequenced as in 5.3.8 and identified using the “Basic Local Alignment Search Tool” BLAST (<http://www.ncbi.nlm.nih.gov/BLAST/>).

5.6 Mammalian cell culture

5.6.1 Cell culture

HeLa L and hTERT-RPE1 cells were cultured at 37 °C and 5 % CO₂ atmosphere in Dulbeccos Modified Eagle Medium (DMEM) containing 10 % fetal calf serum, 100 U/ml penicillin and 100 μg/ml streptomycin (GIBCO, Invitrogen, Carlsbad, CA, USA)

5.6.2 Transient transfection of mammalian cells

HeLa cells were transiently transfected with plasmid DNA constructs using the lipid-based transfection reagent FuGENE6 (Roche, Germany) or the equivalent LT1 (MoBiTec, Germany). For a 24-hour transfection about 50.000 cells per well of a 6-well plate were seeded 24 hours prior to the transfection. Per single well of a 6-well plate 1 μg plasmid DNA was used with 3 μl FuGene6 or LT1 diluted in 100 μl OptiMEM medium (Invitrogen, Carlsbad, CA, USA). After gentle mixing and complex formation for 25 minutes at room temperature the mixture was added drop-wise to the cells. Usually the transfection was left for 24 hours.

5.6.3 RNA interference

In order to selectively knockdown the expression levels of particular proteins, small interfering RNA duplexes (siRNAs) were transfected into HeLa cells. Either 21 nucleotide siRNA duplexes with a 3' overhang of two nucleotides were designed or pre-designed

SMART Pools by Dharmacon Inc. were used. The lyophilised and pre-annealed siRNA duplexes were diluted to a stock solution of 100 μ M and aliquots were stored at -80°C .

HeLa cells were seeded 24 hours prior to transfection to a density of about 25,000 cells per well of a 6-well plate for a typical 72 hours siRNA time course. For transfection the lipid-based transfection reagent Oligofectamine (Invitrogen, Carlsbad, CA, USA) was used. For a single well of a 6-well plate 3 μ l Oligofectamine and 3 μ l of 20 μ M siRNA duplex were added to 200 μ l OptiMEM medium (Invitrogen, Carlsbad, CA, USA) in a RNase-free Eppendorf tube. The mixture was mixed gently and left for 25 minutes at room temperature. The mixture was then added drop-wise to the cells.

5.7 Mammalian cell methods

5.7.1 Immunofluorescence

For immunofluorescence cells were cultured on ethanol-flamed coverslips in 6-well plates. For paraformaldehyde fixation, 3 % paraformaldehyde was prepared by dissolving 3 g paraformaldehyde in 100 ml PBS at 80°C in a fume hood. 10 μ l 1 M CaCl_2 and 10 μ l 1 M MgCl_2 were added while stirring before the solution was allowed to cool to room temperature and pH adjusted to 7.4. The solution was then vacuum-filtered through a 0.45 μ m filter and 15 ml aliquots were stored at -20°C . The coverslips were fixed in 3% paraformaldehyde for 15 minutes and were then washed once in 2 ml quench solution (50 mM NH_4Cl in PBS made freshly prior to use) before incubation in a further 2 ml quench solution for 10 minutes. The coverslips were then washed in 3 x 2ml PBS. If the cells were to be permeabilised, they were incubated for 5 minutes in permeabilisation solution (0.2% TX100 in PBS) before washing in 3 x 2ml PBS.

For methanol fixation, the coverslips were washed twice in PBS. Per well 2ml of -20°C methanol was added, and the 6-well was incubated at -20°C for 5 minutes. Subsequently the coverslips were washed in room temperature PBS twice.

For antibody labelling, primary antibodies were diluted appropriately in PBS. A strip of parafilm was placed on a flat surface and 50 μ l drops of the antibody solution were placed on the strip. Coverslips with fixed cells were then transferred, cell face down, onto the antibody drops. The coverslips were then covered with a moist, dark chamber and left for 1 hour at room temperature. After this incubation the coverslips were returned to the wells and washed in 3 x 2ml PBS. The same procedure as before was followed for incubation with

secondary antibodies conjugated to appropriate fluorophores. After washing in PBS for the final time, coverslips were mounted onto clean microscope slides by placing them, cell face down, onto a 10 μ l drop of Moviol mounting medium. The mounting medium used usually contained 1 μ g/ml DAPI stain. The coverslips were then left overnight at room temperature to allow the Moviol to dry.

Images were collected using an Axioskop-2 with a 63x Plan Apochromat oil immersion objective of NA 1.4, standard filter sets (Carl Zeiss, Göttingen, Germany), a 1300 by 1030 pixel cooled-CCD camera (model #CCD-1300-Y, Princeton Instruments, Trenton, NY) and Metavue software (Visitron Systems, Puchheim, Germany). Images were cropped in Adobe Photoshop CS then sized and placed using Adobe Illustrator CS (Adobe, San Jose, CA).

5.7.2 Cell extracts

In order to detach cells from the cell culture dishes, HeLa cells were treated with PBS containing 1 mM EDTA for 15 minutes at 37 °C, then gently pipetted off from the cell culture dishes into clean plastic vials and centrifuged for 5 minutes at 400 g. Total cell extracts were prepared from cell pellets by addition of ice-cold mammalian lysis buffer containing 1 tablet of complete mini protease inhibitor (Roche, Mannheim, Germany) per 10 ml solution and pipetting up and down several times. After 20 minutes incubation on ice the lysate was cleared by centrifugation at 20000 g at 4 °C for 15 minutes. The supernatant was transferred to a clean Eppendorf and the protein concentration of the extract was determined as described in 5.4.3.

5.7.3 Immunoprecipitation

For immunoprecipitation (IP) cell extracts were incubated with antibodies in an appropriate volume of mammalian lysis buffer. To detect proteins on Western blot IPs were usually performed with cell extracts from one 10 cm dish and 1 μ g purified antibody in a total volume of 1 ml. After addition of 15 μ l of protein- G sepharose (Amersham, UK) the slurry was incubated for 2 hours on a roller at 4 °C for the antibody-antigen complex to form and be extracted. The complex on the sepharose beads was collected by 400g centrifugation at 4 °C for 5 minutes; the supernatant was kept to show depletion of the antigen. The beads were washed three times with 1 ml lysis buffer. After a final centrifugation at top speed for one minute, residual buffer was removed, and boiling in 1.5x SDS sample buffer eluted the bound complex.

To IP intact transmembrane complexes, a different buffer (50mM HEPES-NaOH pH 7.5, 150 mM KCl, 1 mM EGTA, 1 mM EDTA, 5mM MgCl₂, 5% [vol/vol], 1% Digitonin [wt/vol], heated to 95°C prior to use) had to be chosen.

5.7.4 Cell fractionation

For fractionation experiments HeLa cells were grown on 15 cm dishes to 70% confluence. Cells were either transfected using 15 µg of each plasmid DNA and left for 24 hours to express the protein of interest, or incubated for 30 min in growth medium containing 5 µg/ml Brefeldin A. The cells were then harvested and washed twice in ice cold PBS. The cell pellet was resuspended in 1 ml of 25 mM Tris HCl pH 7.4, 130 mM KCl, 5 mM MgCl₂, containing protease inhibitor cocktail tablets (Roche, Germany). Cells were then broken open by passing them 40 times through a 27G needle using a 1 ml syringe. Nuclei and cell debris were removed by centrifugation for 5 min at 1000x g and 4°C. This post-nuclear supernatant was split into two equal aliquots. One was kept on ice and corresponds to the total material. The other half was centrifuged for 30 min at 100,000x g and 4 °C. The supernatant corresponding to the soluble cytosolic fraction was transferred to a fresh tube. The pellet, corresponding to the membrane fraction, was resuspended in 100µl 1.5x sample buffer. Aliquots of the supernatant and total of each sample were precipitated by adding 0.5 µl of 10% 26 [wt/vol] sodium deoxycholate and 30 µl of 100% [wt/vol] TCA. After 30 min incubation on ice, precipitated protein was collected by centrifugation at 20,000x g and 4 °C. Pellets were washed with ice cold acetone, and then resuspended in 100 µl of 1.5x sample buffer.

5.7.5 Carbonate extraction

For carbonate extraction experiments, a 200µl aliquot of the post nuclear supernatant generated as in 5.7.4 was split in two identical halves. One was kept on ice as the total material, while the other was centrifuged at 100,000 x g for 30 min at 4°C to generate a membrane pellet. The pellet was then resuspended in 100 mM Na₂CO₃ and incubated on ice for 30 min. To recover the membrane the sample was centrifuged at 100,000 x g for 30 min at 4°C. The supernatant was precipitated using 25% [wt/vol] TCA, and equal amounts of the total, carbonate extracted supernatant and membrane pellet fractions were analysed by western blotting.

5.7.6 Proteinase K digestion

For proteinase K digestion experiments, HeLa cells from two 70% confluent 15 cm dishes and one 10 cm dish transfected with GFP-tagged TBC1D20 constructs for 24 h were washed twice in cold PBS, then scraped of the dishes, and pooled. The cell pellets were resuspended using 6 passes through a 21G needle in 50 mM HEPES pH 7.5, 200 mM Sucrose, 1 mM MgCl₂, and 1 mM EDTA to give a final volume of 1 ml. This cell suspension was passed through an EMBL cell cracker (European Molecular Biology Laboratories, Heidelberg, Germany) fitted with an 8.002 mm diameter ball. The broken cell suspension was centrifuged twice at 1000 x g and 4°C for 5 min to remove cell debris and leave a post nuclear supernatant. Proteinase K (New England Biolabs, Ipswich, MA) was incubated at 37°C for 30 min prior to use to inactivate any contaminating lipase activity. The post nuclear supernatant was then adjusted to 10 mM CaCl₂, and 100 µl aliquots treated with 2 µg proteinase K, 0.5 [vol/vol] % Triton-X 100, or both proteinase K and Triton-X 100 for 30 min on ice. To stop the reaction, a half volume of 100 [wt/vol] % TCA was added, samples were then vortexed and incubated on ice for 30 min. Proteins were recovered by centrifugation at 20,000 x g for 15 min, the pellets washed in 1 ml of -20°C acetone, resuspended in 100 µl of sample buffer, and 20µl analysed by western blotting.

5.8 Cellular and biochemical assays

5.8.1 EGF uptake assay

EGF coupled to Alexa Fluor 488 (40xstock, 200 µg/ml) and transferrin coupled to Texas Red (100xstock, 5 mg/ml) (Molecular Probes, Karlsruhe) were stored as stock solutions in PBS at -20 °C. For uptake assays, HeLa cells plated on glass cover slips at a density of 50,000 cells/well of a six-well plate were washed three times with serum-free growth medium 36 h after plating, and then incubated in serum-free growth medium for 15–16 h at 37 °C and 5% CO₂. Cover slips were washed three times in ice-cold PBS, and placed on 40 µl drops of uptake medium (DME, 2% [wt/vol] bovine serum albumin, 20mM HEPES-NaOH (pH 7.5) and either 5 µg/ml EGF or 50 µg/ml transferrin on an ice-cold metal plate covered in Parafilm (Pechiney Plastic Packaging, Menasha, WI). After 1 h incubation, the coverslips were washed three times in ice-cold PBS to remove excess ligand. One cover slip was fixed to give the total bound ligand, and the remaining cover slips were transferred to a six-well plate containing pre-warmed growth medium and incubated at 37 °C and 5% CO₂.

At the time points of interest, cover slips were fixed and processed for immune fluorescence microscopy (5.7.1).

5.8.2 VSV-G transport assay

HeLa cells plated on glass cover slips were transfected with a plasmid encoding green fluorescent protein (GFP) tagged VSV G ts045 protein for 2 h at 37°C then 12 h at 39.5°C. The cells were then incubated for 30 minutes at 4°C on ice to promote VSV G protein folding, and afterwards the growth medium was replaced with pre-warmed medium at 31.5°C. Immediately before adding pre-warmed medium a t=0 time point was fixed with 3% [wt/vol] paraformaldehyde in PBS. After the required chase period, usually at 30 and 60 minutes, cover slips were fixed and processed for fluorescence microscopy (5.7.1). Cell surface VSV G was detected with a monoclonal antibody against the VSV G luminal domain. To detect transfected cells or to stain endogenous markers, the cell membrane was permeabilised using 0.2 % TX100 [vol/vol] after staining for cell surface VSV G and cells were incubated with antibodies.

5.8.3 GTP-hydrolysis assay

For Rab loading reactions, 10 µl of assay buffer, 73 µl dH₂O, 10 µl of 10 mM EDTA (pH 8.0), 5 µl of 1 mM GTP, 2 µl of [γ ³²P] GTP (Amersham PB10244; 10 mCi/ml; 5000 Ci/mmol) and 100 pmoles GST–Rab protein were mixed on ice. Initially GTP binding was measured using a nitrocellulose filter-binding assay to determine the optimal time for GTP-loading. To do this a 20µl aliquot of the loading mixture was taken and pipetted immediately onto a nitrocellulose filter on top of a vacuum flask. The filter was washed twice with assay buffer (without BSA) and then dried on Whatman paper, before being transferred to a scintillation vial containing 4 ml of Ultima Gold scintillation liquid (Perkin-Elmer) and was scintillation counted.

After 15 min incubation at 30 °C, loaded Rabs were stored on ice. 5 µl aliquots were taken in duplicate and immediately added to 795 µl of ice cold 5% [wt/vol]-activated charcoal slurry in 50 mM NaH₂PO₄, and left on ice. This is the t=0 value. The Rab loading mix was then split into two equal halves. In one half (+GAP) GTPase- reactions were started by the addition of 0.5- 10 pmoles of GAP. The other half was used to calculate the basal hydrolysis by the Rab (-GAP), so only a corresponding amount of 1x assay buffer was added. Reactions were then incubated at 30 °C, taking 5 µl samples in duplicate at 60 min. The 5 µl aliquots were immediately added to 795 µl of ice cold 5% [wt/vol]-activated

charcoal slurry in 50 mM NaH_2PO_4 , left for 1 h on ice and then centrifuged at 16000 g in a bench-top microfuge to pellet the charcoal. A 400 μl aliquot of the supernatant was scintillation counted in 4ml of Ultima Gold scintillation liquid (Perkin-Elmer).

At the end of the reaction a 2.5 μl aliquot of the assay mix was scintillation counted to measure the specific activity of the reaction in cpm/pmole of GTP, so the amount of GTP hydrolysed during the reaction could be calculated. The measured specific activity was then multiplied by 40 in order to get the specific activity for the full assay of 100 μl . This value was then divided by the total of 5000 pmol GTP in the reaction to obtain the specific activity in cpm/pmole of GTP.

The measured values of the 5 μl aliquots taken from each reaction in duplicate at each time point were averaged and then multiplied by 2 as only 400 μl out of 800 μl charcoal mix were used. The values were then multiplied by 20 as only 5 μl out of 100 μl total reaction mix were measured. To calculate the amount of GTP hydrolysed in pmol, these values were then divided by the specific activity per pmole GTP cpm/pmole. The $t=0$ values were then subtracted to eliminate the background of the reaction. The amount of GTP hydrolysed by the Rabs alone (-GAP) was then subtracted from the stimulated reactions (+GAP). By this calculation the stimulation of GTP hydrolysis by all Rabs upon addition of the same GAP can be compared.

Abbreviations

Abbreviation	Description
aa	Amino acid
ARF	ADP ribosylation factor
ARL	ARF like
BFA	Brefeldin A
CCP	Clathrin coated pit
CCV	Clathrin coated vesicle
CGN	<i>Cis</i> -Golgi network
COP	Coat protein
C-terminus	Carboxyl terminus
EE	Early endosome
EEA1	Early endosomal antigen 1
EGF	Epidermal growth factor
EGFR	EGF receptor
ER	Endoplasmic reticulum
ERGIC	ER-Golgi intermediate compartment
GAP	GTPase activating protein
GDF	GDI displacement factor
GDI	GDP dissociation inhibitor
GDP	Guanosineine 5'diphosphate
GEF	Guanine nucleotide exchange factor
GFP	Green fluorescent protein
GTP	Guanosine 5'triphosphate
Gyp	GAP for Ypt
HGF	Hepatocyte growth factor
Hrs	HGF regulated tyrosine kinase substrate
kDa	Kilo Dalton
LE	Late endosome
LY	Lysosome

MPR	Mannose 6-phosphate receptor
MVB	Multivesicular body
NEM	N-ethyl maleimide
Ni-NTA	Nickel-nitriloacetic acid
NSF	NEM sensitive factor
N-terminus	Amino terminus
PM	Plasma membrane
QDO	Quadruple dropout
Rab	Ras like from brain
RE	Recycling endosome
siRNA	Small interfering RNA
SNAP	Soluble NSF acceptor protein
SNARE	SNAP receptor
TGN	<i>Trans</i> -Golgi network
TMD	Transmembrane Domain
VSV-G	Vesicular stomatitis virus G protein
VTC	Vesicular tubular cluster
x	Any amino acid
Ypt	Yeast protein transport

References

- Aivazian, D., R.L. Serrano, and S. Pfeffer. 2006. TIP47 is a key effector for Rab9 localization. *J Cell Biol.* 173:917-26.
- Albert, S., and D. Gallwitz. 1999. Two new members of a family of Ypt/Rab GTPase activating proteins. Promiscuity of substrate recognition. *J Biol Chem.* 274:33186-9.
- Albert, S., E. Will, and D. Gallwitz. 1999. Identification of the catalytic domains and their functionally critical arginine residues of two yeast GTPase-activating proteins specific for Ypt/Rab transport GTPases. *Embo J.* 18:5216-25.
- Allan, B.B., B.D. Moyer, and W.E. Balch. 2000. Rab1 recruitment of p115 into a cis-SNARE complex: programming budding COPII vesicles for fusion. *Science.* 289:444-8.
- Allin, C., M.R. Ahmadian, A. Wittinghofer, and K. Gerwert. 2001. Monitoring the GAP catalyzed H-Ras GTPase reaction at atomic resolution in real time. *Proc Natl Acad Sci U S A.* 98:7754-9.
- Alvarez, C., H. Fujita, A. Hubbard, and E. Sztul. 1999. ER to Golgi transport: Requirement for p115 at a pre-Golgi VTC stage. *J Cell Biol.* 147:1205-22.
- Appenzeller-Herzog, C., and H.P. Hauri. 2006. The ER-Golgi intermediate compartment (ERGIC): in search of its identity and function. *J Cell Sci.* 119:2173-83.
- Bacon, R.A., A. Salminen, H. Ruohola, P. Novick, and S. Ferro-Novick. 1989. The GTP-binding protein Ypt1 is required for transport in vitro: the Golgi apparatus is defective in ypt1 mutants. *J Cell Biol.* 109:1015-22.
- Barlowe, C., L. Orci, T. Yeung, M. Hosobuchi, S. Hamamoto, N. Salama, M.F. Rexach, M. Ravazzola, M. Amherdt, and R. Schekman. 1994. COPII: a membrane coat formed by Sec proteins that drive vesicle budding from the endoplasmic reticulum. *Cell.* 77:895-907.
- Barr, F.A. 1999. A novel Rab6-interacting domain defines a family of Golgi-targeted coiled-coil proteins. *Curr Biol.* 9:381-4.
- Bascom, R.A., S. Srinivasan, and R.L. Nussbaum. 1999. Identification and characterization of golgin-84, a novel Golgi integral membrane protein with a cytoplasmic coiled-coil domain. *J Biol Chem.* 274:2953-62.
- Behnia, R., and S. Munro. 2005. Organelle identity and the signposts for membrane traffic. *Nature.* 438:597-604.
- Bernards, A. 2003. GAPs galore! A survey of putative Ras superfamily GTPase activating proteins in man and Drosophila. *Biochim Biophys Acta.* 1603:47-82.
- Bi, X., R.A. Corpina, and J. Goldberg. 2002. Structure of the Sec23/24-Sar1 pre-budding complex of the COPII vesicle coat. *Nature.* 419:271-7.
- Bickford, L.C., E. Mossessova, and J. Goldberg. 2004. A structural view of the COPII vesicle coat. *Curr Opin Struct Biol.* 14:147-53.
- Block, M.R., B.S. Glick, C.A. Wilcox, F.T. Wieland, and J.E. Rothman. 1988. Purification of an N-ethylmaleimide-sensitive protein catalyzing vesicular transport. *Proc Natl Acad Sci U S A.* 85:7852-6.
- Bonfanti, L., A.A. Mironov, Jr., J.A. Martinez-Menarguez, O. Martella, A. Fusella, M. Baldassarre, R. Buccione, H.J. Geuze, A.A. Mironov, and A. Luini. 1998. Procollagen traverses the Golgi stack without leaving the lumen of cisternae: evidence for cisternal maturation. *Cell.* 95:993-1003.
- Bonifacino, J.S., and B.S. Glick. 2004. The mechanisms of vesicle budding and fusion. *Cell.* 116:153-66.

- Bonifacino, J.S., and J. Lippincott-Schwartz. 2003. Coat proteins: shaping membrane transport. *Nat Rev Mol Cell Biol.* 4:409-14.
- Bonifacino, J.S., and R. Rojas. 2006. Retrograde transport from endosomes to the trans-Golgi network. *Nat Rev Mol Cell Biol.* 7:568-79.
- Bos, J.L., H. Rehmann, and A. Wittinghofer. 2007. GEFs and GAPs: critical elements in the control of small G proteins. *Cell.* 129:865-77.
- Bourne, H.R., D.A. Sanders, and F. McCormick. 1991. The GTPase superfamily: conserved structure and molecular mechanism. *Nature.* 349:117-27.
- Brennwald, P., and P. Novick. 1993. Interactions of three domains distinguishing the Ras-related GTP-binding proteins Ypt1 and Sec4. *Nature.* 362:560-3.
- Cabezas, A., K.G. Bache, A. Brech, and H. Stenmark. 2005. Alix regulates cortical actin and the spatial distribution of endosomes. *J Cell Sci.* 118:2625-35.
- Cai, H., S. Yu, S. Menon, Y. Cai, D. Lazarova, C. Fu, K. Reinisch, J.C. Hay, and S. Ferro-Novick. 2007. TRAPPI tethers COPII vesicles by binding the coat subunit Sec23. *Nature.* 445:941-4.
- Callebaut, I., J. de Gunzburg, B. Goud, and J.P. Mornon. 2001. RUN domains: a new family of domains involved in Ras-like GTPase signaling. *Trends Biochem Sci.* 26:79-83.
- Carpenter, G. 2000. The EGF receptor: a nexus for trafficking and signaling. *Bioessays.* 22:697-707.
- Carroll, K.S., J. Hanna, I. Simon, J. Krise, P. Barbero, and S.R. Pfeffer. 2001. Role of Rab9 GTPase in facilitating receptor recruitment by TIP47. *Science.* 292:1373-6.
- Ceresa, B.P. 2006. Regulation of EGFR endocytic trafficking by rab proteins. *Histol Histopathol.* 21:987-93.
- Chavrier, P., J.P. Gorvel, E. Stelzer, K. Simons, J. Gruenberg, and M. Zerial. 1991. Hypervariable C-terminal domain of rab proteins acts as a targeting signal. *Nature.* 353:769-72.
- Cherfils, J., and P. Chardin. 1999. GEFs: structural basis for their activation of small GTP-binding proteins. *Trends Biochem Sci.* 24:306-11.
- Christoforidis, S., H.M. McBride, R.D. Burgoyne, and M. Zerial. 1999a. The Rab5 effector EEA1 is a core component of endosome docking. *Nature.* 397:621-5.
- Christoforidis, S., M. Miaczynska, K. Ashman, M. Wilm, L. Zhao, S.C. Yip, M.D. Waterfield, J.M. Backer, and M. Zerial. 1999b. Phosphatidylinositol-3-OH kinases are Rab5 effectors. *Nat Cell Biol.* 1:249-52.
- Clague, M.J., and S. Urbe. 2001. The interface of receptor trafficking and signalling. *J Cell Sci.* 114:3075-81.
- Clary, D.O., I.C. Griff, and J.E. Rothman. 1990. SNAPs, a family of NSF attachment proteins involved in intracellular membrane fusion in animals and yeast. *Cell.* 61:709-21.
- Connerly, P.L., M. Esaki, E.A. Montegna, D.E. Strongin, S. Levi, J. Soderholm, and B.S. Glick. 2005. Sec16 is a determinant of transitional ER organization. *Curr Biol.* 15:1439-47.
- Cook, N.R., P.E. Row, and H.W. Davidson. 2004. Lysosome associated membrane protein 1 (Lamp1) traffics directly from the TGN to early endosomes. *Traffic.* 5:685-99.
- Cooper, A.A., A.D. Gitler, A. Cashikar, C.M. Haynes, K.J. Hill, B. Bhullar, K. Liu, K. Xu, K.E. Strathearn, F. Liu, S. Cao, K.A. Caldwell, G.A. Caldwell, G. Marsischky, R.D. Kolodner, J. Labaer, J.C. Rochet, N.M. Bonini, and S. Lindquist. 2006. Alpha-synuclein blocks ER-Golgi traffic and Rab1 rescues neuron loss in Parkinson's models. *Science.* 313:324-8.
- Cuif, M.H., F. Possmayer, H. Zander, N. Bordes, F. Jollivet, A. Couedel-Courteille, I. Janoueix-Lerosey, G. Langsley, M. Bornens, and B. Goud. 1999. Characterization of

- GAPCenA, a GTPase activating protein for Rab6, part of which associates with the centrosome. *Embo J.* 18:1772-82.
- Curto, M., B.K. Cole, D. Lallemand, C.H. Liu, and A.I. McClatchey. 2007. Contact-dependent inhibition of EGFR signaling by Nf2/Merlin. *J Cell Biol.* 177:893-903.
- Daumke, O., M. Weyand, P.P. Chakrabarti, I.R. Vetter, and A. Wittinghofer. 2004. The GTPase-activating protein Rap1GAP uses a catalytic asparagine. *Nature.* 429:197-201.
- Dautry-Varsat, A. 1986. Receptor-mediated endocytosis: the intracellular journey of transferrin and its receptor. *Biochimie.* 68:375-81.
- De Antoni, A., J. Schmitzova, H.H. Trepte, D. Gallwitz, and S. Albert. 2002. Significance of GTP hydrolysis in Ypt1p-regulated endoplasmic reticulum to Golgi transport revealed by the analysis of two novel Ypt1-GAPs. *J Biol Chem.* 277:41023-31.
- De Craene, J.O., J. Coleman, P. Estrada de Martin, M. Pypaert, S. Anderson, J.R. Yates, 3rd, S. Ferro-Novick, and P. Novick. 2006. Rtn1p is involved in structuring the cortical endoplasmic reticulum. *Mol Biol Cell.* 17:3009-20.
- de Leeuw, H.P., P.M. Koster, J. Calafat, H. Janssen, A.J. van Zonneveld, J.A. van Mourik, and J. Voorberg. 1998. Small GTP-binding proteins in human endothelial cells. *Br J Haematol.* 103:15-9.
- Delprato, A., E. Merithew, and D.G. Lambright. 2004. Structure, exchange determinants, and family-wide rab specificity of the tandem helical bundle and Vps9 domains of Rabex-5. *Cell.* 118:607-17.
- Denzel, A., F. Otto, A. Girod, R. Pepperkok, R. Watson, I. Rosewell, J.J. Bergeron, R.C. Solari, and M.J. Owen. 2000. The p24 family member p23 is required for early embryonic development. *Curr Biol.* 10:55-8.
- Diao, A., D. Rahman, D.J. Pappin, J. Lucocq, and M. Lowe. 2003. The coiled-coil membrane protein golgin-84 is a novel rab effector required for Golgi ribbon formation. *J Cell Biol.* 160:201-12.
- Dominguez, M., K. Dejgaard, J. Fullekrug, S. Dahan, A. Fazel, J.P. Paccaud, D.Y. Thomas, J.J. Bergeron, and T. Nilsson. 1998. gp25L/emp24/p24 protein family members of the cis-Golgi network bind both COP I and II coatomer. *J Cell Biol.* 140:751-65.
- Dong, G., M. Medkova, P. Novick, and K.M. Reinisch. 2007. A catalytic coiled coil: structural insights into the activation of the Rab GTPase Sec4p by Sec2p. *Mol Cell.* 25:455-62.
- Duden, R. 2003. ER-to-Golgi transport: COP I and COP II function (Review). *Mol Membr Biol.* 20:197-207.
- Dunphy, W.G., R. Brands, and J.E. Rothman. 1985. Attachment of terminal N-acetylglucosamine to asparagine-linked oligosaccharides occurs in central cisternae of the Golgi stack. *Cell.* 40:463-72.
- Feng, Y., B. Press, and A. Wandinger-Ness. 1995. Rab 7: an important regulator of late endocytic membrane traffic. *J Cell Biol.* 131:1435-52.
- Feuerstein, J., R.S. Goody, and M.R. Webb. 1989. The mechanism of guanosine nucleotide hydrolysis by p21 c-Ha-ras. The stereochemical course of the GTPase reaction. *J Biol Chem.* 264:6188-90.
- Fiedler, K., M. Veit, M.A. Stamnes, and J.E. Rothman. 1996. Bimodal interaction of coatomer with the p24 family of putative cargo receptors. *Science.* 273:1396-9.
- Fischer, J., T. Weide, and A. Barnekow. 2005. The MICAL proteins and rab1: a possible link to the cytoskeleton? *Biochem Biophys Res Commun.* 328:415-23.
- Fuchs, E., A.K. Haas, R.A. Spooner, S. Yoshimura, J.M. Lord, and F.A. Barr. 2007. Specific Rab GTPase-activating proteins define the Shiga toxin and epidermal growth factor uptake pathways. *J Cell Biol.* 177:1133-43.

- Fujiki, Y., A.L. Hubbard, S. Fowler, and P.B. Lazarow. 1982. Isolation of intracellular membranes by means of sodium carbonate treatment: application to endoplasmic reticulum. *J Cell Biol.* 93:97-102.
- Fukuda, M., T.S. Kuroda, and K. Mikoshiba. 2002. Slac2-a/melanophilin, the missing link between Rab27 and myosin Va: implications of a tripartite protein complex for melanosome transport. *J Biol Chem.* 277:12432-6.
- Futter, C.E., A. Pearce, L.J. Hewlett, and C.R. Hopkins. 1996. Multivesicular endosomes containing internalized EGF-EGF receptor complexes mature and then fuse directly with lysosomes. *J Cell Biol.* 132:1011-23.
- Gallwitz, D., C. Donath, and C. Sander. 1983. A yeast gene encoding a protein homologous to the human c-ha/bas proto-oncogene product. *Nature.* 306:704-7.
- Geng, J., M.E. Shin, P.M. Gilbert, R.N. Collins, and C.G. Burd. 2005. *Saccharomyces cerevisiae* Rab-GDI displacement factor ortholog Yip3p forms distinct complexes with the Ypt1 Rab GTPase and the reticulon Rtn1p. *Eukaryot Cell.* 4:1166-74.
- Giepmans, B.N. 2006. Role of connexin43-interacting proteins at gap junctions. *Adv Cardiol.* 42:41-56.
- Gillingham, A.K., A.H. Tong, C. Boone, and S. Munro. 2004. The GTPase Arf1p and the ER to Golgi cargo receptor Erv14p cooperate to recruit the golgin Rud3p to the cis-Golgi. *J Cell Biol.* 167:281-92.
- Glick, B.S. 2002. Can the Golgi form de novo? *Nat Rev Mol Cell Biol.* 3:615-9.
- Goody, R.S., A. Rak, and K. Alexandrov. 2005. The structural and mechanistic basis for recycling of Rab proteins between membrane compartments. *Cell Mol Life Sci.* 62:1657-70.
- Griffith, K.J., E.K. Chan, C.C. Lung, J.C. Hamel, X. Guo, K. Miyachi, and M.J. Fritzler. 1997. Molecular cloning of a novel 97-kd Golgi complex autoantigen associated with Sjogren's syndrome. *Arthritis Rheum.* 40:1693-702.
- Griffiths, G., and K. Simons. 1986. The trans Golgi network: sorting at the exit site of the Golgi complex. *Science.* 234:438-43.
- Grosshans, B.L., D. Ortiz, and P. Novick. 2006. Rabs and their effectors: achieving specificity in membrane traffic. *Proc Natl Acad Sci U S A.* 103:11821-7.
- Gu, F., C.M. Crump, and G. Thomas. 2001. Trans-Golgi network sorting. *Cell Mol Life Sci.* 58:1067-84.
- Guo, J.H., L. Chen, S. Chen, X. Liu, H. Saiyin, Q. Deng, Y. Zhuang, B. Wan, L. Yu, and S.Y. Zhao. 2003. Isolation, expression pattern of a novel human RAB gene RAB41 and characterization of its intronless homolog RAB41P. *DNA Seq.* 14:431-5.
- Guo, W., F. Tamanoi, and P. Novick. 2001. Spatial regulation of the exocyst complex by Rho1 GTPase. *Nat Cell Biol.* 3:353-60.
- Guo, Y., and A.D. Linstedt. 2006. COPII-Golgi protein interactions regulate COPII coat assembly and Golgi size. *J Cell Biol.* 174:53-63.
- Gurkan, C., A.V. Koulov, and W.E. Balch. 2007. An evolutionary perspective on eukaryotic membrane trafficking. *Adv Exp Med Biol.* 607:73-83.
- Haas, A.K., and F.A. Barr. 2007. COP sets TRAPP for vesicles. *Dev Cell.* 12:326-7.
- Hammer, J.A., 3rd, and X.S. Wu. 2002. Rabs grab motors: defining the connections between Rab GTPases and motor proteins. *Curr Opin Cell Biol.* 14:69-75.
- Hammond, A.T., and B.S. Glick. 2000. Dynamics of transitional endoplasmic reticulum sites in vertebrate cells. *Mol Biol Cell.* 11:3013-30.
- Hauri, H.P., F. Kappeler, H. Andersson, and C. Appenzeller. 2000. ERGIC-53 and traffic in the secretory pathway. *J Cell Sci.* 113 (Pt 4):587-96.
- Horiuchi, H., R. Lippe, H.M. McBride, M. Rubino, P. Woodman, H. Stenmark, V. Rybin, M. Wilm, K. Ashman, M. Mann, and M. Zerial. 1997. A novel Rab5 GDP/GTP

- exchange factor complexed to Rabaptin-5 links nucleotide exchange to effector recruitment and function. *Cell*. 90:1149-59.
- Hutt, D.M., L.F. Da-Silva, L.H. Chang, D.C. Prosser, and J.K. Ngsee. 2000. PRA1 inhibits the extraction of membrane-bound rab GTPase by GDI1. *J Biol Chem*. 275:18511-9.
- Ichioaka, F., M. Horii, K. Katoh, Y. Terasawa, H. Shibata, and M. Maki. 2005. Identification of Rab GTPase-activating protein-like protein (RabGAPLP) as a novel Alix/AIP1-interacting protein. *Biosci Biotechnol Biochem*. 69:861-5.
- Iwahashi, J., N. Hamada, and H. Watanabe. 2007. Two hydrophobic segments of the RTN1 family determine the ER localization and retention. *Biochem Biophys Res Commun*. 355:508-12.
- Jahn, R., and R.H. Scheller. 2006. SNAREs--engines for membrane fusion. *Nat Rev Mol Cell Biol*. 7:631-43.
- Jedd, G., C. Richardson, R. Litt, and N. Segev. 1995. The Ypt1 GTPase is essential for the first two steps of the yeast secretory pathway. *J Cell Biol*. 131:583-90.
- Jena, B.P., P. Brennwald, M.D. Garrett, P. Novick, and J.D. Jamieson. 1992. Distinct and specific GAP activities in rat pancreas act on the yeast GTP-binding proteins Ypt1 and Sec4. *FEBS Lett*. 309:5-9.
- Jones, S., C. Newman, F. Liu, and N. Segev. 2000. The TRAPP complex is a nucleotide exchanger for Ypt1 and Ypt31/32. *Mol Biol Cell*. 11:4403-11.
- Katzmann, D.J., G. Odorizzi, and S.D. Emr. 2002. Receptor downregulation and multivesicular-body sorting. *Nat Rev Mol Cell Biol*. 3:893-905.
- Klumperman, J., A. Schweizer, H. Clausen, B.L. Tang, W. Hong, V. Oorschot, and H.P. Hauri. 1998. The recycling pathway of protein ERGIC-53 and dynamics of the ER-Golgi intermediate compartment. *J Cell Sci*. 111 (Pt 22):3411-25.
- Komada, M., and N. Kitamura. 2001. Hrs and hbp: possible regulators of endocytosis and exocytosis. *Biochem Biophys Res Commun*. 281:1065-9.
- Kotting, C., M. Blessenohl, Y. Suveyzdis, R.S. Goody, A. Wittinghofer, and K. Gerwert. 2006. A phosphoryl transfer intermediate in the GTPase reaction of Ras in complex with its GTPase-activating protein. *Proc Natl Acad Sci U S A*. 103:13911-6.
- Ladasky, J.J., S. Boyle, M. Seth, H. Li, T. Pentcheva, F. Abe, S.J. Steinberg, and M. Edidin. 2006. Bap31 enhances the endoplasmic reticulum export and quality control of human class I MHC molecules. *J Immunol*. 177:6172-81.
- Lafer, E.M. 2002. Clathrin-protein interactions. *Traffic*. 3:513-20.
- Lallemand, D., M. Curto, I. Saotome, M. Giovannini, and A.I. McClatchey. 2003. NF2 deficiency promotes tumorigenesis and metastasis by destabilizing adherens junctions. *Genes Dev*. 17:1090-100.
- Lan, Z., W.E. Kurata, K.D. Martyn, C. Jin, and A.F. Lau. 2005. Novel rab GAP-like protein, CIP85, interacts with connexin43 and induces its degradation. *Biochemistry*. 44:2385-96.
- Lane, J.D., J. Lucocq, J. Pryde, F.A. Barr, P.G. Woodman, V.J. Allan, and M. Lowe. 2002. Caspase-mediated cleavage of the stacking protein GRASP65 is required for Golgi fragmentation during apoptosis. *J Cell Biol*. 156:495-509.
- Lanzetti, L., A. Palamidessi, L. Areces, G. Scita, and P.P. Di Fiore. 2004. Rab5 is a signalling GTPase involved in actin remodelling by receptor tyrosine kinases. *Nature*. 429:309-14.
- Lanzetti, L., V. Rybin, M.G. Malabarba, S. Christoforidis, G. Scita, M. Zerial, and P.P. Di Fiore. 2000. The Eps8 protein coordinates EGF receptor signalling through Rac and trafficking through Rab5. *Nature*. 408:374-7.
- Lawe, D.C., A. Chawla, E. Merithew, J. Dumas, W. Carrington, K. Fogarty, L. Lifshitz, R. Tuft, D. Lambright, and S. Corvera. 2002. Sequential roles for phosphatidylinositol

- 3-phosphate and Rab5 in tethering and fusion of early endosomes via their interaction with EEA1. *J Biol Chem.* 277:8611-7.
- Lawe, D.C., V. Patki, R. Heller-Harrison, D. Lambright, and S. Corvera. 2000. The FYVE domain of early endosome antigen 1 is required for both phosphatidylinositol 3-phosphate and Rab5 binding. Critical role of this dual interaction for endosomal localization. *J Biol Chem.* 275:3699-705.
- Lazar, T., M. Gotte, and D. Gallwitz. 1997. Vesicular transport: how many Ypt/Rab-GTPases make a eukaryotic cell? *Trends Biochem Sci.* 22:468-72.
- Lee, I.K., K.S. Kim, H. Kim, J.Y. Lee, C.H. Ryu, H.J. Chun, K.U. Lee, Y. Lim, Y.H. Kim, P.W. Huh, K.H. Lee, S.I. Han, T.Y. Jun, and H.K. Rha. 2004. MAP, a protein interacting with a tumor suppressor, merlin, through the run domain. *Biochem Biophys Res Commun.* 325:774-83.
- Lippincott-Schwartz, J., L.C. Yuan, J.S. Bonifacino, and R.D. Klausner. 1989. Rapid redistribution of Golgi proteins into the ER in cells treated with brefeldin A: evidence for membrane cycling from Golgi to ER. *Cell.* 56:801-13.
- Liu, J., D. Lamb, M.M. Chou, Y.J. Liu, and G. Li. 2007. Nerve growth factor-mediated neurite outgrowth via regulation of Rab5. *Mol Biol Cell.* 18:1375-84.
- Losev, E., C.A. Reinke, J. Jellen, D.E. Strongin, B.J. Bevis, and B.S. Glick. 2006. Golgi maturation visualized in living yeast. *Nature.* 441:1002-6.
- Lowe, M., and F.A. Barr. 2007. Inheritance and biogenesis of organelles in the secretory pathway. *Nat Rev Mol Cell Biol.* 8:429-39.
- Lu, L., and W. Hong. 2003. Interaction of Arl1-GTP with GRIP domains recruits autoantigens Golgin-97 and Golgin-245/p230 onto the Golgi. *Mol Biol Cell.* 14:3767-81.
- Markgraf, D.F., K. Peplowska, and C. Ungermann. 2007. Rab cascades and tethering factors in the endomembrane system. *FEBS Lett.* 581:2125-30.
- Matsuo, H., J. Chevallier, N. Mayran, I. Le Blanc, C. Ferguson, J. Faure, N.S. Blanc, S. Matile, J. Dubochet, R. Sadoul, R.G. Parton, F. Vilbois, and J. Gruenberg. 2004. Role of LBPA and Alix in multivesicular liposome formation and endosome organization. *Science.* 303:531-4.
- Matsuoka, K., L. Orci, M. Amherdt, S.Y. Bednarek, S. Hamamoto, R. Schekman, and T. Yeung. 1998. COPII-coated vesicle formation reconstituted with purified coat proteins and chemically defined liposomes. *Cell.* 93:263-75.
- Maxfield, F.R., and T.E. McGraw. 2004. Endocytic recycling. *Nat Rev Mol Cell Biol.* 5:121-32.
- Mayer, B.J. 2001. SH3 domains: complexity in moderation. *J Cell Sci.* 114:1253-63.
- Mayor, S., and R.E. Pagano. 2007. Pathways of clathrin-independent endocytosis. *Nat Rev Mol Cell Biol.* 8:603-12.
- McBride, H.M., V. Rybin, C. Murphy, A. Giner, R. Teasdale, and M. Zerial. 1999. Oligomeric complexes link Rab5 effectors with NSF and drive membrane fusion via interactions between EEA1 and syntaxin 13. *Cell.* 98:377-86.
- McLauchlan, H., J. Newell, N. Morrice, A. Osborne, M. West, and E. Smythe. 1998. A novel role for Rab5-GDI in ligand sequestration into clathrin-coated pits. *Curr Biol.* 8:34-45.
- McNiven, M.A., and H.M. Thompson. 2006. Vesicle formation at the plasma membrane and trans-Golgi network: the same but different. *Science.* 313:1591-4.
- Miaczynska, M., L. Pelkmans, and M. Zerial. 2004. Not just a sink: endosomes in control of signal transduction. *Curr Opin Cell Biol.* 16:400-6.
- Miaczynska, M., and M. Zerial. 2002. Mosaic organization of the endocytic pathway. *Exp Cell Res.* 272:8-14.

- Mills, I.G., A.T. Jones, and M.J. Clague. 1998. Involvement of the endosomal autoantigen EEA1 in homotypic fusion of early endosomes. *Curr Biol.* 8:881-4.
- Mironov, A.A., A.A. Mironov, Jr., G.V. Beznoussenko, A. Trucco, P. Lupetti, J.D. Smith, W.J. Geerts, A.J. Koster, K.N. Burger, M.E. Martone, T.J. Deerinck, M.H. Ellisman, and A. Luini. 2003. ER-to-Golgi carriers arise through direct en bloc protrusion and multistage maturation of specialized ER exit domains. *Dev Cell.* 5:583-94.
- Mironov, A.A., P. Weidman, and A. Luini. 1997. Variations on the intracellular transport theme: maturing cisternae and trafficking tubules. *J Cell Biol.* 138:481-4.
- Morozova, N., Y. Liang, A.A. Tokarev, S.H. Chen, R. Cox, J. Andrejic, Z. Lipatova, V.A. Sciorra, S.D. Emr, and N. Segev. 2006. TRAPPII subunits are required for the specificity switch of a Ypt-Rab GEF. *Nat Cell Biol.* 8:1263-9.
- Morrison, H., L.S. Sherman, J. Legg, F. Banine, C. Isacke, C.A. Haipek, D.H. Gutmann, H. Ponta, and P. Herrlich. 2001. The NF2 tumor suppressor gene product, merlin, mediates contact inhibition of growth through interactions with CD44. *Genes Dev.* 15:968-80.
- Morsomme, P., and H. Riezman. 2002. The Rab GTPase Ypt1p and tethering factors couple protein sorting at the ER to vesicle targeting to the Golgi apparatus. *Dev Cell.* 2:307-17.
- Moyer, B.D., B.B. Allan, and W.E. Balch. 2001. Rab1 interaction with a GM130 effector complex regulates COPII vesicle cis--Golgi tethering. *Traffic.* 2:268-76.
- Mu, F.T., J.M. Callaghan, O. Steele-Mortimer, H. Stenmark, R.G. Parton, P.L. Campbell, J. McCluskey, J.P. Yeo, E.P. Tock, and B.H. Toh. 1995. EEA1, an early endosome-associated protein. EEA1 is a conserved alpha-helical peripheral membrane protein flanked by cysteine "fingers" and contains a calmodulin-binding IQ motif. *J Biol Chem.* 270:13503-11.
- Munro, S. 2002. Organelle identity and the targeting of peripheral membrane proteins. *Curr Opin Cell Biol.* 14:506-14.
- Munro, S., and B.J. Nichols. 1999. The GRIP domain - a novel Golgi-targeting domain found in several coiled-coil proteins. *Curr Biol.* 9:377-80.
- Nakamura, N., C. Rabouille, R. Watson, T. Nilsson, N. Hui, P. Slusarewicz, T.E. Kreis, and G. Warren. 1995. Characterization of a cis-Golgi matrix protein, GM130. *J Cell Biol.* 131:1715-26.
- Neuwald, A.F. 1997. A shared domain between a spindle assembly checkpoint protein and Ypt/Rab-specific GTPase-activators. *Trends Biochem Sci.* 22:243-4.
- Nielsen, E., S. Christoforidis, S. Uttenweiler-Joseph, M. Miaczynska, F. Dewitte, M. Wilm, B. Hoflack, and M. Zerial. 2000. Rabenosyn-5, a novel Rab5 effector, is complexed with hVPS45 and recruited to endosomes through a FYVE finger domain. *J Cell Biol.* 151:601-12.
- Nilsson, T., M. Pypaert, M.H. Hoe, P. Slusarewicz, E.G. Berger, and G. Warren. 1993. Overlapping distribution of two glycosyltransferases in the Golgi apparatus of HeLa cells. *J Cell Biol.* 120:5-13.
- Nilsson, T., C. Rabouille, N. Hui, R. Watson, and G. Warren. 1996. The role of the membrane-spanning domain and stalk region of N-acetylglucosaminyltransferase I in retention, kin recognition and structural maintenance of the Golgi apparatus in HeLa cells. *J Cell Sci.* 109 (Pt 7):1975-89.
- Novick, P., and M. Zerial. 1997. The diversity of Rab proteins in vesicle transport. *Curr Opin Cell Biol.* 9:496-504.
- Oertle, T., and M.E. Schwab. 2003. Nogo and its pARTNers. *Trends Cell Biol.* 13:187-94.

- Okada, T., M. Lopez-Lago, and F.G. Giancotti. 2005. Merlin/NF-2 mediates contact inhibition of growth by suppressing recruitment of Rac to the plasma membrane. *J Cell Biol.* 171:361-71.
- Okada, T., L. You, and F.G. Giancotti. 2007. Shedding light on Merlin's wizardry. *Trends Cell Biol.* 17:222-9.
- Ortiz, D., M. Medkova, C. Walch-Solimena, and P. Novick. 2002. Ypt32 recruits the Sec4p guanine nucleotide exchange factor, Sec2p, to secretory vesicles; evidence for a Rab cascade in yeast. *J Cell Biol.* 157:1005-15.
- Pan, X., S. Eathiraj, M. Munson, and D.G. Lambright. 2006. TBC-domain GAPs for Rab GTPases accelerate GTP hydrolysis by a dual-finger mechanism. *Nature.* 442:303-6.
- Panic, B., O. Perisic, D.B. Veprintsev, R.L. Williams, and S. Munro. 2003. Structural basis for Arl1-dependent targeting of homodimeric GRIP domains to the Golgi apparatus. *Mol Cell.* 12:863-74.
- Pei, L., Y. Peng, Y. Yang, X.B. Ling, W.G. Van Eyndhoven, K.C. Nguyen, M. Rubin, T. Hoey, S. Powers, and J. Li. 2002. PRC17, a novel oncogene encoding a Rab GTPase-activating protein, is amplified in prostate cancer. *Cancer Res.* 62:5420-4.
- Pelham, H.R. 2001. Traffic through the Golgi apparatus. *J Cell Biol.* 155:1099-101.
- Peplowska, K., D.F. Markgraf, C.W. Ostrowicz, G. Bange, and C. Ungermann. 2007. The CORVET tethering complex interacts with the yeast Rab5 homolog Vps21 and is involved in endo-lysosomal biogenesis. *Dev Cell.* 12:739-50.
- Pereira-Leal, J.B., and M.C. Seabra. 2000. The mammalian Rab family of small GTPases: definition of family and subfamily sequence motifs suggests a mechanism for functional specificity in the Ras superfamily. *J Mol Biol.* 301:1077-87.
- Pereira-Leal, J.B., and M.C. Seabra. 2001. Evolution of the Rab family of small GTP-binding proteins. *J Mol Biol.* 313:889-901.
- Peter, F., C. Nuoffer, S.N. Pind, and W.E. Balch. 1994. Guanine nucleotide dissociation inhibitor is essential for Rab1 function in budding from the endoplasmic reticulum and transport through the Golgi stack. *J Cell Biol.* 126:1393-406.
- Pfeffer, S. 2003. Membrane domains in the secretory and endocytic pathways. *Cell.* 112:507-17.
- Pfeffer, S.R. 1999. Transport-vesicle targeting: tethers before SNAREs. *Nat Cell Biol.* 1:E17-22.
- Pfeffer, S.R. 2001. Rab GTPases: specifying and deciphering organelle identity and function. *Trends Cell Biol.* 11:487-91.
- Prescott, A.R., J.M. Lucocq, J. James, J.M. Lister, and S. Ponnambalam. 1997. Distinct compartmentalization of TGN46 and beta 1,4-galactosyltransferase in HeLa cells. *Eur J Cell Biol.* 72:238-46.
- Presley, J.F. 2005. Imaging the secretory pathway: the past and future impact of live cell optical techniques. *Biochim Biophys Acta.* 1744:259-72.
- Presley, J.F., N.B. Cole, T.A. Schroer, K. Hirschberg, K.J. Zaal, and J. Lippincott-Schwartz. 1997. ER-to-Golgi transport visualized in living cells. *Nature.* 389:81-5.
- Puthenveedu, M.A., C. Bachert, S. Puri, F. Lanni, and A.D. Linstedt. 2006. GM130 and GRASP65-dependent lateral cisternal fusion allows uniform Golgi-enzyme distribution. *Nat Cell Biol.* 8:238-48.
- Pylypenko, O., A. Rak, T. Durek, S. Kushnir, B.E. Dursina, N.H. Thomae, A.T. Constantinescu, L. Brunsveld, A. Watzke, H. Waldmann, R.S. Goody, and K. Alexandrov. 2006. Structure of doubly prenylated Ypt1:GDI complex and the mechanism of GDI-mediated Rab recycling. *Embo J.* 25:13-23.

- Rak, A., R. Fedorov, K. Alexandrov, S. Albert, R.S. Goody, D. Gallwitz, and A.J. Scheidig. 2000. Crystal structure of the GAP domain of Gyp1p: first insights into interaction with Ypt/Rab proteins. *Embo J.* 19:5105-13.
- Rak, A., O. Pylypenko, T. Durek, A. Watzke, S. Kushnir, L. Brunsveld, H. Waldmann, R.S. Goody, and K. Alexandrov. 2003. Structure of Rab GDP-dissociation inhibitor in complex with prenylated YPT1 GTPase. *Science*. 302:646-50.
- Reits, E.A., and J.J. Neefjes. 2001. From fixed to FRAP: measuring protein mobility and activity in living cells. *Nat Cell Biol.* 3:E145-7.
- Richardson, C.J., S. Jones, R.J. Litt, and N. Segev. 1998. GTP hydrolysis is not important for Ypt1 GTPase function in vesicular transport. *Mol Cell Biol.* 18:827-38.
- Rink, J., E. Ghigo, Y. Kalaidzidis, and M. Zerial. 2005. Rab conversion as a mechanism of progression from early to late endosomes. *Cell*. 122:735-49.
- Rohrer, J., A. Schweizer, D. Russell, and S. Kornfeld. 1996. The targeting of Lamp1 to lysosomes is dependent on the spacing of its cytoplasmic tail tyrosine sorting motif relative to the membrane. *J Cell Biol.* 132:565-76.
- Row, P.E., M.J. Clague, and S. Urbe. 2005. Growth factors induce differential phosphorylation profiles of the Hrs-STAM complex: a common node in signalling networks with signal-specific properties. *Biochem J.* 389:629-36.
- Rubino, M., M. Miaczynska, R. Lippe, and M. Zerial. 2000. Selective membrane recruitment of EEA1 suggests a role in directional transport of clathrin-coated vesicles to early endosomes. *J Biol Chem.* 275:3745-8.
- Sacher, M., Y. Jiang, J. Barrowman, A. Scarpa, J. Burston, L. Zhang, D. Schieltz, J.R. Yates, 3rd, H. Abeliovich, and S. Ferro-Novick. 1998. TRAPP, a highly conserved novel complex on the cis-Golgi that mediates vesicle docking and fusion. *Embo J.* 17:2494-503.
- Salminen, A., and P.J. Novick. 1987. A ras-like protein is required for a post-Golgi event in yeast secretion. *Cell*. 49:527-38.
- Sasaki, T., A. Kikuchi, S. Araki, Y. Hata, M. Isomura, S. Kuroda, and Y. Takai. 1990. Purification and characterization from bovine brain cytosol of a protein that inhibits the dissociation of GDP from and the subsequent binding of GTP to smg p25A, a ras p21-like GTP-binding protein. *J Biol Chem.* 265:2333-7.
- Scales, S.J., R. Pepperkok, and T.E. Kreis. 1997. Visualization of ER-to-Golgi transport in living cells reveals a sequential mode of action for COPII and COPI. *Cell*. 90:1137-48.
- Schamel, W.W., S. Kuppig, B. Becker, K. Gimborn, H.P. Hauri, and M. Reth. 2003. A high-molecular-weight complex of membrane proteins BAP29/BAP31 is involved in the retention of membrane-bound IgD in the endoplasmic reticulum. *Proc Natl Acad Sci U S A.* 100:9861-6.
- Scheffzek, K., M.R. Ahmadian, W. Kabsch, L. Wiesmuller, A. Lautwein, F. Schmitz, and A. Wittinghofer. 1997. The Ras-RasGAP complex: structural basis for GTPase activation and its loss in oncogenic Ras mutants. *Science*. 277:333-8.
- Scheffzek, K., M.R. Ahmadian, and A. Wittinghofer. 1998. GTPase-activating proteins: helping hands to complement an active site. *Trends Biochem Sci.* 23:257-62.
- Schimmoller, F., B. Singer-Kruger, S. Schroder, U. Kruger, C. Barlowe, and H. Riezman. 1995. The absence of Emp24p, a component of ER-derived COPII-coated vesicles, causes a defect in transport of selected proteins to the Golgi. *Embo J.* 14:1329-39.
- Seabra, M.C., and C. Wasmeier. 2004. Controlling the location and activation of Rab GTPases. *Curr Opin Cell Biol.* 16:451-7.
- Seewald, M.J., C. Korner, A. Wittinghofer, and I.R. Vetter. 2002. RanGAP mediates GTP hydrolysis without an arginine finger. *Nature*. 415:662-6.

- Segev, N. 1991. Mediation of the attachment or fusion step in vesicular transport by the GTP-binding Ypt1 protein. *Science*. 252:1553-6.
- Segev, N. 2001. Ypt and Rab GTPases: insight into functions through novel interactions. *Curr Opin Cell Biol*. 13:500-11.
- Serafini, T., L. Orci, M. Amherdt, M. Brunner, R.A. Kahn, and J.E. Rothman. 1991. ADP-ribosylation factor is a subunit of the coat of Golgi-derived COP-coated vesicles: a novel role for a GTP-binding protein. *Cell*. 67:239-53.
- Sheff, D.R., E.A. Daro, M. Hull, and I. Mellman. 1999. The receptor recycling pathway contains two distinct populations of early endosomes with different sorting functions. *J Cell Biol*. 145:123-39.
- Shima, D.T., N. Cabrera-Poch, R. Pepperkok, and G. Warren. 1998. An ordered inheritance strategy for the Golgi apparatus: visualization of mitotic disassembly reveals a role for the mitotic spindle. *J Cell Biol*. 141:955-66.
- Short, B., and F.A. Barr. 2002. Membrane traffic: exocyst III--makes a family. *Curr Biol*. 12:R18-20.
- Short, B., A. Haas, and F.A. Barr. 2005. Golgins and GTPases, giving identity and structure to the Golgi apparatus. *Biochim Biophys Acta*. 1744:383-95.
- Short, B., C. Preisinger, R. Korner, R. Kopajtich, O. Byron, and F.A. Barr. 2001. A GRASP55-rab2 effector complex linking Golgi structure to membrane traffic. *J Cell Biol*. 155:877-83.
- Short, B., C. Preisinger, J. Schaletzky, R. Kopajtich, and F.A. Barr. 2002. The Rab6 GTPase regulates recruitment of the dynactin complex to Golgi membranes. *Curr Biol*. 12:1792-5.
- Sigismund, S., T. Woelk, C. Puri, E. Maspero, C. Tacchetti, P. Transidico, P.P. Di Fiore, and S. Polo. 2005. Clathrin-independent endocytosis of ubiquitinated cargos. *Proc Natl Acad Sci U S A*. 102:2760-5.
- Simonsen, A., J.M. Gaullier, A. D'Arrigo, and H. Stenmark. 1999. The Rab5 effector EEA1 interacts directly with syntaxin-6. *J Biol Chem*. 274:28857-60.
- Simonsen, A., R. Lippe, S. Christoforidis, J.M. Gaullier, A. Brech, J. Callaghan, B.H. Toh, C. Murphy, M. Zerial, and H. Stenmark. 1998. EEA1 links PI(3)K function to Rab5 regulation of endosome fusion. *Nature*. 394:494-8.
- Sivars, U., D. Aivazian, and S.R. Pfeffer. 2003. Yip3 catalyses the dissociation of endosomal Rab-GDI complexes. *Nature*. 425:856-9.
- Sklan, E.H., R.L. Serrano, S. Einav, S.R. Pfeffer, D.G. Lambright, and J.S. Glenn. 2007a. TBC1D20 is a RAB1 GAP that mediates HCV replication. *J Biol Chem*.
- Sklan, E.H., K. Staschke, T.M. Oakes, M. Elazar, M. Winters, B. Aroeti, T. Danieli, and J.S. Glenn. 2007b. A Rab-GAP TBC Domain Protein Binds Hepatitis C Virus NS5A and Mediates Viral Replication. *J Virol*. 81:11096-105.
- Sohn, K., L. Orci, M. Ravazzola, M. Amherdt, M. Bremser, F. Lottspeich, K. Fiedler, J.B. Helms, and F.T. Wieland. 1996. A major transmembrane protein of Golgi-derived COPI-coated vesicles involved in coatomer binding. *J Cell Biol*. 135:1239-48.
- Soldati, T., and M. Schliwa. 2006. Powering membrane traffic in endocytosis and recycling. *Nat Rev Mol Cell Biol*. 7:897-908.
- Soldati, T., A.D. Shapiro, A.B. Svejstrup, and S.R. Pfeffer. 1994. Membrane targeting of the small GTPase Rab9 is accompanied by nucleotide exchange. *Nature*. 369:76-8.
- Stahl, P.D., and M.A. Barbieri. 2002. Multivesicular bodies and multivesicular endosomes: the "ins and outs" of endosomal traffic. *Sci STKE*. 2002:PE32.
- Steiner, P., K. Kulangara, J.C. Sarria, L. Glauser, R. Regazzi, and H. Hirling. 2004. Reticulon 1-C/neuroendocrine-specific protein-C interacts with SNARE proteins. *J Neurochem*. 89:569-80.

- Stenmark, H., R.G. Parton, O. Steele-Mortimer, A. Lutcke, J. Gruenberg, and M. Zerial. 1994. Inhibition of rab5 GTPase activity stimulates membrane fusion in endocytosis. *Embo J.* 13:1287-96.
- Strom, M., P. Vollmer, T.J. Tan, and D. Gallwitz. 1993. A yeast GTPase-activating protein that interacts specifically with a member of the Ypt/Rab family. *Nature.* 361:736-9.
- Sztul, E., and V. Lupashin. 2006. Role of tethering factors in secretory membrane traffic. *Am J Physiol Cell Physiol.* 290:C11-26.
- Tang, B.L., Y. Wang, Y.S. Ong, and W. Hong. 2005. COPII and exit from the endoplasmic reticulum. *Biochim Biophys Acta.* 1744:293-303.
- Tarone, G., G. Galetto, M. Prat, and P.M. Comoglio. 1982. Cell surface molecules and fibronectin-mediated cell adhesion: effect of proteolytic digestion of membrane proteins. *J Cell Biol.* 94:179-86.
- Tisdale, E.J., and W.E. Balch. 1996. Rab2 is essential for the maturation of pre-Golgi intermediates. *J Biol Chem.* 271:29372-9.
- Valsdottir, R., H. Hashimoto, K. Ashman, T. Koda, B. Storrie, and T. Nilsson. 2001. Identification of rabaptin-5, rabex-5, and GM130 as putative effectors of rab33b, a regulator of retrograde traffic between the Golgi apparatus and ER. *FEBS Lett.* 508:201-9.
- van Vliet, C., E.C. Thomas, A. Merino-Trigo, R.D. Teasdale, and P.A. Gleeson. 2003. Intracellular sorting and transport of proteins. *Prog Biophys Mol Biol.* 83:1-45.
- Vetter, I.R., and A. Wittinghofer. 2001. The guanine nucleotide-binding switch in three dimensions. *Science.* 294:1299-304.
- Voeltz, G.K., W.A. Prinz, Y. Shibata, J.M. Rist, and T.A. Rapoport. 2006. A class of membrane proteins shaping the tubular endoplasmic reticulum. *Cell.* 124:573-86.
- Vollmer, P., and D. Gallwitz. 1995. High expression cloning, purification, and assay of Ypt-GTPase-activating proteins. *Methods Enzymol.* 257:118-28.
- Vollmer, P., E. Will, D. Scheglmann, M. Strom, and D. Gallwitz. 1999. Primary structure and biochemical characterization of yeast GTPase-activating proteins with substrate preference for the transport GTPase Ypt7p. *Eur J Biochem.* 260:284-90.
- Wakana, Y., S. Koyama, K. Nakajima, K. Hatsuzawa, M. Nagahama, K. Tani, H.P. Hauri, P. Melancon, and M. Tagaya. 2005. Reticulon 3 is involved in membrane trafficking between the endoplasmic reticulum and Golgi. *Biochem Biophys Res Commun.* 334:1198-205.
- Wang, W., M. Sacher, and S. Ferro-Novick. 2000. TRAPP stimulates guanine nucleotide exchange on Ypt1p. *J Cell Biol.* 151:289-96.
- Ward, T.H., R.S. Polishchuk, S. Caplan, K. Hirschberg, and J. Lippincott-Schwartz. 2001. Maintenance of Golgi structure and function depends on the integrity of ER export. *J Cell Biol.* 155:557-70.
- Watson, P., A.K. Townley, P. Koka, K.J. Palmer, and D.J. Stephens. 2006. Sec16 defines endoplasmic reticulum exit sites and is required for secretory cargo export in mammalian cells. *Traffic.* 7:1678-87.
- Weber, T., B.V. Zemelman, J.A. McNew, B. Westermann, M. Gmachl, F. Parlati, T.H. Sollner, and J.E. Rothman. 1998. SNAREpins: minimal machinery for membrane fusion. *Cell.* 92:759-72.
- Weide, T., J. Teuber, M. Bayer, and A. Barnekow. 2003. MICAL-1 isoforms, novel rab1 interacting proteins. *Biochem Biophys Res Commun.* 306:79-86.
- Wennerberg, K., K.L. Rossman, and C.J. Der. 2005. The Ras superfamily at a glance. *J Cell Sci.* 118:843-6.
- Wildasin, K. 2004. Role of reticulon proteins in Alzheimer's disease. *Lancet Neurol.* 3:576.

- Will, E., and D. Gallwitz. 2001. Biochemical characterization of Gyp6p, a Ypt/Rab-specific GTPase-activating protein from yeast. *J Biol Chem.* 276:12135-9.
- Wittinghofer, A. 2006. Phosphoryl transfer in Ras proteins, conclusive or elusive? *Trends Biochem Sci.* 31:20-3.
- Wittinghofer, A., K. Scheffzek, and M.R. Ahmadian. 1997. The interaction of Ras with GTPase-activating proteins. *FEBS Lett.* 410:63-7.
- Wu, Y.W., K.T. Tan, H. Waldmann, R.S. Goody, and K. Alexandrov. 2007. Interaction analysis of prenylated Rab GTPase with Rab escort protein and GDP dissociation inhibitor explains the need for both regulators. *Proc Natl Acad Sci U S A.* 104:12294-9.
- Wurmser, A.E., T.K. Sato, and S.D. Emr. 2000. New component of the vacuolar class C-Vps complex couples nucleotide exchange on the Ypt7 GTPase to SNARE-dependent docking and fusion. *J Cell Biol.* 151:551-62.
- Yan, R., Q. Shi, X. Hu, and X. Zhou. 2006. Reticulon proteins: emerging players in neurodegenerative diseases. *Cell Mol Life Sci.* 63:877-89.
- Yoshimura, S., J. Egerer, E. Fuchs, A.K. Haas, and F.A. Barr. 2007. Functional dissection of Rab GTPases involved in primary cilium formation. *J Cell Biol.* 178:363-9.
- Yoshimura, S., A. Yamamoto, Y. Misumi, M. Sohda, F.A. Barr, G. Fujii, A. Shakoory, H. Ohno, K. Mihara, and N. Nakamura. 2004. Dynamics of Golgi matrix proteins after the blockage of ER to Golgi transport. *J Biochem (Tokyo).* 135:201-16.
- Yu, S., A. Satoh, M. Pypaert, K. Mullen, J.C. Hay, and S. Ferro-Novick. 2006. mBet3p is required for homotypic COPII vesicle tethering in mammalian cells. *J Cell Biol.* 174:359-68.
- Yuce, O., A. Piekny, and M. Glotzer. 2005. An ECT2-centralspindlin complex regulates the localization and function of RhoA. *J Cell Biol.* 170:571-82.
- Zacchi, P., H. Stenmark, R.G. Parton, D. Orioli, F. Lim, A. Giner, I. Mellman, M. Zerial, and C. Murphy. 1998. Rab17 regulates membrane trafficking through apical recycling endosomes in polarized epithelial cells. *J Cell Biol.* 140:1039-53.
- Zerial, M., and H. McBride. 2001. Rab proteins as membrane organizers. *Nat Rev Mol Cell Biol.* 2:107-17.
- Zhang, X., E. Bi, P. Novick, L. Du, K.G. Kozminski, J.H. Lipschutz, and W. Guo. 2001. Cdc42 interacts with the exocyst and regulates polarized secretion. *J Biol Chem.* 276:46745-50.
- Zheng, J.Y., T. Koda, T. Fujiwara, M. Kishi, Y. Ikehara, and M. Kakinuma. 1998. A novel Rab GTPase, Rab33B, is ubiquitously expressed and localized to the medial Golgi cisternae. *J Cell Sci.* 111 (Pt 8):1061-9.

Publications

Parts of this work are published in:

Haas, A.K., E. Fuchs, R. Kopajtich, and F.A. Barr. 2005. A GTPase-activating protein controls Rab5 function in endocytic trafficking. *Nat Cell Biol.* 7:887-93.

Haas, A.K., S. Yoshimura, D.J. Stephens, C. Preisinger, E. Fuchs, and F.A. Barr. 2007. Analysis of GTPase-activating proteins: Rab1 and Rab43 are key Rabs required to maintain a functional Golgi complex in human cells. *J Cell Sci.* 120:2997-3010.

Fuchs, E., **A.K. Haas**, R.A. Spooner, S. Yoshimura, J.M. Lord, and F.A. Barr. 2007. Specific Rab GTPase-activating proteins define the Shiga toxin and epidermal growth factor uptake pathways. *J Cell Biol.* 177:1133-43.

Yoshimura, S., J. Egerer, E. Fuchs, **A.K. Haas**, and F.A. Barr. 2007. Functional dissection of Rab GTPases involved in primary cilium formation. *J Cell Biol.* 178:363-9.

Yoshimura, S., **A.K. Haas**, and F.A. Barr. 2008. Analysis of Rab GTPase and GTPase-activating protein function at primary cilia. *Methods Enzymol.* 439:353-364. *In Press.*

Reviews:

Haas, A.K., and F.A. Barr. 2007. COP sets TRAPP for vesicles. *Dev Cell.* 12:326-7.

Short, B., **A. Haas**, and F.A. Barr. 2005. Golgins and GTPases, giving identity and structure to the Golgi apparatus. *Biochim Biophys Acta.* 1744:383-95.

Presentations

Poster presentations:

ELSO meeting 2005, Dresden

Haas, A.K., E. Fuchs, R. Kopajtich, and F.A. Barr; A GTPase-activating protein controls Rab5 function in endocytic trafficking

British Society for Cell biology meeting 2007, Liverpool:

Haas, A.K., S. Yoshimura, D.J. Stephens, C. Preisinger, E. Fuchs, and F.A. Barr; Rab1 and Rab43 are key Rabs required to maintain a functional Golgi complex in human cells

Oral presentations:

ASCB meeting 2006, San Diego:

Haas, A.K., S. Yoshimura, D.J. Stephens, C. Preisinger, E. Fuchs, and F.A. Barr; Rab1 and Rab43 are key Rabs required to maintain a functional Golgi complex in human cells

Acknowledgements

I would like to thank Prof. Francis Barr not only for giving me the opportunity to study Rabs and their regulators in his lab for the last years, but also for countless discussions about whatever. I've learnt a lot during these years, but I still wouldn't buy a Mac. (But for free, I guess I would take one...).

Mein besonderer Dank gebührt PD Dr. Angelika Böttger für die Betreuung meiner Dissertation als Erstgutachterin. Ich möchte mich auch bei den weiteren Mitgliedern meiner Prüfungskommission recht herzlich bedanken.

I would also like to thank my colleagues in the Barr group and the Nigg department for their support and friendship in the last years. I would like to particularly mention Ben Short, Christian Preisinger, Rüdiger Neef, Robert Kopajtich, Evelyn Fuchs, Johannes Egerer, Stefan Hümmer and Kerstin Thein. Not to forget about Anni, of course!

Thanks to everybody in Liverpool for their support! Unfortunately I was there too short to get to know you better...

Extra special thanks goes to Shinichiro Yoshimura for becoming a close friend and home mate in Liverpool. Remember to always keep your loops tight and the line wet!

Cheers, Mate!

Besonderer Dank gebührt auch den Fischverrückten.

Abschließend möchte ich mich bei meiner Familie, und im ganz besonderen bei meinen Eltern für das Verständnis und die Unterstützung während der letzten 30 Jahre bedanken. War bestimmt nicht immer ganz leicht.

Silvia, danke für einfach alles! Ohne dich wär' das alles nix geworden...

Curriculum Vitae

Personal details

Name	Alexander Klaus Haas
Date of Birth	19 th November 1977
Place of Birth	Aschaffenburg, Germany

Education and Qualifications

Since 2003	PhD in Biology with Prof. Francis A. Barr at the Max-Planck Institut für Biochemie in Martinsried and the Cancer Research Centre in Liverpool
1997-2003	Ludwig-Maximilians Universität München Subject Biology, Diploma in Biology grade 1,0 Diploma thesis in the Lab of Dr. Francis A. Barr, Topic: “Regulation von Rab GTPasen durch TBC1 Domänen Proteine”
1989-1997	Wilhelm-Hausenstein Gymnasium München (German grammar school), Abitur (university entrance qualification) grade 2,2

Additional skills and experience

- Education as radio safety officer
- Organisation and administration of the 6th Graduate Retreat of the MPI für Biochemie
- Excellent knowledge in computer hardware and software, especially Windows PC, MS Office, Adobe Photoshop, Adobe Illustrator, Macromedia Dreamweaver, Macromedia Fireworks